DOCUMENT 809-10

SIGNATURE MEASUREMENT STANDARDS GROUP

STANDARDS AND PROCEDURES FOR APPLICATION OF RADIOMETRIC SENSORS

WHITE SANDS MISSILE RANGE
REAGAN TEST SITE
YUMA PROVING GROUND
DUGWAY PROVING GROUND
ABERDEEN TEST CENTER
ELECTRONIC PROVING GROUND
HIGH ENERGY LASER SYSTEMS TEST FACILITY

NAVAL AIR WARFARE CENTER WEAPONS DIVISION, PT. MUGU
NAVAL AIR WARFARE CENTER WEAPONS DIVISION, CHINA LAKE
NAVAL AIR WARFARE CENTER AIRCRAFT DIVISION, PATUXENT RIVER
NAVAL UNDERSEA WARFARE CENTER DIVISION, NEWPORT
PACIFIC MISSILE RANGE FACILITY
NAVAL UNDERSEA WARFARE CENTER DIVISION, KEYPORT

30TH SPACE WING
45TH SPACE WING
AIR FORCE FLIGHT TEST CENTER
AIR ARMAMENT CENTER
ARNOLD ENGINEERING DEVELOPMENT CENTER
BARRY M. GOLDWATER RANGE

NATIONAL AERONAUTICS AND SPACE ADMINISTRATION

Report Documentation Page

Form Approved
OMB No. 0704-0188

1. REPORT DATE	2. REPORT TYPE	3. DATES COVERED
JUL 2010		**00-06-2006 to 00-01-2010**

4. TITLE AND SUBTITLE	5a. CONTRACT NUMBER
Standards and Procedures for Application of Radiometric Sensors	5b. GRANT NUMBER
	5c. PROGRAM ELEMENT NUMBER
6. AUTHOR(S)	5d. PROJECT NUMBER
	5e. TASK NUMBER **SMSG-019**
	5f. WORK UNIT NUMBER
7. PERFORMING ORGANIZATION NAME(S) AND ADDRESS(ES) **Range Commanders Council,1510 Headquarters Avenue,White Sands Missile Range,NM,88002**	8. PERFORMING ORGANIZATION REPORT NUMBER **809-10**
9. SPONSORING/MONITORING AGENCY NAME(S) AND ADDRESS(ES)	10. SPONSOR/MONITOR'S ACRONYM(S)
	11. SPONSOR/MONITOR'S REPORT NUMBER(S)

12. DISTRIBUTION/AVAILABILITY STATEMENT
Approved for public release; distribution unlimited

13. SUPPLEMENTARY NOTES

14. ABSTRACT
Defines foundational standards for electro-optical and infrared signature measurements including standardization of the parameters, quantity names, symbols, units, equations, terms, and definitional descriptions of typical and/or standardized electro-optical/infrared test environments.

15. SUBJECT TERMS
Signature Measurement Standards Group; electro-optical signature measurement; infrared signature measurements; radiometer; photometer; spectral domain; spatial domain; temporal domain; EO; IR

16. SECURITY CLASSIFICATION OF:			17. LIMITATION OF ABSTRACT	18. NUMBER OF PAGES	19a. NAME OF RESPONSIBLE PERSON
a. REPORT **unclassified**	b. ABSTRACT **unclassified**	c. THIS PAGE **unclassified**	**Same as Report (SAR)**	**242**	

This page intentionally left blank.

DOCUMENT 809-10

STANDARDS AND PROCEDURES FOR APPLICATION OF RADIOMETRIC SENSORS

July 2010

Prepared by

SIGNATURE MEASUREMENT STANDARDS GROUP
(SMSG)

Published by

Secretariat
Range Commanders Council (RCC)
U.S. Army White Sands Missile Range,
New Mexico 88002-5110

This page intentionally left blank.

TABLE OF CONTENTS

LIST OF FIGURES

This page intentionally left blank.

LIST OF TABLES

This page intentionally left blank.

PREFACE

This document presents the results of work performed by the Signature Measurement Standards Group (SMSG) of the Range Commanders Council (RCC). The work was a three year effort entitled RCC Task SMSG-19, "Development of Electro-optical (EO)/Infrared (IR) Laboratory and Field Inter-Comparison." The scope of Task SMSG-19 was to develop a methodology for comparing calibrations between laboratory and field measurements of EO/IR measurements. The specific objective was to define the measurement and data reduction processes that allow direct comparison between EO signatures collected under laboratory (indoor range) environments and those collected in outdoor range environments. Task SMSG-19 was directed toward developing major foundational standards for EO/IR signature measurements, including standardization of the parameters, quantity names, symbols, units, equations, terms, and definitional descriptions of typical and/or standardized EO/IR test environments. Funding for this effort was provided by the Test Resource Management Center (TRMC) and several other organizations contributed considerable support.

The RCC would especially like to thank the following individual for providing additional technical content, advice, editing, and coordination.

Technical Coordinator: Ms. Kathryn Dietz
Senior Scientist
Science Applications International Corporation (SAIC)

Please direct any questions to:

Secretariat, Range Commanders Council (RCC)
ATTN: TEDT-WS-RCC
1510 Headquarters Avenue
White Sands Missile Range, NM 88002-5110
Phone: (575) 678-1107 DSN 258-1107
Fax: (575) 678-7519 DSN 258-7519
Email: usarmy.wsmr.atec.list.rcc@mail.mil

This page intentionally left blank.

ACKNOWLEDGMENTS

Members of the Signature Measurement Standards Group (SMSG) of the Range Commanders Council (RCC) developed the objectives and designed the structure of this document. Portions of the document were based on writings of several individuals:

a. Unpublished writings of Dr. Henry Register and Mr. George Cameron, with Department of Defense (DoD) oversight by Mr. William Jollie, Eglin Air Force Base (AFB), FL.
b. Unpublished writings of Mr. Jack White, with DoD oversight by Mr. Kevin Young, Point Mugu, CA.
c. New material developed by Ms. Kathryn Dietz and Mr. Donald Philpott, with DoD oversight by Dr. Jim Nichols, Arnold AFB, TN.
d. Ms. Dietz also performed final technical review of inputs and editing of the final product. Ms Dietz wishes to thank the following people for their assistance:

(1) Mr. Jeffrey Burks, Air Force Research Laboratory (AFRL) and Mr. Kevin Norwood, White Sands Missile Range (WSMR), for their detailed review and helpful comments during the final review.
(2) Mr. Dennis Garbo and Mr. David Cocanougher, Eglin AFB, for additional material on standard predictive codes for Chapter 9.
(3) Mr. Roger Davis, SMSG Secretary, for his detailed guidance and support during the planning and execution phases of this task.

Additional key support came from:

e. Dr. Gerald Fraser, National Institute of Standards and Technology (NIST), and Mr. Chris Dobbins, Redstone Arsenal, AL, the current SMSG Chair and Vice Chair, respectively, for their technical assistance.
f. Personnel at the Advanced Missile Signatures Center (AMSC), Arnold AFB, for their review of the first draft.

This work is dedicated to the memories of:
Dr. Henry Register and Mr. George Cameron.

This page intentionally left blank.

ACRONYMS

2D	two dimensional
3D	three dimensional
AEDC	Arnold Engineering Development Center
AF	Air Force
AFB	Air Force Base
AFRL	Air Force Research Laboratory
AMSC	Advanced Missile Signature Center
AR	anti-reflection
ATC	Aberdeen Test Center
ATF	aperiodic transfer function
AVHRR	Advanced Very High Resolution Radiometer
AVIRIS	Airborne Visible/Infrared Imaging Spectrometer
BIPM	International Bureau of Weights and Measures (in French: Bureau International des Poids et Mesures)
BRDF	bidirectional reflectance distribution function
CAD	computer-aided design
CCD	charge-coupled device
cd	candela
CFD	computational fluid dynamics
CHAMP	Composite Hardbody and Missile Plume
CIE	International Commission on Illumination (in French: Commission Internationale de l'Eclairage)
CPIAC	Chemical Propulsion Information Analysis Center
CRAFTAC	Combustion Research and Flow Technology Aircraft
CVF	circular variable filter
CW	continuous wave
DARPA	Defense Advanced Research Projects Agency
DIA	Defense Intelligence Agency
DTIC	Defense Technical Information Center
E2E	end-to-end
EGT	exhaust gas temperature
E-MSIG	Enhanced Missile Signature (model)
EO	electro-optical
EO-3	Earth Observing 3 (NASA program)
EPSS	Exhaust Plume and Signatures Subcommittee
ERIM	Environmental Research Institute of Michigan
EUV	extreme UV
EXTF	external turbo fan
FIR	far IR
FISTA	Flying Infrared Signatures Aircraft
FOR	field of regard
FOV	field of view
FPA	focal plane array
FTIR	Fourier transform IR
FTS	Fourier Transform Spectrometer
FUV	far UV

FWHM	full width at half maximum
GIFTS	Geostationary Imaging Fourier Transform Spectrometer
GPS	Global Positioning System
GTSIG	Georgia Tech Signature (code library)
GTVISIT	Georgia Tech Visible and Infrared Synthetic Imagery Testbed
GUI	graphical user interface
HIL	hardware-in-the-loop
HIRSS	Hover Infrared Suppression System
HYDICE	Hyperspectral Digital Imagery Collection Experiment
Hz	hertz
IDRL	Integrated Data Requirements List
IFOV	instantaneous field of view
IPC	Interagency Propulsion Committee
IR	infrared
IRIA	Infrared Information Analysis Center
IRIG	Inter-range Instrumentation Group
ISO	International Organization for Standardization
JANNAF	Joint Army-Navy-NASA-Air Force
JPL	Jet Propulsion Laboratory
JTAMS	Joint Tactical Missile Signature
JTF	Joint Task Force
KHILS	Kinetic Kill Vehicle Hardware-in-the-loop Simulator
LANDSAT	Land Remote-Sensing Satellite
$LiTaO_3$	lithium tantalate
LWIR	long wave IR
Lya	Lyman-alpha
MANPADS	Man Portable Air Defense System
MDR	material directional reflectance
MIRS	Multispectral Infrared Radiometric System
MODEX	Model Extrapolation Procedure
MODTRAN	Moderate Resolution Atmospheric Transmission
mrad	milliradian
MSIC	Missile and Space Intelligence Center
MuSES	Multi-Service Electro-optics Signature (code)
MUV	Mid UV
MW	megawatt
mW	milliwatt
MWIR	mid-wave IR
NASA	National Aeronautics and Space Administration
NEP	noise equivalent power
NIR	near IR
NIST	National Institute of Standards and Technology
NMP	New Millennium Program
ns	nanosecond
NSP	National Signatures Program
NUV	near UV
OSD	Office of the Secretary of Defense
PbS	lead sulfide
PBV	post boost vehicle

PFF	Plume Flow Field
PLA	power level angle
PNS	Parabolized Navier Stokes
PRISM	Physically Reasonable Infrared Signature Model
Q.E.	quantum efficiency
R&D	research and development
RCC	Range Commanders Council
RCMS	Radiometric Color Measurement System
RPM	revolutions per minute
RTC	Real-Time CHAMP
SAM	surface-to-air missile
SARIS	Spatial/Spectral Airborne Radiometric Infrared System
SBUV	solar blind UV
SEBASS	Spatially Enhanced Broadband Array Spectrograph System
SFPA	staring focal plane array
SI	International System of Units
SIRRMII	Standard Infrared Radiation Model, version II
SMSG	Signature Measurement Standards Group
SNR	signal-to-noise ratio
SPF	Standard Plume Flowfield
SPF	standard plume flowfield
SPIRITS	Spectral and Inband Radiometric Imaging of Targets and Scenes
SPURC	Standard Plume Ultraviolet Radiation Code
sr	steradian
SWIR	short wave IR
TALO	time after lift-off
TATR	time after trigger
TGT	Turbine Gas Temperature
TIT	turbine inlet temperature
TOD	time of day
TRBEXT	turbine exit
TRBEXT	Turbine Exit (model)
TRMC	Test Resource Management Center
TSPI	time-space-position information
UAV	unmanned air (aerial) vehicle
UCSB	University of California, Santa Barbara
UTC	Coordinated Universal Time
UV	ultraviolet (radiation)
UV-A	ultraviolet Type A
UV-B	ultraviolet Type B
UV-C	ultraviolet Type C
VIPER	Viscous Interaction Performance Evaluation Routine
VIS	visible (radiation)
VUV	vacuum UV
W	watt
WSMR	White Sands Missile Range

This page intentionally left blank.

CHAPTER 1

INTRODUCTION

1.1 Background

Several factors affect the ability to compare sets of measured radiometric signatures. These factors include the characteristics of the measurement instrumentation systems used, the effect of the environment on the signature, and the effect of the environment on the instrumentation. This document focuses on the characterization, calibration, and use of radiometric instrumentation for data collection and the reduction and analysis of the data. It addresses procedures to determine the spectral, spatial, and temporal characteristics of typical measurement instrumentation systems and includes mathematical calculations applicable to calibration, reduction, operations, and report documentation. Existing methods, capabilities, and procedures used by major Army, Navy, and Air Force (AF) T&E organizations performing radiometric measurements have been investigated with pertinent techniques addressed in this document. Application of the techniques defined will improve the quality of target data collections and allow a better understanding of comparisons between data sets collected with different measurement systems at different locations and times.

1.1.1 Key Definitions.

a. Electro-optical (EO): The Department of Defense (DoD) Dictionary of Military and Associated Terms (Reference 3a) defines EO as:

"The technology associated with those components, devices and systems which are designed to interact between the electromagnetic (optical) and the electric (electronic) state."

The above definition refers to devices that interact with electromagnetic energy and change electric state proportional to the electromagnetic energy. The electric signal can be a current or voltage, or a changed resistance or temperature that is measured electronically.

b. Optical Radiation. Optical radiation is defined to be electromagnetic energy with wavelengths (measured in micrometers, μm) ranging from 0.01 μm to 1 000 μm. However, the usable wavelength range of concern to the military is limited to wavelengths between 0.2 μm and 25 μm due to severe atmospheric absorption outside this range.

c. Radiometry. Radiometry is the measurement of the electromagnetic energy through measurement of the electric signal. The range of the electromagnetic spectrum is broad, extending from extremely short wavelength cosmic radiation (shorter than 10^{-14} meter) to extremely long wavelength radiation from slowly oscillating electrons (longer than 10^{5} meter).

Radiometry is the science and the craft of measuring radiant power, and is a specialized branch of the general field of remote sensing. A more accurate description might be "remote quantification" because simply sensing that radiation is present, forming images, or qualitatively analyzing spectra to identify chemical constituents is not radiometry. Radiometry is concerned with the measurement of the magnitude of electromagnetic radiant power. Radiometry, as used in this document, includes measurements of the distribution of radiant power across a domain.

d. Photometry. Photometry is related to radiometry, but it is the science of measuring radiation in the visible portion of the electromagnetic spectrum (i.e. in the spectral response of a human observer). The procedures of photometry are similar to those of radiometry for a band system, where the band is the spectral response of the human eye, except photometry has its own set of terms.

Radiometric instruments used to measure target signatures include band radiometers, imaging radiometers, spectral radiometers, and spatial/spectral radiometers. If the radiometer is optically filtered such that the spectral response mimics the response of the human eye it is referred to as a photometer. Each instrument has characteristics which affect signature data collected using the instrument. The characteristics include effective collecting aperture, field of view (FOV), instantaneous field of view (IFOV), spectral response, temporal response, and input/output characteristics. Accurate characterization and calibration of measurement instrumentation systems are necessary to allow the collection of accurate target signature data and the proper interpretation of the measured data. Sources of military interest include stationary or moving surface targets; airborne and space targets; targets in simulation chambers; and standard laboratory calibration sources. Unfortunately, radiometers are simultaneously subjected to radiation from sources other than the target of interest. The unwanted radiation sources include the operating environment background and foreground and radiometer self-radiation. The contribution of extraneous sources to the radiometer output signal must be accurately accounted for and removed, leaving only the actual target signature.

1.1.2 Goal of Electro-optical (EO) measurements. The goal of EO target measurements is to provide accurate target signature descriptions. It is often the case that signatures of the same target, but collected in different environments and with different sensors, will be different. Proper characterization and calibration of the measurement system, as well as accounting for differences in the environments, will account for the variations. The detailed characterization and accurate calibration of EO measurement systems are necessary, but not sufficient to obtain target signature data that are independent of the instrumentation and the environment. Unless the instrumentation is properly characterized and calibrated, and unless the effects of the environment are properly accounted for, there is little reason to expect that different measurements of a target signature data can be compared. The procedures outlined in this document are meant to assist in minimizing the differences and to account for the remainder.

1.2 Scope

This document standardizes the characterization of instrumentation before, during, and after test data collection exercises. Because the radiometric test environment is a complex

system that varies tremendously across time, space, and meteorological conditions, it is critically important to reduce the overall uncertainties relating to the instrumentation employed. Because this document focuses only on the instrumentation part of the overall test environment, it is a useful product for use by a very broad user base.

The document is intended for personnel working in radiometry who have some experience with calibration, measurement, and data reduction, and also have an understanding of the many factors that produce and influence target signatures. Fundamental concepts are briefly reviewed, but without the depth, especially mathematical, that is needed for thorough understanding. This document is designed to supplement, but not replace, other published radiometry documents.

Little of the material contained here will be new to experienced personnel. What may be new for many is the assembly of different concepts and the presentation of how an understanding of the combination and interaction of these concepts can be used to develop strategies to reduce uncertainty. In measurement groups where these strategies are already well known and practiced, this document may also serve as a check list to review before every major measurement program.

The document discusses standard methods to characterize and calibrate banded radiometers, scanning radiometers, and spectral radiometers for applications in testing scenarios currently addressed by major Army, Navy, and Air Force T&E organizations. The scope of this document encompasses measurements within the portion of the electromagnetic radiation that spans the ultraviolet (UV) through the infrared (IR) wavelengths of 0.2 μm to 25 μm (frequencies spanning 1.5×10^{15} Hz to 2×10^{13} Hz). These wavelengths are considered the optical wavelengths.

Data reduction techniques to transfer the raw data signals to engineering unit data are discussed. Quantities, symbols, and units of measure are those sanctioned by the National Institute of Standards and Technology (NIST) and the International Bureau of Weights and Measures (BIPM). It is impossible to address all testing scenarios since they are broad and varied, but the required ancillary data for correct radiometric signature interpretation in four representative testing scenarios are discussed in detail. The four scenarios are in described in Chapter 8:

a. Geometric size considerations. (paragraph 8.1)
b. Low radiance targets. (paragraph 8.2)
c. Long range testing. (paragraph 8.3)
d. Short range testing. (paragraph 8.4)

This document primarily addresses the process of making accurate measurements of the apparent signature through accurate characterization of the measurement instrument, where the term “apparent” indicates that the measured signature includes the effect of the environment. Proper documentation of the environment and the measurement process is also addressed to allow correct interpretation of the data. The correction of the measured data for atmospheric effects is addressed in a Range Commanders Council (RCC) document to be published at a later

date; the document title will be Weather and Atmospheric Effects on the Measurement and Use of Electro-optical (EO) Signature Data.

CHAPTER 2

RADIOMETRY

2.1 Electromagnetic Spectrum

The frequency or wavelength range of the electromagnetic spectrum is broad. The explored range of the spectrum extends over 17 orders of magnitude from extremely short wavelength cosmic radiation to extremely long wavelength radiation from slowly oscillating electrons. Optical radiation is defined to be the narrow portion of the electromagnetic spectrum spanning five orders of magnitude with wavelength ranging from 0.01 μm to 1000 μm. The electromagnetic spectrum and the optical region are illustrated in Figure 2-1. The optical range includes ultraviolet (UV), visible (VIS), and IR radiation. The illustration of the optical spectrum in Figure 2-1(b) is limited to wavelengths ranging from 0.1 μm to 25 μm because this is approximately the range related to military surveillance, reconnaissance, weapon, and countermeasure systems. The UV wavelength range will be further limited in our consideration to wavelengths longer than 0.2 μm because radiation of shorter wavelengths is significantly absorbed by the atmosphere. The atmosphere is also essentially opaque to wavelengths longer than 25 μm.

Electromagnetic radiation, including optical radiation, is characterized by its wavelength (λ), frequency (ν), wavenumber (σ), and photon energy (Q). With c defined to be the speed of light (2.997 924 58 x 10^{8} meters per second (m/s)) and h defined to be Planck's constant (6.626 068 896 x 10^{-34} J s or 4.135 667 33 x 10^{-15} eV s), the quantities are related as seen in Equations 2-1a through Equation 2-1d. Figure 2-2 is a nomograph for convenient conversion between the radiometric quantities.

$$\lambda = \frac{c}{\nu}, \text{ wavelength} \qquad \text{(Eq. 2-1a)}$$

$$\nu = \frac{c}{\lambda}, \text{ frequency} \qquad \text{(Eq. 2-1b)}$$

$$\sigma = \frac{1}{\lambda}, \text{ wavenumber} \qquad \text{(Eq. 2-1c)}$$

$$Q = h\nu, \text{ photon energy} \qquad \text{(Eq. 2-1d)}$$

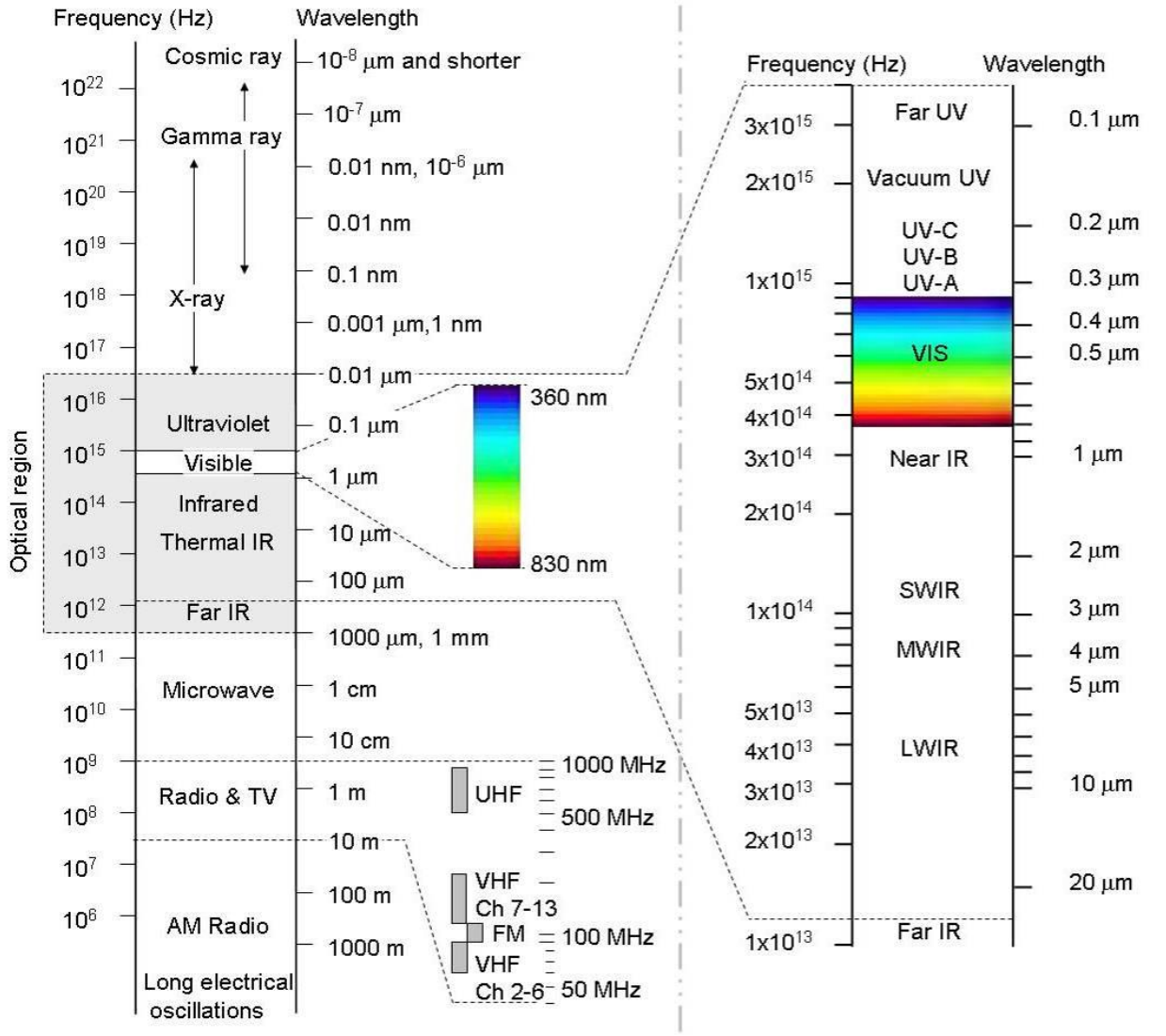

a. Electromagnetic spectrum

b. Portion of optical region from 0.1 μm to 25 μm

Figure 2-1. Electromagnetic spectrum and a portion of the optical region limited to 25 μm, the long wavelength concern of the military.

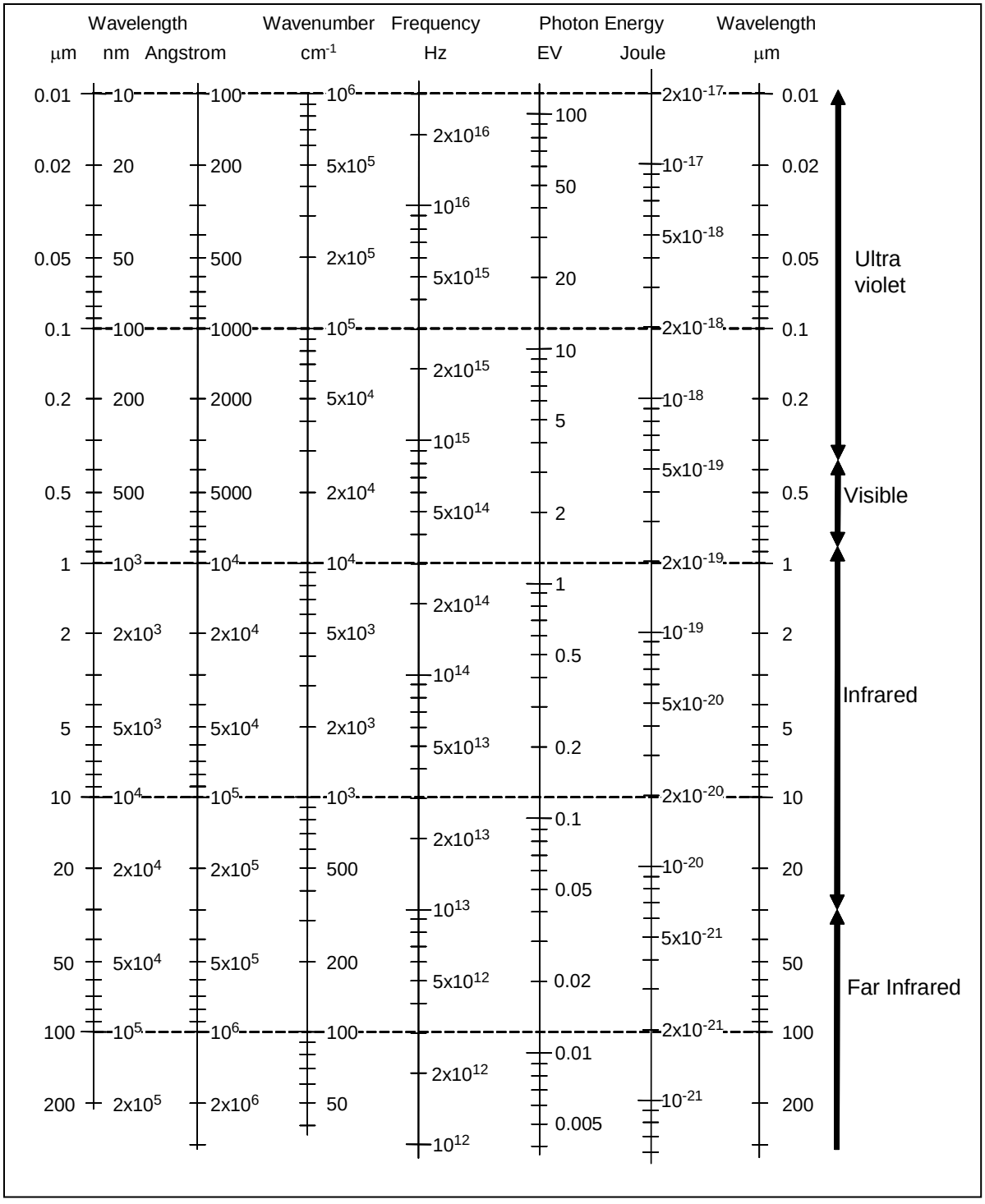

Figure 2-2. Nomograph for conversion between radiometric quantities.

The designations of the named sub-regions in Figure 2-1 are subjective. There are no standard wavelength points to define the named regions nor are there standard names. The names shown in Figure 2-1 are those commonly used by the military. Other disciplines use different designations that better fit their needs. Because of the lack of standardization across disciplines, it is important to always quantify the spectral band of concern. As will be discussed, this quantification is accomplished at a minimum by quantifying the bandpass end points and (optimally) by quantifying the spectral response of the optical instrument.

The visible region is naturally defined by the range of human sight. The word *infrared* is based on the Latin word *infra* for below and indicates the frequencies are less than the red region of human sight. The term *ultraviolet* was coined to indicate frequencies greater than the violet region of human sight. The subgroups are further subdivided into regions based primarily on the phenomenology of atmospheric absorption and atmospheric windows (spectral regions of high transmission), and by the effects of the radiation on biological systems. Table 2-1 lists sub-region terms commonly used by the military compared to terms recommended by the International Commission on Illumination (CIE) and those used in the discipline of astrophysics and atmospheric science (Reference 3b).

TABLE 2-1. GENERAL SUB-REGION TERMS OF THE OPTICAL SPECTRUM

CIE Recommended	Astrophysics	Atmospheric Science	Nominal Military	Band (Micrometers)
Far UV (FUV)				0.01 to 0.1
	Extreme UV (EUV)			0.01 to 0.121
	Lyman-alpha (Lya)			0.121-0.122
	Far UV (FUV)			0.122 to 0.2
	Mid-UV (MUV)			0.2 to 0.3
	Near UV (NUV)			0.3 to 0.4
			Vacuum UV (VUV)	0.01 to 0.2
UV-C		UV-C	UV-C	0.1 to 0.28
UV-B		UV-B	UV-B	0.28 to 0.315
			Solar Blind UV (SBUV)	0.2 to 0.315
UV-A*			UV-A*	0.315 to 0.38
		UV-A		0.32 to 0.4
Visible (VIS)			Visible (VIS)	0.36 to 0.83 (‡)
	Visible (VIS)			0.38 to 0.78
		Visible (VIS)`		0.4 to 0.7
		Near- IR (NIR)		0.7 to 4
		Infrared (IR)		0.7 to 1000
	Near- Infrared (NIR)			0.76 to 1.4
IR-A				0.78 to 1.4
			Near-Infrared (NIR)	0.75 to 1.83
IR-B	Middle Infrared (Mid-IR)			1.4 to 3
			Short Wave Infrared (SWIR)	1.83 to 2.7
			Mid-Wave Infrared (MWIR)	2.7 to 6
IR-C	Far Infrared (FIR)			3 to 1000
		Thermal Infrared		4 to 50
			Long-Wave Infrared (LWIR)	6 to 30
			Far Infrared (FIR), also Terahertz IR	30-1000
		Far Infrared (FIR)		50 to 1000

* Global Solar UV Index designates ultraviolet type A (UV-A) as 0.315 μm to 0.4 μm

‡ The spectral limits of the spectral luminous efficiency for photopic vision (Reference 3c).

Figure 2-3 shows the spectral regions of the atomic and molecular ultraviolet absorbers compared to the ultraviolet sub-region designations (Reference 3d). By convention, atmospheric optical depth is defined along a vertical path from the top of the atmosphere to the earth surface. The dependent variable of Figure 2-3 is the altitude when 63 percent of the solar radiation at a specific wavelength is absorbed, or $I(\lambda)/I_0(\lambda)$ = exp(-1) = 0.37 (Reference 3d). The extreme and far UV regions are defined by absorption bands of atomic and diatomic nitrogen and oxygen in the very high atmosphere. The narrow Lyman-alpha (Lya) region is the prominent solar hydrogen emission at 0.1216 µm that is broadened to 0.1214 µm to 0.1218 µm. The vacuum ultraviolet region includes the extreme and far regions, but also extends to the longer wavelength boundary of 0.2 µm defined by the Schumann-Runge absorption continuum (0.13 µm to 0.175 µm) and bands (0.175 µm to 0.20 µm) of diatomic oxygen (O_2). The region is named the vacuum ultraviolet region because radiation at wavelengths shorter than 0.2 µm will not transmit through the atmosphere over even a very short distance. The UV Type C (UV-C) region is defined by absorption of O_2 and ozone (O_3). Solar UV-C radiation will not penetrate the high ozone level in the upper atmosphere. Ultraviolet wavelengths between 0.2 µm and 0.315 µm are absorbed by the Hartley bands of ozone. The UV Type B (UV-B) region is defined by reduced atmospheric absorption (increased atmospheric window) on the long wavelength side of the Hartley band which allows some solar UV-B radiation to penetrate the upper atmosphere. The spectral region defined by the ozone Hartley band (0.2 µm to 0.315 µm) overlaps both the UV-C and the UV-B regions. It is called the solar-blind region because UV radiation will transmit through the atmosphere at low altitudes where the ozone level is low but the source will not be solar since solar radiation will not penetrate the stratospheric ozone layer. The UV Type A (UV-A) region is defined by the spectral atmospheric window that allows solar radiation to penetrate, but is bound at the longer wavelength end by the start of the visible region.

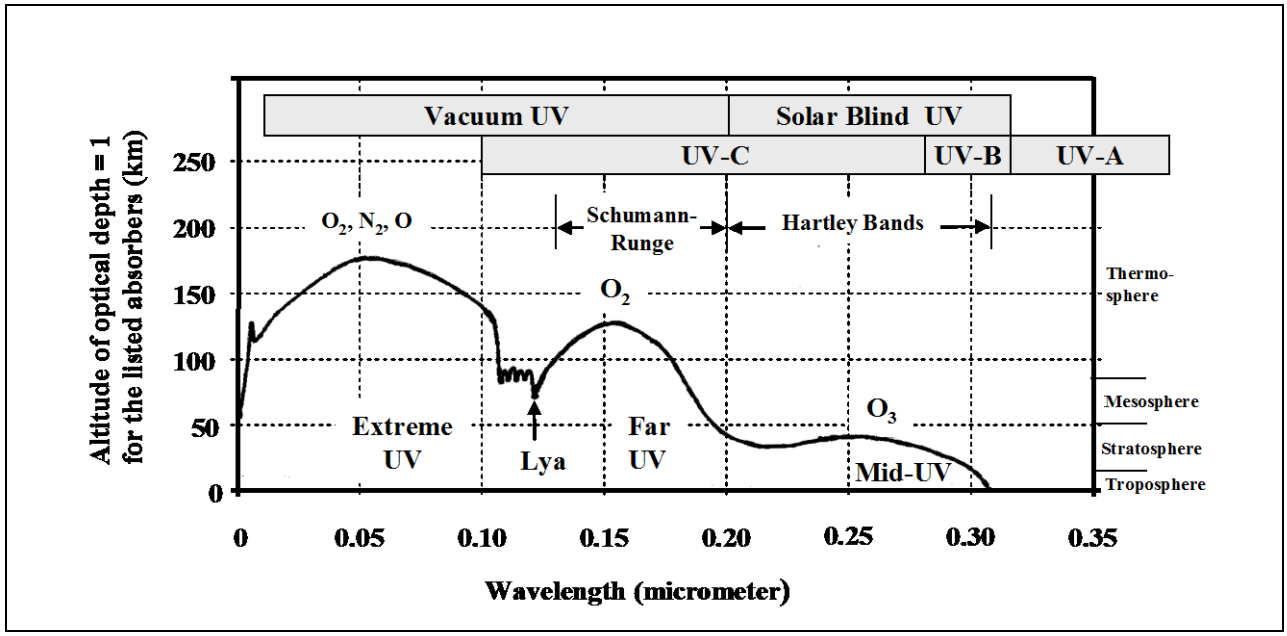

Figure 2-3. Altitude at which 63 percent of solar radiation is absorbed.

Figure 2-4 shows the atmospheric IR spectral transmission function with named IR sub-regions for wavelengths less than 30 μm. For the plot, the atmospheric transmission function was calculated using the Air Force Research Laboratory (AFRL), Space Vehicles Directorate atmospheric model, Moderate Resolution Atmospheric Transmission (MODTRAN, v 4.0), for a 500 m horizontal path at sea-level (see Reference 3e). The MODTRAN model is only valid for wavelengths less than 25 μm, but it is known from measurements that the atmosphere is essentially opaque to longer wavelength optical radiation and is plotted as such. The short wavelength end of the long wave IR (LWIR) region is sometimes labeled as 7 μm instead of 6 μm. Since the low altitude atmosphere is totally opaque to optical radiation between 5.5 μm and 7.2 μm, some practitioners choose the long wavelength edge of the gap as the breakpoint between mid-wave IR (MWIR) and LWIR. Another common variation is that some practitioners quote 8 μm to 12 μm as the end points of the LWIR band to stay within the high transmission window when they have no need to consider wavelengths longer than 12 μm.

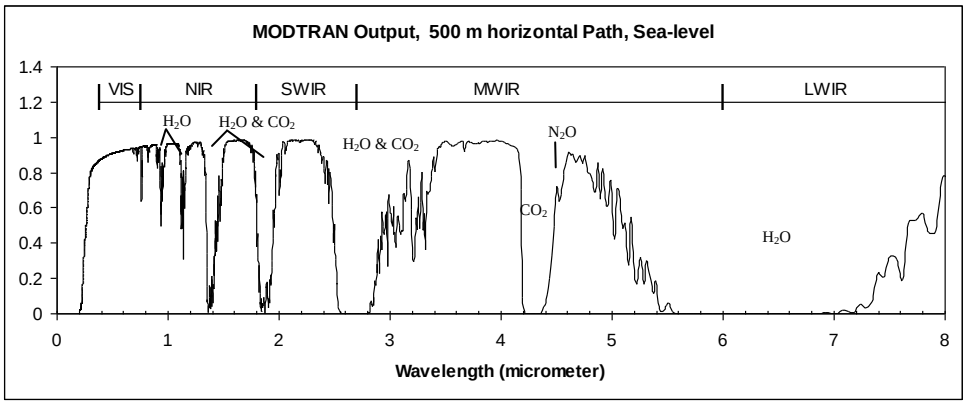

a. VIS to MWIR regions

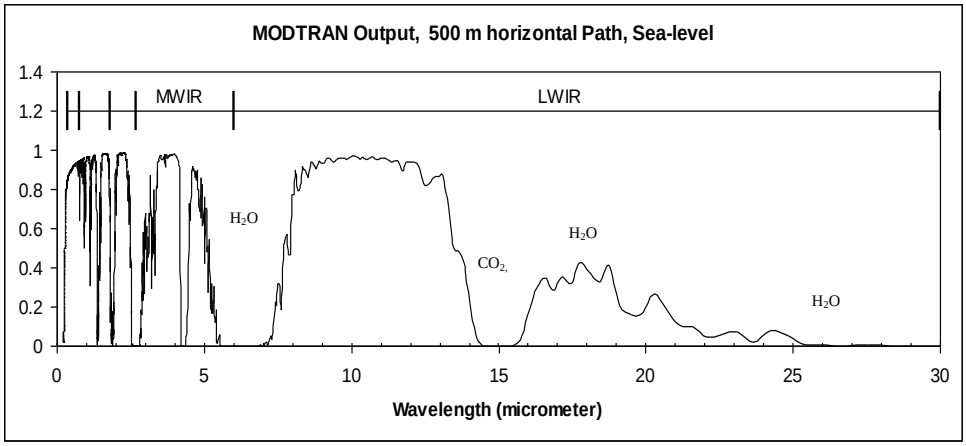

b. MWIR to LWIR regions

Figure 2-4. Infrared (IR) sub-regions defined by regions of atmospheric absorption.

2.2 International System of Units (SI)

Effective communications requires a consistent set of terms with well-understood meanings. This is especially true for technical disciplines, where it is desirable that a consistent set of quantities, definitions, symbols, and units be used. This holds true in the disciplines of radiometry and photometry. The SI, from the French Le Systeme International d'Unites, (Reference 3f, Reference 3g, and Reference 3h) provides a precise set of defined basic quantities from which radiometric and photometric quantities are derived. The following is a brief summary of the standard units and guidance of use. For more information, see Reference 3f, through Reference 3h. Be aware that the 1995 NIST Special Report 811 (Reference 3g) and the 2001 NIST Special Report 330 (Reference 3h) are derivatives of an earlier version of the definitive 2008 BIPM document (Reference 3f). Minor changes have been made by BIPM in the intervening years. For example, the BIPM no longer refers to radian and steradian units as supplementary; instead, the BIPM more completely identify coherent derived units, and they offer recommended symbols for some quantity names. The second printing of the 1995 NIST document acknowledges the elimination of the supplementary units in the preface and footnotes, and offers a definition of coherency in a footnote. The current printing of the 2001 NIST document acknowledges the elimination of the supplementary units in margin notes.

The two types of quantities are base, and derived. The seven base SI quantities are listed in Table 2-2. Examples of derived quantities are listed in Table 2-3. Examples of derived units with special names are listed in Table 2-4. Special names and symbols are simply a compact form for frequently used expressions of combinations of base units. Some special names offer an intuitive description of the quantity involved. Table 2-4 includes derived units made from a combination of base SI units and units with special names.

TABLE 2-2. SI BASE UNITS

Base Quantity		SI Base Unit	
Name	**Symbol (recommended)**	**Name**	**Symbol (mandatory)**
Amount of substance	*n*	mole	*mol*
Electric current	*I, i*	ampere	*A*
Length	*l, x, r, etc.*	meter	*m*
Luminous intensity	I_v	candela	*cd*
Mass	*m*	kilogram	*kg*
Thermodynamic temperature	*T*	Kelvin	*K*
Time	*t*	second	*s*

TABLE 2-3. EXAMPLES OF COHERENT DERIVED SI UNITS IN TERMS OF THE BASE NAME

Derived Quantity		SI Coherent Derived Unit	
Name	**Symbol**	**Name**	**Symbol**
Acceleration	a	meter per second squared	m/s^2
Amount of concentration	c	mole per cubic meter	mol/m^3
Area	A	square meter	m^2
Density, mass density	ρ	kilogram per cubic meter	kg/m^3
Luminance	L_v	candela per square meter	cd/ m^2
Mass concentration	ρ, γ	kilogram per cubic meter	kg/m^3
Refractive index	n	one (dimensionless)	1
Relative permeability	μ_r	one (dimensionless)	1
Speed, velocity	v	meter per second	m/s
Volume	V	cubic meter	m^3
Wavenumber	$\sigma, \tilde{\nu}$	reciprocal meter	m^{-1}

Derived units are expressed algebraically in terms of base units or other derived units, including the radian and steradian which are special dimensionless quantities. Coherent derived units are products of powers of base units that include no numerical factor other than 1. For example, 1 Hz = 1 s^{-1} and 1 N= 1 m kg s^{-2}. The SI units may be used with prefixes but the result will no longer be coherent. For example, 1 kHz = 1000 s^{-1} is not a coherent relationship. The radian and the steradian are dimensionless derived coherent quantities with the unit one but are given special unit names and symbols to be used to express values of plane angle and solid angle, respectively.

TABLE 2-4. EXAMPLES OF SI COHERENT DERIVED UNITS WITH SPECIAL NAMES AND SPECIAL SYMBOLS

Derived quantity	SI Coherent Derived Unit [1]			
Name	Name	Unit Symbol	Expressed in Terms of Other SI Units	Expressed in Terms of SI Base Units
Angular acceleration	radian per second squared		rad/s^2	$m\ m^{-1}\ s^{-2} = s^{-2}$
Angular velocity	radian per second		rad/s	$m\ m^{-1}\ s^{-1} = s^{-1}$
Capacitance	farad	F	C/V	$m^{-2}\ kg^{-1}\ s^4\ A^2$
Electric charge, quantity of electricity	coulomb	C		s A
Electric resistance	ohm	Ω	V/A	$m^2\ kg\ s^{-3}\ A^{-2}$
Energy [2]	electron-volt	eV	J	$m^2\ kg\ s^{-2}$
Energy, work, quantity of heat	joule	J	N m	$m^2\ kg\ s^{-2}$
Force	newton	N		$m\ kg\ s^{-2}$
Frequency	hertz	Hz		s^{-1}
Illuminance	lux	lx	lm/m^2	m^{-2} cd
Inductance	henry	H	Wb/A	$m^2\ kg\ s^{-2}\ A^{-2}$
Irradiance, heat flux density	watt per square meter		W/m^2	$kg\ s^{-3}$
Luminous flux	lumen	lm	cd sr	cd (candela)
Magnetic flux	weber	Wb	V s	$m^2\ kg\ s^{-2}\ A^{-1}$
Magnetic flux density	tesla	T	Wb/m^2	$kg\ s^{-2}\ A^{-1}$
Plane angle	radian	rad	1	m/m
Power, radiant flux	watt	W	J/s	$m^2\ kg\ s^{-3}$
Pressure, stress	pascal	Pa	N/m^2	$m^{-1}\ kg\ s^{-2}$
Radiance	watt per square meter steradian		$W/(m^2 \cdot sr)$	$kg\ s^{-3}$
Radiant intensity	watt per steradian		W/sr	$m^2\ kg\ s^{-3}$
Solid angle	steradian	sr	1	m^2/m^2

[1] Coherent derived units are products of powers of base units that include no numerical factor other than 1. Examples are 1 Hz = 1 s^{-1} and 1 N= 1 m kg s^{-2}. Coherent units may be used with prefixes but they will no longer be coherent; for example, 1 kHz = 1000 s^{-1} is not a coherent relationship.

[2] The electronvolt (eV) is an acceptable unit of energy for use with SI whose value in SI units J is obtained experimentally; 1 eV = 1.602 177 33x10^{-19} J with a combined standard uncertainty of 0.000 000 49x10^{-19} J

Prefixes listed in Table 2-5 are used on SI quantities when it is desirable to avoid the use of an extremely small or extremely large numeric value of the quantity. For example, it is more desirable to write 1.2 nm instead of 0.000 000 001 2 m or 1.2×10^{-9} m. A few rules of prefix usage from Reference 3g are:

a. Compound prefix symbols, that is, prefix symbols formed by the juxtaposition of two or more prefix symbols, are not permitted. This rule also applies to compound prefix names. For example, millimicrosecond is not permitted.
b. Prefix symbols can neither stand alone nor be attached to the number 1 (the symbol for the unit one). Similarly, prefix names cannot be attached to the name of the unit one, that is, to the word one.
c. Prefix names and symbols are never used with the units of time: minute, min; hour, h; day, d. Prefixes, however, may be used with the unit of time second, s, such as millisecond, ms. Also, prefix names and symbols are never used with angle-related symbols and names such as ^{o} for degrees, ' for minutes, and " for seconds.
d. Prefix symbols may be used with the unit symbol ^{o}C and prefixes may be used with the unit name *degree Celsius*. For example, 10 m^{o}C (10 millidegrees Celsius) is acceptable.
e. For historical reasons, the kilogram is the only quantity with a name and symbol that includes a prefix. Names and symbols for decimal multiples and submultiples of kilogram are formed by attaching prefix names to the unit name *gram*, and prefix symbols to the unit symbol *g*. For example, 10^{-6} kg = 1 mg.

TABLE 2-5. SI PREFIXES

Factor	Name	Unit Symbol	Factor	Name	Unit Symbol
10^{1}	deca	da	10^{-1}	deci	d
10^{2}	hecto	h	10^{-2}	centi	c
10^{3}	kilo	k	10^{-3}	milli	m
10^{6}	mega	M	10^{-6}	micro	μ
10^{9}	giga	G	10^{-9}	nano	n
10^{12}	tera	T	10^{-12}	pico	p
10^{15}	peta	P	10^{-15}	femto	f
10^{18}	exa	E	10^{-18}	atto	a
10^{21}	zetta	Z	10^{-21}	zepto	z
10^{24}	yotta	Y	10^{-24}	yocto	y

2.3 Radiometric Quantities

Radiometric quantity terms are used to represent radiant energy and radiant energy per unit time, per unit area, and per unit wavelength as it is emitted, transported, or absorbed. The most significant radiometric quantity is irradiance. Irradiance is significant because it is the only directly measured quantity. Other radiometric quantities are inferred from the measured irradiance. Irradiance is the time averaged flow of radiant energy across a unit area. Time averaging is required because the extreme optical frequencies make it impractical to measure the magnitude of an optical electromagnetic wave at a single point in time.

Radiometric quantities are derived from SI base units and SI derived units. Table 2-6 lists the basic set. Table 2-7 lists similar quantities when photon flux is the concern. Brief definitions of the basic quantities and some special adaptations follow the tables. There are many college level text books on optics that include derivations of the radiometric quantities. Two are listed as Reference 3i and Reference 3j. The 1998 NIST Handbook 152 (Reference 3k) is another excellent source for descriptions of radiometric quantities. To avoid additional complexity, geometric angle is not shown as a variable in Table 2-6 and Table 2-7, but the quantities in general vary with angle. In fact, the variation with angle characterizes a source into special categories of spectral, diffuse, and Lambertian that are described in paragraph 2.3.2.

Source radiation is described by either radiant intensity (point sources) or radiance (extended sources). Radiant intensity and radiance exist at the source and cannot be remotely measured. Radiation propagates away from the source and is measured at a distant point. The resulting radiant flux density at a remote point is described by an irradiance value. Irradiance is a remotely measurable quantity. Characteristic source radiation must be derived from a measurement of irradiance. The qualifying term *apparent* is used to indicate radiant intensity and radiance attenuated by the intervening atmosphere between the source and the remote point of measurement. The quantities are in general functions of wavelengths. If the spectral nature of the quantity is under consideration, the term spectral is used to alter the name and the symbol (λ) or (σ) is added to the symbol. For example spectral radiance, $L(\lambda)$ or $L(\sigma)$, is defined to be radiance per unit wavelength or per unit wavenumber

$$L(\lambda) = \frac{dL}{d\lambda}, \quad L(\sigma) = \frac{dL}{d\sigma} \qquad \text{(Eq. 2-2)}$$

with typical non-coherent units W/(cm^2 sr μm), or W/(cm^2 sr nm) and W/(cm^2 sr cm^{-1}), respectively. The spectrally integrated quantity from wavelength λ_1 to wavelength λ_2 (wavenumber σ_1 to wavenumber σ_2) yields the total radiance within the spectral band λ_1 to λ_2 (σ_1 to σ_2). Total radiance is the second quantity listed in Table 2-6 and is derived from the integral shown in Equation 2-3.

$$L = \int_{\lambda_1}^{\lambda_2} L(\lambda)\mathrm{d}\lambda, \quad L = \int_{\sigma_1}^{\sigma_2} L(\sigma)\mathrm{d}\sigma \qquad \text{(Eq. 2-3)}$$

Figure 2-5 and Figure 2-6 illustrate the concepts of FOV defined by the field stop of the optical system and the solid angle defined by the aperture stop which controls the amount of

irradiance from each point on the source. The figures show simplistic conceptual drawings of an optical system. The field stop is shown as the physical extent of the detector, such as a film plate. The aperture stop is shown as an iris immediately after the collection lens. In reality, optical systems are much more complex, but the concepts are the same. The image of the field stop as seen by the source defines the FOV. In an ideal optical system, no radiation outside of the FOV will be detected. The aperture stop defines the solid angle ω through which radiation flows to the detector. The aperture stop, such as an iris in front of or behind the collection optic, controls the size of the detector area which the irradiance falls on, and therefore controls the amount of irradiance from each point on the source that passes to the detector.

TABLE 2-6. BASIC RADIOMETRIC QUANTITIES, SYMBOLS, AND UNITS

Derived Quantity		SI Coherent Derived Unit				SI Non-coherent Derived Unit [3]	
Name	**Symbol** [1, 2]	**Name** [2]	**Unit Symbol** [2]	**In Terms of Other SI Units**	**In Terms of SI Base Units**	**Name**	**Unit Symbol**
Irradiance	*E*	watt per square meter	W/m^2	$J/(m^2 \cdot s)$	$kg\ s^{-3}$	watt per square centimeter	W/cm^2
Radiance	*L*	watt per square meter steradian	$W/(m^2 \cdot sr)$	$J/(m^2 \cdot s \cdot sr)$	$kg\ s^{-3}\ sr^{-1}$	watt per square centimeter steradian	$W/(cm^2 \cdot sr)$
Radiant energy	*Q*	joule	J		$kg\ m^2\ s^{-2}$	joule or electronvolt	J or eV
Radiant exitance	*M*	watt per square meter	W/m^2	$J/(m^2 \cdot s)$	$kg\ s^{-3}$	watt per square centimeter	W/cm^2
Radiant flux, also called radiant power	*Φ, P*	watt	W	J/s	$kg\ m^2\ s^{-3}$	watt	W
Radiant intensity	*I*	watt per steradian	W/sr	$J/(s \cdot sr)$	$kg\ m^2\ s^{-3}\ sr^{-1}$	watt per steradian	W/sr
Spectral absorptance [4]	$a(\lambda)$	one, (I_a / I_0) [4]	1			one	1
Spectral emissivity [5]	$\varepsilon(\lambda)$	one, (M/M_{BB}) [5]	1			one	1
Spectral irradiance [3]	$E(\lambda)$	watt per square meter wavelength	$W/(m^2 \cdot m)$	$J/(m^2 \cdot s \cdot m)$	$kg\ s^{-3}\ m^{-1}$	watt per square centimeter micrometer watt per square centimeter nanometer	$W/(cm^2 \cdot \mu m)$ $W/(cm^2 \cdot nm)$
Spectral radiance [3]	$L(\lambda)$	watt per square meter steradian wavelength	$W/(m^2 \cdot sr \cdot m)$	$J/(m^2 \cdot s \cdot sr \cdot m)$	$kg\ s^{-3}\ sr^{-1} m^{-1}$	watt per square centimeter steradian micrometer watt per square centimeter steradian nanometer	$W/(cm^2 \cdot sr \cdot \mu m)$ $W/(cm^2 \cdot sr \cdot nm)$
Spectral radiant energy	$Q(\lambda)$	joule per wavelength	J/m		$kg\ m\ s^{-2}$	joule or electronvolt per micrometer joule or electronvolt per nanometer	J/μm, eV/μm J/nm, eV/nm

TABLE 2-6 (CONCLUDED)

Derived Quantity		SI Coherent Derived Unit				SI Non-coherent Derived Unit [3]	
Name	**Symbol** [1, 2]	**Name** [2]	**Unit Symbol** [2]	**In Terms of Other SI Units**	**In Terms of SI Base Units**	**Name**	**Unit Symbol**
Spectral radiant exitance	$M(\lambda)$	watt per square meter wavelength	$W/(m^3)$	$J/(m^3 \cdot s)$	$kg\ m^{-1}\ s^{-3}$	watt per square centimeter micron watt per square centimeter nanometer	$W/(cm^2 \cdot \mu m)$ $W/(cm^2 \cdot nm)$
Spectral radiant flux, also called spectral radiant power	$\Phi(\lambda)$, $P(\lambda)$	watt per wavelength	W/m	$J/(m \cdot s)$	$kg\ m\ s^{-3}$	watt per micrometer watt per nanometer	W/µm W/nm
Spectral radiant intensity [3]	$I(\lambda)$	watt per steradian wavelength	$W/(sr \cdot m)$	$J/(s \cdot sr \cdot m)$	$kg\ m\ s^{-3}\ sr^{-1}$	watt per steradian micrometer watt per steradian nanometer	$W/(sr \cdot \mu m)$ $W/(sr \cdot nm)$
Spectral reflectance [5]	$r(\lambda)$	one, (I_r / I_0) [5]	1			one	1
Spectral transmittance [5]	$\tau(\lambda)$	one, (I_τ / I_0) [5]	1			one	1
Wavelength	λ	meter	m		m	micrometer, nanometer	µm, nm
Wavenumber	σ, $\tilde{\nu}$	reciprocal meter	m^{-1}		m^{-1}	reciprocal centimeter	cm^{-1}

[1] Recommended symbols: Symbols that appear in older documents are U for radiant energy, W for radiant exitance, N for radiance, J for radiant intensity, H for irradiance.
[2] Spectral quantities are shown with wavelength as the independent variable but wavenumber is often used.
[3] Non-coherent units are commonly used by the EO community because they are descriptive of the physical system and to avoid the use of very small or very large numeric values.
[4] Ratio of the object radiance exitance to the radiance exitance of a blackbody at the same temperature.
[5] Ratio of reflected, transmitted, or absorbed radiant intensity (subscripts r, τ, or a) to the incident radiant intensity (subscript 0).

TABLE 2-7. BASIC RADIOMETRIC QUANTITIES, SYMBOLS, AND UNITS FOR PHOTON QUANTA-RATE EMITTED OR RECEIVED

Derived Quantity		SI Coherent Derived Unit		SI Non-Coherent Derived Unit [2]	
Name	**Symbol [1]**	**Name [1]**	**Unit Symbol [1]**	**Name**	**Unit Symbol**
Photon exitance	M_p	rate per square meter	$1/(s \cdot m^2)$	rate per square centimeter	$1/(s \cdot cm^2)$
Photon flux	Φ_p, P_p	rate	1/s	rate	1/s
Photon irradiance	E_p	rate per square meter	$1/(s \cdot m^2)$	rate per square centimeter	$1/(s \cdot cm^2)$
Photon intensity	I_p	rate per steradian	$1/(s \cdot sr)$	rate per steradian	$1/(s \cdot sr)$
Photon radiance	L_p	rate per square meter steradian	$1/(s \cdot m^2 \cdot sr)$	rate per square centimeter steradian	$1/(s \cdot cm^2 \cdot sr)$
Spectral photon exitance	$M_p(\lambda)$	rate per square meter wavelength	$1/(s \cdot m^3)$	rate per square centimeter micrometer rate per square centimeter nanometer	$1/(s \cdot cm^2 \cdot \mu m)$ $1/(s \cdot cm^2 \cdot nm)$
Spectral photon flux	$\Phi_p(\lambda)$, $P_p(\lambda)$	rate	1/s	rate	1/s
Spectral photon irradiance	$E_p(\lambda)$	rate per square meter wavelength	$1/(s \cdot m^2 \cdot m)$	rate per square centimeter micrometer rate per square centimeter nanometer	$1/(s \cdot cm^2 \cdot \mu m)$ $1/(s \cdot cm^2 \cdot nm)$
Spectral photon radiance	$L_p(\lambda)$	rate per square meter steradian wavelength	$1/(s \cdot m^2 \cdot sr \cdot m)$	rate per square centimeter steradian micrometer rate per square centimeter steradian nanometer	$1/(s \cdot cm^2 \cdot sr \cdot \mu m)$ $1/(s \cdot cm^2 \cdot sr \cdot nm)$

[1] Spectral quantities are shown with wavelength as the independent variable but wavenumber is often used.

[2] Non-coherent units are commonly used by the EO community because they are descriptive of the physical system and to avoid the use of very small or very large numeric values.

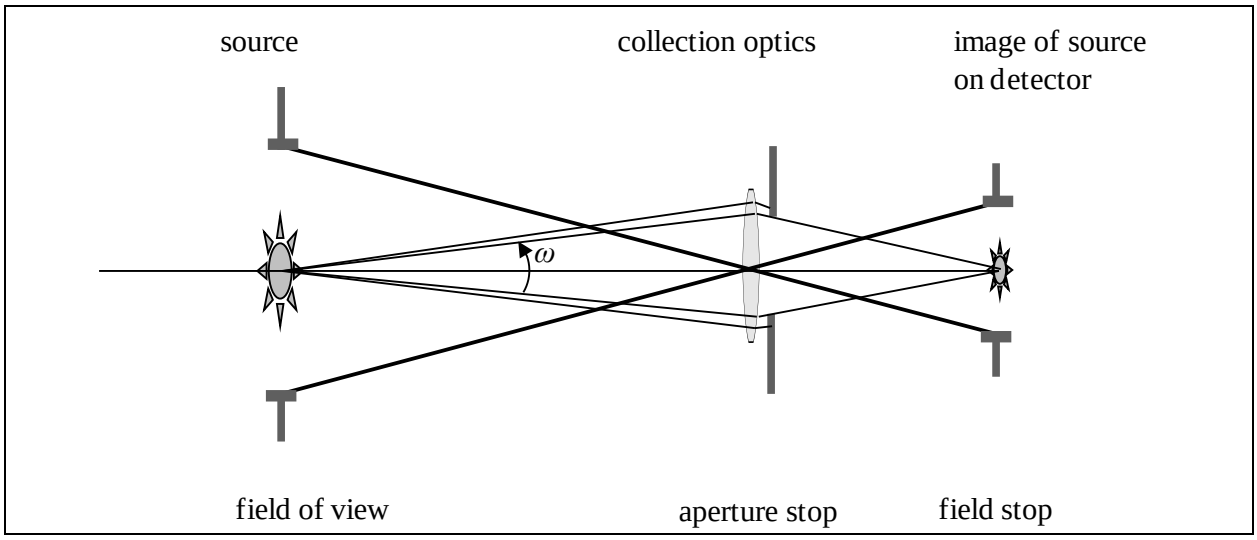

Figure 2-5. Optical system with an FOV larger than the source.

Note: The above configuration would be used to calibrate for irradiance for a determination of radiant intensity.

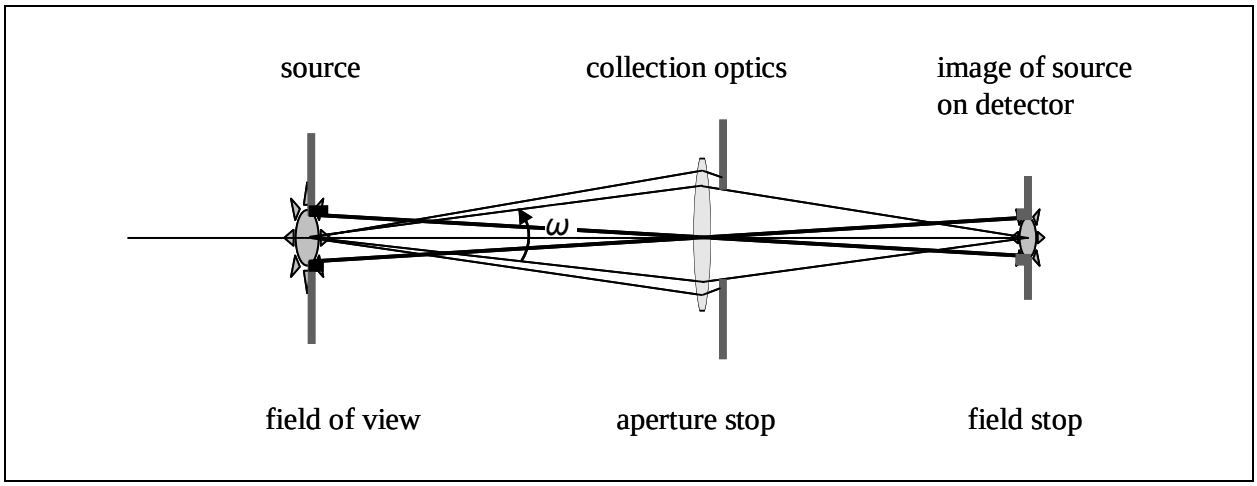

Figure 2-6. Optical system with an FOV smaller than the source.

Note: The above configuration would be used to calibrate a sensor for a determination of radiance.

2.3.1 Radiant Flux $\Phi(\lambda)$ and Radiant Energy $Q(\lambda)$. A significant property of an electromagnetic wave is that it transports energy. The energy flow is in the direction of the wave propagation. The time rate of energy flow is the radiant flux, $\Phi(\lambda)$, in SI units of watt per wavelength. Radiant energy is calculated by integrating radiant flux with respect to time. A time integral is a basic requirement in measuring optical radiation because the high frequencies (10^{14} Hz to 10^{15} Hz) make it impractical to consider measuring a radiometric quantity at any one point in time.

$$Q(\lambda) = \int_{t_1}^{t_2} \Phi(\lambda)\, dt \qquad \text{(Eq. 2-4)}$$

The defining equation of spectral radiant flux is the differential version of Equation 2-4 found in Equation 2-5.

$$\Phi(\lambda) = \frac{dQ(\lambda)}{dt} \qquad \text{(Eq. 2-5)}$$

By Equation 2-4, the output of an integrating detector is a function of the radiant energy transferred during the integration time. The detector is considered a non-integrating detector if it has a short time constant such that (t_2-t_1) can be made small. A non-integrating detector can be used to measure the time varying radiant flux with temporal precision limited to $\Delta t=(t_n-t_{n-1})$. As an application of Equation 2-4, consider the power of a high *power* laser compared to the continuous power of a high energy laser. Radiant flux is commonly used to state the peak power of short pulse lasers and to describe the output of continuous wave (CW) lasers. The peak power of a high power laser is specified in megawatt (MW) units and a high energy CW laser is specified as having an average power also in units MW. It is important to distinguish the specification between a high power laser and a high energy laser. For example, a high power pulsed laser with a 100 MW peak power but a short 10 nanosecond (ns) pulse length and pulse frequency of 10 Hz would have an average power of only 10 W. While each pulse has a high peak power, the laser is not a high energy laser.

2.3.2 Radiant Exitance $M(\lambda)$ and Radiant Irradiance $E(\lambda)$. The time rate of flow of radiant energy is radiant flux. If we divide the radiant flux incident on or exiting a surface by the area of the surface we have radiant flux density in units W/(cm^2 μm), where other commonly used versions of non-coherent units use nm or cm^{-1} for the wavelength unit in the denominator. By convention, radiant flux density exiting a surface is called exitance, and radiant flux density incident on a surface it is called irradiance. Each case is a measure of the time averaged rate of energy flow across a surface. Again, the concept of a time average is required because it is impractical to consider measuring the high frequency optical wave at any single point in time.

Exitance radiates from a surface into a hemisphere. The radiation might originate from a reflection or from the surface itself. Either way, it is defined as exitance since the radiation radiates from the surface. Figure 2-7 illustrates two types of exitance (specular and diffuse), where $\hat{n}$ is the unit vector which is normal to the surface and the exitance is a function of the angle θ. Exitance does not in general irradiate the surface of the hemisphere equally at all angles. This is obvious for a specular surface but also true for a diffuse surface. The total power

radiates into the solid angle 2π sr of the hemisphere but the points on the hemisphere are not necessarily radiated uniformly. The variation with angle θ is a measured property of the surface. If the variation is zero for all angles except for a very narrow range of angles around a single angle, the surface is considered specular. If the variation is non-zero for most angles, then the surface is considered diffuse. Matte paint and etched glass are examples of diffuse surfaces. A special type of diffuse surface is a Lambertian surface. Lambert's Cosine Law (after Johann Heinrich Lambert, 1728-1777) states that a surface is Lambertian if its intensity is proportional to the cosine of the angle between the surface normal and the line of sight, $I(\theta, \lambda)=I(\lambda)\cos(\theta)$. A Lambertian surface would also have the property that its exitance is proportional to the cosine of the angle between the surface normal and the line of sight, $M(\theta, \lambda)=M(\lambda)\cos(\theta)$. It will be shown in paragraph 2.3.3 this proportionality comes from the property of a Lambertian surface that the radiance is constant with viewing angle.

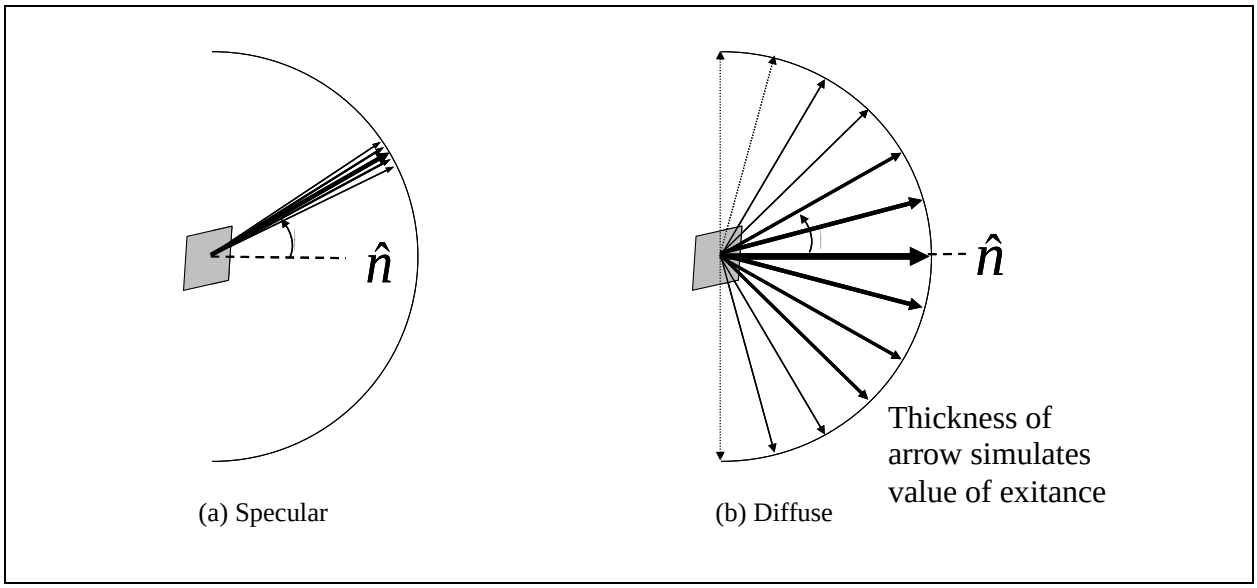

Figure 2-7. Exitance radiating into a hemisphere from an infinitesimal surface area.

Irradiance is the radiant flux density (radiant power) incident on a surface. Irradiance is special in that it is the only observable radiometric quantity at a distant point. Other radiometric quantities characterizing a source are derived from a measurement of irradiance. Irradiance is produced by source radiance $L(\lambda)$ or source radiant intensity $I(\lambda)$ at a remote point and is therefore modified by atmospheric path transmission $\tau(\lambda)$. The irradiance at a remote point has a spectral distribution $E(\lambda)$ that is the product of the source spectral emission and the atmospheric spectral attenuation. The spectral irradiance $E(\lambda)$ due to a source describable by spectral radiant intensity $I(\lambda)$ is given by Equation 2-6. The spectral irradiance $E(\lambda)$ due to a source describable by spectral radiance $L(\lambda)$ is given by Equation 2-7:

Point source, $$E(\lambda) = \frac{I(\lambda)\,\tau(\lambda)}{R^2} = \frac{I'(\lambda)}{R^2}$$ (Eq. 2-6)

Extended source, $$E(\lambda) = L(\lambda)\tau(\lambda)\omega_s = L'(\lambda)\omega_s$$ (Eq. 2-7)

Where

$\tau(\lambda) \leq 1.0$	is the atmospheric spectral transmission
R	is the distance between the source and the sensor
ω_s	is the solid angle subtended by the source area
$I'(\lambda) \equiv I(\lambda)\,\tau(\lambda)$	is defined to be apparent spectral radiant intensity
$L'(\lambda) \equiv L(\lambda)\,\tau(\lambda)$	is defined to be apparent spectral radiance

Note: The term "apparent" is used to qualify a quantity altered by the spectral attenuation of the atmosphere.

The apparent spectral radiant intensity or the apparent spectral radiance of a source is equal to or less than the actual value. A prime superscript is used to indicate an apparent value. Irradiance is due to the apparent radiant intensity or apparent radiance but is not itself an apparent value and therefore does not have a prime superscript.

a. Range-Squared Effect. It can be seen from Equation 2-6 that if the atmospheric transmission is unity, that is $\tau(\lambda)$=1.0, the irradiance is inversely proportional to the square of the range. Figure 2-8 illustrates the range-squared effect for point sources (and infinitesimal areas of larger sources). Because radiation emits into a hemisphere, the irradiance at area A_d decreases as range increases from the source because the solid angle decreases from ω_{d1} to ω_{d2} as range increases from R to xR. The rate of decrease is $(R/xR)^2$.

Caution must be made because this effect is not always true for every source shape; however, it is true for most sources. A rule of thumb is that the range must be greater than ten times the largest spatial dimension of the source for the range-squared effect to hold. The range-squared effect is used extensively in irradiance calibrations and is required to infer radiant intensity from an irradiance measurement of a target. The range-squared effect is a convenient tool to measure linearity of the detector response to irradiance levels; one can accurately increase or decrease the irradiance at the sensor by decreasing or increasing the range.

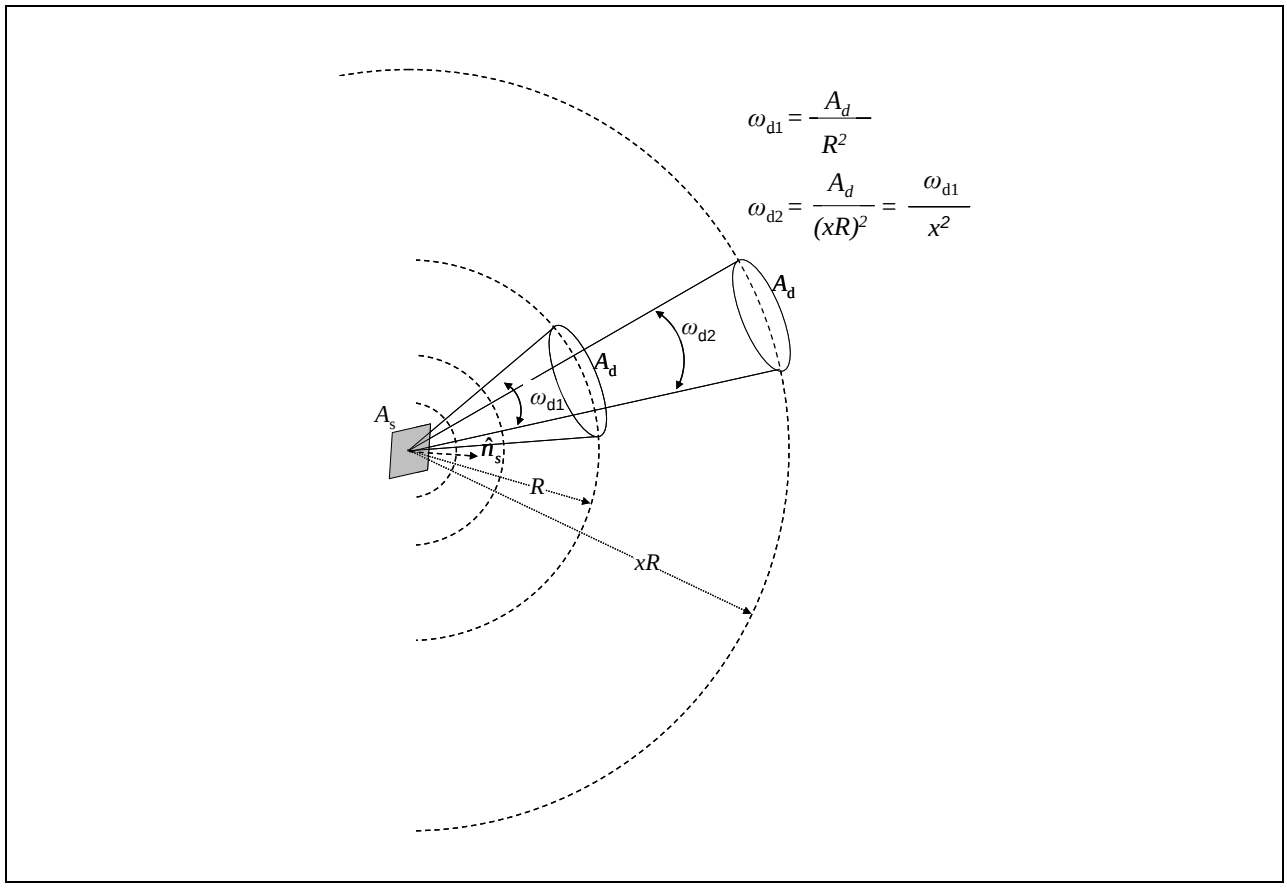

Figure 2-8. Range-squared effect for a point source or an infinitesimal area of a larger source.

b. Solid Angle. It is important to show why the solid angle ω_s in Equation 2-7 is the solid angle subtended by the source area and not the solid angle subtended by the detector. Using the approximation for solid angle described in Appendix C and referring to the geometry of Figure 2-9, we have

$$\omega_s \cong \frac{A_s}{R^2} \qquad \text{(Eq. 2-8a)}$$

$$\omega_d \cong \frac{A_d}{R^2} \qquad \text{(Eq. 2-8b)}$$

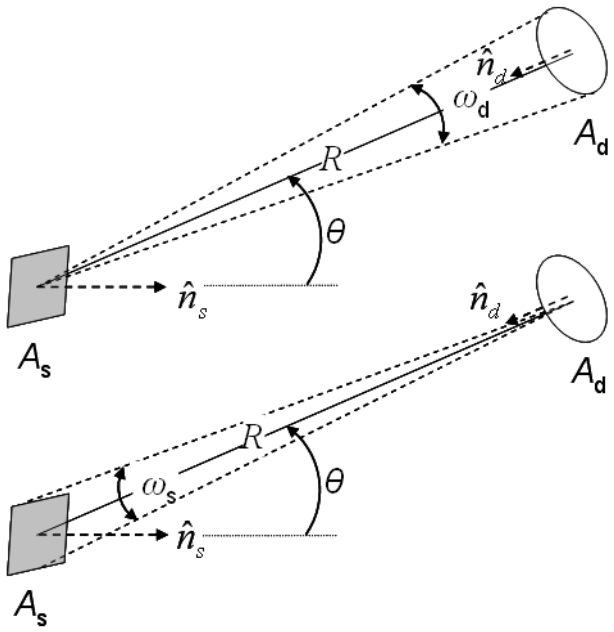

LEGEND

R	= distance between the source and the detector
A_s	= source area (can be an infinitesimal area)
A_d	= detector area (can be an infinitesimal area)
$\hat{n}_s$	= unit vector normal to the source surface
$\hat{n}_d$	= unit vector normal to the detector area
ω_s	= solid angle subtended by the source area
ω_d	= solid angle subtended by the detector area
θ	= angle between the unit vectors $\hat{n}_s$ and $\hat{n}_d$

Figure 2-9. Solid angles subtended by the detector area, ω_d, and subtended by the source area, ω_s.

The definition of radiance is power emitted per unit area perpendicular to the direction of travel into a unit solid angle. Considering the detector area to define the solid angle, we write the equation for radiance of surface S and use the approximations in Equation 2-8.

$$L(\lambda) = \frac{\Phi(\lambda)}{A_s \cos(\theta)\, \omega_d} = \frac{\Phi(\lambda)}{A_s \cos(\theta)\, \frac{A_d}{R^2}} = \frac{\Phi(\lambda)}{\frac{A_s}{R^2} \cos(\theta)\, A_d} = \frac{\Phi(\lambda)}{\omega_s A_d \cos(\theta)} \qquad \text{(Eq. 2-9)}$$

Now, the irradiance at the detector surface is defined to be the power per surface area perpendicular to the direction of travel and the spectral radiant flux from the

source is attenuated by the atmospheric transmission $\tau(\lambda)$. Therefore, the spectral irradiance at the detector from the source spectral radiance is

$$E(\lambda) = \frac{\Phi(\lambda)\tau(\lambda)}{A_d \cos(\theta)} \qquad \text{(Eq. 2-10)}$$

Substituting Equation 2-9 into Equation 2-10 we derive Equation 2-7, $E(\lambda) = L(\lambda)\omega_s\tau(\lambda) = L'(\lambda)\omega_s$, showing that the solid angle subtended by the surface area is a factor used to calculate irradiance from a radiance quantity.

A second derivation of Equation 2-7 is to consider the power at the detector from an infinitesimal area of the extended source. The power into a unit solid angle from an infinitesimal area is

$$\frac{\Phi(\lambda)}{\omega_d} = L(\lambda)\tau(\lambda)\,da$$

Using Equation 2-8a,

$$\frac{\Phi(\lambda)}{A_d} = \frac{1}{R^2} L(\lambda)\tau(\lambda)\,da \qquad \text{(Eq. 2-11)}$$

Recognizing that the left-hand side of the Equation 2-11 is the irradiance, integrating over the total area of the extended source, and using Equation 2-8b, we again derive Equation 2-7.

$$E(\lambda) = \frac{1}{R^2}\int_{A_s} L(\lambda)\tau(\lambda)\,da = L'(\lambda)\,\omega_s$$

It will be shown in paragraph 2.5.2 that when a sensor is calibrated for radiance against an extended radiance source, the solid angle is a constant of the calibration and it is not required to know what it is.

c. Effective Quantities. We now consider the spectral response of the observing system. Band measurement instruments such as radiometers and imagers have system spectral responses shaped by the spectral response of the detector and the spectral transmission of the optics including optical band pass filters. Band instruments must be calibrated in terms of effective irradiance or effective radiance. The qualifying term effective, indicated by a subscript e, is used to indicate a radiometric quantity within the spectral response of the observing system. Effective quantities are not spectral quantities and only have meaning within the spectral response of the observing system. Effective irradiance at the point of observation is the integral of spectral irradiance within limits λ_1 to λ_2 as shown in Equation 2-12 for irradiance attributable to source radiant intensity and Equation 2-13 for irradiance attributable to source radiance. The practical limits of

integration, λ_1 and λ_2, are the wavelengths at which the spectral response is zero beyond them. Equations 2-12b and 2-12d are alternate shorthand forms of Equation 2-12a. Equations 2-13b and 2-13d are alternate shorthand forms of Equation 2-13a.

Point source, $$E_e = \frac{1}{R^2}\int_{\lambda_1}^{\lambda_2} I(\lambda)\tau(\lambda)r(\lambda)d\lambda \quad \text{(Eq. 2-12a)}$$

$$E_e = \frac{1}{R^2}\int_{\lambda_1}^{\lambda_2} I'(\lambda)r(\lambda)d\lambda \quad \text{(Eq. 2-12b)}$$

Defining $$I'_e \equiv \int_{\lambda_1}^{\lambda_2} I'(\lambda)r(\lambda)d\lambda \quad \text{(Eq. 2-12c)}$$

$$E_e = \frac{I'_e}{R^2} \quad \text{(Eq. 2-12d)}$$

Extended source, $$E_e = \omega_s\int_{\lambda_1}^{\lambda_2} L(\lambda)\tau(\lambda)r(\lambda)d\lambda \quad \text{(Eq. 2-13a)}$$

$$E_e = \omega_s\int_{\lambda_1}^{\lambda_2} L'(\lambda)r(\lambda)d\lambda \quad \text{(Eq. 2-13b)}$$

Defining $$L'_e \equiv \int_{\lambda_1}^{\lambda_2} L'(\lambda)r(\lambda)d\lambda \quad \text{(Eq. 2-13c)}$$

$$E_e = \omega_s L_e' \quad \text{(Eq. 2-13d)}$$

Where

R	= the distance between the source and the sensor
ω_s	= the solid angle defined by the FOV of the observing system
$r(\lambda)$	= the spectral response of the observing system
$I'(\lambda) \equiv I(\lambda)\,\tau(\lambda)$	= defined to be apparent spectral radiant intensity
I'_e	= defined to be the apparent effective radiant intensity
$L'(\lambda) \equiv L(\lambda)\,\tau(\lambda)$	= defined to be apparent spectral radiance
L'_e	= defined to be the apparent effective radiance

Not all of the irradiance arriving at remote points is due to a source of interest. Additional irradiance can be due to background and foreground radiation or energy scattered toward the observation point. The signal from this additional irradiance must be removed from the measured data in order to obtain accurate source signature data. If the signal cannot be removed, the additional sources must be understood and documented so that data taken under different conditions can be compared. This is a complicated process since observable effective irradiance from real-world targets varies with spectral band, range effecting target size within the FOV, range effecting atmospheric transmission path, and target aspect angle.

2.3.3 Radiant Intensity $I(\lambda)$. The spectral radiant intensity, $I(\lambda)$, in units W/(sr μm), where other commonly used versions of non-coherent units use nm or cm^{-1} as the wavelength unit in the denominator, describes the radiation from a point source. Radiant intensity is defined as the power (energy per time) emitted from a point source in a certain direction into a unit solid angle.

Radiant intensity is used to characterize a source that is small compared to the viewing distance such that it can be considered a point source. In a more practical sense, it is used to characterize a source that underfills the sensor FOV as illustrated in Figure 2-10. Radiant intensity is measured with non-imaging radiometric sensors such as radiometers and spectrometers with large, single fields of view. A focal plane array imager can be configured with a short focal length telescope that highly magnifies the image of the focal plane array at the source. If the images of the individual array elements at the target can be made large then the small source will underfill the individual array elements and a radiant intensity measurement is made. This non-traditional use of an imager is often made when the target is small and its location has a high degree of uncertainty. The array of fields of view imaged at the target plane increase the probability of capturing the target, while each FOV is not so large that the measurement is saturated with background emissions. Considering that modern focal plane imagers have scan rates approaching 1 kHz and that software offers the capability to electronically tie neighboring elements together to customize the FOV matrix, it is feasible that imagers will begin to replace single detector radiometers as data collection instruments.

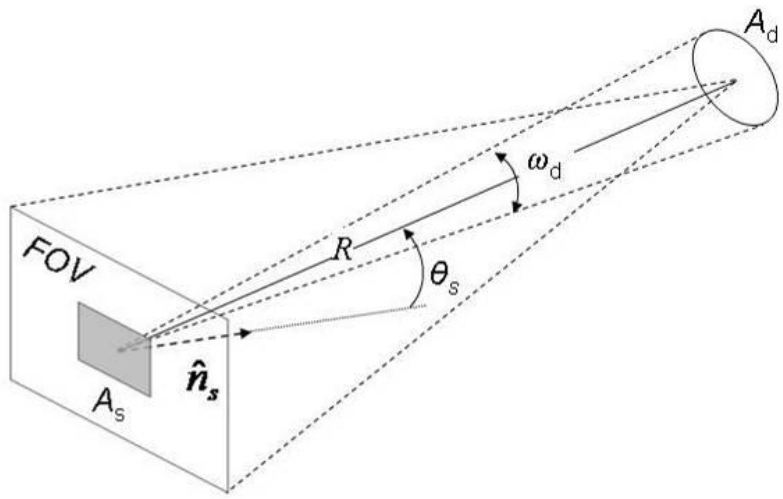

LEGEND

A_s = the total area of the small source
θ_s = the angle between the normal to the surface and the line of sight
ω_d = the solid angle defined by the detector collection optics, $=A_d/R^2$
R = the range between the emitting surface and the detector
A_d = the projected area of the clear aperture of the optics along the line of sight

Figure 2-10. Optical system to characterize radiant intensity generalized to illustrate projected area.

The defining equation for radiant intensity in differential form is

$$I(\lambda) = \frac{d\Phi(\lambda)}{d\omega_d} \qquad \text{(Eq. 2-14)}$$

The differential $d\Phi(\lambda)$ indicates the power received by the detector is differential with respect to the projected solid angle subtended by the detector. This is intuitive if you consider the power at the detector would increase if the detector size increased (collecting more photons). The size of the source is not a factor as long as the entire size is contained within the FOV.

For an arbitrary surface, radiant intensity can vary in a complicated way with viewing angle. The radiant intensity as a function of viewing angle is an experimentally determined property of a surface. Special types of emitting surfaces are diffuse, spectral, and Lambertian. A spectral surface has radiant intensity equal to zero for all viewing angles except for a very narrow range of angles around the specular angle. A diffuse surface has non-zero radiant intensity for all (or most) viewing angles. A Lambertian surface is a subset of a diffuse surface that has constant radiance for all viewing angles. It will be shown in paragraph 2.3.4, (Equation 2-26) that the condition of constant radiance with angle leads to the property that the radiant intensity

of a Lambertian surface is proportional to the cosine of the viewing angle, $I(\lambda) = I_0(\lambda)\cos(\theta)$. This property is known as Lambert's Cosine Law. Blackbody surfaces and exit ports of integrating spheres are Lambertian; however, filament and arc lamps are not.

Radiant intensity describes the angular radiation from a source. Radiant intensity is not directly observable at a remote point but must be inferred from an irradiance measurement at the remote point. A measurement instrument is calibrated in terms of effective irradiance where apparent effective radiant intensity is inferred from the measurement. The calibration process requires that the calibration path spectral attenuation is known and applied to the calibration source spectral distribution; this requirement is because the instrument responds to the effective irradiance that actually exists at the instrument. When the radiometer is calibrated in terms of effective irradiance, the measurement of a source will result in effective irradiance or apparent effective radiant intensity, apparent since the irradiance at the sensor has been reduced by atmospheric attenuation, effective since the sensor must be calibrated in terms of effective quantities. The effective radiant intensity of a source can be determined from measured apparent effective radiant intensity by numerically removing the atmospheric effects. The process is discussed in paragraph 2.6 and in detail in the RCC SMSG report, Weather and Atmospheric Effects on the Measurement and use of Electro-Optical Signature Data to be published later.

Radiant intensity measurement systems are calibrated for irradiance units using a small blackbody, an integrating sphere with a small aperture, or a standard lamp with a small emitting filament or small arc point. Figure 2-11 shows the concept of a non-imaging radiometer being calibrated against the irradiance from a standard 1000 W quartz halogen FEL (2-post) lamp. The irradiance calibration supplied with the lamp will be for a specific geometry, usually with the line of sight perpendicular to the vertical axis of the coil and perpendicular to the flat front of the base.

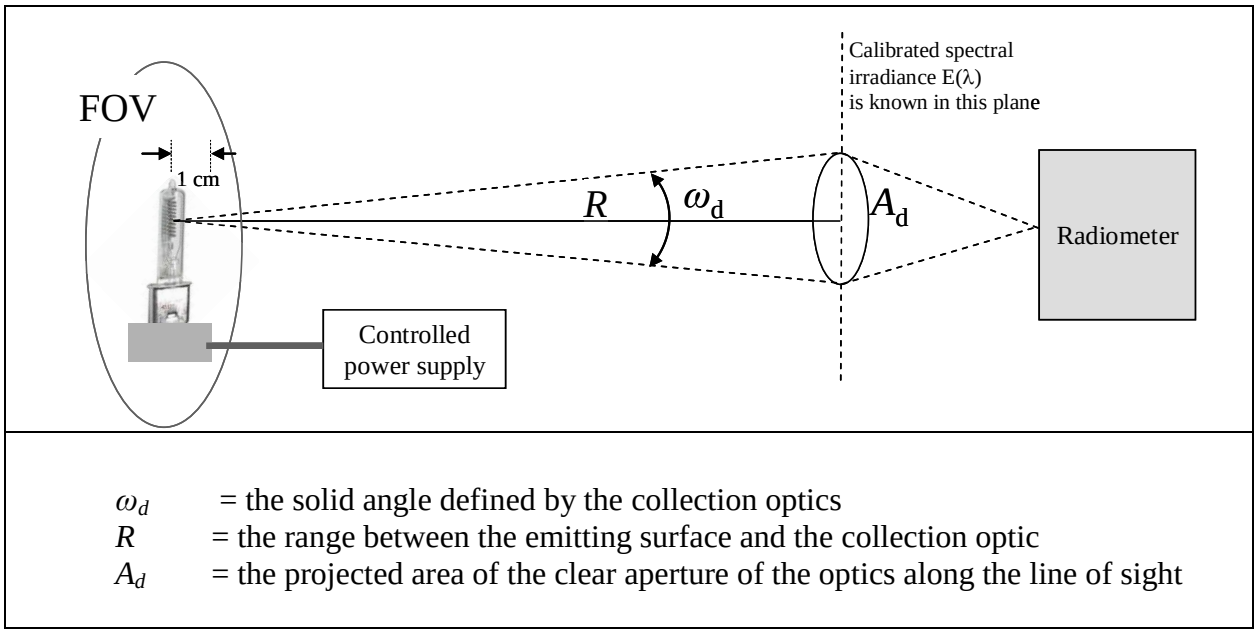

ω_d = the solid angle defined by the collection optics
R = the range between the emitting surface and the collection optic
A_d = the projected area of the clear aperture of the optics along the line of sight

Figure 2-11. Non-imaging radiometer calibrated for irradiance against a small FEL lamp.

The spectral irradiance of an FEL lamp is usually specified at a distance of 50 cm from the lamp base. Because the filament coil is about 1 cm behind the face of the base, the irradiance is actually specified at a distance of 51 cm from the coil. The effective spectral irradiance at a calibration distance of *R* cm is

$$E(\lambda) = E_{cal}(\lambda)\left(\frac{51}{R}\right)^2 \tau(\lambda) \qquad \text{(Eq. 2-15)}$$

Where

$E_{cal}(\lambda)$ = the irradiance calibration supplied with the lamp
R = the range in centimeters
$\tau(\lambda)$ = the atmospheric spectral transmission of path *R*.

The range-squared effect is a convenient tool to measure linearity of the detector response to irradiance levels; one can accurately increase or decrease the irradiance at the sensor by decreasing or increasing the range. For a band instrument, the effective irradiance considers the spectral response of the sensor $r(\lambda)$. For this example, the effective irradiance at calibration distance *R* is

$$E_e = \left(\frac{51}{R}\right)^2 \int_{\lambda_1}^{\lambda_2} E_{cal}(\lambda)\, \tau(\lambda)\, r(\lambda)\, d\lambda\,, \qquad \text{(Eq. 2-16)}$$

Where $r(\lambda)$ is zero beyond the practical limits of integration λ_1 *and* λ_2.

We now consider a calibration against the irradiance originating from the radiant intensity of a blackbody source. The concept of an irradiance calibration against a blackbody is illustrated in Figure 2-12. The same concept can be used for calibration against the output port of an integrating sphere.

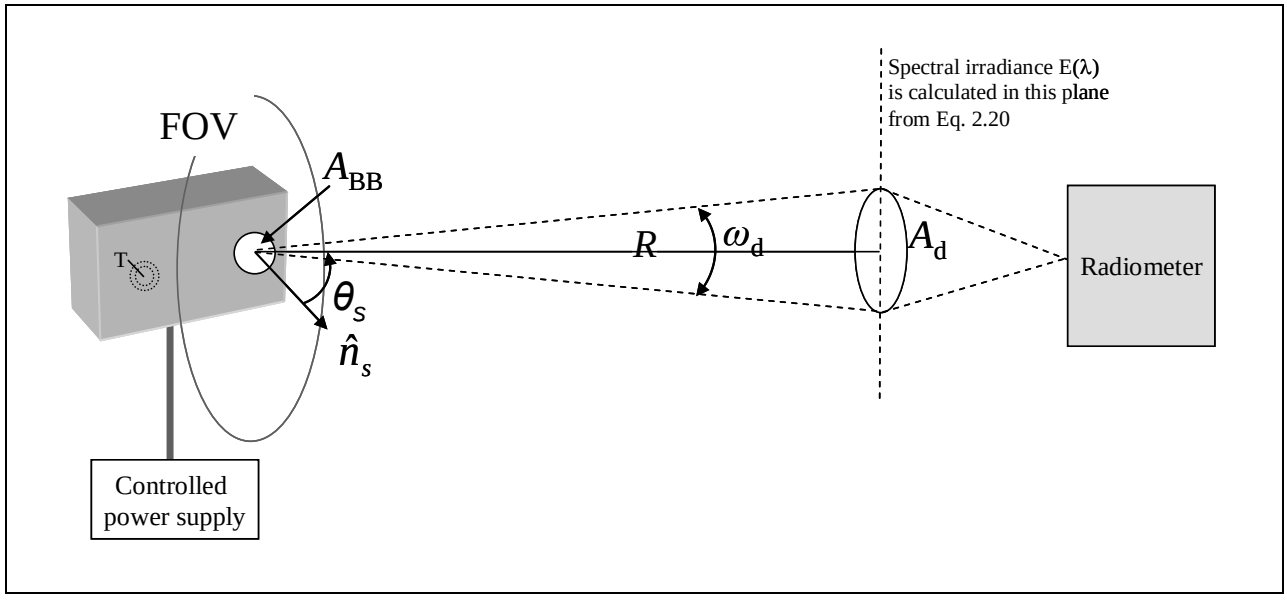

LEGEND

A_{BB}	=	the area of the exit port
θ_s	=	the angle between the normal to the port and the line of sight
ω_d	=	the solid angle defined by the collection optics, $=A_d/R^2$
R	=	the range between the port and the collection optics
A_d	=	the projected area of the clear aperture of the optics along the line of sight
$\hat{n}_s$	=	the unit vector normal to the source surface

Figure 2-12. Non-imaging radiometer calibrated for irradiance against a small blackbody.

Planck's blackbody function gives the radiance of the exit port of a blackbody at temperature T as

$$L_{BB}(\lambda,T) = \frac{2hc^2}{\lambda^5}\frac{1}{e^{\frac{hc}{\lambda kT}}-1} \qquad \text{(Eq. 2-17)}$$

Where

h	=	Planck's constant, $6.626\,069 \times 10^{-34}$ J s
c	=	the speed of light, $2.997\,924\,58 \times 10^{8}$ m s^{-1}
k	=	Boltzman's constant, $1.380\,650\,4 \times 10^{-23}$ J K^{-1}
T	=	the temperature in units Kelvin
e	=	the base of the natural logarithm = 2.718 281

The radiant intensity of the total area of the exit port is

$$I_{BB}(\lambda,T) = \int_{A_{BB}} L_{BB}(\lambda,T)\cos(\theta)\, da \qquad \text{(Eq. 2-18)}$$

Where

The factor $cos(\theta)$ is included to consider the projected area if the blackbody face is not perpendicular to the line of sight. Since the radiance of a good blackbody is uniform across the face of the port, the radiant intensity is more simply the radiance multiplied by the area of the port.

$$I_{BB}(\lambda,T) = L_{BB}(\lambda,T)\, A_{BB}\cos(\theta) \qquad \text{(Eq. 2-19)}$$

The spectral irradiance arriving at the sensor is then

$$E(\lambda) = \frac{I_{BB}(\lambda,T)\,\tau(\lambda)}{R^2} = \frac{L_{BB}(\lambda,T)\, A_{BB}\cos(\theta)\,\tau(\lambda)}{R^2} \qquad \text{(Eq. 2-20)}$$

Note that varying the exit port area A_{BB} is a convenient tool to measure the linearity of detector response with irradiance level. The irradiance level can be increased or decreased by increasing or decreasing A_{BB}.

By Equation 2-12, and using Equation 2-19, the effective irradiance at range R originating from the radiant intensity of a small blackbody is

$$E_e = \frac{1}{R^2}\int_{\lambda} I_{BB}(\lambda,T)\,\tau(\lambda)\,r(\lambda)\,d\lambda = \frac{1}{R^2}\int_{\lambda} L_{BB}(\lambda,T)\,A_{BB}\,\cos(\theta)\,\tau(\lambda)\,r(\lambda)\,d\lambda \qquad \text{(Eq. 2-21)}$$

The effective spectral irradiance for an arbitrary target completely contained within the FOV of the sensor at range R was derived in Equation 2-12d, $E_e = I_v^{'}/R^2$. The effective apparent radiant intensity of the arbitrary target is inferred from the measured irradiance

$$I_e{}' = E_e\,R^2 \qquad \text{(Eq. 2-22)}$$

2.3.4 Radiance $L(\lambda)$. The spectral radiance, $L(\lambda)$, in units $W/(sr\ cm^2\ \mu m)$, where other commonly used versions of non-coherent units use nm or cm^{-1} as the wavelength unit in the denominator, describes the radiation from an extended surface. Radiance is special in that it is the most general quantity to measure the radiant distribution in space from a surface. Radiance is defined as the power (energy per time) emitted from a point per unit area perpendicular to the direction of travel into a unit solid angle.

Typically, modern radiance measurement systems are imaging systems using focal plane array (FPA) detectors. The systems are calibrated for radiance units using an extended source blackbody or an integrating sphere with a large aperture. Extended source blackbodies and integrating spheres with large apertures are convenient radiance standards since they are Lambertian, and radiance is not a function of viewing angle. They can also be made to have spatially constant exitance over the extended surface which, in other words, means they will be spatially uniform across the emitting area.

Radiance is used to characterize an extended source that has appreciable size compared to the square of the viewing distance. In a more practical sense, it is used to characterize a source that overfills the sensor FOV as illustrated in Figure 2-13. Radiance spatial distributions (images) are measured with imaging radiometers. An imaging radiometer can be configured with a single detector with the small FOV that is scanned across the field of regard or, more commonly, a focal plane array detector where each detector element is imaged at the source. Either method offers spatial resolution at the source and produces an image.

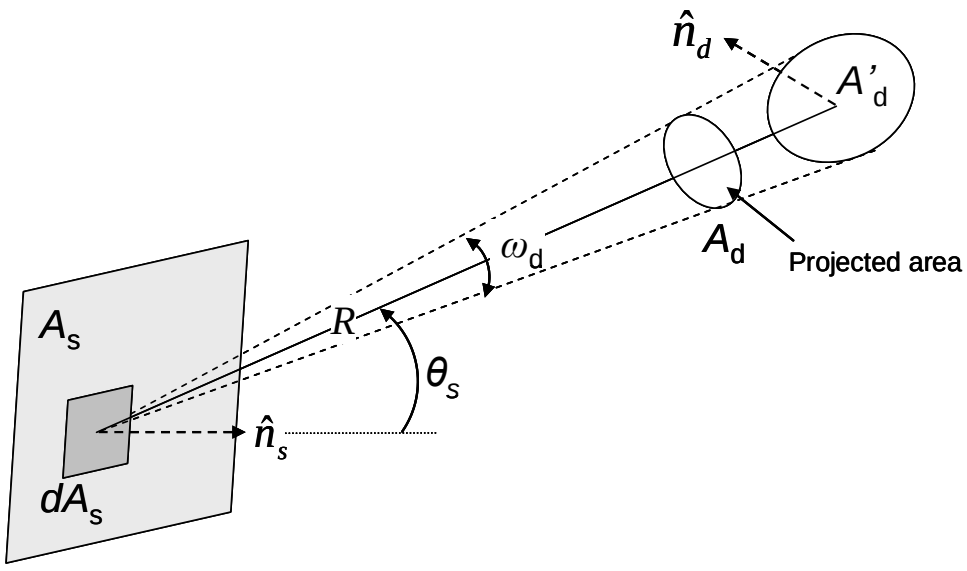

LEGEND

dA_s	=	the infinitesimal area of the source with total area A_s.
θ_s	=	the angle between the normal to the surface and the line of sight.
ω_d	=	the solid angle defined by the detector collection optics.
R	=	the range between the emitting surface and the detector.
A_d	=	the projected area of the detector (or clear aperture of the optics) along the line of sight.

Figure 2-13. Optical system to characterize radiance generalized to illustrate projected area.

Note that in Figure 2-13, to avoid over complicating the drawing, the area of the detector (or clear aperture of the optics) A_d is shown perpendicular to the line of sight. The face of the detector A'_d is tilted away from the line of sight such that A_d is the projected area along the line of sight. The approximation for the solid angle ω_d is $\omega_d = A'_d \cos(\theta_d)/R^2$ where θ_d is the angle between the normal to the detector face and the line of sight.

The defining equation for radiance in differential form is

$$L(\lambda) = \frac{d^2\Phi(\lambda)}{dA_s \cos\theta_s \; d\omega_d} \qquad \text{(Eq. 2-23)}$$

Where

Subscript s	=	reference to the source
Subscript d	=	reference to the detector
$\Phi(\lambda)$	=	the spectral radiant flux, watt per wavelength
dA_s	=	the infinitesimal area of the source with total area A_s
θ_s	=	the angle between the normal to the surface and the line of sight
ω_d	=	the solid angle defined by the detector collection optics

The second differential $d^2\Phi(\lambda)$ indicates the power received by the detector is differential with respect to the projected area of the source along the line of sight and the solid angle subtended by the detector. This observation is intuitive if you consider the power at the detector would increase if the size of the emitting source increases (producing more photons) or the detector size (solid angle) increases (collecting more photons).

Rearranging Equation 2-23 we can integrate independently with respect to the projected area or the solid angle to declare properties of the source from the radiance.

$$d^2\Phi(\lambda) = L(\lambda) dA_s \cos\theta_s \; d\omega_d \qquad \text{(Eq. 2-24)}$$

Integrating over the source surface area returns source intensity in units of watt per steradian.

$$\frac{d\Phi(\lambda)}{d\omega_d} = I(\lambda) = \int_{A_s} L(\lambda)\, dA_s \cos\theta_s \qquad \text{(Eq. 2-25)}$$

Integrating over the solid angle returns exitance in units of watt per area.

$$\frac{d\Phi(\lambda)}{dA_s} = M(\lambda) = \int_{\omega_d} L(\lambda) \cos\theta_s \; d\omega_d \qquad \text{(Eq. 2-26)}$$

For an arbitrary surface, radiance can vary in a complicated way with viewing angle. Special types of emitting surfaces are diffuse, spectral, and Lambertian. A Lambertian surface is a subset of a diffuse surface that has constant radiance for all viewing angles. A Lambertian surface is also called a perfectly diffuse surface. If we assume $L(\lambda)$ in Equation 2-25 is not a function of viewing angle θ_s it comes out of the integral and Equation 2-25 reduces to Lambert's Cosine Law.

$$I(\lambda) = I_0(\lambda) \cos(\theta_s) \qquad \text{(Eq. 2-27)}$$

Equation 2-26 can be reduced in the same manner for a Lambertian surface. If we assume $L(\lambda)$ is not a function of viewing angle θ_s it comes out of the integral and Equation 2-26 reduces to

$$M(\lambda) = M_0(\lambda)\cos(\theta_s) \qquad \text{(Eq. 2-28)}$$

The properties of a Lambertian surface are related in that they can be derived from each other; although most optics text books derive Lambert's Cosine Law (Equation 2-27) from the condition that $L(\lambda)$ is not a function of viewing angle. The three properties of a Lambertian surface are listed as follows:

a. Radiance is not a function of viewing angle. Therefore, a Lambertian surface is a desirable choice for calibrations since it removes a variable. The port of a blackbody source is Lambertian. For the UV/VIS/NIR regions, there are commercially available reflecting materials that are pressed into flat plates that are Lambertian for a very wide angular spread around the normal (on the order of ±60 degrees). The materials can also be coated on the interior of a sphere to create an integrating sphere whose output port is Lambertian.
b. The intensity is proportional to the cosine of the viewing angle; Equation 2-27 which is Lambert's Cosine Law.
c. The exitance is proportional to the cosine of the viewing angle, Equation 2-28.

Radiance describes the spatial radiation from a source and is not directly observable from a remote point. Radiance must be inferred from an irradiance measurement. Radiance from a source results in a measurable irradiance at remote points and a measurement instrument is calibrated in terms of either effective irradiance or apparent effective radiance. Either calibration process requires the calibration path spectral attenuation be known and applied to the calibration source spectral distribution, since the instrument responds to the effective irradiance that actually exists at the instrument. When each pixel of an imaging radiometer is calibrated in terms of apparent effective radiance or effective irradiance, the measurement of a source will result in apparent effective radiance or effective irradiance; apparent since the irradiance at the sensor has been reduced by atmospheric attenuation, effective since the sensor must be calibrated in terms of effective quantities. The effective radiance of a source can be determined from measured apparent effective radiance data by numerically removing the atmospheric effects. The process is discussed in the RCC SMSG report Weather and Atmospheric Effects on the Measurement and use of Electro-optical (EO) Signature Data to be published at a later date.

The spectral irradiance arriving at the radiometer from an extended source was previously given in Equation 2-7, $E(\lambda) = \omega_s L'(\lambda)$. The effective irradiance at the sensor from an extended source, $E_e = \omega_s L_e'$, was previously derived in Equation 2-13d, $E_e = \omega_s L_e'$.

It can be seen from Equation 2-7 and Equation 2-13d that if the atmospheric transmission is unity, that is $\tau(\lambda)$=1.0, the irradiance from an extended source of uniform radiance is independent of range. This phenomenon is caused by the fact that the FOV at the source increases at the same rate as the decrease in irradiance from each infinitesimal area of the source as range increases. To illustrate this we consider two cases, a rectangular FOV and a circular

FOV within an extended source and the range-squared effect previously illustrated in Figure 2-8. Figure 2-14 defines the geometry of Case 1, a rectangular FOV (Figure 2-14a) and Case 2, a circular FOV (Figure 2-14b).

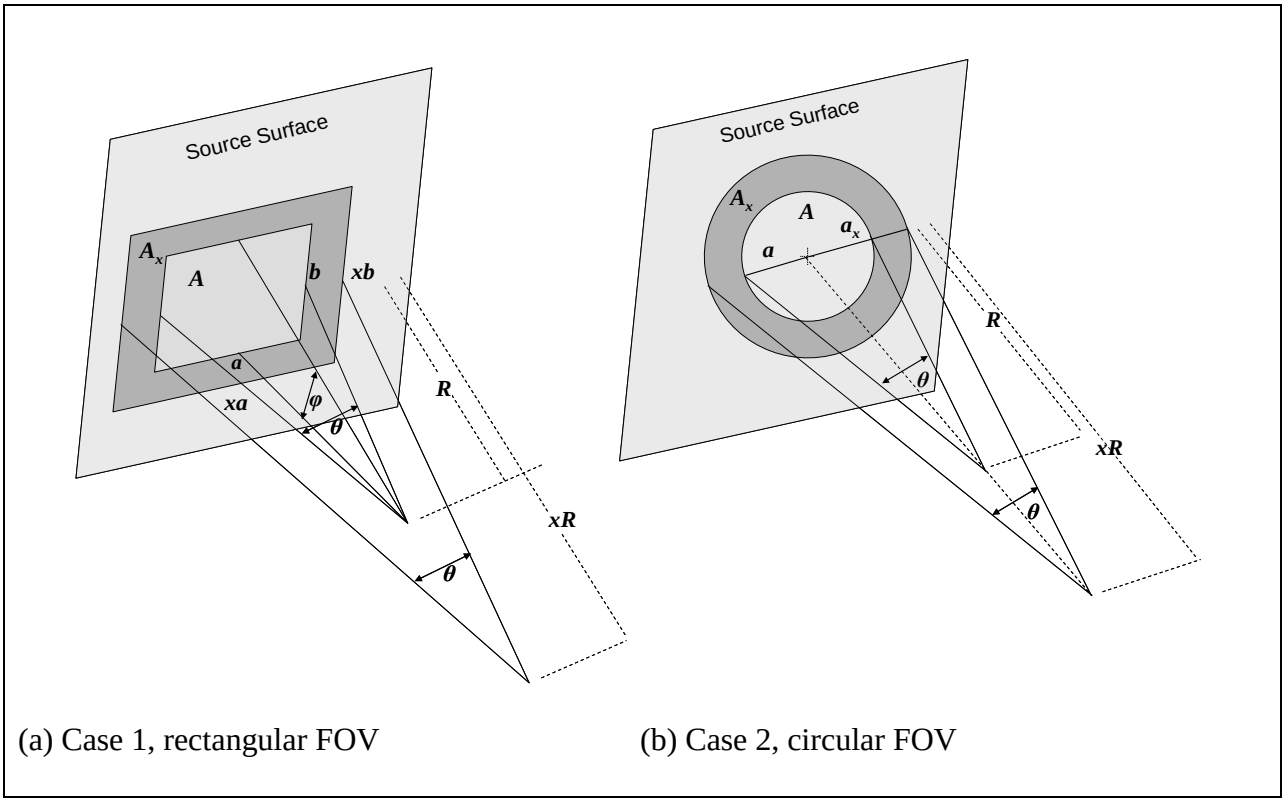

(a) Case 1, rectangular FOV (b) Case 2, circular FOV

Figure 2-14. Geometry for radiance measurements in Case 1 and Case 2.

Case 1. Consider that the irradiance at the sensor is the integral of irradiance contributions from infinitesimally small areas within a rectangular FOV at the source.

Given A rectangular FOV of *a* by *b* at range R in arbitrary units of length.
The horizontal angular FOV is θ in units radian.
The vertical FOV is φ in units radian.
Assume atmospheric transmission is unity (i.e. $\tau(\lambda) = 1.0$).

Then

$$a = 2R \tan(\theta/2)$$
$$b = 2R \tan(\varphi/2)$$
$$A = ab = 4R^2 \tan(\theta/2) \tan(\varphi/2)$$

If the range is increased to *xR*, then

$$a_x = 2xR \tan(\theta/2)$$
$$b_x = 2xR \tan(\varphi/2)$$
$$A_x = a_x b_x = 4x^2R^2 \tan(\theta/2) \tan(\varphi/2) = x^2A$$

Therefore, the integral over area A_x will include x^2 more infinitesimal portions of the source surface contributing to the irradiance at the sensor, exactly cancelling the decrease in irradiance from each infinitesimal area due to the range-squared effect. Atmospheric transmission $\tau(\lambda)<1.0$ would of course reduce the apparent radiance.

Case 2. Consider that the irradiance at the sensor is the integral of irradiance contributions from infinitesimally small areas within a circular FOV.

Given A circular FOV of radius a at range R in arbitrary units of length
The circular angular FOV is θ in units radian
Assume atmospheric transmission is unity, $\tau(\lambda)=1.0$

Then

$$a = 2R \tan(\theta/2)$$
$$A = \pi a = 4R^2 \tan^2(\theta/2)$$

If the range is increased to *xR*, then

$$a_x = 2xR \tan(\theta/2)$$
$$A_x = \pi a_x^2 = 4x^2R^2 \tan^2(\theta/2) = x^2A$$

Just as in Case 1, the integral over area A_x will include x^2 more infinitesimal portions of the source surface contributing to the irradiance at the sensor, exactly cancelling the decrease in irradiance from each infinitesimal area due to the range-squared effect. Atmospheric transmission $\tau(\lambda)<1.0$ would of course reduce the apparent radiance.

Although not shown, the previous analysis holds if the source surface is not perpendicular to the line of sight and the area is the projected source area. Note that if the source is not spatially uniform across the emitting area, the irradiance is a function of the average value within the field-of-view and may increase or decrease with range.

2.4 Summary of Radiometric Quantities

Table 2-8 summarizes radiometric spectral quantities.

TABLE 2-8. SUMMARY OF RADIOMETRIC SPECTRAL QUANTITIES

Name and units	Defined by:	Graphic	Comments
Spectral Exitance M(λ) W/(m^2 μm) W/(cm^2 μm)	power per area per wavelength	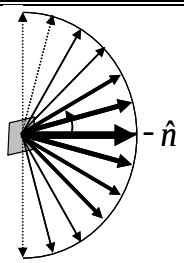	• By convention, power exiting a surface, divided by the surface area • Variation with viewing angle is a property of the surface • Surface is Lambertian if $M(\lambda) = M_0(\lambda)\cos(\theta)$
Spectral Irradiance E(λ) W/(m^2 μm) W/(cm^2 μm)	power per area per wavelength	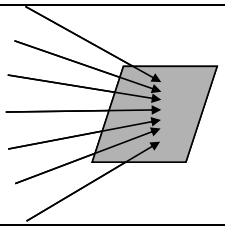	• By convention, power incident on a surface, divided by the surface area • The only measurable quantity
Spectral Radiant Intensity I(λ) W/(sr μm)	power per solid angle per wavelength	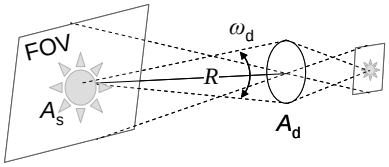	• Sensor has a large field of view (FOV) that encompasses the entire emitting surface • Irradiance at A_d due to source intensity is $E(\lambda) = I(\lambda)\,R^2\,\tau(\lambda)$ • Source is Lambertian if $I(\lambda) = I_0(\lambda)\cos(\theta)$ • Most sources follow range-squared relationship (for $\tau(\lambda)$=1.0) $E_{R_2}(\lambda) = E_{R_1}(\lambda)\left(\frac{R_1}{R_2}\right)^2$
Spectral Radiance L(λ) W/(sr m^2 μm) W/(sr cm^2 μm)	power per solid angle per area per wavelength	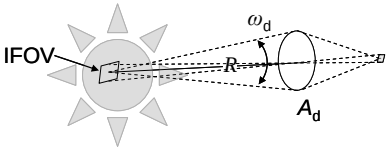	• The most general quantity • Irradiance due to source radiance $E(\lambda) = L(\lambda)\ \omega_s\ \tau(\lambda)$ • Surface is Lambertian if $L(\lambda)$ is constant with viewing angle • $E(\lambda)$ is constant with range as long as FOV is contained within uniform emitting surface area • If the sensor is calibrated against a radiance standard the factor ω_s is a constant of the calibration and does not have to be known

2.5 Radiometric Calibration Techniques

Spectral radiometers are calibrated in terms of either spectral irradiance E(λ) or spectral apparent radiance $L'(\lambda)$. Band radiometers are calibrated in terms of effective irradiance E_e or apparent effective radiance L'_e.

2.5.1 Irradiance Calibration. Calibration in terms of irradiance can be accomplished by several methods as described below.

a. Exposing the radiometer to a standard radiant intensity source such as the 1000 W FEL lamp in the set-up previously illustrated in Figure 2-11. The spectral irradiance at range *R* is given directly by Equation 2-6. The effective irradiance is given by Equation 2-12d. This is a simple set-up that requires minimal hardware. A linearity measurement with irradiance level can be made using the range-squared effect if the alignment in the FOV can be held as *R* is increased or decreased.

b. Exposing the radiometer to a standard radiance extended source directly behind a precision aperture with area A_a used to control the source area exposed to the radiometer. This concept was previously illustrated for a blackbody source in Figure 2-12. The extended source can also be the output port of an integrating sphere. The spectral radiant intensity of the extended source through the aperture is given by

$$I(\lambda) = L(\lambda)\, A_a$$

The spectral irradiance $E(\lambda)$ at range *R* is then given by Equation 2-6. The effective irradiance E_e is given by Equation 2-12d. A linearity measurement with irradiance level can be made by varying the area of the precision aperture as long as the area of the exposed source is well within the FOV of the detecting system.

c. Placing a standard radiance extended source directly behind a precision aperture with area A_a at the focal point of a collimating mirror and placing the radiometer in the collimated beam with the restriction that the physical dimensions of the aperture are small enough to assume a point-like source to the collimating mirror such that aberrations are avoided. This set-up has three advantages, (1) the collimated beam simulates an object at infinity which puts the object at the correct distance for radiometers focused at infinity while the actual calibration path is only focal length *f* + beam length *B*, (2) it can be used to conduct a linearity measurement with irradiance level by varying the aperture area A_a, and (3) an FOV map can be obtained by pivoting the radiometer in the beam around a point in the entrance pupil of the collection optics. The disadvantage is that the spectral reflection of the mirror must be known to correctly calculate the irradiance of the beam. The concept of a collimating mirror is presented in Figure 2-15. To better illustrate the concept, the collimating mirror assembly is unfolded as a small radiance source at the focal point of a thin lens as shown in Figure 2-16.

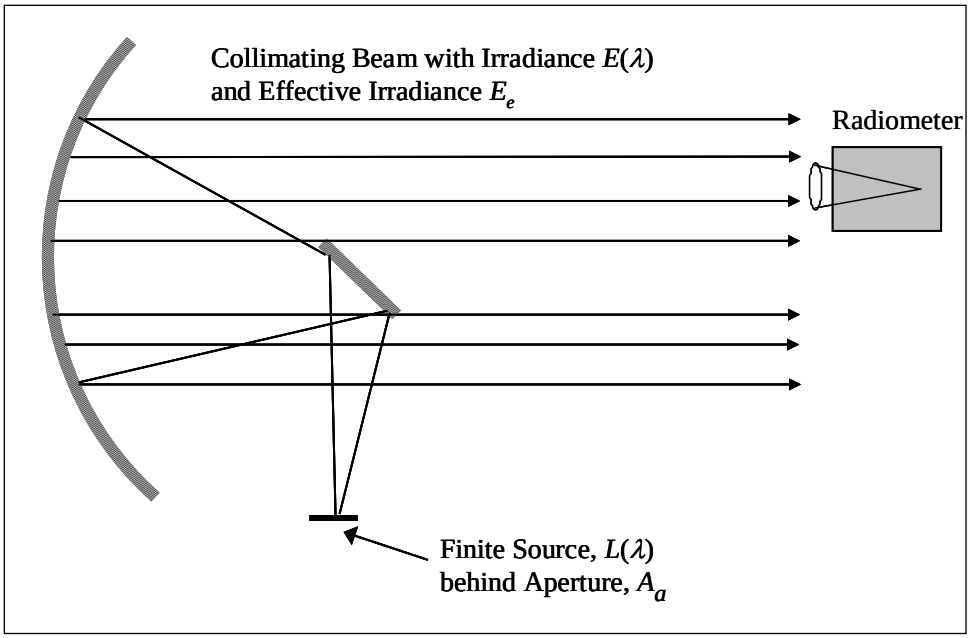

Figure 2-15. Concept of a collimating mirror.

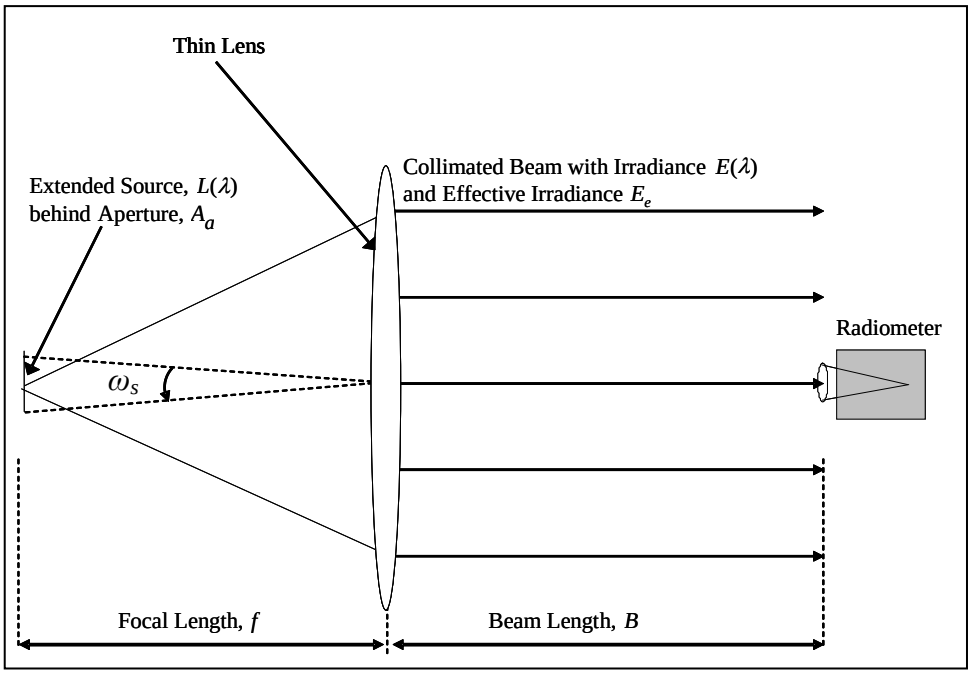

Figure 2-16. Simulation of collimating mirror.

Referring to Figure 2-16, an extended source of calibrated and known spectral radiance is placed at the focal point of the lens. A precision aperture is placed immediately in front of the extended source to limit the area exposed to the lens. The radiant intensity of the source through the aperture is

$$I(\lambda) = L(\lambda) A_a \qquad \text{(Eq. 2-29)}$$

The spectral irradiance at the lens is

$$E(\lambda) = \frac{I(\lambda)\, \tau_f(\lambda)}{f^2} \qquad \text{(Eq. 2-30}$$

The irradiance at the radiometer is

$$E(\lambda) = \frac{I(\lambda)\, \tau_{f+B}(\lambda)\rho(\lambda)}{f^2} \qquad \text{(Eq. 2-31)}$$

Where $\tau_{f+B}(\lambda)$ is the spectral transmission over path $f + B$,*and* $\rho(\lambda)$ is the spectral reflection coefficient of the mirror, or in this model, the spectral transmission of the lens. The effective irradiance of a band radiometer is again given by Equation 2-12d.

During a calibration event, the radiant power in a specific time interval that produces current i_{cal} by the radiometer is, defining A_d to be the effective area of the collection optics of the radiometer,

$$\Phi(\lambda) = E(\lambda)_{cal}\, A_d \qquad \text{(Eq. 2-32)}$$

The calibration response is the ratio of the measured current to the radiant power. The radiance calibration response is then

$$RESP(\lambda) = \frac{i(\lambda)_{cal}}{E(\lambda)_{cal}\, A_d} \quad \text{(amp/W)} \qquad \text{(Eq. 2-33)}$$

Where the measured current is shown as a spectral quantity. When the radiometer is used to view a target under test, the current caused by the target irradiance in the same time interval is

$$i(\lambda)_{target} = RESP(\lambda) \left\{ E(\lambda)_{target}\, A_d \right\} \qquad \text{(Eq. 2-34)}$$

Using Equation 2-33 in Equation 2-34, we solve for $E(\lambda)_{target}$ and recognize that the effective area of the collection optics is a constant of the calibration and cancels out. If the radiometer is calibrated for irradiance against an irradiance standard, the effective area of the collection optics does not need to be known.

$$E(\lambda)_{target} = \frac{i(\lambda)_{target}}{i(\lambda)_{cal}} \frac{E(\lambda)_{cal} A_d}{A_d} = \frac{i(\lambda)_{target}}{i(\lambda)_{cal}} E(\lambda)_{cal} \qquad \text{(Eq. 2-35)}$$

More often than not the radiometer will have an analog-to-digital component of the collection electronics and Equation 2-35 will have the more familiar form

$$E(\lambda)_{target} = \frac{counts(\lambda)_{target}}{counts(\lambda)_{cal}} \frac{E(\lambda)_{cal} A_d}{A_d} = \frac{counts(\lambda)_{target}}{counts(\lambda)_{cal}} E(\lambda)_{cal} \qquad \text{(Eq. 2-36)}$$

The apparent target radiant intensity is calculated from the target irradiance if the range to the target is known.

$$I'_{target}(\lambda) = E(\lambda)_{target} R^2_{target} \qquad \text{(Eq. 2-37)}$$

Equations 2-32 through Equation 2-37 are applicable to band instruments by replacing the spectral quantities with the associated effective quantities. Replace $\Phi(\lambda)$ with Φ_e, $I(\lambda)$ with I_e, $I'(\lambda)$ with I_e', $E(\lambda)$ with E_e, $RESP(\lambda)$ with $RESP$, $i(\lambda)$ with i, and $counts(\lambda)$ with $counts$.

For a spectral measurement, the actual spectral radiant intensity $I_{target}(\lambda)$ can be determined for each wavelength by dividing $I'_{target}(\lambda)$ by the spectral path transmission $\tau(\lambda)$ to remove the path attenuation, where $\tau(\lambda)$ is determined through an independent measurement or by using the MODTRAN model to calculate the function. For an effective measurement, the actual effective radiant intensity $I_{e,target}$ can be determined by dividing $I'_{e,target}$ by a weighted transmission factor which can be calculated if the spectral path attenuation, the radiometer relative spectral response, and the relative spectral function of the target are known. A technique to calculate a weighted transmission factor is discussed in paragraph 2.6.

2.5.2 Radiance Calibration. Calibration in terms of radiance can be accomplished with three configurations.

a. Exposing the imaging system to an extended source of calibrated, known spectral radiance, as is illustrated in Figure 2-17, where θ is the between the normal to the surface and the line of sight, $\hat{n}$ is the unit vector normal to the source surface, ω_d is the solid angle defined by the area of the source in the footprint of the IFOV, and R is the range between the emitting surface and the detector.

   This is a simple set-up with minimal hardware. The source can be an extended blackbody or the output port of a large integrating sphere. It is important that the IFOV of an individual detector element be completely contained within a region of uniform radiance. The spectral irradiance $E(\lambda)$ at the radiometer is given by Equation 2-7. The effective irradiance E_e is given by Equation 2-13d.

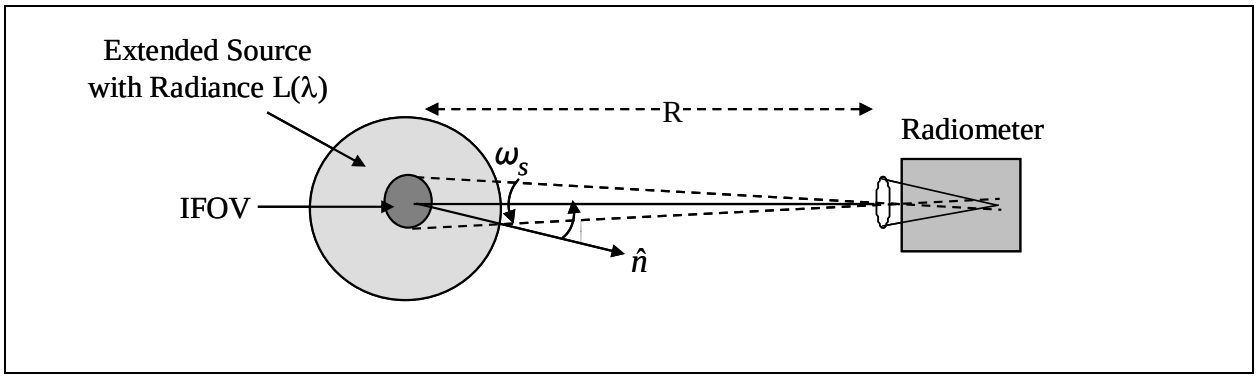

Figure 2-17. Geometry of radiance calibration.

b. Exposing the imaging system to an extended reflective Lambertian plate that is illuminated by an irradiance standard with irradiance $E(\lambda)$ at the specified distance, as illustrated in Figure 2-18, where again θ is the angle between the normal to the surface and the line of sight, $\hat{n}$ is the unit vector normal to the source surface, ω_d is the solid angle defined by the area of the source in the footprint of the IFOV, and R is the range between the emitting surface and the detector.

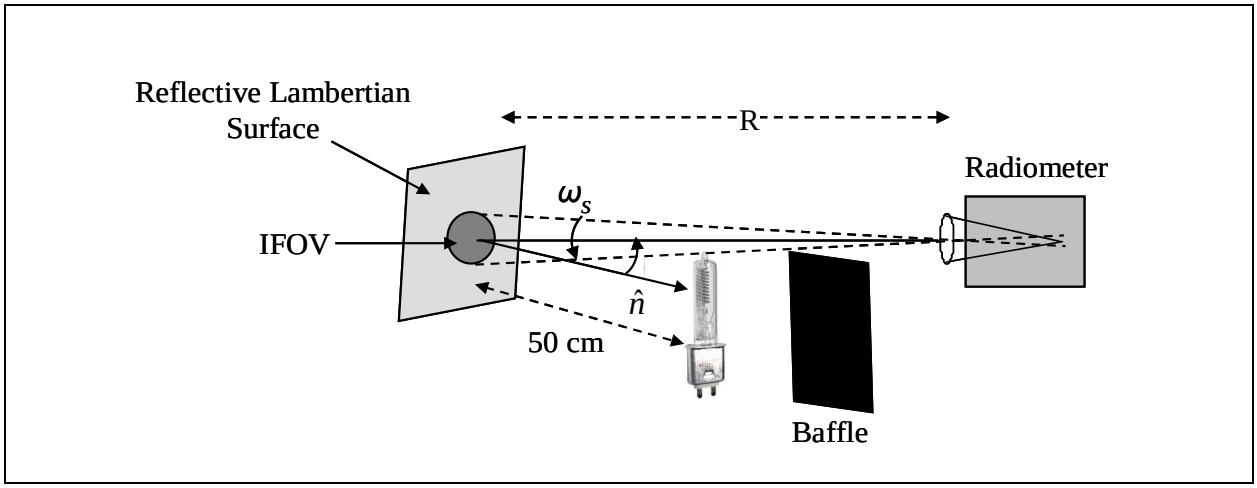

Figure 2-18. Creating a radiance standard with a reflective Lambertian plate and an irradiance standard.

With ρ(λ) defined as the spectral reflection coefficient of the plate, the radiance of the reflective Lambertian plate is

$$L(\lambda) = \frac{E(\lambda)\,\rho(\lambda)}{\pi}$$

The spectral irradiance $E(\lambda)$ at the radiometer is given by Equation 2-7. The effective irradiance E_e is given by Equation 2-13d. The advantage of this set-up is that it can be used to measure linearity with radiance level by exploiting the range-squared effect to decrease the irradiance at the plate by increasing the range R.

c. Placing an extended radiance source at the focal plane of a collimating mirror. Figure 2-19 illustrates this concept by unfolding the collimating mirror assembly shown in the previous Figure 2-15 as an extended radiance source at the focal point of a thin lens and where ω_s is the solid angle defined by the area of the source in the IFOV of the radiometer.

The set-up has the advantage of simulating an object at infinity which puts the object at the correct distance for imaging radiometers focused at infinity while the actual calibration path is only focal length *f* plus beam length *B*. It has the disadvantage that the spectral reflection of the mirror must be known to correctly calculate the irradiance of the beam. It also has a limitation in that the spatial footprint of the detector IFOV at the plane of the extended source cannot be too large since that would require a larger extended source which would introduce aberrations in the collimated beam.

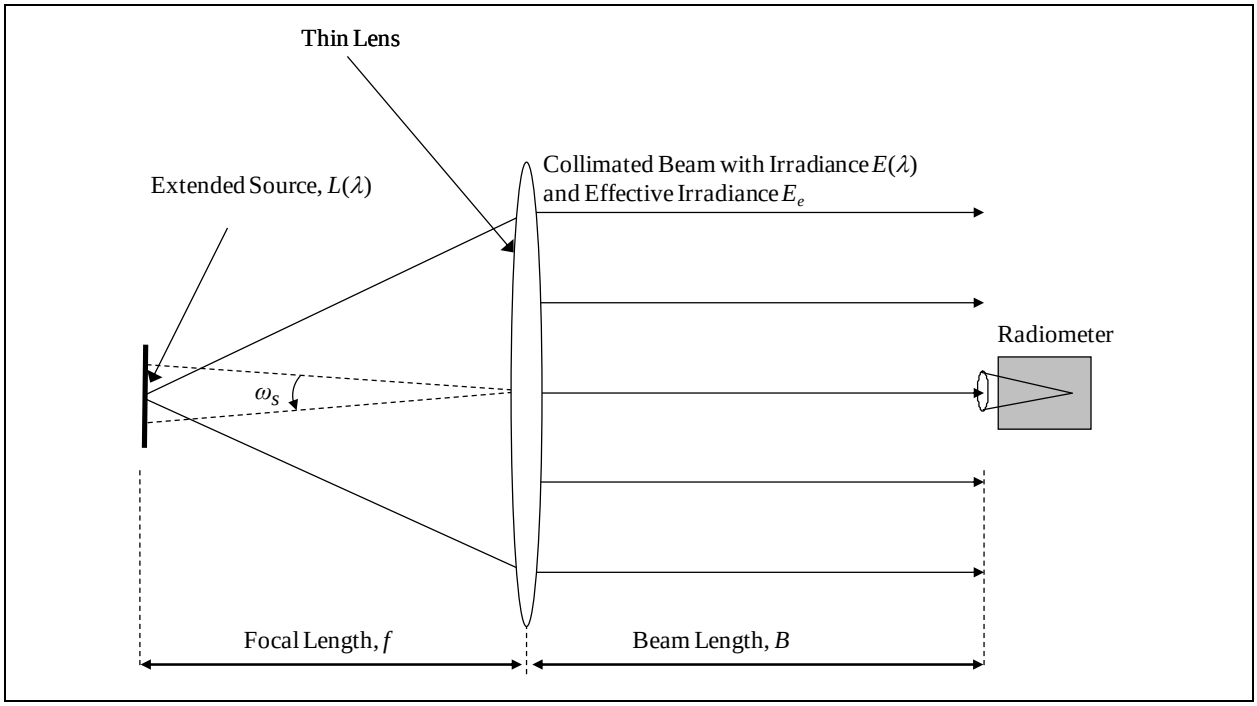

Figure 2-19. Simulation of a collimating mirror with extended source at the focal plane.

The spectral irradiance $E(\lambda)$ at the radiometer is given by Equation 2-7 where the apparent spectral radiance is defined as

$$L'(\lambda) \equiv L(\lambda)\, \tau_{f+B}(\lambda)\, \rho(\lambda) \qquad \text{(Eq. 2-38)}$$

Where $\tau_{f+B}(\lambda)$ is the path transmission along path $f+B$ and $\rho(\lambda)$ is the spectral reflection coefficient of the mirror or, in this model, the spectral transmission coefficient of the lens.

During a calibration event, the luminous power in a specific time interval that produces current i_{cal} by the radiometer is, defining A_d to be the effective area of the collection optics of the radiometer,

$$\Phi_v = E_{v,cal}\, A_d = L_{v,cal}\, \omega_s\, A_d \qquad \text{(Eq. 2-39)}$$

The calibration response is the ratio of the measured current to the luminous power. The radiance calibration response is then

$$RESP = \frac{i_{cal}}{L_{v,cal}\, \omega_s\, A_d} \quad \text{(amp/lm)} \qquad \text{(Eq. 2-40)}$$

When the radiometer is used to view a target under test, the current caused by the target irradiance in the same time interval is

$$i_{target} = RESP\ (L'_{v,\,target}\, \omega_s\, A_d) \qquad \text{(Eq. 2-41)}$$

Using Equation 2-40 in Equation 2-41, we can solve for $L'_{v,\,target}$ and recognize that the effective area of the collection optics and the FOV of the single detector element are constants of the calibration and cancel out. If the radiometer is calibrated for radiance against a radiance standard, the effective area of the collection optics and the FOV of the single detector element do not need to be known.

$$L'_{v,\,target} = \frac{i_{target}}{i_{cal}} \frac{L_{v,\,cal}\, \omega_s\, A_d}{\omega_s\, A_d} = \frac{i_{target}}{i_{cal}}\, L_{v,\,cal} \qquad \text{(Eq. 2-41)}$$

More often than not, the radiometer will have an analog-to-digital component of the collection electronics and we will have the more familiar form

$$L'_{v,\,target} = \frac{counts_{target}}{counts_{cal}} \frac{L_{v,\,cal}\, \omega_s\, A_d}{\omega_s\, A_d} = \frac{counts_{target}}{counts_{cal}}\, L_{v,\,cal} \qquad \text{(Eq. 2-43)}$$

The source radiance can be determined by removing the path atmospheric attenuation if the path spectral atmospheric attenuation $\tau(\lambda)$ is known and the relative spectral function of the target is known. This process is discussed in paragraph 2.6.

2.6 Effective Path Transmission

It is possible to remove the attenuation of the atmospheric transmission from the measured apparent radiant intensity I'_e and apparent radiance L'_e if the spectral transmission function is known and if the relative spectral shape of the target is known.
The desired effective radiometric quantity is

$$X_e = \int_\lambda X(\lambda)\,\tau(\lambda)\,d\lambda \qquad \text{(Eq. 2-44)}$$

Where X_e indicates either L_e or I_e and $X(\lambda)$ indicates either $L(\lambda)$ or $I(\lambda)$. The measured quantity is

$$X_e^{'} = \int_\lambda X(\lambda)\,\tau(\lambda)\,d\lambda \qquad \text{(Eq. 2-45)}$$

We ratio Equation 2-44 to Equation 2-45 and solve for X_e.

$$X_e = X_e^{'}\frac{\int_\lambda X(\lambda)\,\tau(\lambda)\,d\lambda}{\int_\lambda X(\lambda)\,d\lambda} \qquad \text{(Eq. 2-46a)}$$

$$X_e = X_e^{'}\frac{\int_\lambda X(\lambda)\,d\lambda}{\int_\lambda X(\lambda)\,\tau(\lambda)d\lambda} \qquad \text{(Eq. 2-46b)}$$

Since the spectral radiometric quantity $X(\lambda)$ is in both the numerator and denominator, we can replace it with the relative (normalized) spectral function which we define to be $X_{rel}(\lambda)$. Then, we define the weighted transmission to be

$$\tau_{weighted} \equiv \frac{\int_\lambda X_{rel}(\lambda)\,\tau(\lambda)d\lambda}{\int_\lambda X_{rel}(\lambda)\,d\lambda} \qquad \text{(Eq. 2-47)}$$

and Equation 2-46b is rewritten as

$$X_e = \frac{X_e^{'}}{\tau_{weighted}} \qquad \text{(Eq. 2-48)}$$

2.7 Application to Target Radiation with Target Temperature

The spectral irradiance arriving at a distant point (at a measuring device or a weapon system) often has a low value. The accuracy of measured data is affected by the system signal-to-noise (S/N) ratio. It is therefore extremely important that system noise (N) be as low as possible and the signal from the target (S) be as high as possible. The spectral irradiance produced at a range *R* by a point source is shown in Equation 2-49a. The spectral irradiance produced at range *R* by an extended source is shown in Equation 2-49b.

For a point source, $$E(\lambda) = \frac{I'(\lambda)}{R^2} \qquad \text{(Eq.2-49a)}$$

For an extended source, $$E(\lambda) = \omega_t \, L'(\lambda) = L(\lambda)\frac{A_s}{R^2} \qquad \text{(Eq.2-49b)}$$

Where

$I'(\lambda)$ = the apparent spectral radiant intensity of the source.
$L'(\lambda)$ = the apparent spectral radiance of the source.
ω_t = the solid angle subtended by the target area within the FOV.
A_s = the area of the target within the FOV.

For both point sources and extended sources, the irradiance is an inverse function of the square of range R. It is important to use a sensor with low noise when measuring a source at a large distance since the signal will be reduced by the square of the range. The signal is further reduced by range by atmospheric attenuation.

A method to maximize the measurement signal is to choose a detector system with an operational wavelength band optimized for the anticipated target temperature. The spectral radiance of an ideal radiator (a blackbody) is described by the Planck equation previously stated in Equation 2-17 and in Appendix B. As an example, the IR blackbody spectral radiance distributions for three temperatures are shown in Figure 2-20.

Since weapon systems also have a motivation to obtain the highest S/N ratio as possible, they generally choose a spectral region where the target radiance is relatively high. The wavelengths of highest radiation for the different temperatures can be identified in Figure 2-20. It can be seen that a relatively high target temperature is required to obtain useable radiation at short wavelengths. For instance, there is 1×10^9 times more 1 μm radiation at a temperature of 1000 °C than at 100 °C. It can also be seen that the variation of radiation with temperature at long wavelengths is not very great (emissivity is very important at these wavelengths). Although solar temperatures near 6000 °C are not shown in Figure 2-20, a source at this temperature radiates most of its energy in UV and VIS wavelengths. There is very little blackbody UV radiation from sources at temperatures much less than solar temperatures.

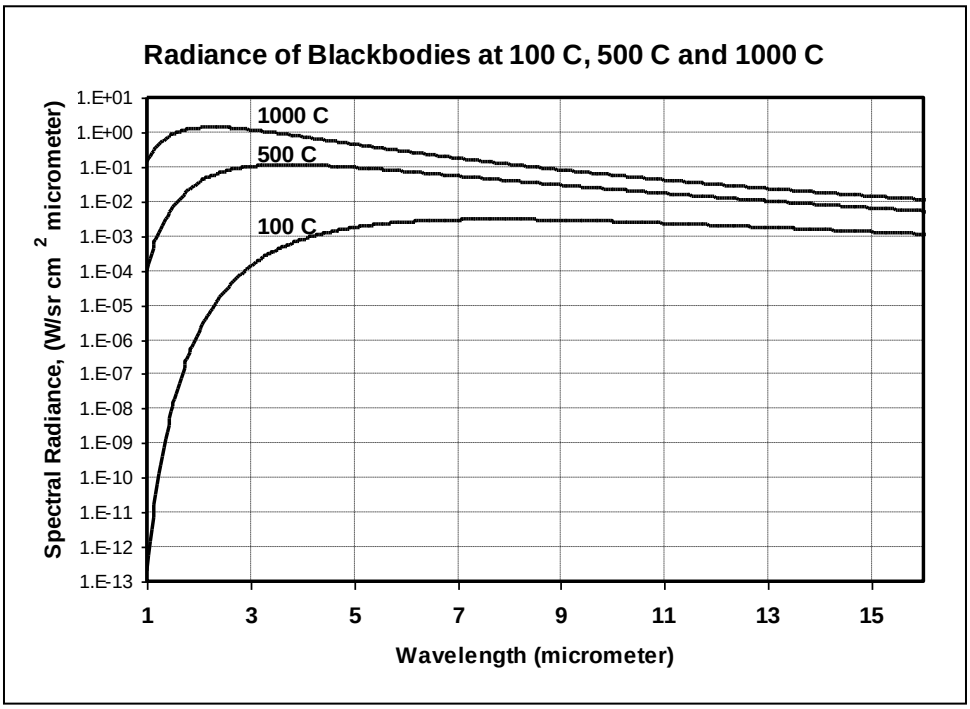

Figure 2-20. Variation of blackbody spectral radiance with temperature.

2.7.1 Spectral Radiation Characteristics of Various Sources. The radiance of a source is a function only of its absolute temperature and spectral emissivity value. A theoretically perfect radiator is called a blackbody. The Planck equation provides values for the radiation of a blackbody at an assigned absolute temperature. A blackbody has a constant emissivity of one. All other radiators have varying emissivity values between zero and one. The spectral radiance of a real radiator is determined by multiplying its emissivity value at each wavelength by the radiance of a blackbody at corresponding temperature and wavelengths. The Planck equation was previously stated in Equation 2-17 and the spectral distribution of blackbodies at various temperatures were shown above in Figure 2-20.

A graybody is defined to be a radiator that has a constant emissivity that is less than one in the spectral interval of interest. Although there may be no radiator that has a constant emissivity over the entire range of EO wavelengths, many materials have an emissivity that is nearly constant over portions of the range. Over the spectral region where the emissivity is constant, the material is considered a graybody, whereas outside that interval it will have a different characteristic.

Many radiators have emissivity values that are wavelength dependent. These radiators are called selective radiators. Solid and liquid radiators often have emissivity values that only change gradually over fairly large wavelength intervals. Gaseous radiators, on the other hand, typically have large variations in their emissivity values over very small wavelength intervals. The earth's atmosphere is composed of a mixture of many gases. Some of these gases, primarily CO_2, O_3, and H_2O molecules, are selective absorbers of certain wavelengths of optical radiation. Since the remote measurement of target signatures involves the measurement of optical radiation

that has passed through an atmospheric path, knowledge of the spectral radiation characteristics of a target, the spectral transmission of the measurement path, and the spectral responsivity of the measurement system are critical to reporting accurate target signature data. Actual target signatures cannot be determined unless all of these spectral quantities are known and correctly applied.

This page intentionally left blank.

CHAPTER 3

MEASUREMENT DOMAINS

Radiant power emitted or reflected from a source is distributed across multiple dimensions or domains. All instruments have some sensitivity to how radiation is distributed in three primary domains. The three domains that are most important to radiometric calibration and measurement are spectral (Figure 3-1), spatial (Figure 3-2), and temporal (Figure 3-3). Knowing how the radiant power from a source is distributed across each domain is important to a measurement and is essential to a calibration.

3.1 Spectral Domain

In the spectral domain, radiation is distributed as a function of wavelength (or wavenumber). Radiation from solid materials is distributed as a continuum in accordance with Planck's blackbody equation. The graph in Figure 3-1 shows the spectral distribution of radiation from a 600 ^{o}C blackbody after passage through the atmosphere. Absorption from atmospheric gases appears at specific wavelengths as narrow lines corresponding to molecular resonances.

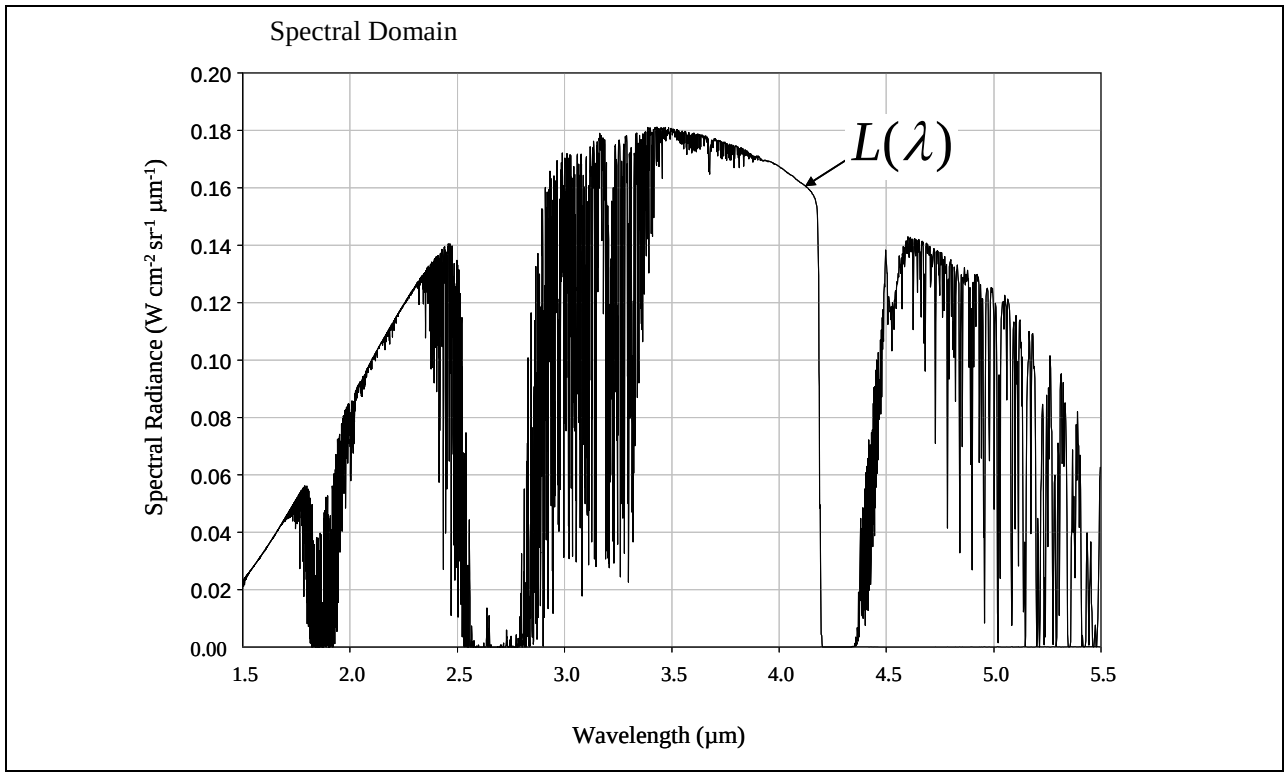

Figure 3-1. Sample spectral distribution of a solid material.

Radiation from each point on a target is a combination of self emission and reflection of radiation from surrounding sources. The radiation from a point depends on the temperature, reflectivity, and emissivity at that point. Radiation, in general, varies from point-to-point. Although the emissivity and reflectivity values are typically constant across a surface, the

temperature can vary considerably across the surface with the target operating state and in response to the environment. A spectrometer is required to measure target spectral radiance. The spectral resolution of band radiometers and band imagers is not any better than their wide spectral response. Band systems are used to measure effective quantities and not spectral quantities.

Considerations for spectral instrument response(s) are that:

a. They may be wide, as in the case of a radiometer or imager, or narrow as in the case of a series of narrow bands of a spectrometer.
b. The spectral response is chosen to measure particular spectral features of interest in a target.
c. Non-uniformity of spectral response is a major concern in measurement uncertainty. Non-uniformity must be taken into consideration when interpreting data collected with a broadband radiometer or imager. However, the spectral response approaches a constant across each narrow band of a spectrometer.

3.2 Spatial Domain

In the spatial domain, radiation is distributed as a function of angle, position, size, shape, or orientation. Figure 3-2 illustrates the radiance, *L(x,y)*, of a circular target as viewed by an imaging system. The radiance is a function of the horizontal (*x*) and vertical (*y*) dimensions.

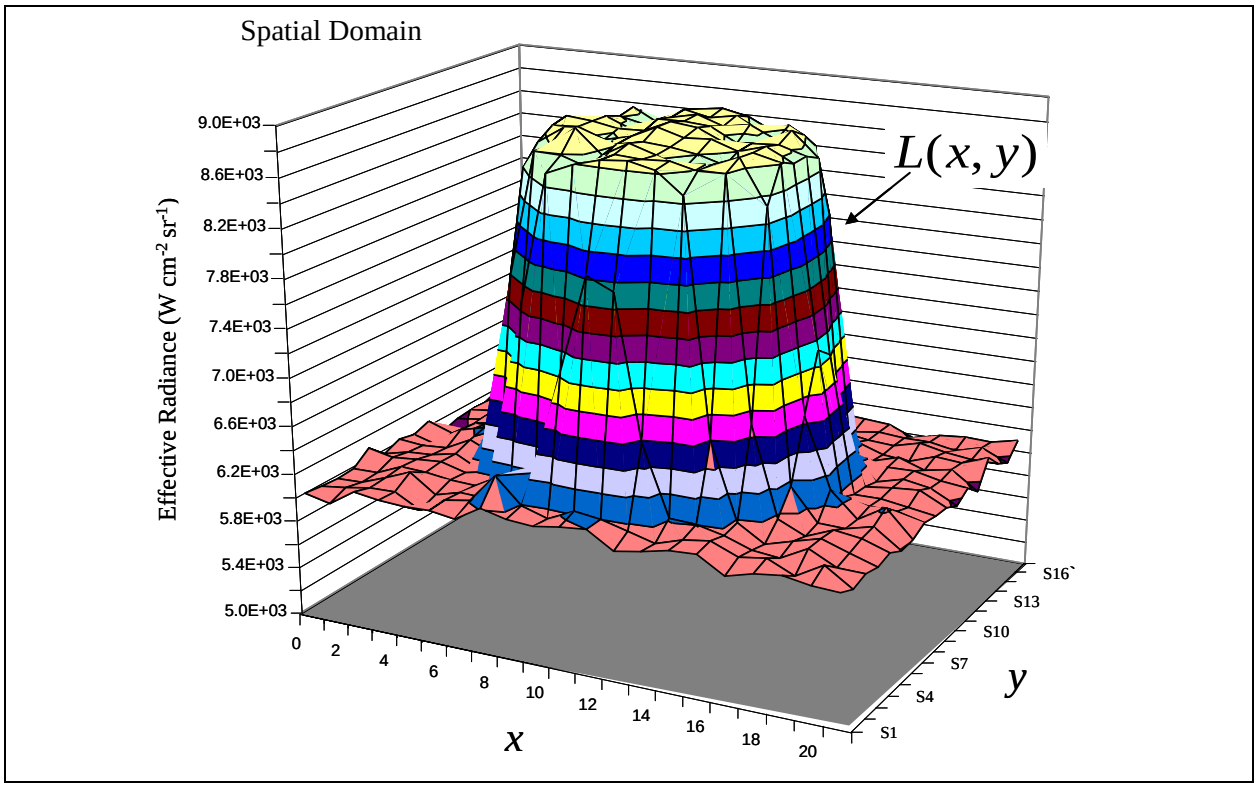

Figure 3-2. Sample spatial distribution of a circular target image.

The temperature and spectral emissivity varies from point-to point on a target, resulting in differences in the spectral radiance at different points on the target. The radiation from each point has a unique angular distribution, resulting in signatures that are aspect angle dependent. Also, the spatial/spectral/aspect angle signature of a target depends on its operating state as well as the environment at the target. An imager is required to measure target spatial characteristics. Radiometers and spectrometers with single, large fields of view do not have the capability to determine spatial variations of radiance.

Considerations for spatial instrument response(s) are that:

a. They may be broad, as in the case of a radiometer or spectrometer, where spatial response takes the form of sensitivity across the instrument FOV, or narrow in the case of an imager, where spatial response takes the form of the resolution of the IFOV.
b. The target measurement range is selected to optimize the spatial resolution using a particular instrument FOV and IFOV.
c. Non-uniformity of spatial response is a major concern in measurement uncertainty. Spatial non-uniformity must be considered when interpreting data collected with a large IFOV radiometers and spectrometers. However, the spatial response approaches a constant across the small IFOV of each pixel of an imager.
d. The response to radiation from the background within the FOV is primarily a spatial response issue and is a major concern in measurement uncertainty.

3.3 Temporal Domain

In the temporal domain, radiation is distributed as a function of time (or frequency) as simulated in Figure 3-3. IR target sources such as aircraft and ground vehicles change slowly with time and can be considered steady state for measurement purposes. However, IR countermeasures systems and devices, such as jammers and decoy flares, have high frequency content that must be considered.

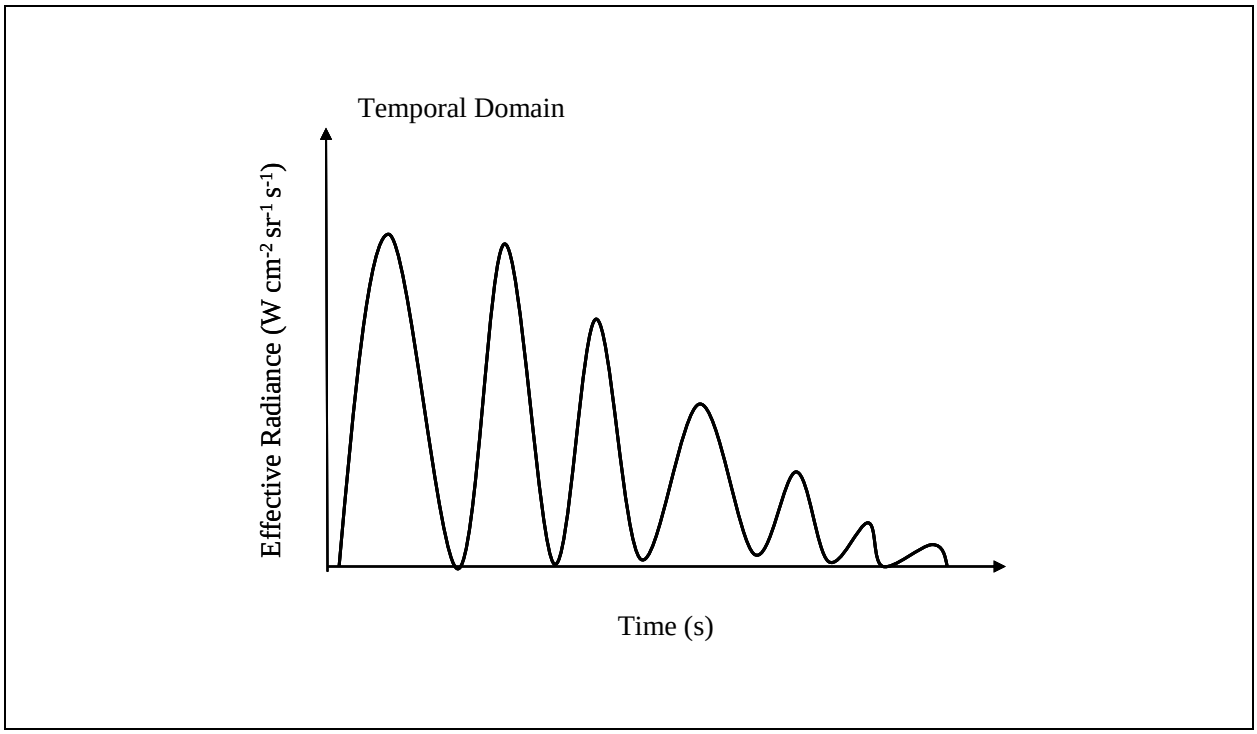

Figure 3-3. Sample temporal distribution of a modulated source.

The spectral/spatial radiation from areas on a target can have a significant temporal dependence. Unless the measurement instrument has an appropriately high frequency response, variation of radiant intensity or radiance values will not be accurately determined. Simply stated, data must be collected at an appropriate rate such that the state of the target can be considered steady during the sampling period.

Considerations for temporal instrument response(s) are that:

a. The temporal response takes the form of bandwidth or, in the case of a digital system, of sampling frequency.
b. Unlike spectral and spatial response, temporal response is usually determined by the full data acquisition and recording system in addition to the basic instrument. The temporal response must be determined for the total system.
c. Non-uniformity across a region is usually not a concern if the sampling rate is higher than target frequencies. Temporal response is usually uniform for target frequencies that fall well below the low-pass or Nyquist breakpoints.

3.4 References for Chapter 1 Through Chapter 3

a. DoD, Operational Plans and Joint Force Development (J-7), Joint Doctrine Division (2001). Department of Defense Dictionary of Military and Associated Terms, (Joint Publication 1-02), as amended through March 4, 2008.

b. Petty, G. (2006). A First Course in Atmospheric Radiation (2nd edition.). Madison, Wisconsin: Sundog Publishing.

c. Zong, Y., Brown, S., and Ohno, Y. (1997). Realization of the Candela, the Lumen,and Other Photometric Units, Optical Technology Division, NIST, http://physics.nist.gov/Divisions/Div844/facilities/photo/Candela/photo.html, Last update February 2008, retrieved June 2008.

d. Tobiska, W., The Development of New Solar Indices for use in Thermospheric Density Modeling (2006). Journal of Atmospheric and Solar-Terrestrial Physics 70 (2008) 803-819. http://sol.spacenvironment.net/~jb2006/, retrieved April 2007.

e. Kirtland Air Force Base. MODTRAN 4 Software Fact Sheet, http://www.kirtland.af.mil/library/factsheets/factsheet.asp?id=7915.

f. International Bureau of Weights and Measures (BIPM) (2006). The International System of Units (SI) (8th edition).

g. Taylor, B. (1995). Guide for the Use of the International System of Units (SI), United States Department of Commerce, National Institute of Standards and Technology (NIST), Special Publication 811, 1995 edition, 2nd printing, April 1995.

h. United States Department of Commerce, National Institute of Standards and Technology (NIST) (2001). The International System of Units (SI), Special Publication 330, 2001 edition, July 2001. Taylor, B., (editor).

i. Moller, K. (1998). Optics. Mill Valley, CA, University Science Books.

j. Dereniak, E., and Boreman, G. (1996). Infrared Detectors and Systems. John Wiley and Sons, New York, NY, 1996.

k. Wyatt, C., Privalsky, V., and Datla, R. (1998). Recommended Practice; Symbols, Terms, Units and Uncertainty Analysis for Radiometric Sensor Calibration, (NIST Handbook 152). United States Department of Commerce, National Institute of Standards and Technology (NIST).

This page intentionally left blank.

CHAPTER 4

PHOTOMETRY

Radiometry is the science and the craft of measuring radiant power across the entire optical region of the electromagnetic spectrum. Photometry is the science of measuring the total integrated visible portion of the electromagnetic spectrum and, more specifically, integrated within the spectral response of the human observer. The primary focus of this document is radiometry since it is the science used by the military for surveillance and threat recognition. The Chapter 2 discussion of radiometers carries directly to a discussion on photometry, which is considered a special branch of radiometry. The following paragraph describes the science of photometry in the context of radiometry.

Photometric units weight radiometric units according to the spectral response of the human eye. Photometric quantities are related to the perceived intensity and brightness of a source to a human observer. Note that the spectral response of the human eye changes with light level. The low light level response is called the scotopic response, and the normal light level response is called the photopic response. The Commission Internationale de l'Eclairage (CIE) defined internationally recognized standard scotopic and photopic spectral responses which are adopted by the International Organization for Standardization (ISO) (Reference 4a). Photopic vision is detected by cones of the eye and scotopic vision is detected by rods. Rods are more sensitive to low light levels, but they do not detect color. Photopic vision is active when luminance levels are greater than 10 cd/m^2. Scotopic vision is active when luminance levels are less than 0.001 cd/m^2 (Reference 4b). The response for intermediate light levels is called mesopic, but there are currently no international standard functions defining a mesopic response. In current practice, all photometric quantities are given in terms of photopic vision, even at low light levels, except for special measurements for research purposes (Reference 4c). The CIE photopic function depicts the photopic luminous efficiency of the human visual system as a function of wavelength and provides the standard weighting function used to convert radiometric quantities to photometric.

4.1 Photopic and Scotopic Response Functions

The visible portion of the electromagnetic spectrum is referred to as "light." The wavelengths of light are between approximately 360 nm and 830 nm (Reference 4d) defined by the human spectral eye response. All units used in stating the various light quantities are based on the candela, which is a base SI unit defining the luminous intensity from a point-like source into a certain direction. The candela and other photometric quantities are defined in terms of the photopic (normal light level) spectral response of the standard observer. The relative photopic luminous efficiency $V(\lambda)$ is shown in Figure 4-1. The photopic response is often called the "standard luminosity curve." The relative scotopic response $W(\lambda)$ is also plotted in Figure 4-1.

Figure 4-2 presents the photopic and scotopic absolute spectral responses, $v(\lambda)$ and $w(\lambda)$ respectively. The values plotted in Figure 4-2 are the same as Figure 4-1 except they are scaled by the respective maximum spectral luminous efficacy; 683 lm/W for photopic vision and 1700 lm/W for scotopic vision. The absolute photopic curve of Figure 4-2 is $v(\lambda) = V(\lambda)$ x 683 lm/W.

The absolute scotopic curve of Figure 4-2 is $w(\lambda) = W(\lambda)$ x 1700 lm/W. The photopic response peaks at 0.555 μm with an absolute value of 683 lm/W. The scotopic response peaks at 0.507 μm with an absolute value of 1700 lm/W. It should be noted that the spectral responses listed are for the average observer. Individuals will have a spectral response slightly different from the listed values.

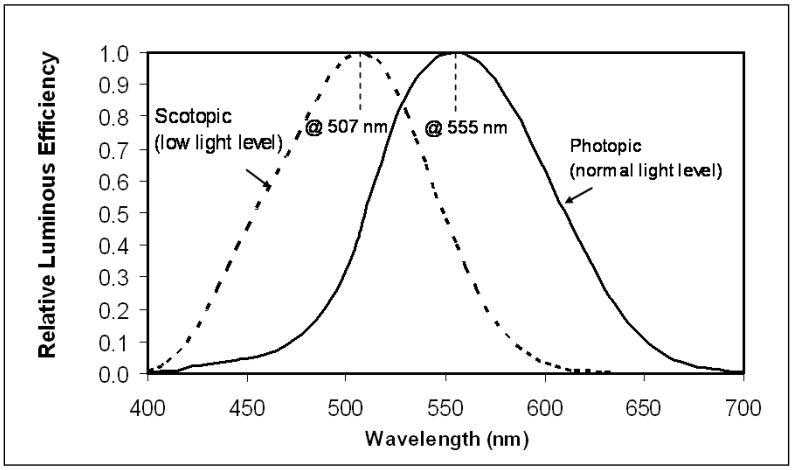

Figure 4-1. Relative CIE photopic and scotopic photometric luminous efficiency functions of the standard observer.

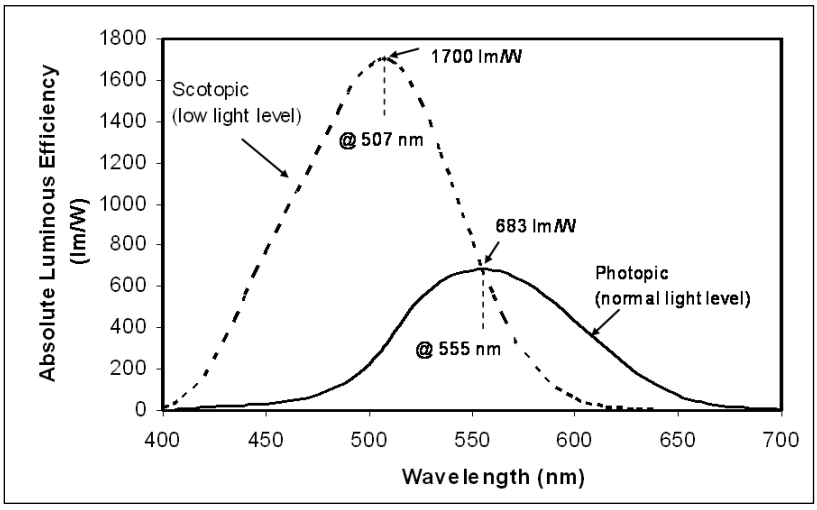

Figure 4-2. Absolute CIE photopic and scotopic photometric luminous efficiency functions of the standard observer.

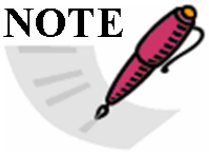

The definition of the candela previous to 1979 was based on the luminous emission of a blackbody at the freezing temperature of platinum (2045 K). This definition was abrogated in 1979 and replaced with the following definition, noting that optical radiation at 540 $x10^{12}$ Hz has a wavelength of 555 nm, the peak of the photopic response:

The candela is the luminous intensity, in a given direction, of a source that emits monochromatic radiation of frequency 540×10^{12} Hz and that has a radiant intensity in that direction of 1/683 W/sr.

The scaling factor 683 lm/W for the absolute photopic luminous efficiency is chosen to make the magnitude of luminous intensity unit as close as possible to that under a previous 1948 definition of the candela and to maintain the continuity of the unit. The scaling factor 1700 lm/W for the scotopic luminous efficiency is chosen to cause agreement of the luminous efficacy (lm/W) for the photopic and scotopic luminous efficiency functions at optical frequency 540 x 10^{12} Hz (λ = 555 nm) (Reference 4a). The scaling factor 1700 lm/W for the scotopic function is in reasonable agreement with the previous scaling factor (1746 lm/W) used before the redefinition of the candela in 1979.

Photometric quantities are determined from spectral radiometric quantities by weighting their radiometric spectral distribution with the photopic luminous efficiency. To illustrate this concept, consider the emission beams of small common laser diode pointers. Two popular laser pointer types have red beams at 650 nm and 635 nm and a third popular pointer has a green beam at 532 nm. Figure 4-3 presents the spectral position of the three laser emission lines compared to the photopic and scotopic eye responses. The relative photopic response values at 650 nm, 635 nm, and 532 nm are 0.11, 0.22, and 0.88, respectively. Class 3R laser pointers are limited to 5 mW radiant power. If we assume each laser pointer outputs the maximum allowable 5 mW radiant power into the same beam diameter, the three outputs will be as follows:

a. 650 nm laser pointer: (683 lm/W)(0.11)(0.005 W) = 0.376 lm
b. 635 nm laser pointer: (683 lm/W)(0.22)(0.005 W) = 0.75 lm
c. Green laser: (683 lm/W)(0.88)(0.005 W) = 3.0 lm

Even though the lasers emit the same radiant power, to a human observer the 635 nm laser will appear 2 times brighter and the green 532 nm laser beam will appear 8 times brighter than the red beam of the 650 nm laser. Another interesting feature that can be seen in Figure 4-3 is that the green laser at 532 nm emits in a very high spectral region of the scotopic response while the red lasers emit in a region of very low response. As a matter of fact, the green laser will appear 1150 times brighter than the 650 nm laser and 350 times brighter than the 635 nm laser in low light level conditions. This is why green laser pointers are becoming popular for pointing at objects in the nighttime sky; a small amount of radiation scatters out of the beam from dust particles and appears bright enough to act as an arrow to the object. A red laser beam will also have some radiation scattered out of the beam but the lumen level will be too low to be seen, making a very poor arrow.

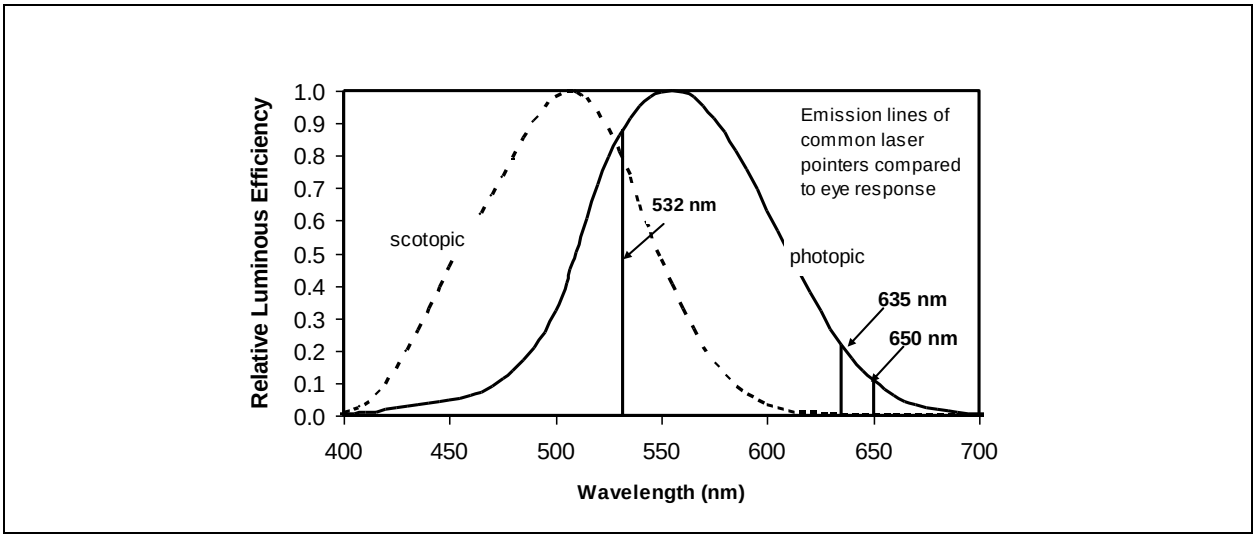

Figure 4-3. Photopic and scotopic eye response with spectral position of common laser pointers.

Photometric instruments are fabricated with optical filters that, when combined with the spectral response of the detector and other optical components, create a total spectral response equal to the CIE photopic response shown in Figure 4-1. Photometric instruments are therefore a special subset of band instruments. They are calibrated in terms of effective irradiance where the spectral response is the photopic response. Photometric quantities are, therefore, effective radiometric quantities using the CIE photopic response. It is important to understand there are no defined spectral photometric quantities. Photometric quantities are always effective and are always related to the spectral response of human vision.

4.2 Photometric Quantities

Photometric quantities can be determined from spectral radiometric quantities by weighting the radiometric spectral distribution with the relative photopic response and integrating under wavelength as is shown in Equation 4-1. The subscript *v* on the photometric symbol indicates the quantity is related to the visual response to visible light. The limits of integration in Equation 4-1 may be zero to infinity but the limits are shown as 360 nm and 830 nm since these are the practical limits with the scotopic and photopic functions being zero beyond them.

$$X_v = 683\ \text{lm/W} \int_{360nm}^{830nm} X(\lambda)\, V(\lambda)\, d\lambda = \int_{360nm}^{830nm} X(\lambda)\, v(\lambda)\, d\lambda \qquad \text{(Eq. 4-1)}$$

Where

X_v = the photometric quantity
$V(\lambda)$ = the relative photopic luminous efficiency
$X(\lambda)$ = the spectral radiometric quantity
$v(\lambda)$ = the absolute photopic luminous efficiency, $V(\lambda)$*683 lm/W

Table 4-1 is the basic set of photometric quantities. A short definition of these quantities and some special adaptations are provided below the table.

The science of photometry has a long history and is used in various and diverse disciplines. Therefore, there are numerous terms for additional photometry quantities that might still be encountered but are not recognized as SI quantities. Included are illuminance quantities foot-candle (lm/ft^2) and phot (lm/cm^2), and the luminance quantity stilb (cd/cm^2). There are other quantities that apply only to Lambertian sources, including apostilb ($cd/m^2/\pi$), Lambert ($cd/cm^2/\pi$), and foot-Lambert (cd/ft^2). Refer to Appendix E for a listing of historical photometric quantities. Practitioners are encouraged to use the new quantities of Table 4-1 based on the candela and to avoid the use of other derived quantities.

TABLE 4-1. BASIC PHOTOMETRIC QUANTITIES, SYMBOLS, AND UNITS

Base Quantity		SI Base Unit			
Name	**Symbol**	**Name**	**Unit Symbol**	**Expressed in Terms of Other SI Units**	**In Terms of SI Base Units**
Luminous intensity	I_v	candela	cd	J/(s·sr) and lm/sr	$kg\ m^2\ s^{-3}\ sr^{-1}$
Derived Quantity		**SI Coherent Derived Unit**			
Name	**Symbol**	**Name**	**Unit Symbol**	**Expressed in Terms of Other SI Units**	**In Terms of SI Base Units**
Illuminance	E_v	lux	lx	$J/(m^2 \cdot s)$ and lm/m^2	$kg\ s^{-3}$
Luminance	L_v	candela per square meter [1]	cd/m^2	$J/(m^2 \cdot s \cdot sr)$	$kg\ s^{-3}\ sr^{-1}$
Luminous energy	Q_v	lumen second [2]	lm·s	J	$kg\ m^2\ s^{-2}$
Luminous exitance	M_v	lux	lx	$J/(m^2 \cdot s)$ and lm/m^2	$kg\ s^{-3}$
Luminous flux	Φ_v	lumen	lm	J/s	$kg\ m^2\ s^{-3}$

[1] Has the special name nit.
[2] Has the special name talbot.

As an example of transferring a radiometric quantity to a photometric quantity, we consider the spectral irradiance of a 1000 W FEL (2-pin base) tungsten halogen lamp typically used to calibrate VIS and NIR radiometers and spectrometers. Figure 4-4 presents the spectral irradiance of a Newport Oriel® Model 6315 1000 W FEL lamp at 50 cm from the lamp base (Reference 4e). Figure 4-5 is the geometry of using a 1000 W FEL lamp as an irradiance standard.

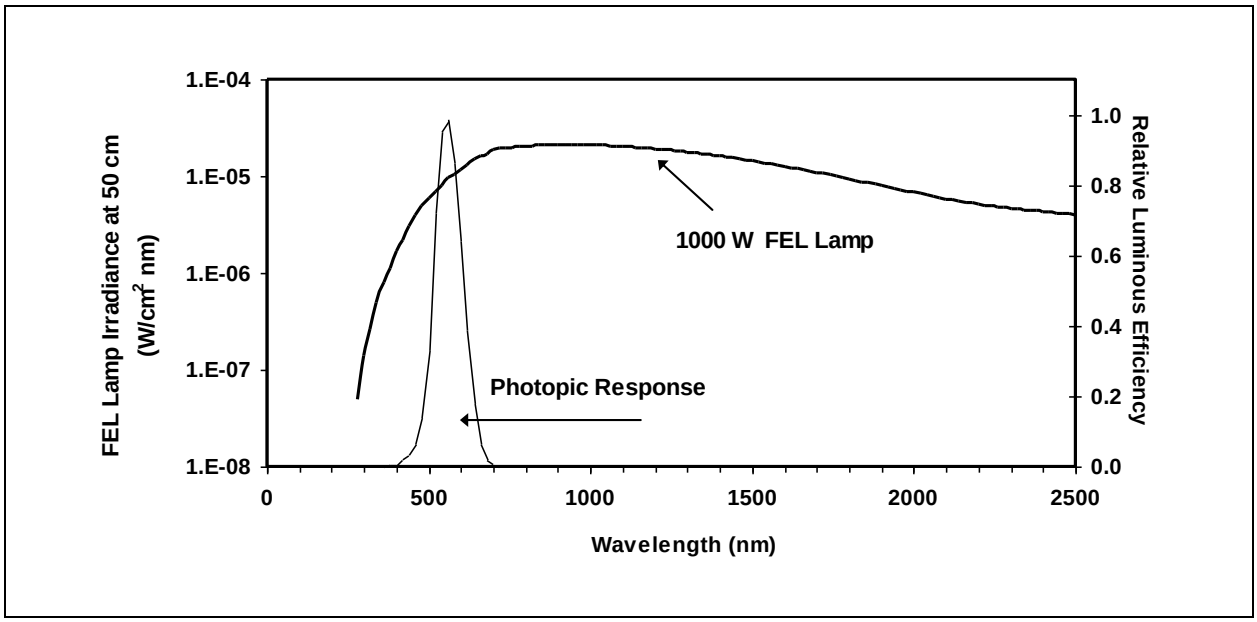

Figure 4-4. Spectral irradiance of a Newport Oriel Model 6315 1000 W FEL lamp and the photopic spectral response.

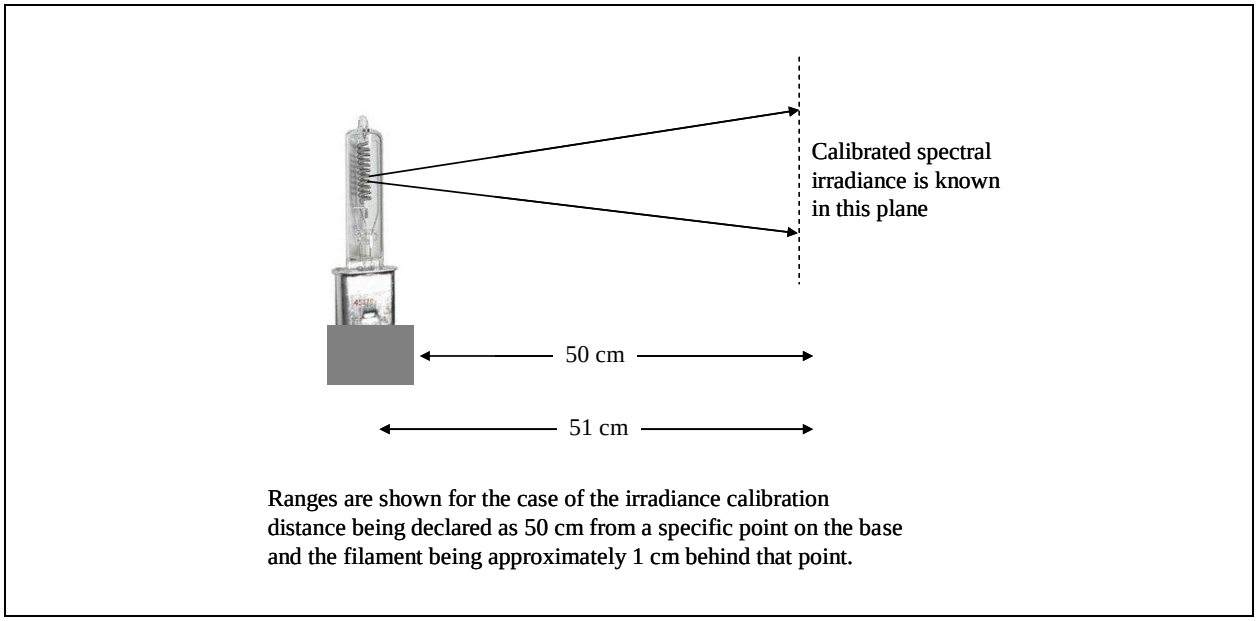

Figure 4-5. Geometry for irradiance calibration against a 1000 W FEL lamp.

The illuminance E_v at the calibrated distance of 50 cm from the base is calculated by the integral of Equation 4-2, where E(λ) is the spectral irradiance of the quartz halogen lamp in units W/cm^2 nm. Path attenuation is insignificant at the 50 cm range and is ignored in Equation 4-2.

$$E_v = 683 \text{ lm/W} \int_{360nm}^{830nm} E(\lambda)\, V(\lambda)\, d\lambda \;\; = 0.7 \text{ lm/cm}^2 \qquad \text{(Eq. 4-2)}$$

The luminous intensity of the lamp is calculated from the illuminance by multiplying by the range-squared, where 51 cm is the range to the filament as illustrated in Figure 4-5.

$$I_v = E_v\,(51cm)^2 \;\; = 1.8\text{x}10^3 \text{ lm/sr (cd)} \qquad \text{(Eq. 4-3)}$$

It is important to realize that photometric quantities are effective and only have definition within the photopic spectral response. It is possible for non-unique spectral radiant quantities to yield equivalent photometric quantities. Figure 4-6 illustrates this concept. Figure 4-6 presents the spectral irradiance of two fictitious sources, $E_1(\lambda)$ and $E_2(\lambda)$.

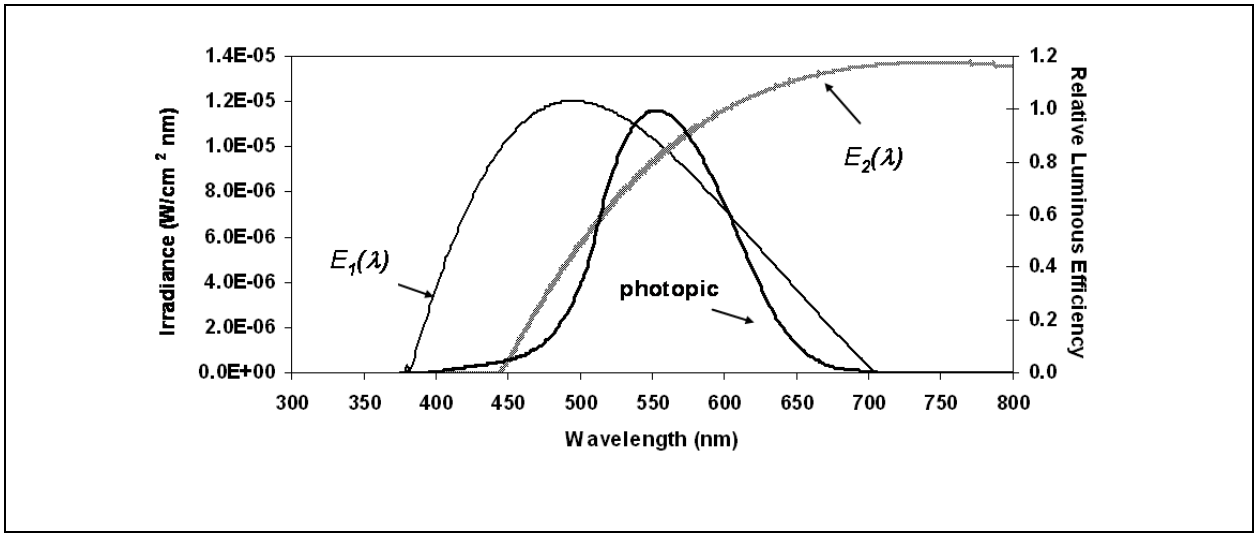

Figure 4-6. Spectral irradiances of two fictitious sources that yield equivalent illuminance values.

The illuminance from each source is calculated as:

$$E_{1v} = 683 \text{ lm/W} \int_{360nm}^{830nm} E_1(\lambda)\, V(\lambda)\, d\lambda \;\; = 0.690 \text{ lm/cm}^2 \qquad \text{(Eq. 4-4)}$$

$$E_{2v} = 683 \text{ lm/W} \int_{360nm}^{830nm} E_2(\lambda)\, V(\lambda)\, d\lambda \;\; = 0.690 \text{ lm/cm}^2 \qquad \text{(Eq. 4-5)}$$

Note that Equation 4-4 and Equation 4-5 illustrate that it is possible to have non-unique spectral radiometric functions that yield equivalent photometric values. Subsequently, it is impossible to infer a spectral radiant power function of a source from its photometric value.

4.2.1 Luminous Flux, Φ_v. Luminous flux corresponds to the fundamental radiometric quantity radiant flux, $\Phi(\lambda)$, measured in watts. The unit of luminous flux is the lumen (lm). Luminous flux is derived from spectral radiant flux by Equation 4-1 as

$$\Phi_v = 683\ \text{lm/W} \int_{360nm}^{830nm} \Phi(\lambda)\, V(\lambda)\, d\lambda \qquad \text{(Eq. 4-6)}$$

4.2.2 Luminous Energy, Q_v. Luminous energy is also known as the quantity of light. It is measured in units lumen second (lm s). It is the time integral of luminous flux over a time interval Δt.

$$Q_v = \int_t \Phi_v\, dt \qquad \text{(Eq. 4-7)}$$

4.2.3 Luminous Intensity, I_v. Luminous intensity corresponds to the radiometric quantity radiant intensity $I(\lambda)$, measured in watt/sr. The unit of luminous intensity is the candela or lumen per steradian (lm/sr). The candela is coherent to the unit lm/sr which is often chosen for use over cd since it is descriptive of the quantity.

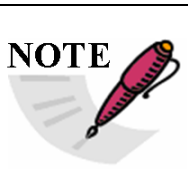

Coherent derived units are products of powers of base units that include no numerical factor other than 1. Examples are 1 Hz = 1 s^{-1} and 1 N= 1 m kg s^{-2}. Coherent units may be used with prefixes but they will no longer be coherent. For example, 1 kHz = 1000 s^{-1} is not a coherent relationship.

Luminous intensity describes the quotient of the luminous flux exiting a surface into an elemental solid angle in a given direction. The source is a point-like source such that the IFOV of a single detector contains the entire spatial extent of the source. It is the quantity of choice for describing the radiation from such "point source" targets. The differential definition is

$$I_v = \frac{d\Phi_v}{d\Omega} \qquad \text{(Eq. 4-8)}$$

Luminous intensity can be derived from spectral radiant intensity by Equation 4-1 as

$$I_v = 683\ \text{lm/W} \int_{360nm}^{830nm} I(\lambda)\, V(\lambda)\, d\lambda \qquad \text{(Eq. 4-9)}$$

Luminous intensity is a property of a target. It cannot be measured remotely, but must be inferred from a measurement of illuminance at a remote observation point. Luminous intensity is normally determined by measuring illuminance using a photometer or spectral photometer with a single detector having a relatively large field-of-regard. Luminous intensity can also be obtained from data collected with an imaging or scanning photometer by integrating target luminance data over the total surface area of a target. Photometers used to measure luminous intensity are normally calibrated in terms of illuminance using a point source illuminance "standard." These calibration techniques are presented in paragraph. 4.3.

4.2.4 Luminance, L_v. Luminance corresponds to the radiometric quantity radiance $L(\lambda)$, commonly measured in watt/m^2 sr or watt/cm^2 sr. The unit of luminance is lumen per area per steradian, lm/(m^2 sr) or lm/(cm^2 sr). Luminance describes the quotient of the luminous flux exiting an elemental surface area at a given point into an elemental solid angle in a given direction. The differential definition is

$$L_v = \frac{d\Phi_v}{dA\cos(\theta)\,d\Omega} \qquad \text{(Eq. 4-10)}$$

Where

dA = the incremental area at the point on the surface,
$d\Omega$ = the incremental solid angle the beam is propagating into
θ = the angle between the normal to the surface and the direction of propagation.

Luminance can be derived from spectral radiance by Equation 4-1 as

$$L_v = 683\ \text{lm/W}\int_{360nm}^{830nm} L(\lambda)\,V(\lambda)\,d\lambda \qquad \text{(Eq. 4-11)}$$

Luminance describes the "brightness" of an extended surface to an observer, noting that brightness is a term only used in photometry; it has no meaning in radiometry. Luminance is the quantity of choice to describe the spatial luminous flux from a target with sufficient angular size that it is spatially resolved by the photometer.

The area (m^2) to be considered in the definition of luminance is the projected surface area perpendicular to the viewing angle (line-of-sight to the observation point). For an arbitrary surface, luminance may vary in a complicated way with viewing angle. For a Lambertian surface luminance is independent of viewing angle. Many sources of military interest are near-Lambertian.

Luminance describes the photometric characteristics of a source and is not directly measurable. Luminance results in a measurable illuminance value at remote points and a measurement instrument can be calibrated in terms of either illuminance or apparent luminance. Either calibration process requires that calibration path spectral attenuation be determined and applied to the calibration source spectral distribution, since the instrument responds to the illuminance that actually exists at the measurement instrument. The transmission of short calibration path in the visible portion of the spectrum is near unity, and therefore is generally ignored. Luminance measurement systems are often imaging systems using charge-coupled device (CCD) array detectors. They are commonly calibrated using a standard extended luminance source such as an integrating sphere or high temperature blackbody. When an imaging radiometer is calibrated in terms of apparent luminance or illuminance, the measurement of a target will result in apparent luminance data. The actual luminance signature of a target can be determined from measured apparent illuminance data if the path transmission

is known and the relative spectral function of the target is known. An example of this process is given in paragraph 4.4.

4.2.5 Luminous Exitance, M_v. Luminous exitance corresponds to the radiometric quantity radiant exitance $M(\lambda)$, commonly measured in watt/m^2 or watt/cm^2. Luminous exitance is measured in units lx (lm/m^2). Luminous exitance is the quotient of luminous flux Φ_v exiting an incremental area of a surface at a given point. The differential definition is

$$M_v = \frac{d\Phi_v}{dA} \text{ (lx) or (lm/m}^2\text{)} \qquad \text{(Eq. 4-12)}$$

By convention, luminous exitance is defined to be the flux exiting a surface. It has the same units as illuminance but by convention, illuminance is defined to be the flux incident on a surface.

4.2.6 Illuminance, E_v. Illuminance corresponds to the radiometric quantity irradiance $E(\lambda)$, commonly measured in watt/m^2 or watt/cm^2. Illuminance E_v in units lux (lx) describes the luminous flux Φ_v per unit area at a distant point from a source. The differential definition is

$$E_v = \frac{d\Phi_v}{dA} \text{ (lx) or (lm/m}^2\text{)} \qquad \text{(Eq. 4-13)}$$

The unit lx is coherent to the unit lm/m^2 which is often chosen for use over lx since it is descriptive of the quantity. Illuminance, similar to irradiance, is by convention defined to describe the luminous flux incident on a surface. Luminous exitance M_v, similar to radiant exitance, is by convention defined to describe luminous flux exiting a surface. Illuminance is special in that it is the only remotely observable photometric quantity. Illuminance is produced by target luminance L_v and/or target luminous intensity I_v, modified by path transmission $\tau(\lambda)$. We will define apparent luminance L'_v and apparent luminous intensity I'_v but, similar to irradiance, illuminance is considered a detector quantity and is never qualified by the term "apparent."

For a point source, illuminance is the integral over the visual spectral band 360 nm to 830 nm of the target spectral irradiance weighted by the photopic response and the path atmospheric transmission.

$$E_v = 683 \text{ lm/W} \int_{360nm}^{830nm} E(\lambda)\, \tau(\lambda)\, V(\lambda)\, d\lambda \qquad \text{(Eq. 4-14)}$$

Using the relationship $E(\lambda)=I(\lambda)/R^2$ Equation 4-14 can be rewritten as

$$E_v = \frac{683 \text{ lm/W}}{R^2} \int_{360nm}^{830nm} I(\lambda)\, \tau(\lambda)\, V(\lambda)\, d\lambda \qquad \text{(Eq. 4-15)}$$

Defining the apparent luminous intensity as

$$I_v^{'} \equiv 683\ \text{lm/W} \int_{360nm}^{830nm} I(\lambda)\ \tau(\lambda)\ V(\lambda)\ d\lambda \qquad \text{(Eq. 4-16)}$$

Equation 4-15 can be rewritten as

$$E_v = \frac{I_v^{'}}{R^2} \qquad \text{(Eq. 4-17)}$$

For an extended source we use the relationship $E(\lambda) = \omega_s L(\lambda)$, where ω_s is the solid angle subtended by the FOV of the detecting system at the target (and is the two-dimensional angular FOV of the detecting system), to rewrite Equation 4-14 as

$$E_v = \omega_s\ 683\ \text{lm/W} \int_{360nm}^{830nm} L(\lambda)\ \tau(\lambda)\ V(\lambda)\ d\lambda = \omega_s\ L_v^{'} \qquad \text{(Eq. 4-18)}$$

Defining the apparent luminance as

$$L_v^{'} \equiv 683\ \text{lm/W} \int_{360nm}^{830nm} L(\lambda)\ \tau(\lambda)\ V(\lambda)\ d\lambda \qquad \text{(Eq. 4-19)}$$

Equation 4-18 can be rewritten as

$$E_v = \omega_s\ L_v^{'} \qquad \text{(Eq. 4-20)}$$

Where we have used the following for Equations 4-14 through Equation 4-20:

E_v = the illuminance at distance R
$I_v^{'}$ = the apparent luminous intensity
$L_v^{'}$ = the apparent luminance
$\tau(\lambda)$ = the spectral path transmission coefficient through distance R
$E(\lambda)$ = the spectral irradiance at distance R
$I(\lambda)$ = the source spectral radiant intensity
$L(\lambda)$ = the radiance
ω_s = the solid angle at the source subtended by the FOV of the detector

4.3 Photometer Calibration Techniques

Photometers are calibrated in terms of either illuminance E_v (Equation 4-17) or apparent luminance $L_v^{'}$ (Equation 4-20). The following derivations of calibration procedures include the path atmospheric transmission factor but it is recognized that over the typically short calibration paths, the atmospheric transmission across the visible spectral region is near unity and can often be justifiably ignored. Figure 4-7 presents atmospheric spectral transmission for various

horizontal, ground level paths predicted by the Air Force Research Laboratory (AFRL) Space Vehicles Directorate atmospheric model, Moderate Resolution Atmospheric Transmission (MODTRAN) v 4.0. The conditions are the 1976 standard atmosphere at mid-latitude with normal high visibility (23 km). Laboratory conditions will have these visibilities or better.

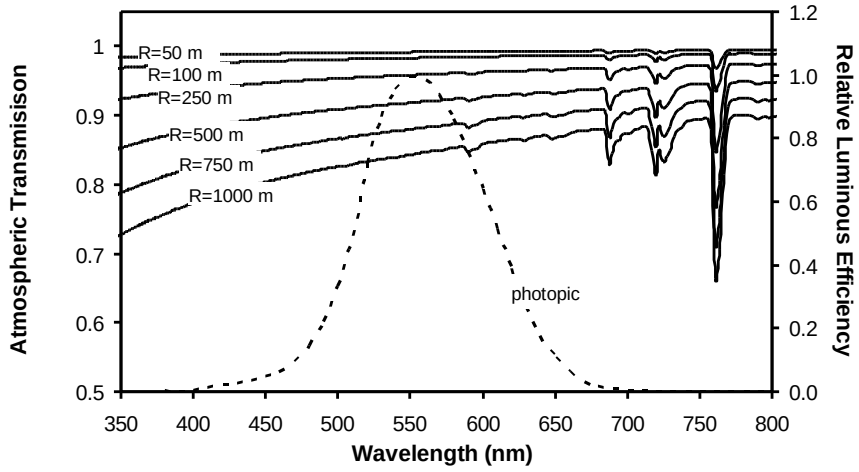

Figure 4-7. MODTRAN model predictions of atmospheric transmission, horizontal path; 1976 standard atmosphere, mid-latitude summer with normal high visibility.

Using the following integral to calculate the weighted transmission within the photopic response, the weighted transmission is calculated for the various ranges and listed in Table 4-2.

$$\tau_{photopic} = \frac{\int_{360nm}^{830nm} \tau(\lambda)\, V(\lambda)\, d\lambda}{\int_{360nm}^{830nm} V(\lambda)\, d\lambda} \qquad \text{(Eq. 4-21)}$$

TABLE 4-2. WEIGHTED ATMOSPHERIC TRANSMISSION WITHIN THE PHOTOPIC RESPONSE FOR SPECTRAL TRANSMISSION FUNCTIONS OF FIGURE 4-7.

Horizontal Range	$\tau_{photopic}$
50 m	**0.99**
100 m	**0.98**
250 m	**0.96**
500 m	**0.91**
750 m	**0.88**
1000 m	**0.84**

4.3.1 Illuminance Calibration. Calibration in terms of illuminance can be accomplished by the methods shown below.

a. Method 1: Expose the photometer to a standard luminous intensity source such as the 1000 W FEL lamp previously shown in Figure 4-5. The illuminance at range R is given directly by Equation 4-17 where the apparent luminous intensity is given by Equation 4-16. This is a simple set-up that requires minimal hardware. A linearity measurement with illuminance level can be made using the range-squared effect if the alignment in the FOV can be held when R is increased or decreased.

b. Method 2: Expose the photometer to a standard luminance extended source directly behind a precision aperture with area A_a used to control the source area exposed to the photometer. The extended source can be the output port of a blackbody cavity or the output port of an integrating sphere. The apparent luminous intensity of the extended source through the aperture is given by

$$I'_v = L'_v \, A_a \qquad \text{(Eq. 4-22)}$$

Note that the apparent luminance L'_v is given by Equation 4-19. The illuminance at range R is then given by Equation 4-17. A linearity measurement with illuminance level can be made by varying the area of the precision aperture as long as the area of the exposed source is well within the FOV of the detecting system.

c. Method 3: Place a standard luminance extended source directly behind a precision aperture with area A_a at the focal point of a collimating mirror, and place the photometer in the collimated beam with the restriction that the physical dimensions of the aperture are small enough to assume a point-like source to the collimating mirror such that aberrations are avoided.

(1) Advantages of this Set-up.

- The collimated beam simulates an object at infinity which puts the object at the correct distance for photometers focused at infinity while the actual calibration path is only focal length f + beam length B.
- It can be used to conduct a linearity measurement with illuminance level by varying the aperture area A_a.
- An FOV map can be obtained by pivoting the photometer in the beam around a point in the entrance pupil of the collection optics.

(2) Disadvantage of this Set-up. The spectral reflection of the mirror must be known to correctly calculate the illuminance of the beam. The concept of a collimating mirror is presented in Figure 4-8. To better illustrate the concept, unfold the collimating mirror assembly as a small luminous source at the focal point of a thin lens as shown in Figure 4-9.

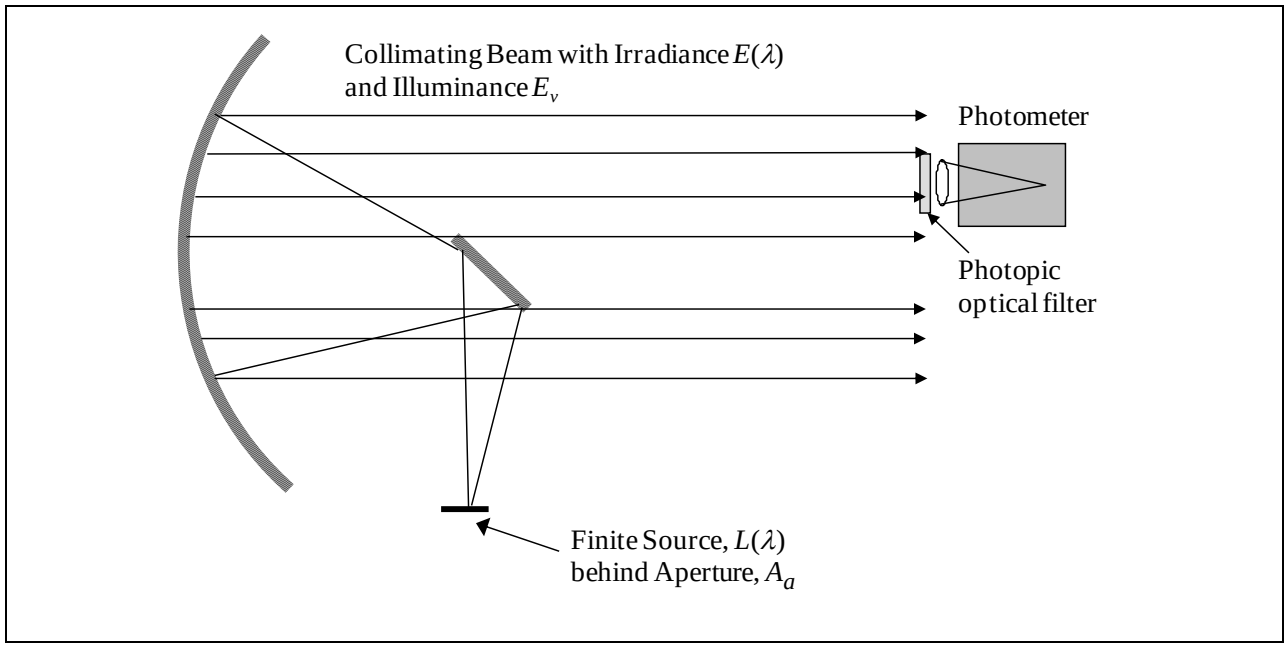

Figure 4-8. Concept of a collimating mirror.

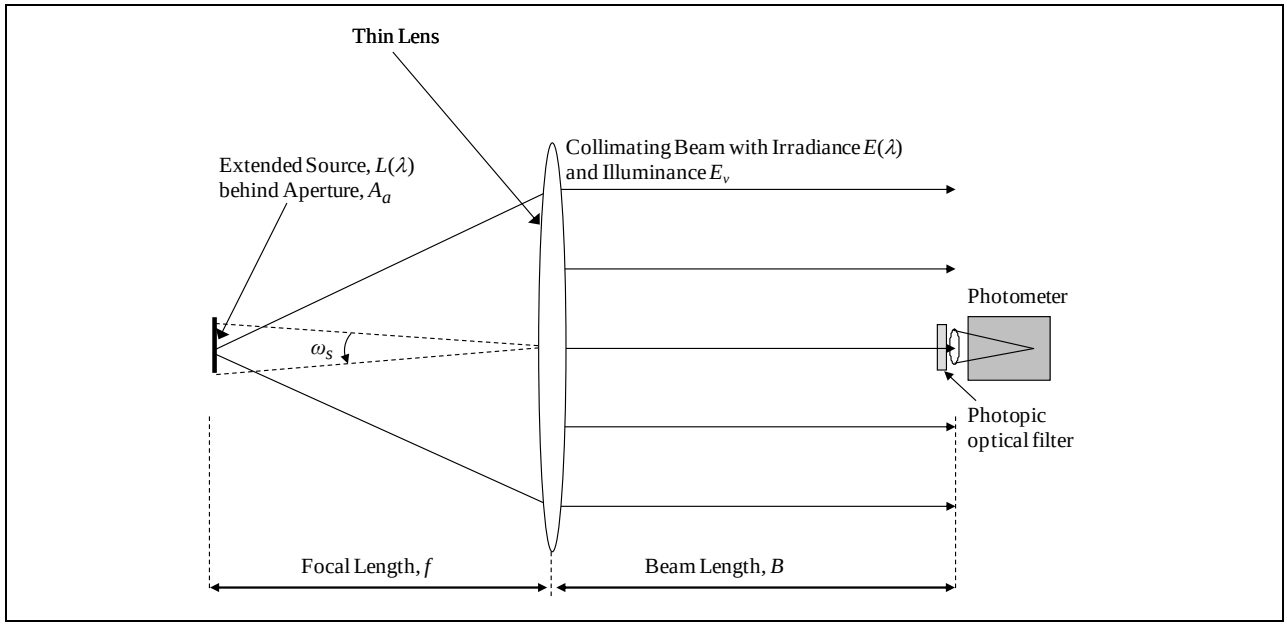

Figure 4-9. Simulation of collimating mirror.

Referring to Figure 4-9, an extended source of calibrated, known, spectral radiance is placed at the focal point of the lens. A precision aperture is placed immediately in front of the extended source to limit the area exposed to the lens. The radiant intensity of the source through the aperture is

$$I(\lambda) = L(\lambda) A_a \qquad \text{(Eq. 4-23)}$$

The irradiance at the lens is

$$E(\lambda) = \frac{I(\lambda)\, \tau_f(\lambda)}{f^2} \qquad \text{(Eq. 4-24)}$$

The illuminance at the photometer is

$$E_v \equiv \frac{683\ \text{lm/W}}{f^2} \int_{360nm}^{830nm} I(\lambda)\, \tau_{f+B}(\lambda)\, \rho(\lambda)\, V(\lambda)\, d\lambda \qquad \text{(Eq. 4-25)}$$

Where

$\tau_{f+B}(\lambda)$ = the spectral transmission over path $f + B$
$\rho(\lambda)$ = the spectral refection coefficient of the mirror, or in this model, the spectral transmission of the lens

During a calibration event, the luminous power in a specific time interval that produces current i_{cal} by the photometer is, defining A_d to be the effective area of the collection optics of the photometer,

$$\Phi_v = E_{v,cal}\, A_d \qquad \text{(Eq. 4-26)}$$

The calibration response is the ratio of the measured current to the luminous power. The luminance calibration response is then

$$RESP = \frac{i_{cal}}{E_{v,cal}\, A_d}\ \text{(amp/lm)} \qquad \text{(Eq. 4-27)}$$

When the photometer is used to view a target under test, the current caused by the target illuminance in the same time interval is

$$i_{target} = RESP\ (E_{v,\,target}\, A_d) \qquad \text{(Eq. 4-28)}$$

Using Equation 4-27 in Equation 4-28 we can solve for $E_{v,target}$ and recognize that the effective area of the collection optics is a constant of the calibration and cancels out (see Figure 4-29). If the photometer is calibrated for illuminance against an illuminance standard, the effective area of the collection optics does not need to be known.

$$E_{v,target} = \frac{i_{target}}{i_{cal}} \frac{E_{v,cal} A_d}{A_d} = \frac{i_{target}}{i_{cal}} E_{v,cal} \qquad \text{(Eq. 4-29)}$$

More often than not the photometer will have an analog-to-digital component of the collection electronics and Equation 4-29 will have the more familiar form of Equation 4-30.

$$E_{v,target} = \frac{counts_{target}}{counts_{cal}} \frac{E_{v,cal} A_d}{A_d} = \frac{counts_{target}}{counts_{cal}} E_{v,cal} \qquad \text{(Eq. 4-30)}$$

The apparent target luminous intensity is calculated from the target illuminance if the range to the target is known.

$$I'_{v,target} = E_{v,target} R^2_{target} \qquad \text{(Eq. 4-31)}$$

The actual luminous intensity can be determined by removing the path atmospheric attenuation if the path spectral atmospheric attenuation $\tau(\lambda)$ is known and the relative spectral function of the target is known. A practical example of this technique is at paragraph 4.4.

4.3.2 Luminance Calibration. Calibration in terms of luminance can be accomplished in the following methods:

a. Method 1: Expose the imaging system to an extended source of calibrated, known spectral radiance, as is illustrated in Figure 4-10. The source can be an extended blackbody or the output port of a large integrating sphere. It is important that IFOV of an individual detector element be completely contained within a region of uniform radiance. This is a simple set-up with minimal hardware.

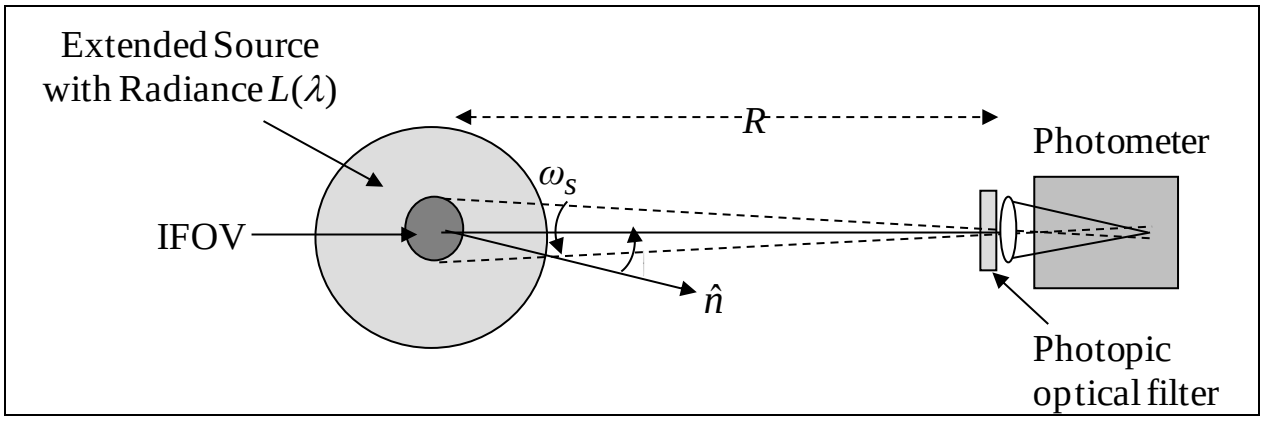

Figure 4-10. Geometry of luminance calibration.

The illuminance at the photometer is given by Equation 4-20 where the apparent luminance is defined in Equation 4-19.

b. Method 2: Expose the imaging system to an extended reflective Lambertian plate that is illuminated by an irradiance standard with irradiance $E(\lambda)$ at the specified distance, as illustrated in Figure 4-11. With $\rho(\lambda)$ defined as the spectral reflection coefficient of the plate, the radiance of the reflective Lambertian plate is

$$L(\lambda) = \frac{E(\lambda)\,\rho(\lambda)}{\pi} \qquad \text{(Eq. 4-32)}$$

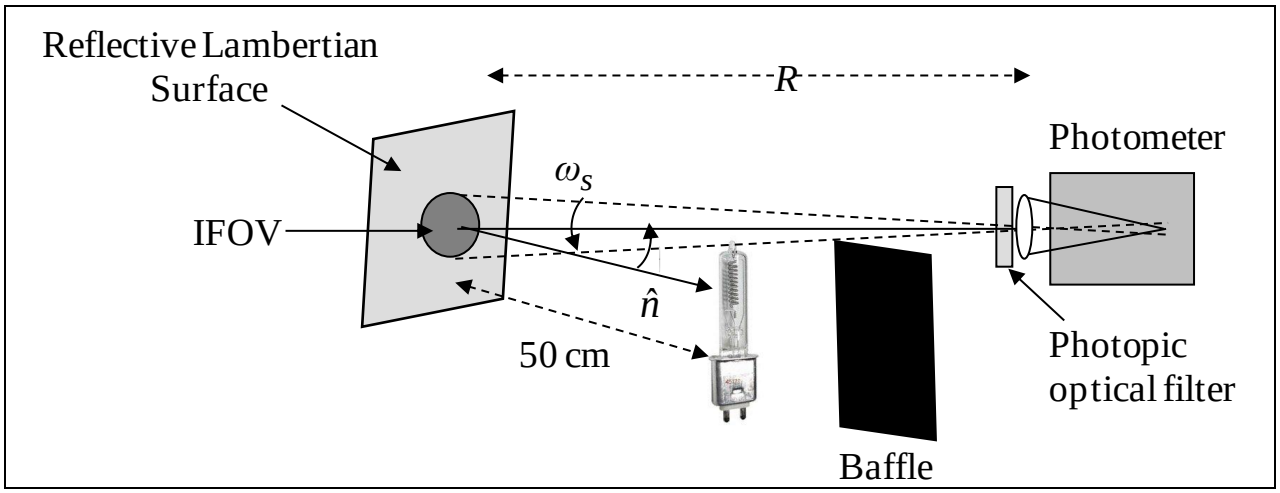

Figure 4-11. Creating a luminance standard with a reflective Lambertian plate and an irradiance standard.

This set-up has the advantage in that it can be used to measure linearity with luminance level by exploiting the range-squared effect to decrease the irradiance at the plate by increasing the range R.

c. Method 3: Place an extended radiance source at the focal plane of a collimating mirror. Refer to Figure 4-8 for the concept of a collimating mirror. To better illustrate the concept, unfold the collimating mirror assembly as an extended luminance source at the focal point of a thin lens as shown in Figure 4-12.

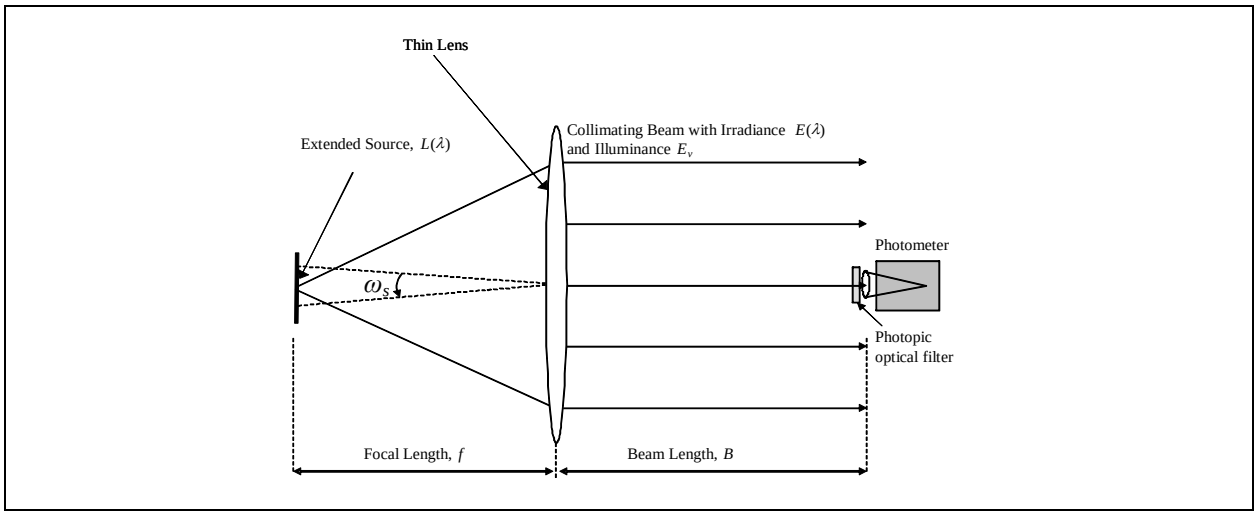

Figure 4-12. Simulation of a collimating mirror with extended source at the focal plane.

The set-up has the advantage of simulating an object at infinity which puts the object at the correct distance for imaging photometers focused at infinity while the actual calibration path is only focal length f + beam length B. It has the disadvantage that the spectral reflection of the mirror must be known to correctly calculate the illuminance of the beam. It also has the disadvantage that the spatial footprint of the IFOV of the single detector at the plane of the source can be large, requiring a larger extended source which could introduce aberrations in the collimated beam.

The illuminance at the photometer is given by Equation 4-20 where the apparent luminance is defined as:

$$L_v^{'} \equiv 683 \text{ lm/W} \int_{360nm}^{830nm} L(\lambda)\, \tau_{f+B}(\lambda)\, \rho(\lambda)\, V(\lambda)\, d\lambda \qquad \text{(Eq. 4-33)}$$

Where

$\tau_{f+B}(\lambda)$ = the path transmission along path f+B
$\rho(\lambda)$ = the spectral reflection coefficient of the mirror or, in this model, the spectral transmission coefficient of the lens

During a calibration event, the luminous power Φ_v in a specific time interval that produces current i_{cal} by the photometer is given by Equation 4-34, where A_d is defined to be the effective area of the collection optics of the photometer.

$$\Phi_v = E_{v,cal}\, A_d = L_{v,cal}\, \omega_s\, A_d \qquad \text{(Eq. 4-34)}$$

The calibration response is the ratio of the measured current to the luminous power. The luminance calibration response is then

$$RESP = \frac{i_{cal}}{L_{v,cal}\,\omega_s\,A_d} \quad \text{(amp/lm)} \qquad \text{(Eq. 4-35)}$$

When the photometer is used to view a target under test, the current caused by the target illuminance in the same time interval is

$$i_{target} = RESP\,(L'_{v,\,target}\,\omega_s\,A_d) \qquad \text{(Eq. 4-36)}$$

Using Equation 4-35 in Equation 4-36 we can solve for $L'_{v,\,target}$ and recognize that the effective area of the collection optics and the FOV of the single detector element are constants of the calibration and cancel out. If the photometer is calibrated for luminance against a luminance standard, the effective area of the collection optics and the FOV of the single detector element do not need to be known.

$$L'_{v,\,target} = \frac{i_{target}}{i_{cal}}\frac{L_{v,\,cal}\,\omega_s\,A_d}{\omega_s\,A_d} = \frac{i_{target}}{i_{cal}}\,L_{v,\,cal} \qquad \text{(Eq. 4-37)}$$

More often than not, the photometer will have an analog-to-digital component of the collection electronics and Equation 4-37 will have the more familiar form

$$L'_{v,\,target} = \frac{counts_{target}}{counts_{cal}}\frac{L_{v,\,cal}\,\omega_s\,A_d}{\omega_s\,A_d} = \frac{counts_{target}}{counts_{cal}}\,L_{v,\,cal} \qquad \text{(Eq. 4-38)}$$

The "source" luminance can be determined by removing the path atmospheric attenuation if the path spectral atmospheric attenuation $\tau(\lambda)$ is known and the relative spectral function of the target is known. A practical example of this technique is presented in Paragraph 4-4.

A typical target is not likely to have the same luminance value at all points on its surface, or to have the same spectral distribution from point-to-point. Calibration sources are designed to have a uniform spatial luminance and a known spectral distribution over their surface. Unless a target has a uniform luminance within a measurement instrument IFOV, the measurement will yield an average luminance value for that IFOV. Luminance measurement systems may not have the same resolution as the human eye (1 arc-minute = approximately 0.3 mrad). Therefore, a measurement of a source having a very non-uniform spatial radiance may result in average radiance measurements that are different from that seen by the eye (or another photometer with a different IFOV).

4.4 Effective Path Transmission

4.4.1 Correcting for Atmosphere Attenuation. It is possible to remove the attenuation of the atmospheric transmission from the measured apparent luminous intensity $I_v^{'}$ and apparent luminance $L_v^{'}$ if the spectral transmission function is known and if the relative spectral shape of the target is known.

The desired photometric quantity is

$$X_v = 683\ \text{lm/W} \int_{360nm}^{830nm} X(\lambda)\, V(\lambda)\, d\lambda \qquad \text{(Eq. 4-39)}$$

Where

X_v indicates either L_v or I_v
$X(\lambda)$ indicates either $L(\lambda)$ or $I(\lambda)$.

The measured quantity is

$$X_v^{'} = 683\ \text{lm/W} \int_{360nm}^{830nm} X(\lambda)\, V(\lambda)\, \tau(\lambda)\, d\lambda \qquad \text{(Eq. 4-40)}$$

We ratio Equation 4-39 to Equation 4-40 and solve for X*v*.

$$X_v = X_v^{'} \frac{683\ \text{lm/W} \int_{360nm}^{830nm} X(\lambda)\, V(\lambda)\, d\lambda}{683\ \text{lm/W} \int_{360nm}^{830nm} X(\lambda)\, V(\lambda)\, \tau(\lambda) d\lambda} \qquad \text{(Eq. 4-41a)}$$

$$X_v = X_v^{'} \frac{\int_{360nm}^{830nm} X(\lambda)\, V(\lambda)\, d\lambda}{\int_{360nm}^{830nm} X(\lambda)\, V(\lambda)\, \tau(\lambda) d\lambda} \qquad \text{(Eq. 4-41b)}$$

Since the spectral radiometric quantity $X(\lambda)$ is in both the numerator and denominator, we can replace it with the relative (normalized) spectral function which we define to be $X_{rel}(\lambda)$. Then, we define the weighted transmission to be

$$\tau_{weighted} \equiv \frac{\int_{360nm}^{830nm} X_{rel}(\lambda)\, V(\lambda)\, \tau(\lambda)\, d\lambda}{\int_{360nm}^{830nm} X_{rel}(\lambda)\, V(\lambda)\, d\lambda} \qquad \text{(Eq. 4-42)}$$

and Equation 4-41b is rewritten as

$$X_v = \frac{X_v'}{\tau_{weighted}} \qquad \text{(Eq. 4-43)}$$

4.4.2 Correcting for Atmosphere Attenuation: an Example. As a practical example of this technique, we consider the solar radiance at the top of the atmosphere and at ground level. Figure 4-13 presents the solar spectrum at the top of the atmosphere (extraterrestrial) and the solar spectrum through the atmosphere (Reference 4f). The spectral atmospheric transmission used to attenuate the solar spectrum is presented in Figure 4-14, which (for this exercise) was calculated by dividing $E_2(\lambda)$ by $E_1(\lambda)$ irradiances given by Reference 4f.

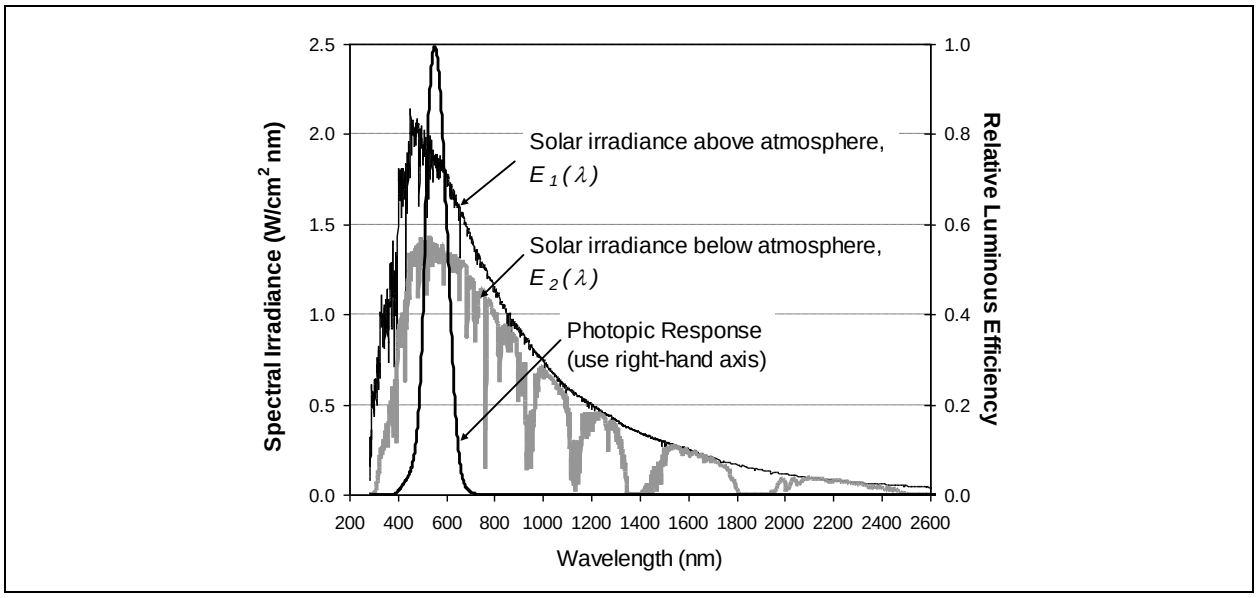

Figure 4-13. Solar irradiance at the top of the atmosphere (extraterrestrial) and at ground level.

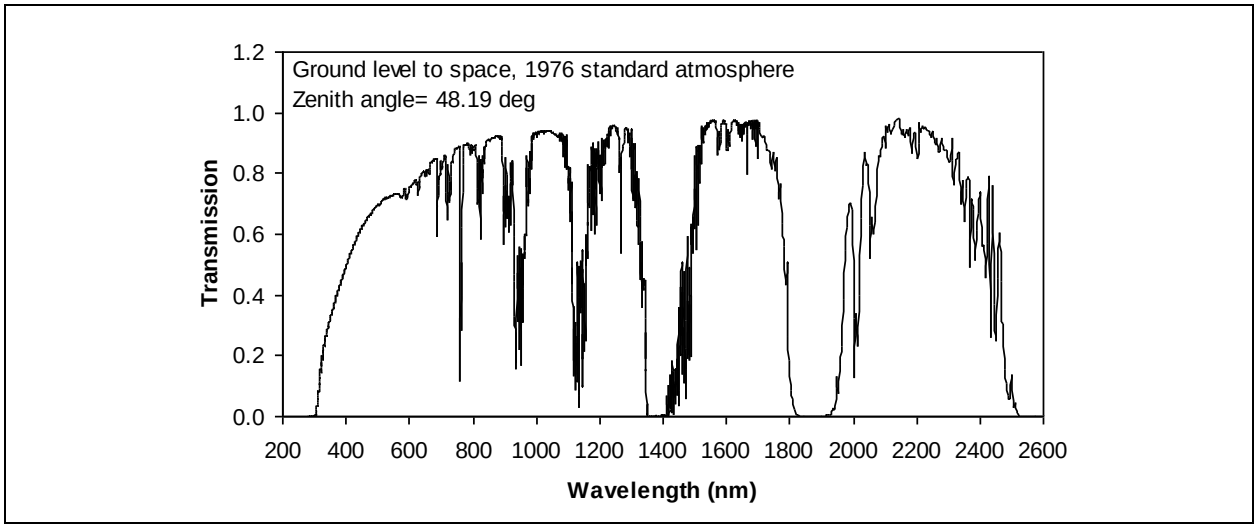

Figure 4-14. Spectral atmospheric transmission used for this exercise.

As a side note, the spectrally integrated irradiance of the extraterrestrial solar irradiance is the standard solar constant, E_e, which equals

$$E_e = \int_0^{4000\,\mathrm{nm}} E_1(\lambda)\, d\lambda = 1.35\mathrm{x}10^3\ \mathrm{W/m^2}$$

It is interesting to note that about half the radiant flux of the solar constant is within the VIS spectral region. If we integrate the extraterrestrial solar spectral irradiance from 360 nm to 830 nm, the effective irradiance is 734 W/m^2, which is 54 percent of the solar constant.

The illuminance for the extraterrestrial and ground level solar powers are calculated from Equation 4-39, as

$$E_{1,v} = 683\ \mathrm{lm/W} \int_{360nm}^{830\,nm} E_1(\lambda)\, V(\lambda)\, d\lambda = 1.35\mathrm{x}10^5\ \mathrm{lm/m^2} \qquad \text{(Eq. 4-44)}$$

$$E_{2,v} = 683\ \mathrm{lm/W} \int_{360nm}^{830\,nm} E_2(\lambda)\, V(\lambda)\, d\lambda = 0.982\mathrm{x}10^5\ \mathrm{lm/m^2} \qquad \text{(Eq. 4-45)}$$

The following is an example problem to illustrate the extraterrestrial and ground level solar powers.

a. Problem. Given the ground level solar illuminance 0.982 x 10^5 lm/m^2, and given the relative (normalized) solar spectral function and the path atmospheric transmission plotted in Figure 4-15, derive the extraterrestrial solar illuminance.

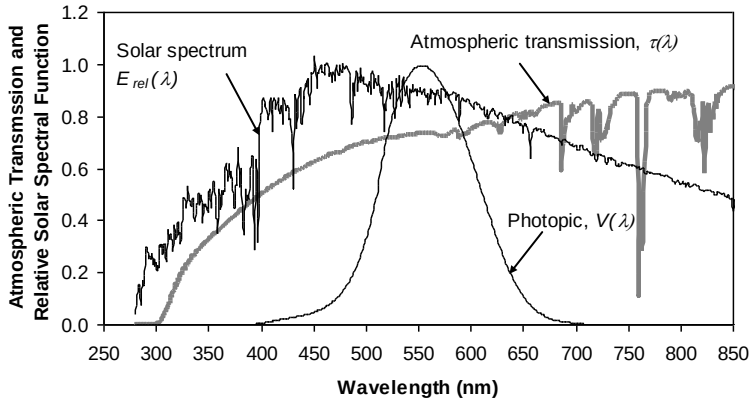

Figure 4-15. Relative (normalized) solar spectrum and path atmospheric transmission.

b. Answer. Using Equation 4-38 to calculate a weighted atmospheric transmission, $\tau_{weighted,}$

$$\tau_{weighted} \equiv \frac{\int_{360nm}^{830nm} E_{rel}(\lambda)\, V(\lambda)\, \tau(\lambda)\, d\lambda}{\int_{360nm}^{830nm} E_{rel}(\lambda)\, V(\lambda)\, d\lambda} = 0.729$$

Equation 4-39 is then used to calculate the extraterrestrial solar illuminance, which agrees with the known extraterrestrial solar illuminance $E_{1,v}$ shown in Equation 4-40.

$$E_v = \frac{0.982x10^5 \text{ lm/m}^2}{0.729} = 1.35\text{x}10^5 \text{ lm/m}^2$$

4.5 References for Chapter 4

a. International Organization for Standardization (ISO) (2005). Photometry-The CIE System of Physical Photometry, ISO 23539 (CIE S 010/E:2004) (1st edition, Aug 1, 2005).

b. International Bureau of Weights and Measures (BIPM) (2006). The International System of Units (SI) (8th edition) pg.173.

c. Ohno, Y. (1997). Photometric Calibrations, NIST Special Publication 250-37. U.S. Department of Commerce Technology Administration, National Institute of Standards and Technology (NIST).

d. Zong, Y., Brown, S., and Ohno, Y. (1997). Realization of the Candela, the Lumen,and Other Photometric Units, Optical Technology Division, NIST, http://physics.nist.gov/Divisions/Div844/facilities/photo/Candela/photo.html, Last update February 2008.

e. Newport Corporation. Oriel Product Training, Spectral Irradiance, (Figure. 16, pg 32), www.newport.com/file_store/Supporting_Documents/Tech_Ref_Spectral_Irradiance37.pdf and www.newport.com/600---1000-W-QTH-Spectral-Irradiance-Data/409214/1033/catalog.aspx (Figure 16). Web pages retrieved June 2008.

f. American Society for Testing and Materials (ASTM). Terrestrial Reference Spectra for Photovoltaic Performance Evaluation, http://rredc.nrel.gov/solar/spectra/am1.5/ASTMG173/ASTMG173.html. Retrieved July 7, 2008

This page intentionally left blank.

CHAPTER 5

TYPES OF MEASUREMENT SYSTEMS

Measurement instrumentation systems are as varied as the targets they are designed to measure. Commonly used names of some of these measurement systems are radiometers, photometers, spectrometers, spectral radiometers, imagers, and spectral imagers. Some systems are referred to as "staring" because they are designed to measure transient phenomena or modulated sources. Some systems are referred to as "scanning" in that they are designed to measure constant or slowly changing sources. Instruments may have a single detector, a linear detector array, or a two dimensional detector array. Some instruments are thermoelectrically cooled, others are cryogenically cooled, and some are not cooled at all. However, all these instruments have one thing in common; that is, when placed in a flux field of optical energy, they produce recordable outputs that have a calibrated relationship to the level of the optical flux arriving at the measurement system. Target signature data is derived from these outputs and other recorded data. Table 5-1 contains a list of instrument types. Table 5-2 contains a list of domains of spatial/spectral radiometers (commonly called spectral imagers) with typical spectral resolution and applications (Reference 5a). The descriptions in Table 5-1 and Table 5-2 are not identical throughout the scientific community because of the variances in instruments and their associated technologies. However, there is general agreement with the descriptions by the experimenters associated with DoD radiometric testing.

TABLE 5-1. INSTRUMENT TYPES

Name	Common names	Attributes
Band radiometer	Radiometer	Fast data rates. Simple designs, highly reliable, good signal-to-noise. Data is most difficult to interpret because no spatial or spectral resolution.
Spectral radiometer	Spectrometer	
Spatial radiometer	Imager, scanning or staring	
Spatial/spectral radiometer	Hyperspectral	High spectral resolution. Usually based on FTIR technology or grating spectrometer technologies for high spectral resolution.
	Multispectral	Lower spectral resolution compared to hyperspectral systems but usually have greater spatial resolution. Usually based on optical filter technology.
	Broadband or Panochromatic	Very wide spectral band. Usually based on optical filter technology.
Band photometer	Photometer	Banded within CIE eye response
Spectral photometer	Spectral photometer	Spectral response follows CIE eye response
Spatial photometer	Photometric imager	Banded within CIE eye response

TABLE 5-2. DOMAINS OF SPECTRAL IMAGING

Category	Spectral Band Count	Spectral Resolution	Application	Example System
VIS Broadband (Panchromatic)	One	0.5 μm Broad, 0.4 μm to 0.9 μm	Monitor solar radiation	
IR Broadband (Panchromatic)	One	2 μm Broad, 3 μm to 5 μm	Monitor atmosphere	
Multispectral	A few dozen	0.020 μm to 0.1 μm	• Multispectral classification of dissimilar materials (vegetation, soils, water, etc.) • Military target detection, camouflage detection	• LANDSAT, space based (Dept. of Commerce) • AVHRR, space based (Jet Propulsion Lab) MTI, Dept. of Energy/Sandia/LANL
Hyperspectral	Hundreds to a few hundred	0.01 μm to 0.015 μm	• Precise surface material identification • Environmental monitoring • Military target identification • Detection of selected gases • Atmospheric effects must be known to detect gases	• Hyperspectral Digital Imagery Collection Experiment (HYDICE) – airplane based (Naval Research Laboratory) • AVIRIS, space based, (Jet Propulsion Lab) • SEBASS, airplane based (Aerospace Corp.) GIFTS, space based (NASA EO-3 NMP)
Ultraspectral[(a)]	Several hundreds	0.1 cm^{-1} to 0.3 cm^{-1}	• Gas species detection • High resolution permits in-situ correction of atmospheric effects due primarily to water and ozone	• Mostly single detector ground-based systems • Fourier-Transform spectrometers abound here

(a) The use of wavenumbers (cm^{-1}) for the spectral units in ultraspectral applications show the influence of spectroscopists.

Reprinted with permission of Dr. Terrence S. Lomheim, UCSB Extension Short Course: Modern Infrared Detectors and System Applications, June, 2009

5.1 Radiometer

The word "radiometer" is used to describe any instrument that is capable of quantitatively measuring the level of electromagnetic radiation in some spectral band. The term is usually used with a modifier, such as an "IR radiometer" or a "microwave radiometer." When placed in an

electromagnetic field, radiometers collect flux and generate a numeric output signal related to the power flux density (irradiance in units W/cm^2). Radiometers may use a single detector covering a fairly large FOV (staring radiometer), use a single detector with a small IFOV that scans a fairly large FOV (scanning radiometer) or use a focal plane array (FPA) imager which consists of an array of small detectors with small IFOV to continually measure radiation arriving within a fairly large FOV. One of the defining quantities for a radiometer is that each detector produces a single output representing the total radiation within a certain spectral band. It produces no data to determine the spectral distribution within the defined band.

5.1.1 Staring Band Radiometer. A staring band radiometer is the simplest of the signature measurement systems. It consists of an optical system to collect EO flux and focus that flux onto a single detector. The detector converts the collected flux into an electrical signal that has a calibrated relationship to the level of the existing flux density. The system generally has a relatively large FOV, often much larger than the angular size of a target being measured. A large FOV collects a large amount of flux from existing backgrounds and foregrounds, both of which may be highly variable during target signature measurements. Often background and foreground radiance produces flux at the measurement system that is much larger than the flux produced by the target being measured. Signal processing, such as the use of spatial filtering (reticles, choppers) is often used to discriminate in favor of small targets. Reticles are commonly used in non-imaging seekers and are effective in enhancing the signal from targets of small extent and suppressing signals from larger sources, but they have faults when used in radiometers. Such systems may produce target signatures which are a function of the angular size of a target, an effect which is very difficult to remove. In such a case, although the signal from the smaller target is measured, it would be difficult to quantify the signal in engineering units.

While staring band radiometers are simple in design, converting the radiometer output signal to target signature data is can be complicated. Removing residual background signals and accounting for variations of radiometer response to a target when measurements are made at various ranges is difficult. Since the spectral response of a radiometer is typically not uniform and the transmission of the measurement path varies with wavelength, correcting measured data from band radiometers must take into the account the weighted atmospheric transmission, $\tau_{weighted.}$ A weighted transmission factor can be calculated if the spectral path attenuation, the radiometer relative spectral response, and the relative spectral function of the target are known. A technique to calculate a weighted transmission factor is discussed in paragraph 2.6 and is shown in Equation 2-47.

5.1.2 Scanning Radiometer. Reducing the FOV of a staring radiometer proportionally reduces the level of irradiance received from the background. The FOV is often controlled by reducing the size of the detector, which has the advantage of also reducing the internal radiometer noise. However, if the FOV is made too small, accurately pointing on a target becomes an issue and the FOV may not include radiation from the entire target. One way to overcome these problems is to use a system which has a small IFOV and scan the IFOV over a larger FOV. For targets whose signature is fairly stable over time, such systems are satisfactory. However, if the target signature changes too rapidly, signature measurements with such a system may have serious errors because of the time gap between subsequent scans. All radiometer detectors have a finite time constant and therefore scanning from pixel-to-pixel must allow sufficient time on each pixel

for the system output to arrive at a stable value. One advantage of a scanning system is that there is only one detector to be calibrated.

A scanning radiometer produces a single output in time in response to radiation within a relatively wide spectral band that typically does not have a uniform spectral response. A scanning radiometer does not produce spectral information; instead it is calibrated in terms of effective irradiance or effective radiance to produce effective target signature data. Converting measured effective data to actual target signature data requires knowledge of the target spectral emission function and the spectral atmospheric attenuation function.

5.1.3 Staring Imaging Systems. The use of modern FPA imagers allows a large FOV to be constantly observed by using an array of small detectors producing small IFOV. This capability eliminates some of the problems of a scanning radiometer because each detector is not required to move quickly from pixel-to-pixel to cover the larger FOV in a reasonable time. Spatial/ temporal variations in a target's signature are, therefore, more easily determined using a staring imaging system. An FPA based system may have millions of pixels. Since many target signatures are spatially variable, the high spatial resolution possible with FPA based systems produces more detailed target signatures than most systems. This capability however, is not without problems. Electrical and optical crosstalk, variations in the characteristics of individual detector elements, and dynamic range are areas of concern that must be characterized.

A staring imaging radiometer produces an output in time for each detector in response to radiation within a relatively wide spectral band that typically does not have a uniform spectral response; in other words, no spectral information is produced. Just as for the scanning radiometer, the staring imaging radiometer is calibrated in terms of effective irradiance or effective radiance to produce effective target signature data. Converting measured effective data to actual target signature data requires knowledge of the target spectral emission function and the spectral atmospheric attenuation function.

5.1.4 Spectral Radiometer. Band radiometers and imagers use optical filters which are usually changeable to obtain the desired measurement system spectral response. These systems do not produce spectral distribution data within that band. Spectral radiometers add a capability to break a wide band into a large number of small spectral intervals and produce an output for each of these intervals. This capability may be obtained in a variety of ways, including:

a. Using a number of narrow band filters and sequentially placing them within the measurement system optical train.
b. Using a continuously variable filter which is rotated within the optical train.
c. Using a dispersive element, such as a grating or prism, to either scan the spectrum across a single detector or onto a linear array of detectors.
d. Using an interferometer technique such as a Fourier Transform System to produce an output that can be mathematically processed into spectral data.

5.1.5 Staring Spectral Radiometer. A staring spectral radiometer is most often referred to as a spectrometer. It is basically the same as the staring band radiometer described in paragraph 5.1.1, except that the fixed optical filter is replaced by an optical dispersing component and the single detector is replaced by a detector array. The dispersing component

breaks the wide spectral band into narrow spectral bands and the array of detectors individually measures the narrow spectral bands, therefore producing a spectrally resolved target signature. The spectral resolution is defined by the dispersion (wavelength/angle or wavelength/length) of the dispersing component and the width of the individual detector elements along the dispersion dimension. For example, if the dispersion is 20 nm/mm in the plane of the array and the detector elements have a 0.025 mm pitch, the spectral resolution (ignoring point spread function and cross talk) is 0.50 nm.

The staring spectral radiometer has some of the same shortcomings as staring band radiometers mentioned in paragraph 5.1.1. It does, however, have several advantages in addition to providing a spectral signature. Since, within a narrow spectral interval, the radiometer spectral response is generally nearly uniform and the fact that the atmospheric attenuation is nearly constant within that band, correcting measured data for atmospheric effects is much easier and more precise. A spectral radiometer does not have to be calibrated in terms of effective irradiance, but can be calibrated in terms of spectral irradiance. The measured target data will be in terms of spectral irradiance. As an illustration of this concept, refer to Equation 2-12a (repeated below as Equation 5-1) for the effective irradiance of a point source. For each narrow band of a spectral measurement, the quantities inside the integrals are constants (as shown in Equation 5-2a, Equation 5-2b, and Equation 5-2c). Therefore, the integral of Equation 5-1 reduces to Equation 5-3 for the irradiance in the one narrow spectral band at wavelength λ. The irradiance in the narrow band is a spectral quantity and not an effective quantity.

$$E_e = \frac{1}{R^2}\int_{\lambda_1}^{\lambda_2} I(\lambda)\tau(\lambda)r(\lambda)d\lambda \qquad \text{(Eq. 5-1)}$$

$$\tau(\lambda) = \tau_\lambda \qquad \text{(Eq. 5-2a)}$$

$$r(\lambda) = r_\lambda \qquad \text{(Eq. 5-2b)}$$

$$I(\lambda) = I_\lambda \qquad \text{(Eq. 5-2c)}$$

$$E_\lambda = \frac{I_\lambda\, \tau_\lambda\, r_\lambda}{R^2} \qquad \text{(Eq. 5-3)}$$

Where:

R	=	the distance between the source and the sensor.
$r(\lambda)$	=	the spectral response of the observing system, a constant r_λ within a narrow spectral band at wavelength λ.
$\tau(\lambda)$	=	the spectral atmospheric transmission, a constant τ_λ within a narrow spectral band at wavelength λ.
$I(\lambda)$	=	the spectral radiant intensity of the source, a constant I_λ within a narrow spectral band at wavelength λ.

Targets of military interest have different spectral distributions for different points on the target. A staring spectral radiometer produces only an average spectral distribution for an entire target and therefore provides less target signature information than a spatial/spectral radiometer. If a target's spatial/spectral signature was stable over a long time period, one could envision measuring the spatial/spectral signature by moving a small FOV over the target, either manually or using FOV scanning technique while scanning each IFOV spectrally. However, targets of military interest are much too variable to use such a technique. Characterization and calibration of a spectral radiometer requires more effort and additional equipment than does the characterization and calibration of a band radiometer.

5.1.6 Spatial/Spectral Radiometer. By combining a staring FPA with an interferometer, such as a Michelson interferometer cube, one can have a system that breaks a target into a very large number of pixels and rapidly and repetitively produces high resolution spectral distribution data for each pixel. Although such instruments are much more complicated than other systems and require significantly more detailed characterization, calibration, and data reduction, the data produced by these instruments have significantly more general use than does that collected using other types of measurement systems.

Several spatial/spectral systems have been developed in the last few years, including the Multispectral Infrared Radiometric System (MIRS) at the Aberdeen Test Center (ATC) and the Spatial/Spectral Airborne Radiometric Infrared System (SARIS) at Eglin AFB. Both are based on FPA and the Michelson interferometer technologies.

5.2 Photometer

Basic differences between a radiometer and a photometer are very small. A photometer is basically a radiometer equipped with a filter that matches the spectral response of a "standard" human eye under normal illumination conditions. A photometer is calibrated in terms of illuminance (lm/m^2) whereas a radiometer is calibrated in terms of irradiance (W/m^2). Illuminance is basically the effective irradiance for a system with the response of the human eye. The photopic and scotopic response of the eye were previously discussed in Chapter 4.

5.2.1 Staring Photometer. These instruments are the least complex of the visible signature measurement systems. They consist of an optical system that collects optical flux and then focuses that flux onto a single detector. The detector converts the collected flux into an electrical signal that has a calibrated relationship to the level of the existing luminous flux density. Photometers make measurements in a region of the spectrum where radiation from the sun is at its peak level. Targets must be very hot to produce visible radiation, much less to compete with solar radiation at a temperature of the order of 6000 K. In fact, target signatures are often dominated by reflected sunlight or skylight.

The capability to detect and identify targets is very important in military operations. Photometric data of targets and backgrounds over a wide range of luminance levels is required to make estimates of the capability of a human observer to accomplish this task.

While staring photometers are not complex, converting the output signal to actual target signature data is difficult. Removing residual background signals and accounting for variations

of photometer response to a target when measurements are made at various ranges is very difficult. Since the spectral response of photometers is intentionally not uniform and the transmission of the measurement path varies with wavelength, correcting measured target photometric signature data for these effects often results in target signature errors. Fortunately, clear air atmospheric attenuation is relatively low in the visible. However, attenuation due to scattering of target radiation may be difficult to quantify.

5.2.2 Staring Imaging System. The use of photographic film has long been used to record visible scene luminance distributions. When the camera/film system is filtered to approximate the spectral distribution of the human eye, it can collect target and background spatial signature data. The development of the film must be carefully controlled and the spatial density of scenes must be scanned and calibrated to obtain data; this process is fairly laborious. Until recently, film produced a spatial resolution much greater than was possible using electronic imaging systems.

The use of modern FPA and CCD detectors allows a large FOV to be constantly observed by using an array of small detectors producing images of high spatial resolution. Therefore, spatial/temporal variations in a target signature can be determined in real time. Typically, CCD based systems have millions of pixels and (currently) can approach the resolution capability of film. Since many target signatures are spatially variable, the high spatial resolution possible with CCD-based systems produces more detailed target signatures than most other systems. This capability, however, does not come without problems. Electrical and optical crosstalk, variations in the characteristics of individual detector elements, internal system reflections, and dynamic range are some of the possible areas which must be characterized.

A staring imaging photometer produces a single output for each individual detector (pixel) in response to radiation within the visible band; however, it does not produce spectral information within that band. This type of photometer is calibrated in terms of illuminance or luminance, and when used to measure targets through an attenuating atmospheric path, it produces band "apparent" luminance signatures. Accounting for the atmospheric path attenuation requires target spectral distribution data and atmospheric spectral transmission data.

5.2.3 Spectral Photometer. Photometers and imaging photometers use an optical filter to obtain a system spectral response matching that of a human observer. These systems do not produce spectral distribution data within that band. Spectral photometers/radiometers add a capability to break the visual band into a large number of smaller spectral intervals and produce an output for each of these intervals. Spectral photometers are identical to spectral radiometers operating at visible wavelengths, except that they may be calibrated in terms of photometric or radiometric quantities. The CIE photometric curve can be used to convert spectral radiometric data directly into spectral photometric data.

A spatial/spectral photometric signature measurement system, the Radiometric Color Measurement System (RCMS) has recently been developed by ATC.

5.3 Reference for Chapter 5

a. Lomheim, T. (2009, June). Introduction to Infrared Systems. Presented at the 42nd Annual Modern Infrared Detectors and Systems Applications, June 15-19, 2009, University of California, Santa Barbara, Goleta, CA.

CHAPTER 6

SENSOR CHARACTERIZATION

Target signatures consist of spectral, spatial, and temporal characteristics. Data collections can require measurements made with radiometers in a wide range of environments of temperature, pressure, acceleration, vibration, and background lighting. Measurement system characterization is the process of determining the combined effect of all parameters which may affect the determination of the desired target signature from the raw measurement data. Calibration is the process of determining the input/output relationship of the measurement system. Although calibration is a very important step in the process of instrument characterization, it is not the only required step. The characteristics of a radiometer are determined by a combination of the characteristics of many system components. In addition to the determination of the total measurement system characteristics, a description of each system component must be documented. An extensive list of required system parameters to be documented was developed during 1993-1996 with the Office of the Secretary of Defense (OSD) Joint Tactical Missile Signature (JTAMS) Joint Task Force (JTF). The list continues to be refined under the National Signatures Program (NSP). The Integrated Data Requirements List (IDRL) resulting from the 1993-1996 OSD JTAMS program presents required system parameters for UV and IR radiometers, spectroradiometers, and imagers for measuring tactical missile signatures (Reference 6a). The IDRL was adopted by the RCC as Standard 802-98 (Reference 6b). The NSP effort continues to evolve an even more extensive list of parameters since the NSP focus covers more varied targets and environments. Table 6-1 lists the usual measurement system component parameters that require documentation. The left column of Table 6-1 lists component parameters that are usually supplied by the manufacturer, or at most require a one-time measurement. The right column of Table 6-1 lists total system parameters whose determinations require laboratory measurements after the system is configured for the test; an example is the optical filter spectral response. The remainder of this chapter defines parameters and offers methods of determination.

TABLE 6-1. MEASUREMENT SYSTEM COMPONENT PARAMETERS INSTRUMENT TYPES	
Component Documentation	**Requires Measurements**
Detector material	Optical filter spectral response
Nominal detector spectral response	System spectral response
Collection optics material	Spectral resolution
Number of pixels (2D)	Spectral range
Pixel size (2D)	FOV spatial response (2D)
Pixel pitch (2D)	FOV uniformity
Fill factor	Time constants
Digital range (bits)	Frequency response
Optical system focal length	Integration time effects
Effective optical aperture	System noise level
Grating groove density for dispersive system	Input/output calibration curves or factors
Type and length of dispersive spectrometer	System irradiance dynamic range
Entrance slit width for dispersive spectrometer	Temperature effects
Wavenumber resolution for Fourier system	
Cryogenic system description	

6.1 Parameter Definitions

6.1.1 Detector Material. The detector material is the dominant component that determines the possible spectral response of the system. This parameter is supplied by the manufacturer (see IDRL 605 Reference 6b). Documenting the detector type and material identifies the nominal wavelength region of applicability and the nominal sensitivity.

The two types of detectors principally used to measure optical radiation are photon detectors and thermal detectors. Photon detectors are based on semiconductor materials and are most useful for measurement of UV to MWIR radiation. Thermal detectors have a broad spectral response across the entire IR region and are the only choice for measurements of LWIR. Both detector types, and their subsets, have attributes which determine their suitability for a specific measurement.

For an in-depth discussion of detector types and methods to determine their figures of merit, the reader is referred to The Infrared Handbook by Wolfe and Zissis (Reference 6c). Table 6-2 is based on Reference 6c, Section 11.1.4, which lists the methods used by various detector types to transfer optical radiation to a measurable electrical quantity.

TABLE 6-2. DESCRIPTION OF THE PROCESSES OF TRANSDUCTION

Thermal	
Bolometric	Changes in temperature of the responsive element, induced by the incident radiation, causes changes in the electrical conductivity, monitored electrically.
Thermovoltaic	The temperature of a junction of dissimilar metals is varied by changes in the level of incident radiation absorbed at the junction and thus causes the voltage generated by the junction to fluctuate.
Thermopneumatic	The radiation incident on a gas in a chamber causes the temperature, and thus the pressure, of the gas to rise. The varying pressure causes an exterior wall (usually a thin membrane) to move. The movement of the exterior wall is monitored optically and related to the level of incident radiation.
Pyroelectric	The incident radiation increases the temperature of the crystalline responsive element. The temperature change alters the dipole moment which produces a measurable external electric field.
Photon	
Photoconductive	A change in the number of incident photons on a semiconductor causes a change in the number of free charge-carriers in the material. The change in the semiconductor conductivity is directly proportional to the change in the number of incident photons. The measurable quantity is a current or voltage.
Photovoltaic	A change in the number of incident photons on a semiconductor p-n junction causes a measurable change in the voltage by the junction.
Photo-electromagnetic	Photons absorbed at or near the surface of a semiconductor generate free charge-carriers which diffuse into the bulk of the material and are separated by a magnetic field. The charge separation produces a measurable voltage which is directly proportional to the number of incident photons.

Thermal detectors have broad, flat spectral responses but they are slow to respond to changing flux. The efficiency of a thermal detector varies significantly with the frequency of flux variations. This variation would make them unsuitable for detectors in a Fourier transform spectrometer which must react to the highly fluctuating interferogram.

Although semiconductor detectors have high efficiencies and good temporal responses over a broad frequency range, their spectral responses are narrow and non-flat. The narrow spectral response limits their use, which means a laboratory will need a set of sensors to service a broad spectral region. However, the narrow spectral response can be a positive attribute if the user must discriminate between wavelength regions. The burden on optical filtering is eased because the detector is insensitive to wavelengths outside its spectral region.

Figure 6-1 illustrates the D* figure of merit for three photoconductive materials and four thermal detectors. Figure 6-2 compares the variation in D^*_{max} of thermal detectors and a PbS (lead sulfide) photon detector as functions of the chopping frequency of the incident flux, where D^*_{max} is the spectral maximum of D*. Note that the plots in Figure 6-1 and Figure 6-2 present only characteristics of a few of the many choices in detector materials and types. The plots are presented only to illustrate the compromises that must be made in choosing a detector type and material (see Reference 6c and Reference 6d). Even for those materials presented, the actual

values can vary by an order of magnitude depending on manufacturing processes. Refer to Appendix A for additional information on detector materials.

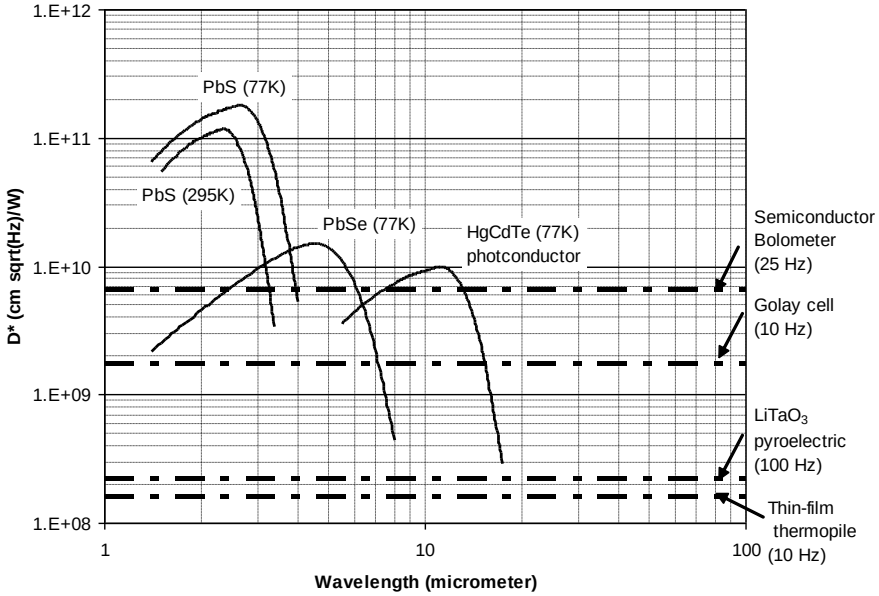

Figure 6-1. Comparison of spectral response of four photon detectors to four thermal detectors.

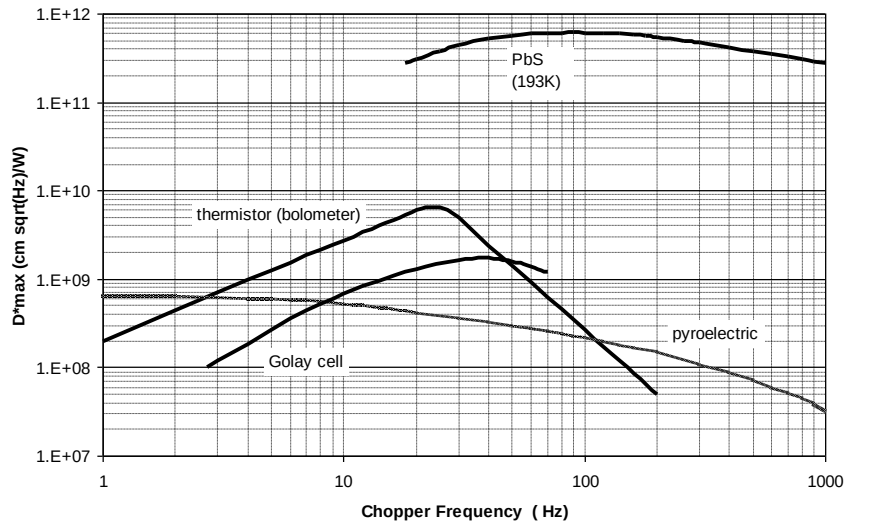

Figure 6-2. Frequency response of D^*_{max} for three thermal detectors compared to a PbS semiconductor detector.

6.1.2 Nominal Detector Spectral Response. This parameter is supplied by the manufacturer. Even though the usable spectral regions of most detector types are well known, it is still important to document the band for the specific detector since the manufacturer can shift the nominal spectral response through variations in impurities, other manufacturing processes, and through the inclusion of filters and windows. The parameter can be documented as the 50 percent response end points of the nominal spectral range or as the spectral function.

The detector spectral response is defined as the ratio of the change in output electrical signal (current or voltage) to the change in incident radiant power. This response is determined by the ratio of the root-mean-square of the electrical signal to the root-mean-square of the input radiation per the wavelength band as shown in Equation 6-1. Note that $R(\lambda)$ will have the units volt per watt per wavelength or ampere per watt per wavelength.

$$R(\lambda) = \frac{V_s}{\Phi_s(\lambda)\,\Delta\lambda}, \quad \text{or} \quad R(\lambda) = \frac{I_s}{\Phi_s(\lambda)\,\Delta\lambda} \qquad \text{(Eq. 6-1)}$$

The spectral response is also sometimes referred to as the quantum efficiency (*Q.E.*) since it can be related to the number of photons required to produce a free electron which results in the measurable current. The spectral response is most likely a function of the bias voltage and the operating electrical frequency.

The spectral response supplied by the manufacturer might be the spectral D* figure of merit as illustrated in Figure 6-1 or it might be a spectral *Q.E.*. The following derives the relationship between the response at a specific wavelength in units amp per watt and the *Q.E* (which is unitless). Consider the energy per photon (reference Equation 2-1d)

$$Q(\lambda) = \frac{hc}{\lambda} \qquad \text{(Eq. 6-2)}$$

Where

h is Planck's constant, 6.626 069 x10^{-34} J s
c is the speed of light, 2.997 924 58 x 10^{8} m s^{-1}

Note. Consider that the detector *Q.E.* is defined to be the ratio of the number of photons that produce electron-hole pairs, N_e, in the detector element to the number of incident photons, N_ν.

$$Q.E.(\lambda) = \frac{N_e}{N_\nu} \qquad \text{(Eq. 6-3)}$$

Using Equation 6-2, the radiant power per photon in unit time Δt is

$$\Phi(\lambda) = \frac{\mathrm{hc}}{\lambda\ \Delta t} \qquad \text{(Eq. 6-4)}$$

The radiant power from the incident photons is the number of incident photons multiplied by the power per photon.

$$\Phi_{\nu}(\lambda) = N_{\nu}\ \frac{\mathrm{hc}}{\lambda\ \Delta t} \qquad \text{(Eq. 6-5)}$$

The current from the electron-holes pairs created in the detector element is the number of free electrons times the charge per electron, e, per unit time, Δt.

$$I_e = \frac{N_e\ e}{\Delta t} \qquad \text{(Eq. 6-6)}$$

The response function is the ratio of the current to the incident radiant power.

$$R(\lambda) = \frac{I_e}{\Phi_{\nu}(\lambda)} = \frac{N_{\mathrm{e}}\ \mathrm{e}\ \lambda}{N_{\nu}\ \mathrm{h\,c}} = [Q.E.]\ \frac{e\lambda}{\mathrm{h\,c}} \qquad \text{(Eq. 6-7a)}$$

Using h=6.626x10^{-34} J s, c=2.997x10^{8} m/s, e=1.6x10^{-19} A s, and wavelength λ in units of micrometer, Equation 6-7a is rewritten as

$$R(\lambda) = 0.805\ [Q.E.]\ \lambda(\mu m)\ \frac{\mathrm{A}}{\mathrm{W}} \qquad \text{(Eq. 6-7b)}$$

Figure 6-3 and Figure 6-4 illustrate the difference in documenting the spectral quantum Q.E and the spectral response function. For Figure 6-3, a simulated *Q.E.* function for a fictional UV/VIS detector is transferred to a spectral response function using Equation 6-7b. Figure 6-4 presents the normalized (by division by the maximum value) of both functions. The spectral functions are similar but the spectral shape is altered by the wavelength factor in Equation 6-7b (obvious in the shift of the full-width-half-maximum end points in Figure 6-4).

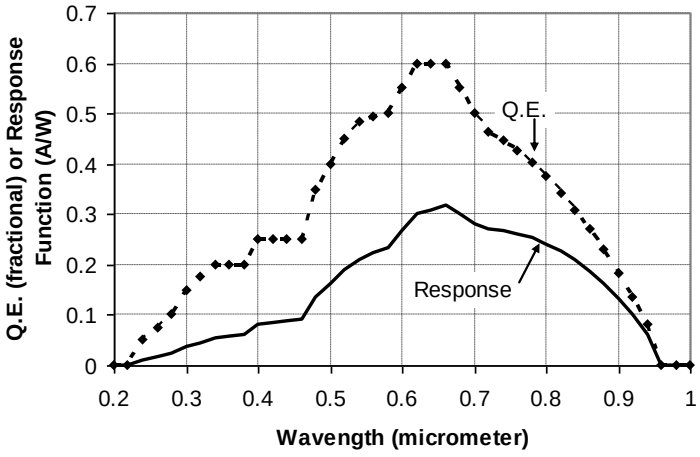

Figure 6-3. Comparison of spectral a *Q.E.* to a spectral response function.

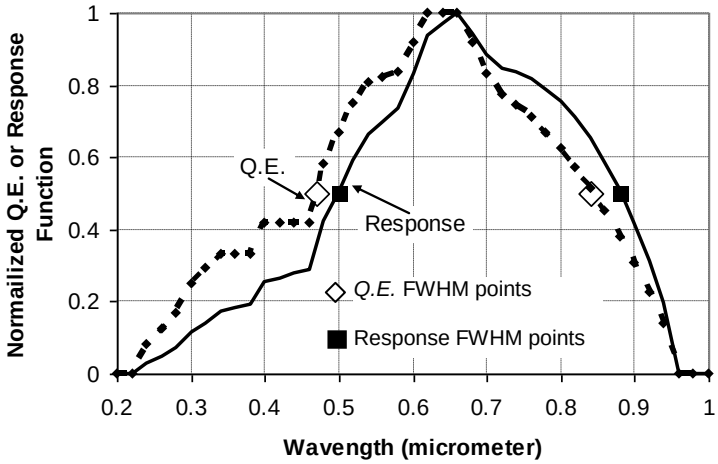

Figure 6-4. Comparison of normalized spectral *Q.E.* to normalized spectral response function.

6.1.3 Collection Optics Material. This parameter is the material list used to fabricate optical components, including beam splitters, but not including the band pass filter which is covered under other parameters. The parameter also includes any coating material used for protection or anti-reflection. If the optical components are reflective, note the reflective material (such as aluminum or gold) and any coating material.

The optical components have as strong an influence on the spectral range as the detector type.

6.1.4 Number of Pixels (2D). This parameter (Ref 6b IDRL 815) is the number of horizontal pixels and the number of vertical pixels. If the pixels are electronically tied together by the data acquisition software, the parameter should be the reduced number of horizontal and vertical pixels.

6.1.5 Pixel Size (2D). This parameter is the horizontal and vertical physical size of the pixels. If the pixels are electronically tied together by the data acquisition software, the parameter is the increased horizontal and vertical size.

6.1.6 Pixel Pitch (2D). This parameter (Ref 6b IDRL 804 and 805) is the center-to-center physical distance of pixels in the horizontal and vertical dimensions. If the pixels are electronically tied together by the data acquisition software, the parameter is the increased horizontal and vertical size.

6.1.7 Fill Factor. This parameter is the ratio of the area per pixel times the number of pixels to the total area of the detector face. An optimum fill factor would be 1.0 although this is never realized because some dead space between pixels is required to avoid, or at least minimize, cross talk. In practice, knowing the Fill Factor parameter is usually not required because it becomes a constant of the calibration and falls out of the data reduction equations.

6.1.8 Digital Range (Bits). This parameter is the digitization capability of the data acquisition system in digital bits. An 8-bit capability can recognize $2^8 = 256$ levels. A 16-bit capability can recognize $2^{16} = 65\,536$ levels.

6.1.9 Optical System Focal Length. This parameter (Ref 6b IDRL 608) is the effective focal length of the optical system. It is the distance from the second principal plane (back focal plane) of the combined optical components to the image plane for an object at infinity. If the optical system has refractive components (lenses) the parameter considers chromatic aberration and is the focal length for the center wavelength of interest.

The second principal plane is most often a virtual surface as illustrated in Figure 6-5. Its position can be calculated from geometrical optics (not covered here).

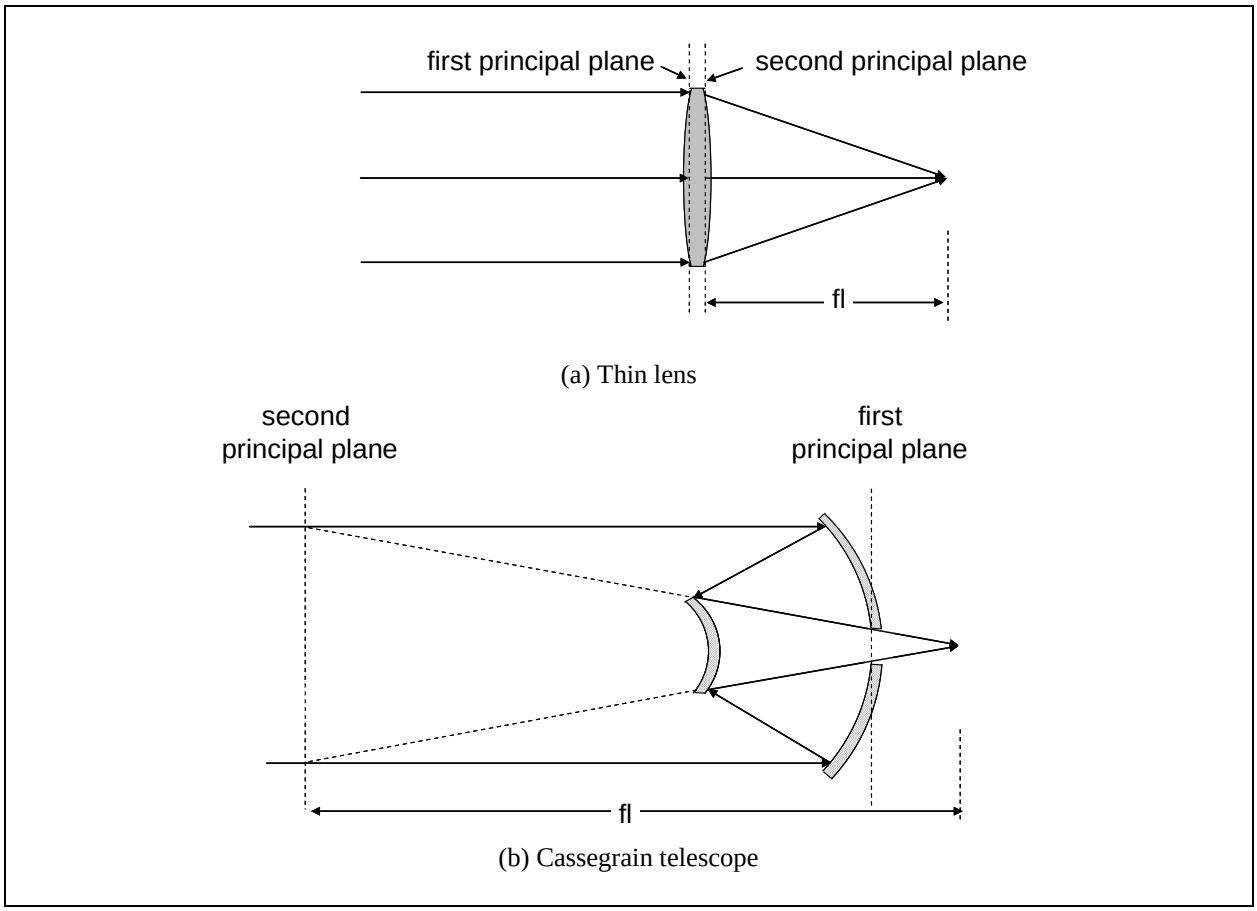

Figure 6-5. Principal planes and focal length for a thin lens and a Cassegrain telescope.

6.1.10 Effective Optical Aperture. Also called the aperture stop, the effective optical aperture (Reference 6b IDRL 609) is the diameter of the surface that limits the amount of energy reaching the image. It can be the diameter of an iris used to reduce the effective size of the collection optic or it can be the diameter of a reflective telescope minus obstructions. The effective aperture for a field lens telescope is the size of the image of the detector at the first principal plane (front focal plane) as seen by the source.

Note that for a non-circular or obscured aperture, Effective Optical Aperture parameter is the diameter of an equivalent circle having the same effective area.

6.1.11 Grating Groove Density for Dispersive System. This parameter (Reference 6b IDRL 605) is supplied by the manufacturer and is documented in grooves per millimeter.

6.1.12 Type and Length of Dispersive Spectrometer. These parameters (Reference 6b, IDRL 605) are supplied by the manufacturer. Two of the most common designs are the Fastie-Ebert, Czerny-Turner, and the double Czerny-Turner. The length is the distance between the entrance slit and the first collimating mirror. In the case of a double spectrometer the length is the distance between the second entrance port and the first collimating mirror of the second spectrometer.

6.1.13 Entrance Slit Width for Dispersive Spectrometer. This parameter (Reference 6b IDRL 605) is the width of the entrance slit in micrometers. Some spectrometers use a circular aperture to couple to an integrating sphere at the input and, in this case, the width is the diameter of the circular aperture. If a fiber optic linear stack is coupled to the entrance slit, the parameter is the width of the limiting aperture.

6.1.14 Wavenumber Resolution for Fourier Spectrometer. This parameter is a function of the length of the interferogram (Reference 6b IDRL 1013) and is recorded in units of wavenumber (cm^{-1}).

6.1.15 Spectral Resolution for Dispersive Spectrometer. This parameter is the full width at half maximum (FWHM) of a single emission line from a standard emission line lamp. The lamps used for UV and VIS systems are usually Pen-Ray® low pressure, cold cathode UV lamps made of double bore quartz tubing filled with mercury or argon gas that emit a series of known, single atomic emission lines. The emission lines are used for spectral calibration (pixel or grating position versus wavelength) and the spectral resolution.

For a spectrometer with a linear detector array, spectral dispersion in units wavelength per pixel is determined by collecting a spectrum of the line emission lamp and documenting pixel number versus wavelength. Since most spectrometers are non-linear in wavelength dispersion, the set of pixel-wavelength pairs is used to determine polynomial coefficients for a polynomial fit of the wavelength range.

$$Y(\text{wavelength}) = a_0 + a_1(\text{pixel}) + a_2(\text{pixel})^2 + a_3(\text{pixel})^3$$

The coefficient a_0 is the beginning of the wavelength region. The coefficient a_1 is approximately the linear dispersion in units of wavelength per pixel. The FWHM of the single emission line in units of number of pixels is transferred to units of wavelength by multiplication by a_1.

6.1.16 Instantaneous Field of View (IFOV). The IFOV represents the spatial resolution of an EO system. It is a function of the detector element size and the focal length of the optical system (Reference 6b IDRLs 826 and 827). When the detecting system is focused for sources at long distances compared to its focal length (which is the most common application) the image of the source is at the focal distance of the optical system. This is illustrated in Figure 6-6, with the optical system being represented by a thin lens and the active detector area is the field stop. With s_o as the object distance, and s_i as the image distance, f as the focal length, the thin lens equation is

$$\frac{1}{f} = \frac{1}{s_o} + \frac{1}{s_i} \qquad \text{(Eq. 6-8)}$$

Solving for s_i,

$$s_i = \frac{s_s f}{s_o - f} \qquad \text{(Eq. 6-9)}$$

In the limit that s_o is large, s_i equals f.

$$s_i = \lim_{s_o \to \infty} \frac{s_s f}{s_o - f} = f \qquad \text{(Eq. 6-10)}$$

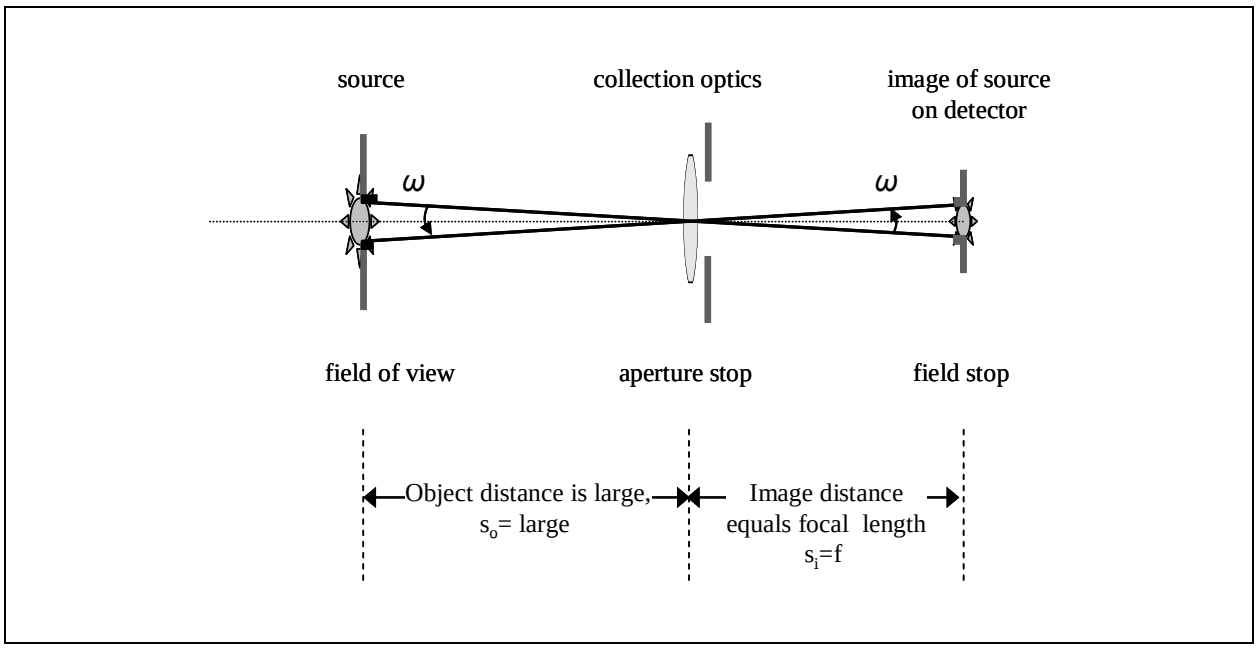

Figure 6-6. Simple example of an imaging system.

By similar triangles, and using the approximation to the solid angle derived in Appendix C, the IFOV is the solid angle subtended by the detector area.

$$\omega = \frac{A_d}{f^2} \qquad \text{(Eq. 6-11)}$$

Where

A_d = the active area of the detector
f = the effective focal length of the optical system.

Another option is to define the IFOV by the one-dimensional angle subtended by the detector area. For a square detector, $A_d = d^2$ and $\theta = d/f$ is the linear IFOV in radians. For a rectangular detector, one refers to the horizontal IFOV and the vertical IFOV. For a circular detector, one refers to the diameter IFOV.

If the image blur circle is smaller than the size of a detector element, the spatial resolution is the IFOV of the solid angle. If the blur circle is larger than the pixel size, the spatial resolution is considered to be diffraction limited. For circular aperture telescopes, the diameter of the blur circle is given by the well known Airy disk equation

$$x = 2.44\left(\frac{\lambda f}{d}\right) = 2.44\,\lambda\,(f/\#) \qquad \text{(Eq. 6-12)}$$

Where

d = the diameter of the telescope aperture
f/# = the dimensionless f-number.

Note. There is a lower limit to the size that individual detector elements can be produced from the various types of detector materials, although detector elements with 10 to 30 micrometer widths are common.

Table 6-3 lists Airy disk diameters calculated with Equation 6-12 for common f/# optics for wavelengths ranging from 0.2 μm to 25 μm. In the UV and VIS, the spatial resolution is optimized with the smallest pixel size available. In the NIR and MWIR the best resolution is had with a low f/# telescope. The spatial resolution in the LWIR is significantly limited by diffraction and a low f/# telescope is strongly required for reasonable resolution.

TABLE 6-3. BLUR CIRCLE DIAMETERS FOR COMMON F/# OPTICS

Wavelength	Blur Circle Diameter		
	f/# = 2	**f/# = 4**	**f/# = 8**
micrometer	micrometer	micrometer	micrometer
0.2	0.98	1.95	3.90
0.5	2.44	4.88	9.76
1	4.88	9.76	19.52
2	9.76	19.52	39.04
5	24.4	48.8	97.6
10	48.8	97.6	195.2
25	122	244	488

6.1.17 Field of View (FOV) and Field of Regard (FOR). Focal plane arrays and charge-coupled device (CCD) arrays consist of a large number of individual detector elements in a rectangular pattern (Reference 6b IDRLs 644, 645, 806, and 807). The total FOV of a measurement system in units of steradian is a function of the size of the array and the focal length of the optical system.

$$\Omega = \frac{A_a}{f^2} \qquad \text{(Eq. 6-13)}$$

Where

Ω = the solid angle FOV of the detector array in steradian
A_a = the active area of the array
f = the effective focal length of the optical system

If one wishes to refer independently to the horizontal and vertical FOVs for an array with rectangular dimensions X and Y, then

$$\theta_x = \frac{X}{f} \quad , \quad \theta_y = \frac{Y}{f}$$

Where

θ_x = the one dimensional horizontal FOV of the detector in units of radian.
θ_y = the one dimensional vertical FOV of the detector in units of radian.

Field of regard is a term indicating an IFOV, such as that from a single detector with a small area, which is mechanically scanned over a wider angle. This process scans the footprint

of the IFOV over a larger area in target space. This was a common practice of imaging systems built around a single detector and an optical scanning component that scanned the image of the detector in a horizontal and vertical pattern in the target plane as illustrated in Figure 6-7. Field of regard is also a term that describes the total FOV extent of the projection of a linear or two-dimensional detector array that is mechanically scanned over a larger angle. One method of performing this procedure is to mount the measurement system in an aircraft and fly it over a ground target. Figure 6-8 is an illustration of the descriptive nickname "push broom" for a field of regard made by scanning the projection of a linear array detector perpendicular to the array axis to cause a rectangular field of regard.

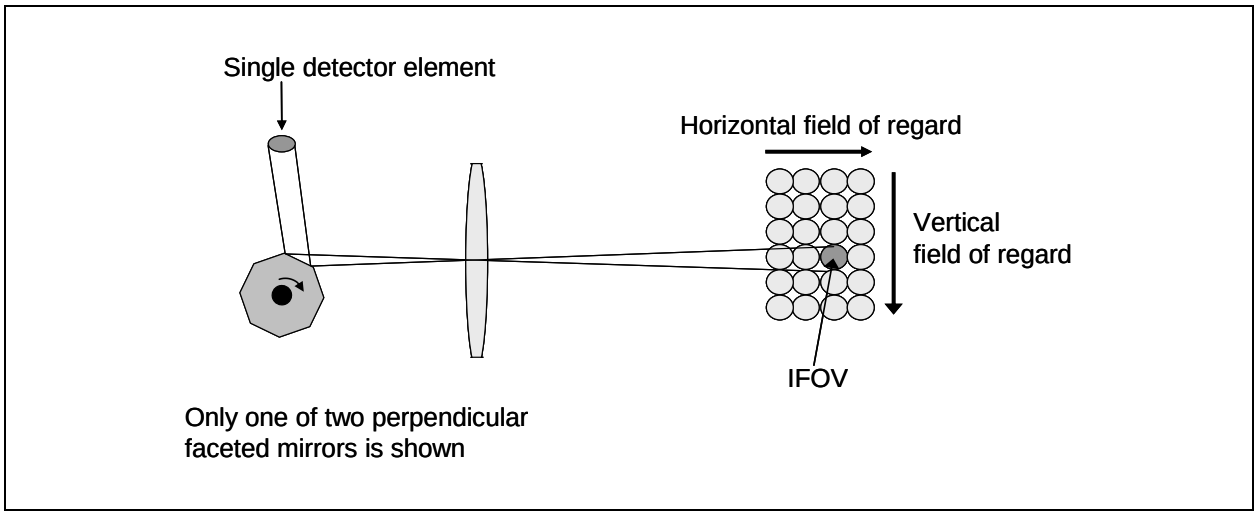

Figure 6-7. Field of regard from mechanically scanning a single IFOV over a larger area.

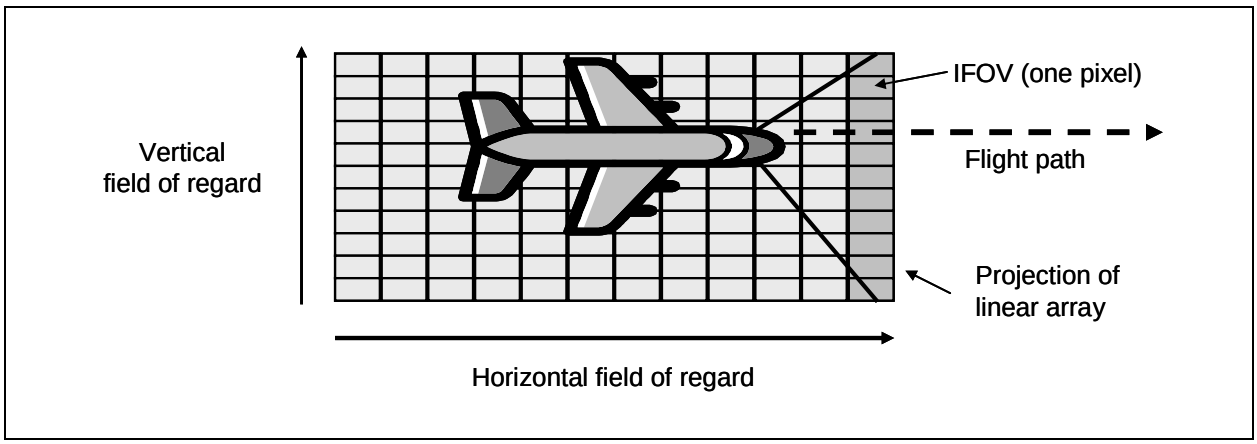

Figure 6-8. Push broom field of regard.

6.1.18 Dynamic Range. The dynamic range is typically documented in decibels (db). It is defined to be the ratio of the greatest level of measurable irradiance before saturation (or before the level is beyond the linearity range of the system response) to the noise equivalent power (NEP) in units of irradiance. The parameter is typically documented in terms of the unitless decibel. The decibel is the base-ten log of the ratio. It states the possible measurable dynamic

range in powers of ten. For example, if the ratio of saturation limit to NEP limit is 1600, the dynamic range is 32 db (calculated as 10 log(1600) = 32 db).

Large dynamic ranges are desirable in a measurement system. There are methods used to extend the total dynamic range. A few common examples are to have a variable gain setting on an amplifier, to have a variable iris that can step down the entrance aperture, and to have the ability to insert neutral density (ND) filters into the optical train. If these methods are used, it is important that a system calibration be conducted for each step. Also, it is still desirable that each step have a large dynamic range of its own.

6.1.19 Detector Time Constant. This parameter is the time required for the detector output to reach 63 percent of a stable value in response to a step change in input flux. The detector parameter can be supplied by the manufacturer, but the total system time constant should be measured. The time constants are illustrated in Figure 6-9 and are documented in units of microsecond. It is important to measure both "on" and "off" time constants since the decay mechanisms might be different than the initiation mechanisms.

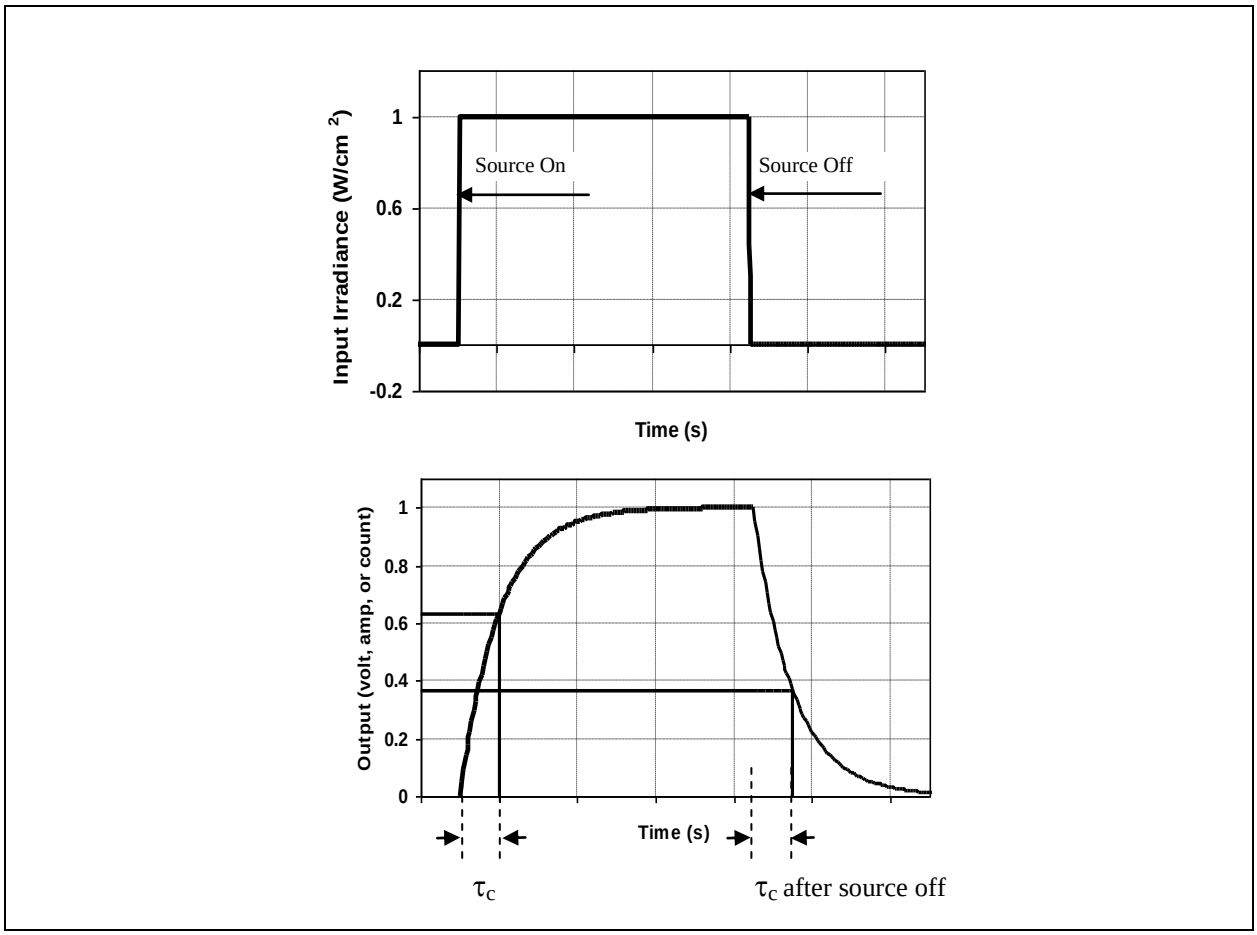

Figure 6-9. Experimentally determining the time constant of a detector.

6.1.20 Frequency Response. This parameter f_{BW} (Reference IDRL 903) is the frequency at which the response falls to 50 percent of the response at slow temporal flux levels, documented

in units of hertz. A system frequency response is related to the time constant where the system response has its maximum at low flux frequencies. For a system utilizing a chopper, the response will decrease at higher chopping frequencies and is theoretically related to the detector time constant by Equation 6-14. An example of the relative frequency response of a detector with a time constant of 1 μs calculated with Equation 6-14 is shown in Figure 6-10. Figure 6-11 is also an example of the data required to determine this characterization.

$$\Re_f = \frac{\Re_0}{\sqrt{(1+4\pi^2 f^2 \tau^2}} \qquad \text{(Eq. 6-14)}$$

Where

$\Re_0$ = responsivity at low chopping frequencies
$\Re_f$ = the responsivity at chopping frequency f
τ = the detector time constant assuming equal "on" and "off" time constants

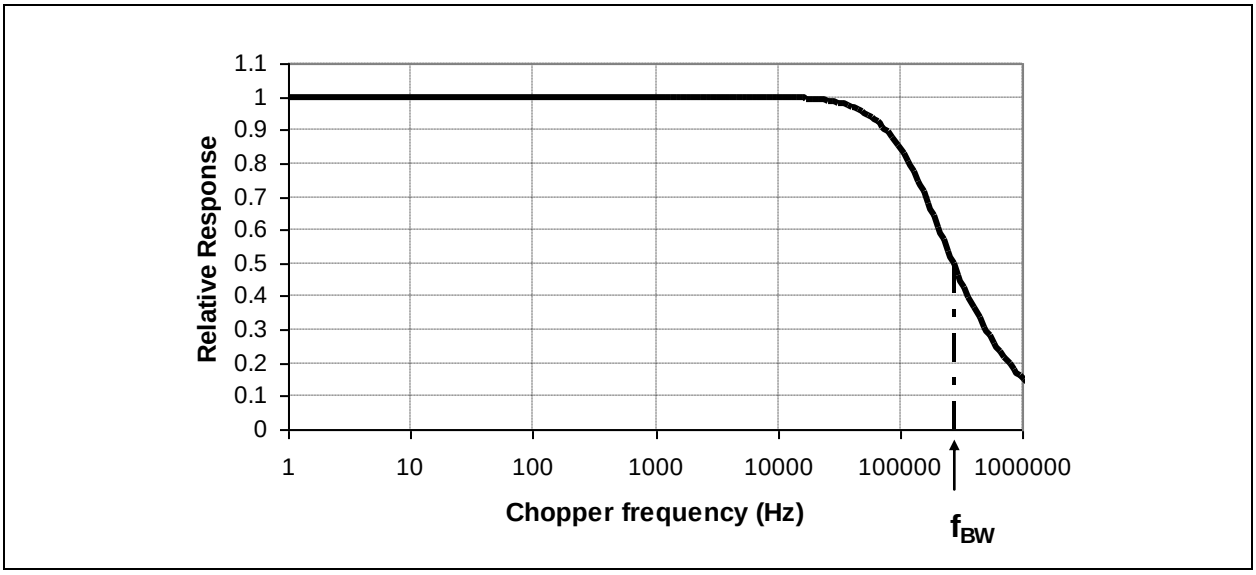

Figure 6-10. Responsivity with frequency for a detector with a 1 μs time constant.

Figure 6-11 shows four increasing chopper or shutter frequencies. For clarity, only the slowest frequencies are shown, but in practice they would increase as in the x-axis range of Figure 6-10. It is obvious that within the same time period, say 1 s, the shutter is open to the radiation source for the same total amount of time. The measurement is count per time versus shutter rate. At some frequency threshold, the system is no longer able to reach full response before the shutter is closed and the count level is reduced. The characterization is determined by monitoring count per time as the frequency of the chopper or shutter is increased. A plot similar to Figure 6-10 is produced and the frequency at which the response falls to 50 percent is documented as f_{BW}.

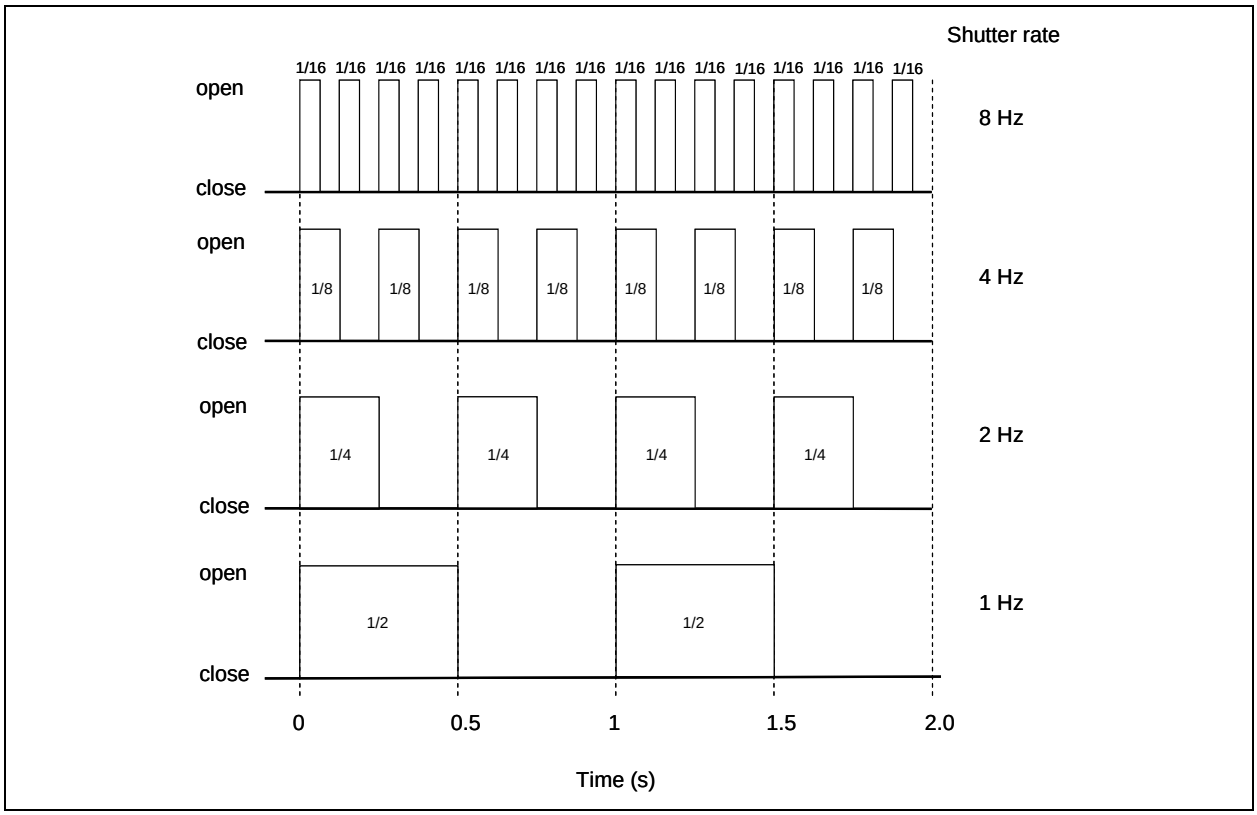

Figure 6-11. Shutter open/close positions for four frequencies.

6.1.21 Optical Filter Spectral Response. This parameter is a function of relative transmission versus wavelength or wavenumber for the optical filter used to limit the bandpass of the system. An example is in Figure 6-12. The function should be measured for the temperature and angle to the optical axis that will be used during test since both can shift the peak wavelength of the response curve. The spectral filter transmission function is documented as a plot or stored as a text file and the FWHM wavelength points can be recorded in the test report and file header.

If the source is predicted to have significant emissions in the out-of-band region, then it is required to measure the filter response to the limits of the detector response to characterize possible leakage in the out-of-band region. Paragraph 6.1.22 includes an example of the consequences of out-of-band leakage for total system spectral response.

Note that measuring the filter spectral response is important, but not sufficient, to define the spectral response of the system. It is required to measure the full end to end system response described in paragraph 6.1.22.

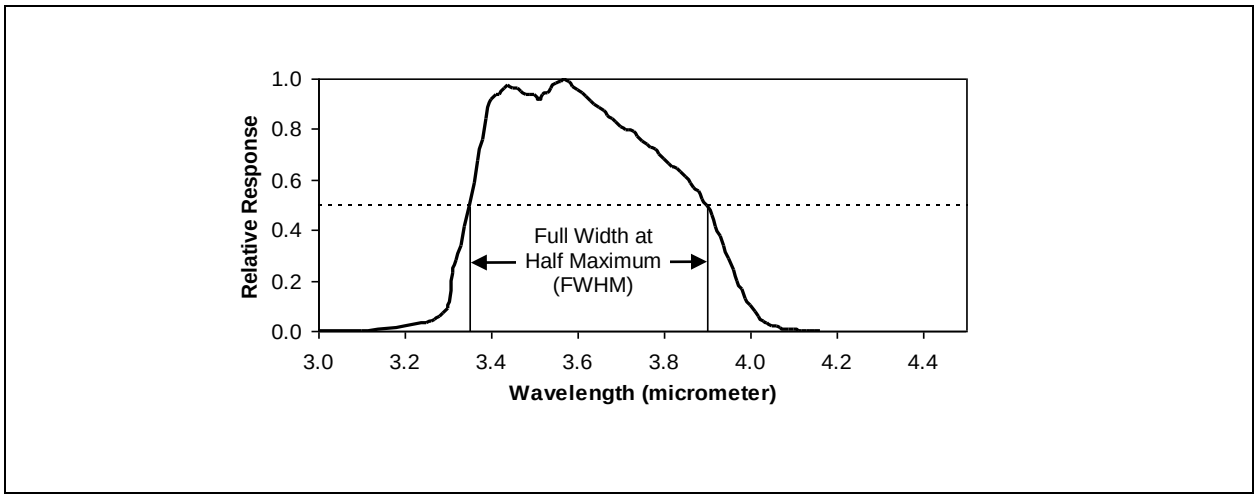

Figure 6-12. Relative spectral response of IR band pass filter.

6.1.22 System Spectral Response. This parameter (Ref 6b IDRL 824) is the relative spectral response of the end-to-end system, documented as a spectral function. An example is shown in Figure 6-13. The measurement is made with all optical elements in place. It is not sufficient to only state the FWHM power limits of a system spectral response. The full system spectral response is required to calculate the effective integrals of paragraph 2.3.2, Equation 2-12 and Equation 2-13.

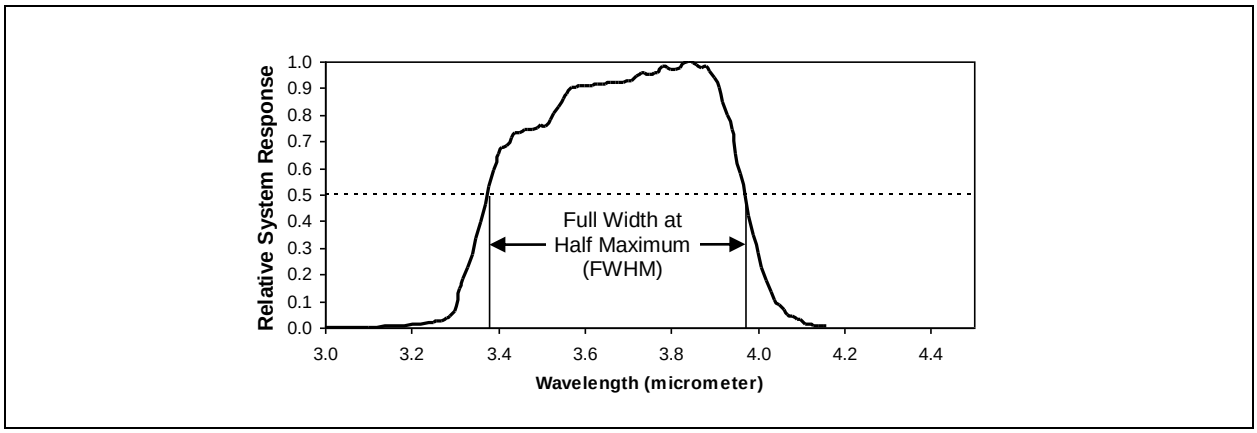

Figure 6-13. Relative spectral response of band IR system.

Knowledge of the out-of-band spectral response must also be characterized if it is predicted that the source will have significant emissions in spectral regions outside the band pass. As an example, consider the spectral response of a visible radiometer using a low quality blue band pass filter and a broadband silicon detector as plotted in Figure 6-14. The blue band pass filter has a second mode that allows some leakage at longer wavelengths. If, for example, the radiometer is used to view the solar radiance, a significant amount of the radiant energy (34 percent) comes from the out-of-band spectral region. If the out-of-band leakage cannot be eliminated by using additional optical filters or by using a detector that has no response in the out-of-band region, then the full system response must be used to understand the data.

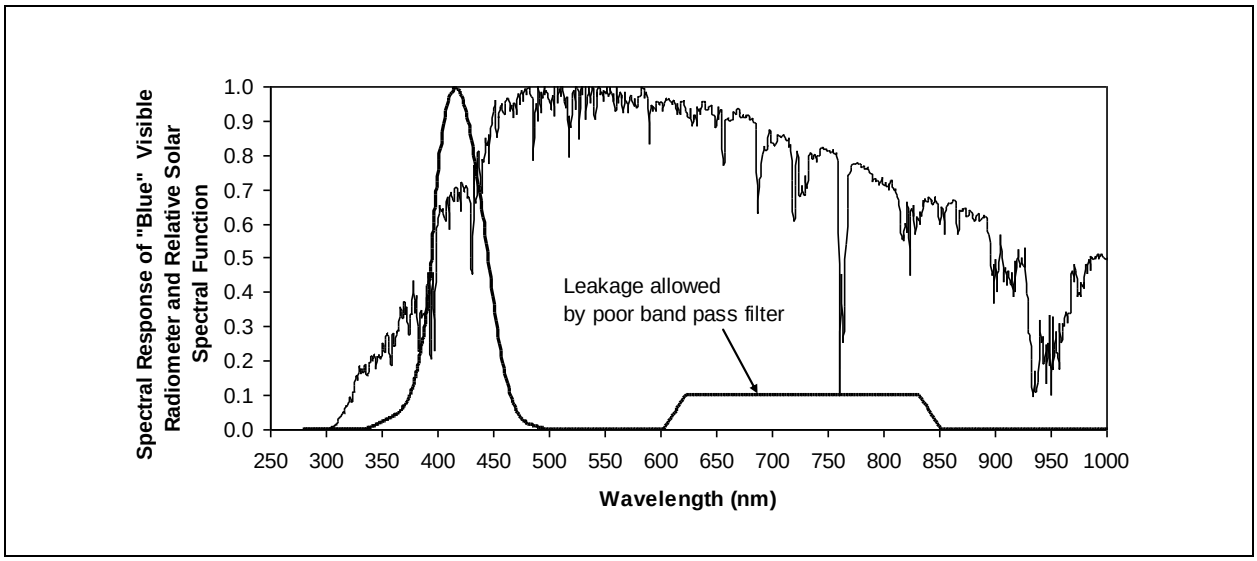

Figure 6-14. Example of a spectral system response with out-of-band leakage.

6.1.23 Cryogenic System Description. The detector responsivity is substantially improved by lowering its temperature. There are four fundamental categories of cooling systems. These are:

a. Open cycle expendable systems using stored cryogens as liquids or in a high pressure state.
b. Passive radiators (radiation to deep space).
c. Closed cycle mechanical refrigerators.
d. Thermoelectric coolers using the Peltier cooling effect.

Note. The parameter to document is simply the type of cryogenic system.

Table 6-4 is a listing of several cryogenic liquids and their properties. Liquid nitrogen is commonly used to cool detectors in radiometers. Sensor detectivity curves are commonly given for the 77 K temperature (liquid nitrogen boiling point). The liquid nitrogen is stored in vacuum bottles and then poured into the small radiometer reservoir where the detector is in close thermal contact with the liquid through copper conducting fingers. Vaporization of the fluid absorbs the waste heat and rejects this heat through the vented gas. The cryogen supply must be maintained to allow uninterrupted testing with a consistent detector temperature.

TABLE 6-4. PROPERTIES OF SOME CRYOGENIC LIQUIDS

Material	Boiling Point at 1 atm Pressure (K)	Liquid Density at Boiling Point (g/ml)	Heat of Vaporization at Boiling Point (J/g)	Critical Temperature (K)	Critical Pressure (atm)
Helium He_4	4.2	0.125	20.5	5.2	2.3
Hydrogen H_2	20.4	0.071	448.0	33.2	13.0
Nitrogen N_2	77.4	0.808	199.0	126.1	33.5
Nitrous Oxide N_2O	183.6	1.230	250.2	399.7	71.7
Carbon Dioxide CO_2	194.6	1.510	574.0	304.5	73.0
Ammonia NH_3	239.8	0.683	1363.0	405.0	111.2
Sulfur Dioxide SO_2	263.1	0.80	388.0	430.0	77.7

6.2 Characterization Overview

The output of every instrument is proportional to an integral of the received radiation that is weighted by the instrument response function in that domain. Every measurement of radiant power is influenced by the characteristics of the instrument used to perform the measurement. In other words, every measurement value starts as an effective value. There are no exceptions; there are only differing degrees of influence.

6.2.1 Response Shape. Characterization quantifies the instrument response shape. Knowledge of response shape is essential to calibration and to application of the measurement data, but is used in a number of other ways as well. Response shape is needed to:

a. Select an instrument that is capable of obtaining the desired target information.
b. Select the calibration source or sources appropriate for the instrument and for the target characteristics.
c. Calculate the calibration coefficients that will be used to convert raw readings into radiance or irradiance.
d. Plan the measurement distance so that the target falls within the instrument's uniform response region.
e. Select measurement conditions such as background behind the target to minimize influence.
f. Use the measurement result for any purpose, from comparing with other instruments or sensors to validation of computer models.

Determining the linearity and dynamic range of an instrument are rightfully a part of the characterization as well, but are usually quantified during the calibration process.

6.2.2 Environment Changes. Characterization also determines the sensitivity of the instrument to changes in its environment. Sensitivity to the environment usually doesn't require precise quantification, but knowing whether the influence is great or small determines what, if anything,

must be done to control or, if that is not possible, to compensate or correct. Examples include sensitivity to:

a. Changes in ambient temperature.
b. Changes in pressure (of concern to airborne instruments).
c. Radiation sources that are outside the nominal FOV.

6.2.3 Non-uniformity Consequences. The consequence of every radiometric measurement being affected by the responses of the instrument used is that a measurement value is only valid for that specific instrument's spectral, spatial, and temporal response shapes and for no others. Two instruments with different response shapes measuring the same target at the same time will produce two different values. A different response shape would produce a different value for the integral, but one that would be equally valid. The difference in measurement values between two dissimilar instruments depends upon how different the shapes of the response curves are and upon the distribution of the target radiation in that domain. In practice, this consequence is not as limiting as it may sound, but failure to understand response effects and to document response shapes in every measurement report is the main cause of data misuse and the main reason why radiometric measurements have such a well-earned reputation for poor comparability.

6.2.4 Ideal Instruments. An ideal instrument with uniform responses would respond equally to all received radiation regardless of its distribution across the different domains. With spectral response, an ideal instrument would respond equally to radiation at all wavelengths within the band of interest and not respond to radiation outside the band limits. Spectral response is the primary response concern of imaging systems, radiometers, and other broad-band instruments. With a uniform spatial response, an ideal instrument would show no sensitivity to target size, shape, orientation, or position within the FOV and would have no response to sources outside the defined FOV. Spatial response, especially to target position in the FOV and to background radiation, is the primary concern and main source of error in spectrometers and other non-imaging instruments. With a uniform and sufficiently broad temporal response, an ideal instrument would respond faithfully to all the time-varying components and harmonics of a modulated or rapidly-changing target source. Temporal response is a primary concern in the measurement of countermeasures sources.

6.2.5 Normalization. Characterization and calibration would ideally be the same process. Ideally, the absolute instrument response would be mapped over a domain with a traceable standard laboratory source that was tunable across the range of interest. In the spectral domain, for example, this would require a tunable monochrometer whose output beam would provide a level of spectral irradiance traceable to a radiation standard and that also would have a cryogenically-cooled background source. The result would be an absolute spectral response function in units of output reading per unit radiance (or irradiance) as a function of wavelength. In practice, it is sufficient and much more practical to separate the characterization and calibration processes so that characterization determines only the relative (rather than the absolute) response shape. Calibration then incorporates the results of the shape characterization to determine the absolute instrument response. Characterization uses a variety of different methods and sources to map relative response shapes. The response curve is then normalized and this normalized curve is used in the later derivation of the calibration coefficients. Different normalizations, such as normalization to an average value, are possible, but the convention

throughout most of the measurement community today is to normalize response curves to unity at the peak.

6.2.6 Instrument Types and Required Characterizations. The instrument type, the instrument design, the characteristics of the target, the target environment, and the information desired from the measurement all determine the characterizations that must be performed. This is especially true when the expected target features approach the limits of the instrument resolution in a domain. Determining exactly which characterizations are needed for all possible instruments for all possible targets is far beyond the scope of this document. Consequently, the procedures described herein will only cover the most common instrument types and are intended only as an overview of general concepts. The final choices and methods used must ultimately be a judgment call made by experienced measurement personnel. Table 6-5 lists the three most common instruments and their typical resolution in each domain. Whether the resolution is high or low determines the response characterization that will most likely be required.

TABLE 6-5. COMMON INSTRUMENTS AND REQUIRED CHARACTERIZATIONS

	Typical resolution in each domain. Response domains with wide instrument resolution require response characterization.		
Instrument Type	**Spectral**	**Spatial**	**Temporal**
Radiometer	Wide	Wide	Narrow
Imager	Wide	Narrow	Wide
Spectrometer	Narrow	Wide	Wide

Resolution and response are actually the same parameter, with resolution being the ultimate, narrowest limit of response. The classification of an instrument resolution in Table 6-5 as being narrow or wide is relative to the target features and information requirements. Resolution may be judged sufficiently narrow to resolve and measure the features of one target, but too wide for another. A practical rule of thumb for narrow resolution is a factor of five because a resolution width that is five times narrower than the target feature of interest will usually impact accuracy of the measurement by one percent or less. Figure 6-15 is an example of a roll off curve for the effect of spatial resolution on a measurement of target radiance. The laboratory collimated source was held at constant radiance and the angle subtended was varied from 10.15 mrad to 0.32 mrad by changing apertures. The imager used in this experiment had an optical resolution width of 1.0 mrad. At a target angle subtending 5.56 mrad, the measured radiance was 99 percent of actual. The measured radiance decreased to 68 percent of actual when the subtended angle was reduced to 1.01 mrad. Another factor in using resolution to determine characterization requirements is curve shape. If the resolution is judged to be narrow for a particular target, then the shape of the response/resolution curve will no longer have a significant effect on the measurement value and the exact shape (which is usually Gaussian) will not need to be characterized.

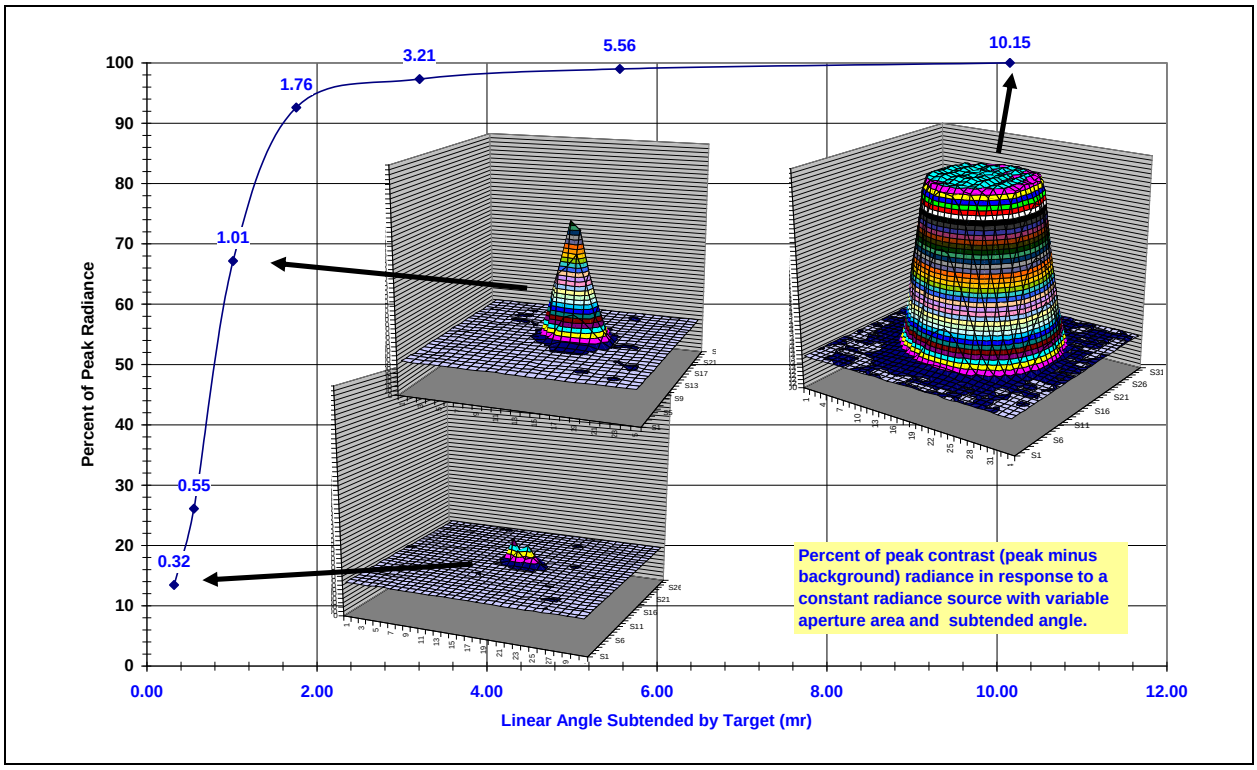

Figure 6-15. Measured percent peak radiance versus target angle (imager resolution = 1.0 mrad).

6.3 Calibration

6.3.1 Calibration Standards. Every calibration rests on the premise that the radiant power from the calibration source that is incident at the instrument optics is known to an acceptable degree of accuracy. This premise means knowing the absolute magnitude and spectral, spatial, and temporal distributions of radiation received at the instrument. Knowing the characteristics of the calibration source by itself is essential, but is only the starting point.

a. Blackbody Calibration Sources. The most common calibration sources are commercially-available blackbody sources. In physics, a blackbody is a perfect absorber and emitter. All radiation entering the blackbody is absorbed. All radiation exiting the blackbody is distributed spectrally as a function of temperature and emissivity in accordance with Planck's formula. Strictly speaking, a source must have a perfectly uniform temperature and have an emissivity of one to be "black." Any source with lower emissivity is a graybody. In practice, a source with an emissivity greater than about 0.95 is considered adequately black for most field and airborne calibration purposes as long as the value of emissivity is known. An in-depth discussion of blackbodies is beyond the scope of this document; however, a great deal of information is available in the open literature and from the various manufacturers. An old term for radiation from a blackbody source is "cavity" radiation. The ideal shape for a blackbody is a spherical cavity with an infinitely small entrance/exit aperture. Radiation within the cavity undergoes multiple reflections from the surface, which enhance the net emissivity as seen through the

aperture. Spherical sources are expensive to make and difficult to control in temperature and to achieve a uniform temperature. The compromise shape most often used is a cone with a total angle of (typically) 12 degrees to 14 degrees. Radiation entering or exiting the cone undergoes multiple reflections from the interior surface and emissivities on the order of 0.999 are claimed by manufacturers.

b. Extended-Area Sources. The advent of imaging systems created a need for calibration sources that are physically larger than is practical with a cavity source. The result is the extended-area sources that are now commercially available. These are electrically heated and temperature-controlled flat plates that are coated black. Typical active area dimensions are available from around four by four inches to a one foot square or larger. A flat plate can never achieve the emissivity of a cavity due to the lack of multiple reflections. Surface emissivities of around 0.98 are claimed for low temperature sources and around 0.95 for high temperatures. These sources are adequate for the calibration of most field and airborne instruments, but there are two concerns about emissivity:
   (1) At low temperature: A lower emissivity means higher reflectivity. For an opaque material, reflectivity = (1 – emissivity). At source temperatures much below that of the room, reflections from the warmer surroundings will elevate the surface radiance above that of the direct emissions
   (2) At high temperature: The emissivity of coatings for high temperature sources vary slightly with temperatures above approximately 600 ^{o}C.

The need for extended-area calibration sources is sufficiently great to accept the increased uncertainty that results from a lower emissivity. Another source of uncertainty is the temperature of the radiating surface. With a conical cavity, a good measurement of temperature is achieved by inserting a precision thermocouple into the apex of the cone. Because the thermocouple is within a cavity, thermal contact with the wall is not critical. With a plate, however, good thermal contact with the coated surface is difficult to achieve. Most commercial sources have a thermocouple embedded within the plate and a digital readout that displays temperature to high precision. Because of radiation and convective heat loss, there will inevitably be some thermal gradient between the point measured by an embedded thermocouple and the exterior of the surface coating. The gradient size and the amount of uncertainty it introduces is difficult to establish. Concern about uncertainty in any radiometric measurement begins with the calibration source. Temperature and emissivity, and their ultimate traceability back to a recognized standard, are always areas of consideration, but in most cases, the uncertainty these introduce is much less than from other causes. One of the chief sources of uncertainty results from the effects of non-uniform instrument response discussed in paragraph 6.2.2.

6.3.2 Wavelength Calibration of Spectral Systems.

a. Weighted Integrals. Instruments respond to received radiant power by integrating the power distribution in each domain under the corresponding response curve. Instruments respond in multiple domains, so output is proportional to a multi-dimensional, weighted integral. Figure 6-16 illustrates response-weighting, or convolution, of radiation with instrument response in the spectral domain. The concept applies equally in the spatial domain.

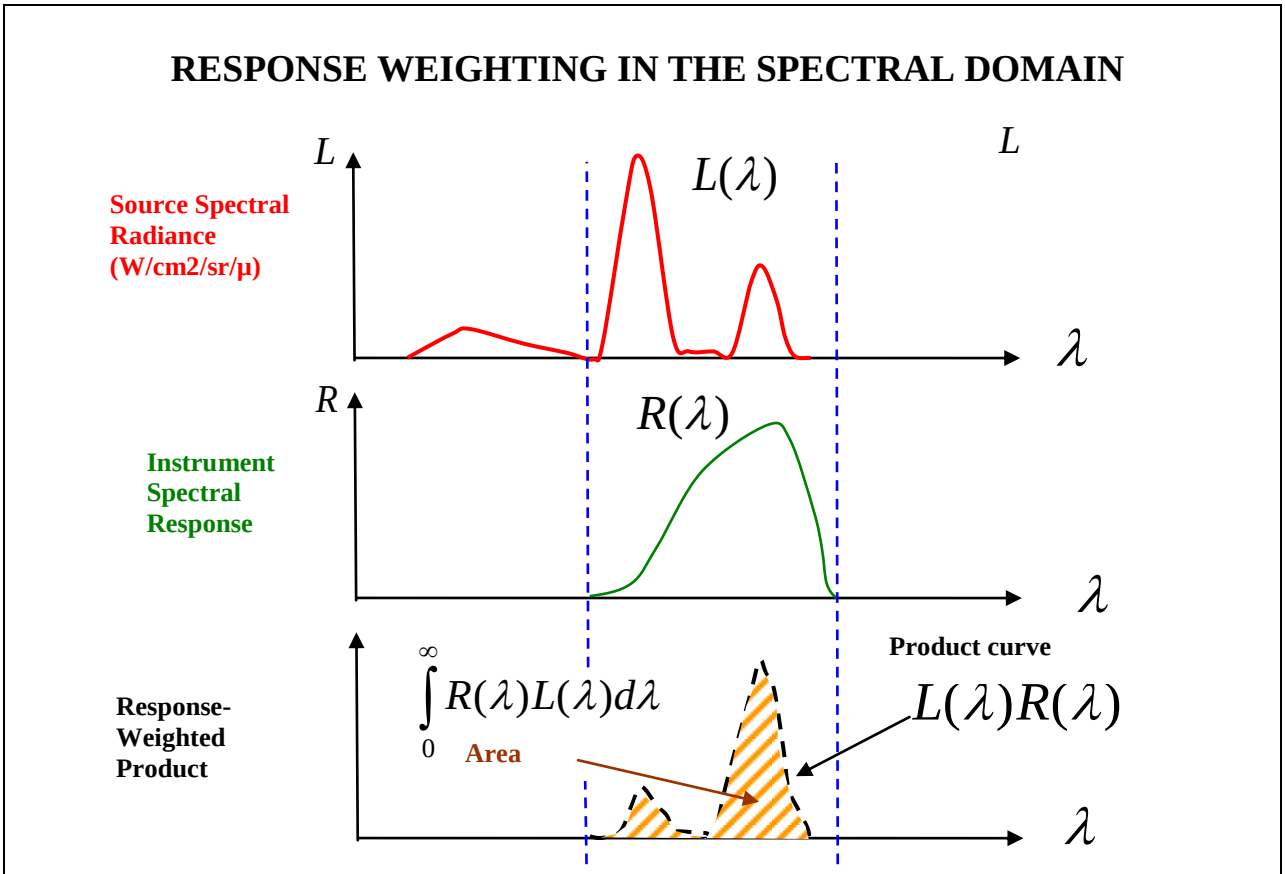

Non-uniform instrument response across a domain distorts the distribution of received radiant power by weighting the radiation at some wavelengths differently than others. Instrument output is proportional to the integral of this weighted product, which makes instrument response shape an embedded part of both the measurement and the calibration. Some consequences of non-uniform response are:

a. Two different sources with identical power, but different distributions will produce different measurement values.

b. If two different sources (such as the calibration and the target) have similar relative power distributions, the relative weighting by the instrument will be the same for both sources, so the shape and degree of non-uniformity has little or no effect. This will be discussed in more detail later as a key strategy in calibration to reduce measurement uncertainty.

Figure 6-16. Response weighting in the spectral domain.

The consequence of instrument output being proportional to multiple weighted integrals is that the characteristics of the instrument affect the measured value in ways that cannot be easily extracted or corrected. Measured values that contain instrument response are termed, effective values. All radiometric quantities begin (and most end) as effective.

Correcting for a non-uniform response requires two basic operations:

(1) Additional outside information must be brought in about how the target radiation is distributed across that domain. This information may come from either of the following two ways:
   - Measurements by another, different type of instrument. Examples are:
     a) For a radiometer or imager, measurements with a spectrometer.
     b) For a spectrometer, measurements with an imager.
   - From knowledge about the nature of the target source and its radiation environment. Examples are:
     a) Target is a solid emitter and consequently is distributed in accordance with Planck's formula where target temperature and emissivity are known. In this case, the spectral distribution is assumed to be that of a graybody or blackbody and a spectral measurement is not required.
     b) Where solar illumination of the target is known and the reflectance properties of the target surface is known.
     c) Where the atmospheric absorption and radiance of the measurement path are known.

(2) A correction factor must be derived based upon calculation of the instrument response (known from characterization) integrated with the estimated target distribution (from step 1 above).

A correction of measurement data for non-uniform response should never be undertaken without giving considerable thought to all the possible contributing factors. If insufficient or incorrect information is used or if erroneous assumptions about the target or its environment are made, the corrected value will be less correct than the original effective value. These kinds of operations will be discussed in greater detail in the paragraph on data reduction (paragraph 7.9).

b. The High-Resolution Solution. Every instrument has some degree of response non-uniformity in the spectral and spatial domains that is uncorrectable or, is at least very difficult to correct. The best solution to this problem is to reduce the width of the response until it is much narrower than any target features of interest in that domain. Using an instrument with a narrow response width (resolution element), has three important benefits:

(1) Additional information about the target can be obtained. Specifically, the distribution of target radiation across that domain can be extracted from the integral and quantified. If the resolution element is sufficiently narrow, the mathematical operation is that of a Dirac delta function.

(2) If the resolution element is much narrower than any target features of interest, then its response shape becomes insignificant. Instruments designed for the two domains are:

- Spectral domain: A spectrometer.
- Spatial domain: An imaging system, or camera. The terms imaging system, imager, and camera are synonymous terms. Usage is largely a personal preference and unimportant as long as the instrument is defined and described as one capable of performing calibrated radiometric measurements. For example, a camera may imply only the capability to produce uncalibrated images.

(3) In calibration, independent calibration factors are derived for each resolution element and applied in reduction of the measurement data. The result can be near perfect response uniformity across that domain. The ability to correct for non-uniformity in the spectral and spatial domains with calibration factors is thus a matter response width, as shown in Table 6-6.

TABLE 6-6. ABILITY TO CORRECT FOR NON-UNIFORM RESPONSE

Type	Response Resolution and Typical Non-Uniformity	
	Spectral	**Spatial**
Radiometer	Broadband & non-uniform: Uncorrectable	Wide FOV, non-uniform: Uncorrectable
Imager	Broadband & non-uniform: Uncorrectable	Narrow resolution: Calibration correctable
Spectrometer	Narrow resolution: Calibration correctable	Wide FOV, non-uniform: Uncorrectable

Use of the word "uncorrectable" in the different categories means that instrument response in that domain cannot be made uniform through calibration factors alone. Additional information about the target source distribution must be introduced and the correction performed mathematically using operations described in paragraph 6.3.3 and paragraph 6.3.4. State of the art imagers and spectrometers have scan rates that are great enough they can often replace the function of fast scanning radiometers although radiometers are still used today because they are typically inexpensive, reliable, and uncomplicated. When radiometers are used in a test along with high speed imagers and spectrometers, the radiometers are considered backup systems and the data collected by them is used for data validation. Having a non-uniform response does not, by itself, induce uncertainty as, for example, having noise in a reading does. The uncertainty caused by non-uniform response results mainly from our own lack of knowledge and erroneous assumptions. The most common erroneous assumption is to assume a uniform response. The resulting error will be systematic rather than random, which makes it more difficult to detect and to quantify without independent, outside knowledge.

6.3.3 Spectral Response of Banded Systems. Imagers typically have wide spectral response extending over a part of the spectrum which may include atmospheric absorption regions and target line emissions. For these cases, the shape of the response curve, and especially its cut-on and cut-off points, must be measured as accurately as possible. For imagers, the shape of the spectral response curve is determined by the product of the spectral transmission curves of each

element in the optical chain, from the objective lens to the detector, and the spectral responsivity of the detector. Staring, focal-plane array (SFPA) imagers are now the most common design used for imaging radiometry. The response-determining elements of an SPFA imager in the order encountered by entering radiation are shown in Table 6-7.

TABLE 6-7. THE RESPONSE-DETERMINING ELEMENTS OF AN SPFA IMAGER

Element[1]	**Comments**
Objective lens	The lens for an SPFA imager usually has four or more refractive elements made from materials selected and ground to correct for chromatic aberration and to give a flat focal plane. The lenses are anti-reflection (AR) coated to give relatively good average transmission across the specified wavelength region.
Dewar window	Also an AR coated material with good average transmission. Like the lens, the dewar window will only have significant effect on spectral response near the limits of its useful transmission region. Operation near the transmission limits of either the lens or dewar window is never recommended because, in the mid to far IR (FIR), these can be significant unwanted sources that vary with ambient temperature.
Interference filter	The filter should be the primary determining element for spectral response cut-on and cut-off. For IR imagers, the filter is usually a "cold filter" located within the dewar and consequently is at liquid nitrogen temperature, which greatly reduces the direct emissions from the filter as well as keeping the temperature and consequent emissions constant with varying outside ambient.
Detector array	Most detector arrays in use now are operated photovoltaic, which gives them a positive slope with increasing wavelength until reaching a steep cutoff on the long wavelength side. For IR imagers, most arrays must be cooled, usually with liquid nitrogen, which also keeps the array temperature constant as well as cold. As with the lens and window transmission, the filter should be the main response-determining element and not the detector.

[1] Shown in the order encountered by entering radiation.

a. Characterization Methods. The two most common methods of characterizing spectral response are the component method and the direct measurement method. The component method uses a composite of individual component transmissions and detector responsivity. The direct measurement method incorporates the total system using a tunable monochromatic source. Direct measurement of total system is the better method, but obtaining and perhaps modifying a tunable monochrometer and assuring its adequacy can be an expensive and formidable task.

(1) Component Method. The component method starts with transmission versus wavelength curves for each of the optical components described above. The net transmission at each wavelength will be the product of the component transmissions. Transmission curves are available from manufacturers. The task is made more tedious because most optical manufacturers provide only a curve and not discrete tabulations, so each curve must be digitized and interpolated to the same wavelength increments. Since the filter is the primary response determining component, the other components mainly affect slope across the bandpass and perhaps skew the turn on and off points slightly. The chief pitfall with interference filters is their temperature sensitivity. Because interference filters work by constructive and destructive interference between deposition layers, their transmission curve translates with temperature according to their coefficient of expansion. Unless specified, most filters come with transmission curves run at a room ambient temperature of 23 ^{o}C (296 K). If the filter is to be mounted within a liquid nitrogen dewar, a curve must be provided at the temperature 77 K. The difference can be significant. Figure 6-17 shows a sample filter transmission with a bandpass of approximately 4.55 μm to 5.0 μm at 77 K. The bandpass at 23 ^{o}C is 4.65 μm to 5.11 μm. Because this is on the long wavelength "red spike" side of carbon dioxide emission, the approximately 0.1 μm difference would have a significant impact on measurement values of exhaust plumes.

The final component in the optical chain is the detector. Detector spectral responsivity can usually be obtained from the manufacturer or, failing that, from published literature for that detector type at the planned operating temperature (usually 77 K). As long as the bandpass of interest does not lie too close to the cutoff wavelength, the main effect of detector responsivity is to give a tilt to the net spectral response curve. When the contributions of all the components are combined into one curve, the result is then peak normalized and this, now unitless, curve is used in the calibration calculations.

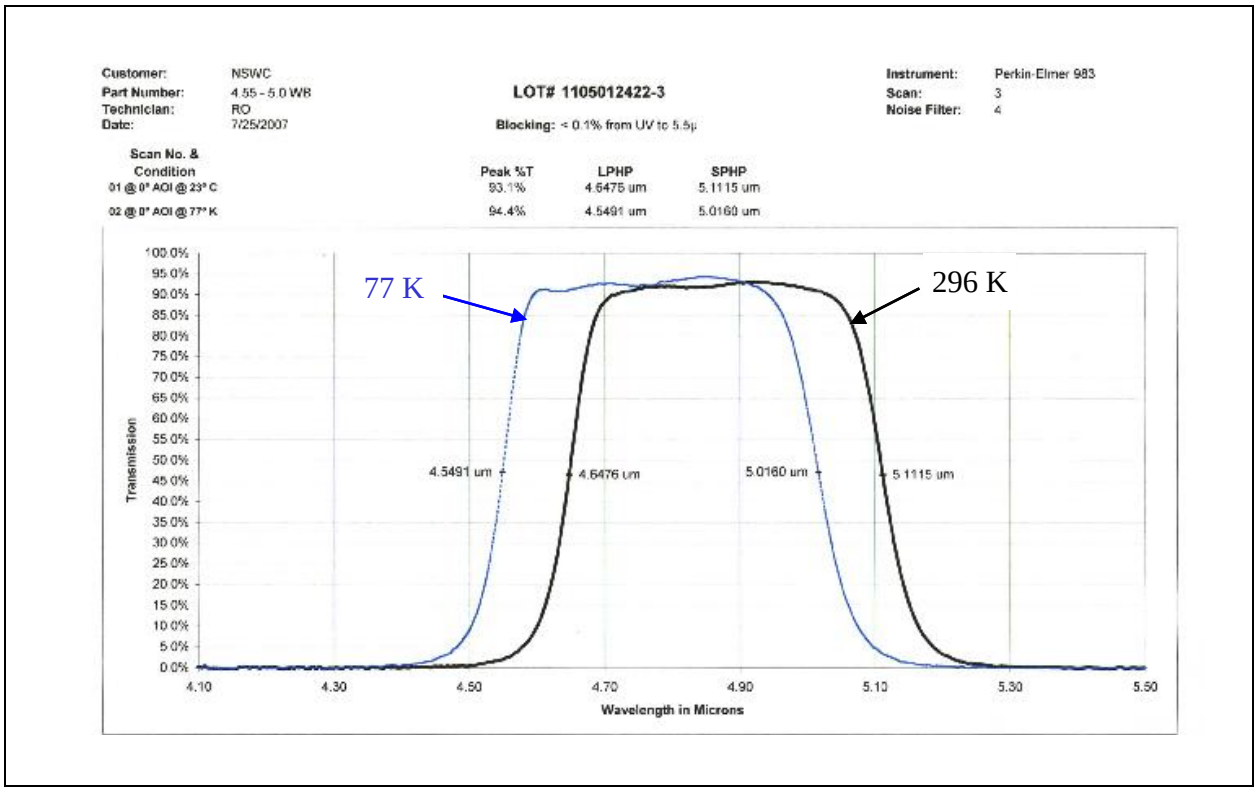

Figure 6-17. Interference filter transmission at two temperatures.

(2) Direct Measurement Method. Direct measurement of spectral response with a tunable monochromatic source has the considerable advantage of measuring the total response of every component in combination and at the temperature at which the imager will be operated. The difficulty usually lies with the requirements for the monochromatic source. Most tunable monochrometers consist of a high-temperature graybody source followed by either: (1) diffraction gratings with blocking filters or (2) a prism of appropriate dispersive material. Diffraction gratings use constructive and destructive interference to separate a beam with narrow spectral width from the broad spectrum. Prisms use the change in index of refraction of the prism material with wavelength (dispersion) to achieve the same result. In practice, "monochromatic" is not literally "one color" as the name implies, but only a source whose spectral width is narrow relative to the spectral features of interest. A system of lenses then brings out a partially collimated beam that is directed into the instrument under test. To measure spectral response, the monochrometer is "tuned" (i.e., the center wavelength varied) across the spectrum and the instrument output at each wavelength increment is measured and recorded. The theory is simple enough, but the practice involves careful laboratory work characterizing the monochrometer to assure validity of the instrument response curve to be measured. The requirements for an adequate tunable monochrometer are shown in Table 6-8.

TABLE 6-8. REQUIREMENTS FOR AN ADEQUATE TUNABLE MONOCHROMETER

Circumstance	Requirements/Comments
Purged atmosphere	Carbon dioxide and water vapor must be removed from the path between the monochrometer and the instrument by purging with a flow of dry nitrogen or by evacuation.
Known spectral irradiance (or radiance if source is spatially resolved)	The irradiance of the monochromatic beam must be measured with an independent, broad-spectrum radiometer whose calibration is traceable to a standard source. Tunable monochrometers are sometimes capable of operating in either of two modes: (1) constant-output variable-resolution or (2) variable-output, constant-resolution, which is more common today.
Known background	Unless the monochromatic source subtends an angle greater than the optical resolution of the imager (not usually the case), the instrument's view of the monochromatic beam will include some of the internal housing as background, i.e., the measurement will be contrast. At wavelengths shorter than approximately 3 μm, the contrast between the beam and its background may be sufficiently great that background radiation can be ignored, but this should never be assumed and high contrast is almost never the case at longer wavelengths. This means that the independent radiometer referred to in Chapter 2 must have a similar field of view (FOV) as the instrument under test to assure the backgrounds seen by each are similar.
Narrow spectral resolution of the beam relative to the imager response width	Intensity of the monochromatic beam is inversely proportional to the spectral width. An instrument under test with narrow spectral response may require the monochrometer resolution to be too narrow to give adequate contrast irradiance for measurement. Exactly where this limit is becomes a judgment call for the measurement personnel

(3) The Hybrid Solution. The problem of compromise between a sufficiently narrow monochromatic beam and sufficiently high contrast irradiance (described in Table 6-8 above) can largely be solved by performing a characterization that combines the component and direct methods. Imager spectral response is determined by the lens, dewar window, filter, and detector spectral responsivity. In a typical imager, the lens, window, and detector have broad response across the active region without large spectral variation or structure that must be resolved. The filter is (and should be) the most critical element in the chain. A hybrid solution is to use both methods. First, use the direct, tunable monochrometer method to characterize the imager response without a filter installed. Second, use the component method to characterize the transmission curve of the filter from the manufacturer's curve or in your laboratory with a spectrophotometer. The final

spectral characterization is the combination of these two curves, which is then peak-normalized.

(4) Characterization Summary.

- Run transmission curves of interference filters at their operating temperature.
- Perform and compare results from both component and direct methods.
- Use a hybrid characterization if monochrometer requirements are too stringent.

6.3.4 Spatial Response of Spectrometers.

a. Uncertainty From Spatial Effects. Often, spectrometer spatial response does not get the characterization and attention it should because the focus is on the spectral data and, perhaps, because spectrometers do not produce pictures and therefore measurement uncertainty from spatial effects is more difficult to visualize. The uncertainty that can result from spatial effects, like every other aspect of radiometry, depends upon the interaction between the characteristics of the target scene with the response of the instrument.

b. Spectrometer Designs and Target Spatial Features.

(1) Spectrometer Design. Spectrometers for field and airborne target signature measurements commonly use one of four different designs to separate received radiant power by wavelength:

- Michelson interferometer spectrometer (also known as a Fourier transform IR (FTIR) spectrometer).
- Circular variable filter (CVF) spectrometer.
- Prism spectrometer.
- Diffraction grating spectrometer.

In all cases, uniformity of the spatial response is sacrificed to some degree by the design aim of good spectral resolution. Spatial response acts as a weighting function on the integral of received target radiation, just as spectral response does in the spectral domain. Characterization of the special response and its treatment in measurement can be a significant source of uncertainty in measurements.

(2) Target Spatial Features. Spatial features of the target and target scene include:

- Angular direction of the target relative to the instrument optical axis.
- Solid angle subtended by the target.
- Background radiance level.
- Area (or solid angle) of the background obscured by the target.
- For multiple targets, angular separation of the targets in addition to the above features.

c. Typical Spectrometer Spatial Response. The dominant spatial response is usually a non-uniform weighting of the target that depends on position in the FOV, specifically to angular direction from the optical axis. Figure 6-18 is an example of a typical spectrometer spatial response in one dimension, with an FOV that is 10 mrad at the 90 percent response points, 14 mrad at the 50 percent points, and 20 mrad at

10 percent. This curve will be the basis for examples of uncertainty in measurements caused by spatial response.

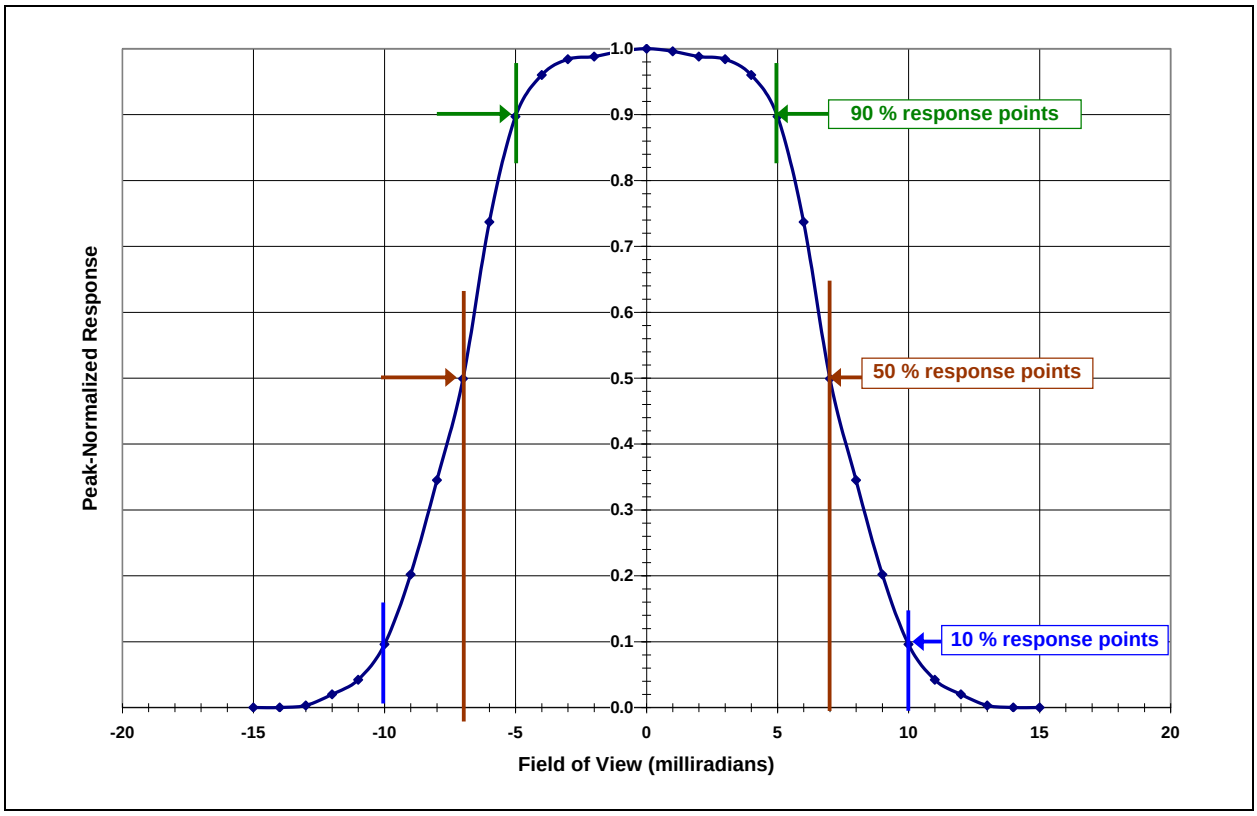

Figure 6-18. Typical spectrometer spatial response in one dimension.

d. "Point-Source" Mapping Method. The most common method of mapping a response curve such as Figure 6-18 is to use a collimated blackbody source with an aperture diameter that subtends an angle much smaller than the spectrometer FOV. The spectrometer is mounted on a rotary table and placed in the collimated beam with the spectrometer objective lens fully illuminated by the beam. A point source at the focal point of a collimator simulates a source at infinity. Pivoting the optical system while in the collimated beam simulates the point source moving laterally across the FOV.

From the maximum reading, which hopefully occurs near the center of the FOV, the rotary table is incremented and readings taken versus angle on either side until there is no measurable response. This completes the raw horizontal mapping. The spectrometer can then be laid on its side and the operation repeated to map elevation or, better yet, horizontal scans can be made at vertical increments to complete a matrix. Mapping a complete matrix is recommended where the FOV is not circular or where it may have some off-center skew. A useful way to visualize spatial response is as a contour map impressed on the target radiance scene, where contours are weighting factors. The final response curve or matrix is then peak-normalized.

e. Spatial Strategies. Mathematically, instrument spatial response acts exactly like spectral response in convolving with target radiation distribution across the domain

and could be used to calculate effective values as is done with spectral response. This is required in situations where the spatial response is complex, as in a missile that uses a reticle to obtain tracking information. In radiometry, however, where spatial response is typically much simpler, the spatial response curve is used primarily to restrict measurement conditions to those target scene conditions where spatial effects will not introduce significant uncertainty. These restrictions lead to the two main strategies for reducing uncertainty from spatial effects: target size and target background. Most measurements with spectrometers are made spatially unresolved, where the target subtends angles less than the total FOV. In Figure 6-18, only targets subtending angles less than 10 mrad fall within the 90 percent response region. Calibration is typically done with a collimated source that subtends a small angle in the center of the FOV. As a result, only the flat center region is actually calibrated. Without the creation of an image, it is difficult to know and, consequently, to correct for regions beyond center. The safest strategy is usually to plan the measurement distance in advance for a given target size so the target image is contained within the flat, calibrated region. If the target is fully resolved so it fills the FOV (an example would be a close-up measurement of airframe), the instrument output will be proportional to the mean of the target radiance weighted by the spatial response. To measure a fully-resolved target, the laboratory calibration source should also be fully-resolved. If these conditions are met, the non-uniformity of the spatial response will largely be compensated. In summary:

(1) For unresolved targets, limit angle subtended to the uniform response region.
(2) For fully-resolved targets, calibrate with an extended source.

f. Background Uncertainty. Where the target subtends an angle smaller than the spectrometer FOV, background radiation is an unavoidable and inseparable part of the measurement. A method known as "background subtraction" is frequently used to reduce the contribution by background to the total. A measurement of an adjacent area of background without the target is subtracted from the measurement of the target scene containing background. Uncertainty is introduced by spatial response non-uniformity or, to be exact, by a false assumption of response uniformity. If the target subtends a substantial area and the response is not uniform, then the area of the background obscured by the target will not be weighted the same as the surrounding background. This difference in weighting is rarely taken into account, in large part because of the many unknowns involved. Background effects and subtraction will be discussed in more detail later. The amount of uncertainty from background depends upon the target contrast (difference between radiance of the target and radiance of the background) and the response non-uniformity. Uncertainty is greatly reduced for low background, high contrast targets.

g. Automatic Background Subtraction. A class of radiometers and spectrometers are designed to automatically subtract background radiation from an area of the scene adjacent to that containing the target to produce contrast rather than absolute measurement values. The spatial response of these instruments can be complex and their analysis and recommended characterization method is beyond the scope of this paper. The chief measurement strategy with automatic background-subtracting

instruments is to restrict their use to measurements of single, high-contrast, small-area targets, such as jet engines, flares, or solid propellant missile plumes.

6.3.5 Temporal Response. Refer to paragraph 6.1.19 and paragraph 6.1.20.

6.3.6 Irradiance Response. Refer to paragraph 2.5.1 "Irradiance Calibration."

6.3.7 Radiance Response. Refer to paragraph. 2.5.2 "Radiance Calibration."

6.3.8 Basic Calibration Techniques. The calibration of an instrument quantifies its absolute response function. Calibration provides the information needed to transform an *indication*, sensing that some radiant quantity is present into a *measurement* (putting a number value to the quantity). Measurements of every type, such as common measurements of length or weight, are made by comparing the unknown object with some known and accepted standard. This is usually done via a lengthy chain of instruments, devices, and tertiary and secondary standards that are ultimately traceable back to a primary standard. In concept, the measurement of radiation is no different. The measuring instrument provides a connection linking the unknown target radiation to a known intermediate radiation standard (the calibration source), which is ultimately traceable back to a primary standard. This connection between the target and the calibration source is made via the instrument responses in all of its active domains. Calibration quantifies the relationship between the output voltage or reading and the input radiant power, which is usually expressed in units of either radiance or irradiance. This relationship is the calibration function or calibration "curve". Calling the calibration function a "curve" acknowledges that the function may be approximated as linear over a limited dynamic range, but is always non-linear to at least some degree.

a. Calibration Function. The calibration function is the inverse of the more familiar electronic circuit transfer function, which is usually expressed as the ratio of output to input. It is a matter of what you know and what you wish to find out. With a circuit, you usually know the input and want to find out what the output will be in response to that input. With radiometry, we usually know the output reading and wish to find out what input radiation produced it. Multiplication by the calibration function gives values for the radiation received. Because radiometry is remote sensing, the measurement process is one of "working backwards." From measurements of the radiation received by an instrument, deductions are made about the radiation that was emitted from the distant target source. This is done by working back from the instrument towards the target, accounting for all of the possible influences along the way. The instrument calibration is the first element in this chain of deductions, presented in Figure 6-19.

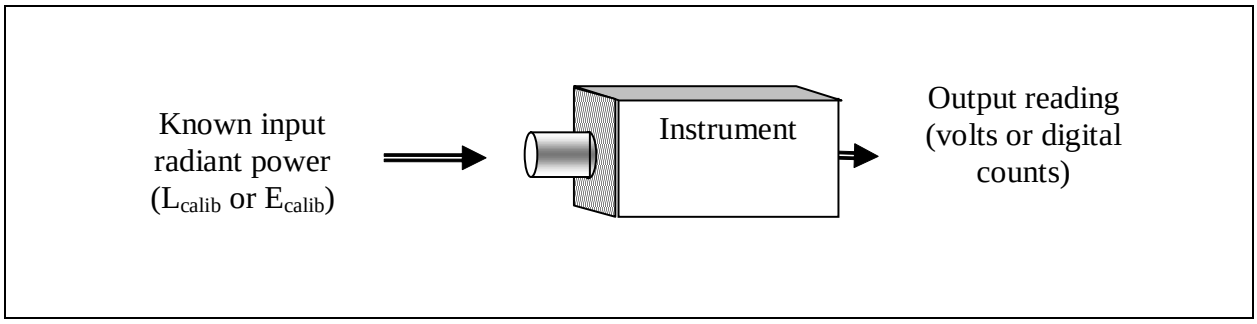

Figure 6-19. Calibration process.

Calibration quantifies the relationship between input radiant power and output readings and relates input to output by quantifying the calibration function, C, shown in simplified form in Equation 6-15 and Equation 6-16. In the complete form all radiant quantities are functions of their spectral, spatial, and temporal distributions and all instruments respond to weighted integrals in a particular domain. Expressed in units of radiance, the calibration function is:

$$C = \frac{Input}{Output} = \frac{L_{calib}}{x_{calib}} \text{ in units of radiance} \qquad \text{(Eq. 6-15)}$$

$$C = \frac{Input}{Output} = \frac{E_{calib}}{x_{calib}} \text{ in units of irradiance} \qquad \text{(Eq. 6-16)}$$

Where

L_{calib} = known radiance level of calibration source (W sr^{-1} cm^{-2})
E_{calib} = known irradiance level of calibration source (W cm^{-2})
x_{calib} = instrument output reading at calibration (volt, ampere, digital count)

In this simplified example, the calibration function, *C*, is the slope of a line that passes through the origin. An output reading, x_{target}, is collected while viewing the unknown target source. The radiance or irradiance value of the target is derived by multiplication of the target reading by *C*. Notice that for this simple instrument the radiance or irradiance of the unknown target is basically a ratio calculated from the known radiance or irradiance of the calibration source. For example, if $x_{target} = 2\ x_{calib}$ would yield a radiance or irradiance value twice that of the calibration source.

$$L_{target} = C \cdot x_{target} = \left[\frac{L_{calib}}{x_{calib}}\right] x_{target} \text{ in units of radiance} \qquad \text{(Eq. 6-17)}$$

$$E_{target} = C \cdot x_{target} = \left[\frac{E_{calib}}{x_{calib}}\right] x_{target} \text{ in units of irradiance} \qquad \text{(Eq. 6-18)}$$

Thinking of the instrument as a connection between the unknown and the known is important because the characteristics of the instrument play such a significant role in the measurement result. The expressions above assume a perfect instrument. Specifically, they assume that the following is true.

(1) First, zero radiation input produces a zero reading out, i.e., there is no offset. Even if zero radiation were possible, in practice, all instruments have some offset reading that must be quantified as part of the response function.
(2) Second, the instrument responds linearly. In fact, all instruments have some degree of nonlinearity. Where dynamic range is limited, as with a staring focal plane array (SFPA) camera, it may be possible to approximate the response as linear, but linearity should never be assumed without supporting data.
(3) Third, the instrument response across the active region is uniform. As discussed in Chapter 2, all instruments have non-uniform (and non-correctable) response in either the spectral or spatial domains or both.

- Offset Voltage. Consider the first assumption. There are several reasons why instrument output is not allowed to go to zero even if a hypothetical zero-radiance source were possible. All electronic circuits have some amount of direct current drift. In addition, internal radiation sources such as the lens and windows, contribute a radiation component to the offset that varies with instrument ambient temperature. To prevent clipping of the signal if this drift should go below the lower limit of the analog-to digital converter, the "bottom end" level is adjusted up to some offset level. The consequence of this offset voltage is the addition of a y-intercept term (*b*) which also must be quantified by the calibration, as shown in Figure 6-20.

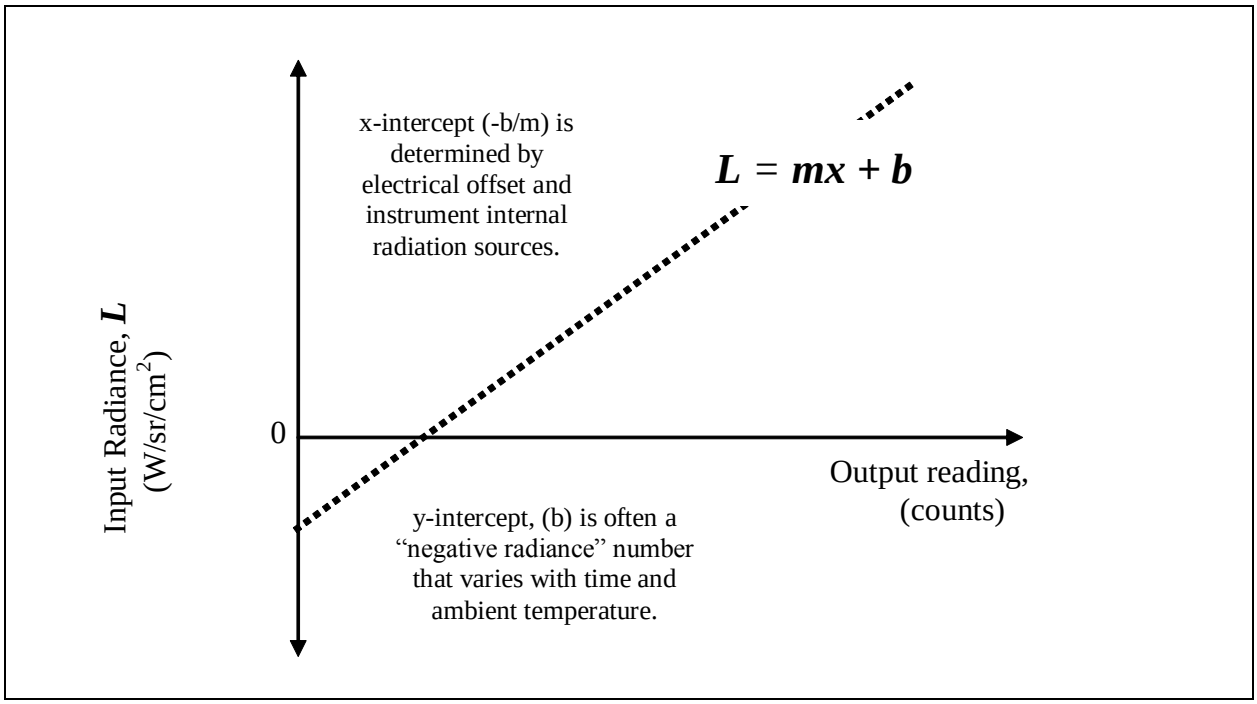

Figure 6-20. Consequences of offset voltage.

- Linearity and Dynamic Range. For the second assumption, most instruments are linear over a limited dynamic range, but that should never be assumed without verification. In IR cameras with staring focal plane arrays, for example, the detector arrays have limited, (typically less than a factor of 1000) dynamic range from the lowest to greatest radiance level in any gain or integration-time setting. Over this range, error introduced by assuming a linear response function is small in comparison with the many other sources. Where different gain/integration-time settings are used to span a greater range, the total curve can be represented as piece-wise linear, with different slope and offset terms for each setting. For these small dynamic-range cases, a conventional least-squares fit of the response function to calibration data points is usually adequate. However, for a single detector in a radiometer, spectrometer, or mechanically-scanned camera, the dynamic range of a single gain setting may be 50 000 or greater. Here, the error from assuming linearity may be substantial, especially for low levels. In this case, the response function usually must be represented as a second-order polynomial and a conventional least squares fit may not be adequate. It is rare that a higher-order polynomial than second is required. The shape of a second-order curve has a single "bow." A third-order curve has an "S" shape and higher orders have additional curves. If a third-order or higher appears to be necessary, it is advisable to investigate the mechanism that is causing the curve to bend back upon itself. This may be a symptom of deeper instrument problems, such as saturation of an intermediate amplifier stage that should be resolved before worrying about calibration. A function that is derived from conventional least-squares fit may introduce substantial systematic error for low-level measurements. The aim of a conventional least-squares fit is to minimize the average difference between the curve and data points. This means that the high level points dominate at the expense of a good fit at the low-level points. With radiometry, we usually want to minimize the difference between the curve and data points as a percentage of reading, in effect, to weight the lower level calibration points more heavily than the higher level points. A poor fit due to conventional least-squares calculations may not be apparent if the data and curve are only plotted on a linear graph. A linear graph itself only displays a dynamic range of less than 100 because all of the low-level points bunch together. To check the goodness of fit over a wide dynamic range, experiment with plotting the data and curve on a log-log graph. A poor fit at the lower points will be immediately apparent.

b. Sensitivity to Operating Temperature. The measurement process relates the unknown target to the known calibration source by way of the measuring instrument and its responses. As a result, the integrity of the measurement requires that the response functions of the instrument be the same during the target measurement as it was for the laboratory calibration, or that any differences be compensated. Among the differences in environment between field and lab that can affect a measurement are changes in ambient temperature, pressure, and radiation from sources outside the

FOV, such as the sun. In most measurement situations with IR instruments, especially staring focal plane array (SFPA) imagers, the critical sensitivity is to ambient temperature.

(1) Temperature Influence on SFPA Imagers. SFPA imagers do not use optical scanning or mechanical modulation. As a consequence, photoelectrons created from illumination of the array by the target source are indistinguishable from those received from the lens, from the window (if used), reflected from the housing, and also from any electrical bias or offset voltage on the array or any subsequent electronic gain stage. For an imager that is sensitive to wavelengths longer than around 3 μm, radiation from the objective lens and other internal sources is a significant contributor to the offset. If lens temperature changes with changes in ambient, the result is a translation of the whole calibration curve (described below). Characterization of imager sensitivity to ambient requires distinguishing between changes (if any) that affect gain and changes that only affect offset. Both require correction or compensation with a field calibration. The important distinction is that a change in gain requires two field calibration sources to determine the changed slope. A change that only affects offset only requires a single field reference source. For a SFPA imager, frequent reference readings must be made throughout a field test.

(2) Gain Sensitivity Elimination.

- Linear System. A basic method of determining sensitivity of SPFA imagers to temperature is to eliminate gain change as a source of uncertainty. For an imager with a linear calibration curve, gain is the slope. For an imager whose calibration curve has previously been established as linear, this can be done with a temperature chamber and two extended-area calibration sources. Temperatures of the calibration sources are chosen to give radiance values near the low and high ends of the most sensitive gain range of the imager, but above dew point to avoid condensation. The basic procedure is as follows:
  a) With the imager stabilized at laboratory ambient, readings are taken and recorded for the low and the high temperature sources at close range with the sources overfilling the imager FOV.
  b) The imager is then placed in a temperature chamber set at some higher temperature, such as 40o C. A lower temperature could also be used, but must be above dew point. Power does not need to be applied. The imager is then allowed to "soak" for a half hour or so for all components to stabilize in temperature.
  c) The imager is removed from the chamber, turned on, and readings immediately taken on the two sources.

Most SFPA imagers are quite gain-stable with temperature. For a typical SFPA imager, the readings will have translated substantially in offset with imager temperature, but the difference between readings on the two sources will have changed little if gain has not been affected. Expressed as a percentage in change of slope, a typical SFPA imager will show a gain change of less than half a percent. In such a case, gain change with ambient can be eliminated as a significant source of uncertainty and field reference readings

only need be taken at a single temperature. If gain is found to change with ambient, plan on using a minimum of two field calibration sources at different temperatures.

- Non-Linear System. For an instrument with a non-linear relationship between output reading and input radiance or irradiance, two calibration source temperatures are not sufficient. In this case, a full calibration over the instrument dynamic range at the two ambient temperatures is required to establish that only the offset term of the calibration coefficients changes with temperature.

c. Sensitivity to Operating Pressure. Airborne instruments that are carried in an unpressurized pod may have some sensitivity to atmospheric pressure. When the detector is maintained at constant temperature by the boiling point of liquid nitrogen, changes in pressure result in slight changes in detector operating temperature. Sensitivity to pressure can be tested in the laboratory by viewing a constant calibration source and connecting a vacuum pump to the dewar vent. If a change in pressure causes a change in instrument reading, attachment of an absolute pressure regulator to the dewar will be required.

d. Sensitivity to Out of Field of View (FOV) Sources. Using the response curve of Figure 6-5 as an example, the figure appears to show that any source located more than 15 mrad off the optical axis will produce no response. The reality is that for most instruments there is some response well beyond the nominal region. How seriously off-axis response may affect a measurement depends upon the irradiance from the target relative to that from the unwanted source. With imagers, a strong off-axis source can cause reflections and false images that, at least, are obvious to the operator. With spectrometers, the influence may not be apparent and, consequently, can be a greater threat. Whether these are radiometrically significant can be determined by viewing a low radiance laboratory source while moving a high intensity source around the instrument, starting from approximately 90 degrees off axis to near the active FOV, while taking readings at regular angle increments. A problem with off-axis sources is difficult, if not impossible, to compensate for, especially after the measurement. A better approach, where possible, is to shade the target or to choose a viewing angle away from the unwanted source.

e. Instrument Response Uniformity. In the third simplifying assumption, the instrument is assumed to produce the same output reading for the same input radiant power, regardless of how the power was distributed across the instrument active region in that domain. The reality is that an instrument will produce an output that is proportional to the integral of the received radiation weighted by a response curve that may be highly non-uniform. How non-uniformity is treated (or not treated) in calibration has a large impact upon the final measurement uncertainty.

6.4 References for Chapter 6

a. Brown, Col. R. (April 1996). Tactical Missile Signatures Measurement Handbook, Gerber, G. (Editor), Joint Tactical Missile Signature (JTAMS) Joint Task Force (JTF), Infrared Information Analysis Center at Veridian Environmental Research Institute of Michigan (ERIM) International, Ann Arbor, MI.

b. Inter-range Instrumentation Group (IRIG) (Dec 1998). Range Commanders Council (RCC) Standard 802-98: Tactical Missile Signatures Measurement Standard and Definitions.

c. Wolfe, W., and Zissis, G. (1993). The Infrared Handbook (4th printing of 1985 edition). Infrared Information Analysis (IRIA) Center, Environmental Research Institute of Michigan, for the Office of the Naval Research, Washington DC.

d. Dereniak, E., and Boreman, G. (1996). Infrared Detectors and Systems. John Wiley and Sons.

CHAPTER 7

MEASUREMENT PROCESS

7.1 Overview

A typical radiometric measurement progresses through a number of stages from initial concept and planning to final data product. The exact number of stages and the tasks within each depend upon a variety of factors, including measurement objectives, instrument types, target characteristics, atmospheric path, radiance background, and data applications.

The methods and mathematics given here are not intended as all-inclusive step-by-step recipes for success, but rather to give a sufficient level of understanding and insight into the mechanisms of measurement to enable personnel to create and apply their own tools to their unique situation. Complete documentation of the particular method used is almost always more important than the method itself.

The steps involved in a typical measurement include:

a. Measurement Program Planning
b. Instrument Selection Strategies
c. Instrument Characterization Calibration Strategies
d. Instrument Calibration Strategies
e. Overall Measurement Strategies
f. Supporting Measurements and Recordings
g. Daily and Post Test Calibration
h. Data Reduction and Uncertainty
i. Documentation and Data Presentation

These steps are generally, but not necessarily, performed in the order above. Measurement planning must be done first. The measurement objectives and target characteristics determine the required instrument types, wavelength bands, dynamic range, FOV, and temporal, spatial and spectral resolutions. In turn, characterization must be done prior to calibration because all of the calculations for calibration are based on the response curves that come from characterization.

A daily and post-measurement calibration is needed to compare with the pre-measurement calibration to assure that no changes or malfunctions to the instrument have occurred during the measurement period. Calibration repeatability doesn't establish accuracy, but good accuracy can never be attained without first establishing and verifying good repeatability. Documentation, while listed in the last step in the measurement process, is by no means insignificant. Documentation is a continuous process beginning with Step 1 and concluding with Step 9, Documentation and Data Presentation. Unfortunately, testers can be in a hurry to see the test results and once that is satisfied, the documentation is poorly prepared and often not submitted with the final data package. Lack of documentation makes it virtually impossible to correlate data taken with several instruments from two or more measurement teams. For this reason, documentation will be emphasized throughout the measurement process.

7.2 Measurement Program Planning

Planning for any measurement starts with defining, to the extent it is known or surmised, everything about the expected characteristics of the target, the conditions under which it will be measured, the information needed from the measurement, and the application of the measurement results. Information about the objectives, expectations, and the application of the results is essential. The better these are understood and defined before the measurements, the more useful the final product will be. These target definitions determine the following:

a. The type of instruments to be used, whether band radiometers, imaging systems or spectrometers, their spatial and spectral ranges and spectral, spatial, temporal resolutions.
b. The characterizations performed on each instrument.
c. The calibration source and calibration path characteristics.
   (1) Temperature range to bracket the radiance or irradiance levels expected from the target.
   (2) Viewing geometry, whether extended-area or collimated.
   (3) Calibration path and whether it must be purged with dry nitrogen or a vacuum.
   (4) Calibration quantities, whether calibrated in radiance or irradiance.
d. Arrangement of the target and target scene.
   (1) Slant range from instrument to target.
   (2) Target size in the instrument FOV.
   (3) The background against which the target will be viewed (if controllable).
   (4) Aspect angles for measurements.
   (5) Target operating conditions during measurements.
e. Supporting ancillary data that must be collected along with the measurement. Common examples are:
   (1) Weather readings or radiosonde soundings.
   (2) Time-space-position information.
f. Data reduction procedures.
g. Operations to be performed on the measurement data to extract the needed information.
h. The method to organize and present the data and the documentation to accompany the data.

7.3 Instrument Selection Strategies

7.3.1 Instruments should be selected according to target information requirements. Measurement programs have, or should have, very specific information needs about a target. These are driven by the characteristics of the target and its environment and by the application of the measurement data. Select instruments according to the information needed and for the complexity of an anticipated target radiation distribution and the scene in which the target is embedded. Additional discussions of instrument characteristics needed to measure different types of targets will be given in the following paragraphs.

7.3.2 Prioritize radiometric and ancillary instrument. The list of instruments that will be used in a measurement should be lengthy. From that list, however, there will be some instruments

that are essential, some that are important, and some that are nice to have, but will only become important if one of the essential instruments fail.

7.3.3 Instrument priority should be reviewed and a "no-go" list agreed upon. In some measurement programs, the no-go list may change at different stages of the test. With aircraft, for example, the no-go list that would be cause for canceling a test will be longer before the aircraft have taken off and before the start of the range period. After the aircraft are airborne and the aircraft and the full range costs are incurred, the no-go list will be much shorter. Cancellation at that point would result in little savings. A priority list might also change as the test progresses and first priority data are successfully collected. The second tier priority measurements move up in priority as first priority data are successfully collected, and so for forth.

7.4 Instrument Characterization Strategies

7.4.1 Use Similar Spatial Distributions. Measurement uncertainty is reduced if the calibration source subtends solid angles similar to those expected for the target. Defining or estimating the target spatial characteristics is an important part of the measurement planning. The information from this planning is used in selecting a calibration source or sources with similar spatial extent.

Non-uniform weighting of spatial response across an instrument FOV is mathematically identical with weighting in the spectral domain. An effective calibration unit, from a weighted integral, can be calculated in the spatial domain just as it is done in the spectral domain, but that is not always necessary. Source spatial distributions typically do not have as much structure as spectral distributions and instrument spatial response is usually more uniform than spectral.

It is often adequate to categorize a target spatially based on the target image size in the instrument FOV and to treat accordingly. The two spatial categories are:

a. Unresolved. The target subtends a solid angle less than the instrument IFOV.
b. Resolved. The target subtends a solid angle substantially greater than the IFOV. A target whose angular extent falls in between, that is, one which is partially resolved or is near the instrument resolution, should be treated as unresolved.

The two target spatial categories determine which of two calibration units to use. The two most common units of radiometric calibration are:

c. Irradiance (*E*). Irradiance is the radiant power density incident on the instrument entrance aperture. Irradiance is usually expressed in units of W/cm^2.
   (1) Irradiance varies as the inverse square of distance between the instrument and the target (assuming no atmospheric absorption).
   (2) Irradiance calibrations are used for measurement situations where the target is expected to be unresolved.
   (3) Radiometers and spectrometers are calibrated in irradiance.

d. Radiance (*L*). Radiance is the source radiant power density per unit solid angle. Radiance can be thought of as the intensity (power per solid angle) per unit area of

the source. Although radiance is a source quantity rather than a receiver quantity, radiance in measurement is concerned with the source as perceived by a distant receiver. Radiance is usually expressed in units of W/(sr cm^2).

(1) Radiance is independent of distance to the source (assuming no atmospheric absorption and a spatial homogeneous source).
(2) Radiance calibrations are used for measurement situations where the target will be highly resolved.
(3) Imagers are usually calibrated in units of radiance.

7.4.2 Use Similar Spectral Distributions. The same mechanisms described in the spatial domain apply equally in the spectral domain. The greater the similarity between the target and the calibration source spectral distributions, the less uncertainty will be introduced by inaccuracies in the spectral response.

Unfortunately, target distribution in the spectral domain usually has much greater variability across the range of interest than the spatial domain. Absorption by the atmosphere adds an additional complication. In practice, the only two controls over spectral distribution of the calibration source are the spectral output of the source through the temperature of a blackbody for the MWIR and LWIR, and the choice of lamp for the UV/VIS/NIR and atmospheric absorption window across the spectral range. The atmospheric window can be controlled through the calibration range in that it might be possible to calibrate at short enough range to neglect absorption and it might be possible to purge the calibration path to completely eliminate atmospheric absorption.

7.4.3 Use Similar Source Temperatures. Blackbody sources are chosen for calibration because they emit a known amount of radiant power with a known spectral distribution; in other words, they radiate in accordance with Planck's Law. As the temperature of a source increases, two things happen: total radiation increases and the peak of the radiation shifts towards shorter wavelengths.

If the approximate temperature of the target is known, and if the target source is a solid and not a gas, using a calibration source with the same temperature will reduce uncertainty from spectral response. There are practical limitations to spectral matching using temperature that depend upon the calibration type.

Temperature matching works well for a radiance calibration, when the target geometry is constant. Temperature matching becomes more complicated for an irradiance calibration, when different calibration irradiance levels are achieved by varying both temperature and source aperture area, which causes changes in both the calibration source spatial extent and the area of background seen by the instrument.

Although less than perfect, matching the calibration source temperature to the target is still good practice and should be done wherever practical.

7.4.4 Use Similar Atmospheric Paths. An air path between the instrument and the source contains water vapor and carbon dioxide, whose molecules have resonant frequencies in the MWIR. Gases absorb and re-emit radiation at their resonant frequencies. The result affects the received radiation in two ways:

a. Atmospheric transmission. Selectively absorbs radiation in spectral regions. The depth and width of an absorption region depends upon the number of molecules over the path. Absorption is greater over longer paths and at lower altitudes.
b. Path radiance. The atmosphere appears as a source between the instrument and target or calibration source. Path radiance results from two different mechanisms:
   (1) Thermal emission. Gases emit in the same spectral regions where they absorb. Emission magnitude depends upon ambient air temperature.
   (2) Scattering. Radiation from sources, such as the sun, that lie outside the FOV of the instrument is scattered into the instrument view. Scattering involves diffraction of the electromagnetic wave by the molecules and by its absorption and re-emission by the oscillating dipoles of the molecules. The intensity distribution of a vibrating dipole is mathematically presented as (Reference 7a).

$$I = (\text{const})\frac{p^4}{\lambda^4}\cos^2\theta \qquad \text{(Eq. 7-3)}$$

Where

p	=	the magnitude of the dipole moment
θ	=	the angle between the direction of the emitted light and the viewing angle
λ	=	the wavelength
const	=	experimentally derived constant
Note:		Scattering is inversely proportional to the fourth power of wavelength, so scattering is stronger at shorter wavelengths. Scattering from sunlight can dominate path radiance at wavelengths shorter than approximately 3.0 μm.

There are two approaches to treatment of the atmospheric path between the instrument and the calibration source. Each approach has limitations and therefore both should be used where possible. The two approaches are:

c. Purge or Evacuate the Calibration Path. Eliminate water vapor and carbon dioxide by purging the path with dry nitrogen gas or by performing the calibration in a vacuum. A variant of this method is to mathematically correct for absorption and path radiance using the AFRL Space Vehicles Directorate atmospheric model MODTRAN 4.0 (Reference 3e). This method is not as good as purging because MODTRAN introduces additional uncertainties.
d. View a Calibration Source Through the Same Atmospheric Path as the Target. This approach can be done if the target is on the ground at a fixed distance from the instrument. However, this approach is difficult to perform for an airborne target.

Radiation from the calibration source undergoes the same absorption as the target radiation.

Viewing a calibration source over the same path as the target can give a valuable quantitative measurement of the atmosphere to use as supporting data. This method does not allow direct correction for the atmosphere because of differences between the calibration and target source spectral distributions. Among the limitations and sources of uncertainty are the introduction of background radiation into the measurement and often less stable source temperature due to wind.

7.4.5 Bound Expected Parameters with Pre-Test Predictions. Whether a calibration is irradiance or radiance, good practice dictates that the span of the calibration extends beyond the levels expected from the target on both the low-level and high level ends. Interpolation between calibrated points always involves lower uncertainty risk than extrapolation into an uncalibrated region. For irradiance calibrations, select temperatures and apertures to bound the expected irradiance levels to be measured and recorded.

7.5 Instrument Calibration Strategies

Four basic strategies can be used in calibration to reduce uncertainty in the final measurement. Three of these involve instrument response. Chapter 2 described how the output reading of an instrument is proportional to the integration of received radiation as weighted by the response curve in that domain. This makes the instrument response a part of the measurement in a manner that cannot be easily extracted because response is a variable inside an integral. The more non-uniform the response shape, the greater the influence.

The influence of response is not, by itself, a source of uncertainty. Uncertainty is caused by using an inaccurate or incorrectly assumed response shape in the calculations for a calibration. Poor instrument characterization and/or incorrect application of instrument response are among the largest causes of uncertainty in radiometry.

A good habit to follow is to minimize response effects whenever possible, even when complete spectral and spatial characterizations are available. In calibration, the basic strategy for reducing response effects is to choose a calibration source whose spectral and spatial distributions are as similar to those of the target as is practical. Temporal characterization should also be included if the target is modulated or transient.

If the calibration source distributions exactly match those of the target, then instrument response becomes unimportant. Their radiant power then differs by a constant, which can be pulled from under the integral. The actual instrument response could be nearly any shape, known or unknown, and could be incorrectly assumed without affecting the calibration and measurement result.

A perfect match is never possible in practice. The target may be a complex mix of source types with different distributions in different, unknown proportions. A typical example is a jet aircraft with emissions from the engine exhaust plume, hot parts, and airframe, whose mix changes with viewing angle. Or, the target may have a distribution, such as the line spectra of an

exhaust plume that cannot be approximated with any available calibration source. These types of targets are very common in field and airborne radiometry. In such cases, two operations are vital:

a. Accurate and complete characterization of the instrument spectral and spatial responses must be performed.
b. The response shapes, especially spectral, must be applied in calibration calculations, (i.e., the calibration function must be in effective units. This is the first calibration strategy).

7.5.1 Calibrate in Effective Units. Using response shape in calibration calculations is more than just good practice. The use of effective units eliminates differences between the calibration and target source distributions as a cause of uncertainty. Because effective values are calculated for that quantity that the instrument responds to, they are valid and accurate for any distribution of power.

Effective does mean that the measurement results are only valid for that particular instrument response shape, but this limitation is inescapable. Unless the calibration and target distributions are identical, that limitation will be true regardless of whether or not the label is applied. Failure to apply the effective label will deprive the data user of critical information and this lack of information will almost certainly lead to misuse or invalid comparisons with other data.

If different target values are needed, such as for a different response shape than that of the measuring instrument or for a different atmospheric path, these values can be calculated later if sufficient outside information about the target is available. The following paragraph describes some of these calculations/extrapolations.

All extrapolations of measured values should be approached with caution and each should be performed as a separate, well-documented operation. This simplified case involves a radiance measurement of a graybody in the MWIR spectral region (3 μm to 5 μm) and projects a radiance value in the LWIR spectral region (8 μm to 12 μm). The surface emissivity in both bands is known and the range to target is known for both cases.

Step 1: Derive the source temperature from the radiance measurement.

T_{source} = Inverse solution of Planck's equation for MWIR

$$\text{Use Radiance equal to } \left[\frac{L'_{e,meas}}{\varepsilon_{MWIR}\ \bar{\tau}_{R(meas)}} \right] \qquad \text{(Eq. 7-1)}$$

Where

$L'_{e,meas}$ = Measured apparent effective radiance MWIR value to be extrapolated

ε_{MWIR} = Known surface emissivity of the target for the MWIR region

$\bar{\tau}_{R(meas)}$ = MWIR band weighted atmospheric transmission of the path R usually calculated using the MODTRAN model

Step 2: Calculate the LWIR radiance at the new range using the derived source temperature.

$$L'_{e,LWIR} = \left[\varepsilon_{LWIR}\ \bar{\tau}_{R(new)}\right] \text{ X Planck's Equation for LWIR Using } \left[T_{source}\right] \quad \text{(Eq. 7-2)}$$

Where

T_{SOURCE} = Derived source temperature of target

$L'_{e,LWIR}$ = Extrapolated apparent effective LWIR radiance

ε_{LWIR} = Known surface emissivity of the target for the LWIR region

$\bar{\tau}_{R(new)}$ = LWIR band weighted atmospheric transmission of the new path R(new), usually calculated using the MODTRAN model

7.5.2 Irradiance Calibration. An irradiance calibration can be done with either of two source geometries.

a. Source solid angle < IFOV. A small irradiance source at the focal point of a collimator simulates a point target at infinity.

b. Source solid angle >> IFOV. Usually done with an extended-area blackbody placed directly in front of instrument objective. The technique relies on knowledge of the IFOV.

Both source geometries have inherent uncertainties and it is often a matter of judgment which is better for a given situation. For the first condition, where the source is less than the IFOV, the background radiation from the collimator aperture plate is a part of the measurement and must be considered. The effects and treatment of background radiation are discussed in greater detail in the section on types of measurement systems (Chapter 5) and data reduction later in this chapter. For the second condition, where the source is greater than the IFOV, background radiation is eliminated, but instrument spatial response becomes a part of the calibration. In a perfect instrument with uniform response across the IFOV and no response beyond, irradiance is the product of the source radiance times the solid angle subtended by the IFOV.

7.5.3 Radiance Calibration. Radiance is independent of distance to the source, assuming no atmospheric path effects, because the footprint of the IFOV increases at the same rate as irradiance decreases due to the range-squared effect. Radiance calibrations are typically used for measurement situations where the target is highly resolved. Imagers are typically calibrated in radiance units.

7.6 Overall Measurement Strategies

The measurement phase involves assembling all the instruments and their data acquisition systems, performing the actual target measurements, recording the instrument readings together with all supplementary data, and documenting the conditions of measurement. Strategies for reducing uncertainty during the measurement phase will vary greatly due to the variety of types and characteristics of targets and the instruments being used. Some strategies, such as performing the measurements from very close range or against a low radiance background, are always desirable, but are not always physically possible.

The information that should be collected to supplement measurements will also vary with the type of target being used. For example, supplementary data for measurements of an aircraft airframe are very different from those for a rocket motor plume. The strategies listed below will always reduce uncertainty, but are not applicable to all targets, nor are they all inclusive. Every target measurement scenario is unique and measurement personnel must develop and apply a strategy that best suits the specific scenario.

7.6.1 Provide and Measure a Common Source. When multiple measurement systems and/or multiple measurement teams participate in joint tests, a common radiation source can provide valuable information to analysts. The source does not have to be a primary calibration standard; however, it should provide a sufficient source of radiation that can be measured by all systems when positioned at a slant range appropriate for all sensors at the test. The range requirement can be up to 5 km for typical free range tactical missile and ground vehicle tests. The source should also be mounted such that it can be rotated and sequentially pointed at all measurement platforms. The source should also be protected to prevent sunlight, wind, or other atmospherics from affecting the radiation. Sensors can be used to monitor and record the source changes during the testing period.

In addition to providing valuable data with which analysts can compare and correlate the field test data, the common source can provide analysts with the ability for a quick check to insure all instruments are working properly and with assistance in bore sighting all instrumentation to their tracking platforms.

7.6.2 Measure the Target at Short Range. The quality of radiometry measurement is always better when the sensing is not too remote. Measuring from as close as possible becomes more important with increases in target complexity and reductions in target radiation level. Measuring from a short distance has two main benefits:

a. The target can be well-resolved spatially.
   (1) A well-resolved target can be measured as a radiance quantity rather than an irradiance quantity, which eliminates the inverse range squared dependence as well as adding valuable information about the target spatial distribution.
   (2) Background radiation is largely eliminated for opaque targets. This characteristic of opaque targets is very important because the lower the target radiance relative to background radiance, the lower the contrast.
   (3) Individual target features and components can be resolved and their contributions to total target emissions can be isolated and quantified.

b. Atmospheric effects are less.
   (1) Less absorption occurs. Uncertainty is much less when measuring a target at short range and calculating the effects of absorption for a long path than from measuring at long range and calculating the effects for a shorter range.
   (2) Path radiance is lower. Radiance of the measurement path has two components:
   - Scattering. Scattering is the less predictable of the two components. The amount of solar radiation scattered into the measurement path depends upon a number of factors including sun angle, viewing angle, wavelength, and path length. Scattered radiation is low for short paths and can often be considered negligible.
   - Thermal Emission. Direct emission by the atmosphere in regions of high absorption, such as that of carbon dioxide around 4.25 micrometers, depends mainly upon ambient air temperature and can be calculated with greater certainty than can scattering.

7.6.3 Measure the Target against a Low-radiance Background. Positioning the target against a low, uniform-radiance background is always good practice, but the importance is much greater if the target is un-resolved than if it is a well-resolved. If the target is well-resolved with an imaging system and is opaque, the background can be eliminated spatially. However, if the target is unresolved or is transparent or translucent, background radiation becomes an inherent part of the measurement.

7.6.4 Measure the Same Target with Different Instruments.

a. Spectral and Spatial Domains. The choice of instrument type to use for a particular measurement is based on the expected target contrast and area as well as on the information needed about the target distribution in a domain. The rules of thumb for choosing instrument type based upon the extremes in target characteristics are:
   (1) High-contrast, small-area target. A spectrometer will produce more useful information with less uncertainty.
   (2) Low-contrast, extended-area target. An imager will produce more useful information with less uncertainty.

   For targets with characteristics that fall somewhere between these extremes, simultaneous measurements with both a spectrometer and an imager are recommended. At least one of the two instrument types will not be optimum and may not be used quantitatively because of its inherent uncertainty. However, having high resolution in another domain can sometimes provide valuable insight into the nature of the target and the component contributors to its total value.

b. Spatial Domain, Different Spectral Bands. Multiple imagers filtered for selected wavelength bands can also be used to gain valuable target information. The choice of bands depends upon the nature of the expected target emissions and upon atmospheric transmission as well as on particular target information needed. The atmosphere has a number of spectral regions of relatively high transmission, called "windows," interspersed between regions of absorption and emission. Refer to Figure 2-4 for an illustration of the IR atmospheric windows.

Filtering an imager for specific bands can allow determination of target properties, such as temperature, with greater certainty than can be done with broadband measurements. Some common bands in the MWIR spectrum are presented in Table 7-1.

TABLE 7-1. COMMON INFRARED (IR) BANDS

Target Emission Type	Atmospheric Windows	Line Emission/Absorption
Solid, Planck emitter	2.0 μm-2.5 μm 3.5 μm -4.0 μm 4.7 μm -4.9 μm	
Gas line emission		H_2O: 2.5 μm -3.0 μm CO_2: 4.0 μm -4.7 μm

7.6.5 Measure the Same Target under Different Conditions. A target is often measured under a variety of different conditions to determine the range of values expected. The emissions from a jet aircraft engine, for example, will often be measured at power settings from idle through intermediate and maximum power with and without afterburner and at altitudes from a thousand feet or so above ground level to the maximum sustained ceiling of the aircraft. Depending on the target type, different conditions can also be used to reduce uncertainty in the usage of the measurement result by isolating and quantifying different contributors. This is most commonly done with aircraft airframe. Radiation from an airframe has two main causes:

a. Thermal. Direct emission from standard paints is distributed spectrally in accordance with Planck's equation. Depending upon speed of the aircraft, temperature of the airframe is approximately recovery temperature (ambient air temperature plus aerodynamic heating).

b. Reflected illumination. The airframe is illuminated by sunlight from above and by the earth from below. Depending upon the paint emissivity, a portion of this illumination is reflected in both a broad, diffuse pattern and narrow, specular glints.

Varying temperature and illumination conditions allow the different causes to be isolated and quantified. Airframe temperature can be changed by varying the speed and altitude. At a given altitude and for the same sun and viewing angles, reflected illumination will not be affected by temperature changes.

Solar illumination can be varied by viewing the airframe via sunlit, backlit, or at night. At aircraft speeds above approximately 200 knots, solar illumination will not have a large effect upon airframe temperature.

Measuring the effects of these changes in temperature and illumination in multiple wavelength bands can be a powerful tool in validating computer signature models.

7.7 Supporting Measurements and Recordings

7.7.1 Perform Frequent Reference Measurements. However stable an instrument may be over time and during changes in ambient temperature, some radiation reference readings must be taken throughout the target measurement period. The reference readings assure that the calibration has not been influenced by any malfunctions, drifts, fogging of lenses, condensation on detector dewars, or other events.

It is a good idea to have point and extended calibration sources readily accessible during the measurement event so that each measurement system can be periodically checked to determine whether or not changes in each instrument response have been affected due to weather or other conditions. These calibration sources should be shielded or covered to prevent extraneous sources from the measurement systems fields of view. These measurements should be documented and time correlated to assist in data reduction.

Repeatability of the pre-test laboratory calibration is extremely important in establishing the integrity of the measuring instrument. Repeatability does not establish measurement accuracy, but accuracy can be no better than repeatability. If good agreement is achieved between the pre and post-test calibrations, the likelihood of any instrument anomalies or malfunctions affecting the target measurement is small. The 1993-1996 Office of Secretary of Defense (OSD) Joint Tactical Missile Signature (JTAMS) Joint Task Force (JTF) (Reference 7b) endorsed the procedure of daily calibrations against a standard source to monitor possible drift.

7.7.2 Plan for Additional Measurements. Time and funding do not always permit additional measurements. Also, some targets, such as rocket motor firings, may be a one-time opportunity. When possible, however, planning for backup tests or measurements can save a program.

In field and airborne measurements, the number of things that can go wrong is not infinite, but it often seem so. Bad weather can delay testing for days. Aircraft can go hard down for maintenance. Critical measurement instruments and acquisition systems can fail, usually at the most inconvenient times. You cannot plan for everything that can possibly go wrong, but planning for backup measurements is the next best thing. As a rule of thumb, if five flights are required to complete a measurement matrix, plan for at least one or, optimally, two additional flights. Little is lost if you do not need them but they can be vital if you do.

In addition to lost measurement periods due to failures and delays, backups can give an opportunity to explore unexpected target features and phenomena that are discovered during quick look reduction of data. It is a rare measurement program that doesn't raise new questions or uncover mysteries that need to be revisited and resolved.

Redundancy in radiometric and ancillary instruments is preferred. The basic planning will determine the types of instruments required to obtain the needed target information. At this stage, the measurement list should be prioritized. It is recognized that providing backup instruments adds cost, but having backup systems for priority measurement should be factored into the measurement planning.

7.7.3 Measure Additional Sources and Surroundings. In addition to the target, also measure and record surrounding sources in the environment. Slow elevation pans from look-down at terrain to a high-look up at sky usually work well. Performing the elevation pans at two or three azimuth angles relative to the sun is also recommended. One pan should be in the direction of the target, one should be directly away from the sun, and one or more should be at right angles to the sun. This allows measurement of the solar scattering component of sky radiance, which is affected by relative azimuth to the sun. These environmental sweeps can be used for two purposes:

a. To directly measure and help validate any modeling of the terrestrial illumination of the target.

b. As another check on the instrument calibration. At a high look-up elevation, the measured radiance of clear sky should agree reasonably well with that predicted with the MODTRAN model.

7.7.4 Prepare for Background Subtraction. For such an unresolved target, the effects of background can be reduced by performing a separate measurement of background alone and subtracting that result from the measurement of target and background. Some instruments perform this subtraction automatically in real-time. With other instruments, the subtraction is done as a separate operation during data reduction. The result is the same for both cases. Subtraction does not eliminate the influence of background radiation. The background subtraction produces a new unit of measurement for the target called a "contrast value." Refer to paragraph 7.9.3 for a more detailed discussion on contrast and absolute values. For now, note that a contrast quantity is always lower than the absolute quantity, but will approach the absolute for conditions of high contrast. The degree of influence and consequent uncertainty introduced by background radiation is difficult to quantify. The amount of uncertainty depends upon several factors, including:

a. Background non-uniformity. A more cluttered or structured background will introduce greater uncertainty.
b. Background radiance level. Higher background radiance will introduce greater uncertainty.
c. Size of the target in the instrument FOV. The target obscures some area of background. The intensity of this obscured area of background is the difference between target absolute and contrast intensity. A larger target size in the FOV introduces greater uncertainty when the target is contrast against a non-uniform background and/or weighted by a non-uniform instrument response.
d. Non-uniformity of the instrument spatial response. The less uniform the instrument response across the FOV, the greater will be the uncertainty for a given background radiance level.

Background subtraction is not an option for some types of targets. Jet engine exhaust plumes and certain types of IR decoys are examples of targets that are optically "thin." Thin, in this context, means that their particles and components do not have areas subtending sufficient solid angle to obscure the background radiation behind. Their measurement always includes background, which must be subtracted.

7.7.5 Record Environmental and Target Operating Conditions. All weather data required as an input to atmospheric models should be collected and recorded with Inter-range Instrumentation Group (IRIG) or other time stamp. Instrumented weather balloons can be released on site during the measurement period. This is especially important for missions running several hours as atmospheric parameters change significantly and rapidly from early morning to afternoon.

It is wise to use automation to collect and record important parameters. Hand recording of parameters is better than none at all, but dependence on hand recording for critical values is highly error prone, especially for a pilot or other active participant during the test event. The use of videotaping, computer logging, or other automated means should be maximized. Equally important is synchronizing all recording equipment to IRIG time.

All target parameters or operating conditions should be documented with time correlation during each measurement. For airborne targets, parameters such as turbine inlet temperature/exhaust gas temperature (TIT/EGT), power settings, fuel flow rates, and engine RPM must be recorded. Background conditions, such as cloud cover, should also be measured and recorded. For ground targets, parameters should not only include target operating conditions but detailed descriptions of the background conditions, time of day, sunlight conditions, etc.

Position information includes slant range, aspect angles, velocities, headings, sun angles, altitudes, and many others. All target position information must be time correlated. It is suggested that all position information be time tagged with the range-provided IRIG time which is accurate to one millisecond.

The radiant properties of any target are highly condition dependent. Although the primary focus of the measurement stage is the collection of radiometric data, these are of limited value unless all of the parameters and conditions that can affect the result are also recorded. The exact data will vary with target type and should be defined during the pre-measurement planning sessions.

A general list of target parameters for aircraft includes, as a minimum:

a. Engine parameters.
   (1) Power setting or power level angle (PLA)
   (2) Exhaust gas or turbine inlet temperature
   - Fuel flow
   - Turbine (N1 and N2) speed

b. Flight parameters. If air-to-air, will need the following for both aircraft:
   (1) Airspeed (indicated and true)
   (2) Altitude
   (3) Outside air temperature
   (4) Heading
   (5) Latitude and longitude

c. Range parameters. Include, as a minimum,
   (1) Meteorological soundings from ground level to a minimum of 3 km above the target altitude. Soundings should be taken during the measurements, if possible.
   (2) Time-space-position information (TSPI) data as well as hand-held Global Positioning System (GPS) units, if available

7.8 Daily and Post Calibration

As endorsed by JTAMS JTF (Reference 7b), daily and post-test calibrations are required to monitor possible drift away from the laboratory calibration results. Since the primary calibration source used in the laboratory is often complex and expensive, a satisfactory procedure is to use a less expensive secondary standard as the field irradiance source. In such a case, fewer calibration points are collected in the field as long as the number of collected points is adequate to monitor possible drift.

Dispersive spectrometer systems must also be checked daily against an emission line source to confirm the wavelength dispersion did not drift. Wavelength drift can be caused by vibrations during transportation to the test site and by daily fluctuations in environmental temperature.

7.9 Data Reduction and Uncertainty

Simply stated, data reduction is the transformation of raw instrument readings into radiant power values that quantify a target signature in engineering units. Instrument readings are multiplied by the appropriate calibration function coefficients, as described earlier, to produce values of target radiance or irradiance. From radiance, intensity can be calculated if target projected area is known. From irradiance, target radiant intensity can be calculated if range is known.

Data reduction is the stage in testing where all of the separate data from the instrument characterizations, laboratory calibrations, field calibrations, meteorological data, TSPI data, etc. are brought together, correlated, and used each in their own way to operate on the raw readings. This data assembly, correlation, and integration are usually the most time consuming effort in data reduction. Many checks and comparisons and judgment calls about the quality of the emerging product are made during the reduction process.

As with the other phases of the testing process, there are a number of strategies for reducing uncertainty in the final result. In data reduction, most of these strategies take the form of providing clear, unambiguous labels and documentation to reduce the likelihood of mistakes by the data user.

7.9.1 Documentation of the Reduction Process. The documentation that takes place in data reduction should provide a factor and formula trail sufficient to allow a knowledgeable data user to start with the raw instrument readings taken of the target and, with the complete calibration, reproduce the same final result. If questions or disagreements come up later, such a trail is invaluable in understanding the measurements and in establishing credibility. It is also invaluable for the measurement activity that generated the data to be able to come back at some future time, perhaps years later, and reproduce the results.

Note that the documentation described here is of the reduction *process*. Documentation of the target conditions, measurement path, etc. are collected and provided separately. The topics of documentation and presentation will be discussed in paragraph 7.10.

The format of this process documentation is not important. Some of the entries may be as simple as references to a provided CD-ROM or formula in a commercial spreadsheet such as Microsoft® Excel or they may be documented and displayed in provided software, but as a minimum, the contents of a reduction trail should be:

a. The Complete Calibration. The credibility and the interpretation of all subsequent data, including the units of measurement, rest upon all of the calibration calculations. Details will depend upon instrument type. For an imager or radiometer, the minimum details needed from the calibration are
   (1) Blackbody emissivity, temperatures, other calibration sources, apertures (if appropriate), collimator transmission, etc
   (2) Raw instrument readings
   (3) Spectral response curve for band radiometer and imager
   (4) FOV spatial response
   (5) Radiance or irradiance calculation formulae including use of spectral response curve and atmospheric path calculations (if not purged)
   (6) Calibration radiance (or irradiance) values, identified as effective (if appropriate)
   (7) Calibration curve coefficients
b. Instrument readings from reference source(s) during the measurement period.
   (1) Time of readings
   (2) Temperatures, emissivities, etc
   (3) History of reference readings through the measurement period
c. Instrument readings from the target.
   (1) Date and time of the reading(s) to enable connection with supporting data and conditions
   (2) An image showing target position in FOV or area of the target measured
   (3) Identification of whether background radiation is contained in the reading and whether background subtraction was performed
d. Instrument readings from environment sweeps.
e. Calculation of apparent effective target values.
   (1) Use of reference readings in calculations
   (2) Calculation of final values from calibration coefficients

7.9.2 Reduction of Measured Values to Apparent Effective. Apparent effective values are reduced values in their most basic form. Apparent means that the effects of atmospheric

absorption and, if absolute values, of path radiance are present in the data. No attempt has been made to correct or extract their effects.

Effective means that the spectral, and perhaps also spatial, response shape of the measuring instrument is embedded in the reduced value. No attempt has been made to mathematically extrapolate the values to another response shape.

Beginning all data reduction with apparent effective values has at least two virtues:

a. Apparent effective values have the least uncertainty. All mathematical operations that may follow are based to some degree upon assumptions about the distribution of target radiation in a domain or upon outside information from another instrument. These bring in additional uncertainties that are often difficult or impossible to quantify.
b. Correction operations, if performed, are done as separate and well documented procedures. This full disclosure provides the data user with information needed to correctly interpret, compare, and apply the results.

7.9.3 Reduction of Measured Data as Both Absolute and Contrast Values. If optically-resolved data were collected, reduce first as absolute quantities without background contribution. Absolute quantities have two benefits, which:

a. Are required for any computer model validation. Even if development and validation of a computer model is not planned at the time of the measurement, it often will be required at some future date. Calculation of absolute quantities does not involve significant additional effort and can be a good investment in the long run.

b. Allow yet another quality control check. Because absolute quantities do not contain background radiation, they are easier to predict from estimates of target temperature and emissivity. This is particularly true of aircraft airframe with standard paint.

When unresolved data are collected, it may be required to subtract the background contribution resulting in a target signature. The general equation used to define a bandpass signature is shown in Equation 7-4.

$$I'_c(R) = I_o\,\bar{\tau}(R) + L_p(R)\,A - L_{bkg}\,A \qquad \text{(Eq. 7-4)}$$

Where

$I'_c(R)$ = Apparent (at range) contrast intensity
I_o = Source intensity
$\bar{\tau}(R)$ = Atmospheric transmittance (weighted over the spectral band)
$L_p(R)$ = Atmospheric path radiance
A = Projected area of target
L_{bkg} = Background radiance

The measured part of Equation 7-4 is that shown in Equation 7-5.

$$I_m(R) = I_o\,\bar{\tau}(R) + L_p(R)\,A \qquad \text{(Eq. 7-5)}$$

Note that in order to compute the contrast intensity, the target projected area as well as the background radiance must be known. The projected area, *A*, may be determined by a photograph reference dimension, X_{photo}, the same actual reference dimension, X_{actual}, and the photograph target area, A_{photo}, as in Equation 7-6.

$$A = A_{photo}\,\frac{X_{actual}}{X_{photo}} \qquad \text{(Eq. 7-6)}$$

Each of the aircraft aspect angles requiring signature measurements would need to be photographed in order to determine the projected area to compute the required signatures.

7.9.4 Reduction and Graphing of Reference Readings Versus Time. A graph of the reference readings as a function of time through the test period is an invaluable tool for establishing the credibility of the instrument. The history of reference readings should be part of the data package for future reference.

7.9.5 Data Operations on Data to Derive Target Characteristics.

a. Mathematical Operations. A variety of mathematical operations can be performed on the reduced apparent effective values described in the previous section. Three general categories of calculations are
   (1) Quantities that cannot be measured directly with conventional radiometry. Two examples are:
      - Temperature.
      - Emissivity.

(2) What the target values would be under different atmospheric conditions other than those measured. Examples are:
- No atmosphere (i.e., at source).
- Longer atmospheric path or slant path.
- Different atmospheric conditions.

(3) What the target values would be if measured with a different instrument spectral response. Examples are:
- Different wavelength band.
- Different spectral response shape (i.e., square band rather than actual curve).

All of these operations require bringing in additional outside information and/or making assumptions about the target characteristics. Consequently, no matter how rigorously done, additional uncertainty is always introduced as the operations take the results further away from the original apparent-effective measurement values.

NOTE 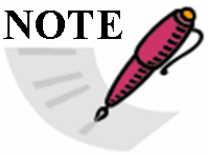	Because outside information or assumptions about the target are required, it is essential for the current and future data use to know what assumptions were made, where the information came from, and how it was used. Failure to provide at least this level of documentation leaves the data user with measurement results that have insufficient information to compare with other measurements or with model results. It is essential to keep the Level 2 data as part of the data archive with Level 3 data being presented only with assumptions made in its derivation.

b. Temperature and Emissivity Operations. Although direct emissions from a solid source follow Planck's equation as a function of temperature and emissivity, operations to determine temperature and emissivity from conventional radiometric measurements can be difficult to make accurately. The most accurate way to measure temperature is with a thermocouple or resistance thermometer in direct physical contact with the surface of interest.

Temperature can be determined accurately from a radiometric measurement only if emissivity is known to be high, i.e., a near blackbody. Two examples of problem situations are:

(1) Low emissivity allows reflections from radiation from the surroundings. This radiation can be spectrally complex. The main sources are:
- Solar radiation involving wavelength dependent absorption and scattering. Scattered solar radiation arrives from a wide angle.
- Terrestrial radiation is at longer wavelengths so scattering is less, but is more likely to undergo absorption. This has both a direct component from earth temperature by emissivity and a reflected component from solar. This radiation also arrives from a wide angle.

(2) Components within a cavity, for example within a jet engine tail pipe. Components with different temperatures and emissivities undergo multiple reflections and are difficult to isolate. High-resolution imager (spatial)

measurements can allow isolation of components. Multiple wavelength bands can help arrive at coarse spectrum, i.e., band ratios looking through atmosphere rich in combustion products (carbon dioxide, water vapor, and carbon particles). Spectral measurements are valuable, but are not usually spatially resolved, so are typically dominated by the single highest temperature component.

(3) Note. The methods are:
- With imager data: Ratios of different, well-separated bands taken within atmospheric windows.
- With spectrometer data: Fits of Planck's curve to spectrum.

(4) Note. Both methods assume that:
- Emissivity is the same across the measured spectrum.
- The target source is a single temperature (or dominated by a single temperature). Multiple sources with different temperatures in the FOV result in a non-Planckian spectral shape.

c. Atmospheric Operations. Because atmospheric absorption and emission is spectrally selective, any operations with atmosphere require spectral quantities for the atmosphere, the target radiation, and the instrument response.

Less uncertainty results from measurement at short range and calculation for long range, i.e., a more accurate value results from taking away via absorption what has been measured than replacing what was not measured. This is especially true of exhaust plume emissions measured through the cold CO_2 absorption region where absorption broadens with range on the long-wavelength edge of the absorption feature.

The reader is referred to the RCC SMSG report Weather and Atmospheric Effects on the Measurement and use of Electro- Optical Signature Data. (to be published at a later date). The reference provides a thorough discussion of the atmosphere and its constituents and their effects on the transmission of EO radiation.

d. Spectral Response Operations for Band Instruments. A data product commonly requested by customers is data that have been corrected for atmosphere; that is, measurement values that characterize a target source as if there were no atmosphere. Usually, the at source value requested is an intermediate term that will be used to calculate how a particular target source would appear to another sensor at a different range and different atmospheric conditions than that of measurement. Prediction of missile lock-on range is one such application, where measurements are made at close range and target characteristics are calculated for a much greater range.

If the source is known to be a hot solid material, then the spectral distribution will usually be in accordance with Planck's Law. If spectral measurements of the target are available, the correction of a solid source with a black or graybody spectrum can be done using the same method as temperature determination. The Planck's curve that was fit to the measured spectrum represents the source without atmosphere.

For more spectrally complex sources, such as gaseous line emission or those in the problem scenarios described for temperature determination, correction for atmosphere requires division of the target spectral power by the atmospheric spectral transmission as shown in Equation 7-7.

$$I_{tgt}(\lambda) = \frac{I'(\lambda)}{\tau_{meas}(\lambda)} \qquad \text{(Eq. 7-7)}$$

Where

$I_{tgt}(\lambda)$ = Desired spectral intensity of the target without atmosphere

$I'(\lambda)$ = Measured apparent spectral intensity of the target

$\tau_{meas}(\lambda)$ = Spectral transmission of the measurement path, usually calculated using the MODTRAN model. Spectral resolution of the transmission data must match the resolution of the target measurement data

Direct measurements of atmospheric spectral transmission are rarely available, so the information must usually be derived from a computer model, such as MODTRAN. Inputs to MODTRAN include meteorological conditions for the time and location of the measurement, the altitudes of the instrument and of the target, path length, and viewing direction relative to the sun. The required meteorological inputs for IR are temperature, pressure, and humidity. Other parameters and gas constituents can use the model defaults. If the measurement involves a slant path, the meteorological data will need to be input as layers.

Matching of the spectral resolutions of the measured spectra and the modeled atmospheric transmission is necessary to avoid introducing unwanted artifacts into the resulting spectrum. This can be done by operating on the higher resolution spectrum with a sliding average to degrade its resolution to that of the other.

e. Correction Factor Creation for Band Data. Where only band measurement data are available, the correction for atmosphere is more involved because the instrument spectral response appears inside a weighted integral with atmospheric spectral transmission. The operation involves deriving a correction factor with which to multiply the measurement values.

A basic correction factor is the ratio of weighted integrals. The numerator contains the new, desired conditions of atmospheric absorption (in this case, no atmosphere). The denominator contains a weighted integral that is believed to be identical to the measured apparent effective value. Variations on this approach can be used for a variety of atmospheric, range, and band corrections. An example for atmosphere is shown in Equation 7-8.

$$I_e = I_e^{'} \times \left[\frac{\int_0^{\infty} r(\lambda) I_{tgt}(\lambda) d\lambda}{\int_0^{\infty} r(\lambda) I_{tgt}(\lambda) \tau_{meas} d\lambda} \right] \qquad \text{(Eq. 7-8)}$$

Measured value

Correction factor is the inverse of the weighted transmission

Where

I_e = Desired effective intensity as seen by an instrument without atmosphere
I'_e = Measured apparent effective intensity value to be corrected
$r(\lambda)$ = Instrument spectral response. Spectral response is usually peak-normalized so values lie between 0 and 1; unitless
$I_{tgt}(\lambda)$ = Known (or postulated) relative spectral intensity of the target
$\tau_{meas}(\lambda)$ = Atmospheric spectral transmission of the measurement path, usually calculated with the MODTRAN model, unitless

Note. The practical limits of integration are the lower and upper wavelengths at which $r(\lambda)$ are zero.

7.9.6 Data Uncertainty. Every physical measurement has some degree of uncertainty. The causes of uncertainty in a radiometric measurement are many and varied. Uncertainty is easier to quantify in static and simulation chamber test events but in most field and airborne measurement cases, the amount of uncertainty is difficult to estimate. The causes are usually known, but the degree of influence may not be. Examples of uncertainties that can be determined are quantities such as the temperature and emissivity of an IR calibration source in a controlled laboratory environment.

Moving from the lab into the field or, worse, into an airborne environment introduces sources of uncertainty that are more difficult to quantify. A typical field or airborne scenario might attempt to measure a target source when:

a. The spectral and spatial distributions are very different from those of the calibration source.
b. Viewing through a long atmospheric path.
c. The target is in contrast against a high-radiance, cluttered background.
d. The target is illuminated by sunlight filtered through thin, broken clouds.
e. Measurement is performed using an instrument with non-uniform spectral and spatial responses.
f. At an ambient temperature warmer or colder than that of the laboratory calibration.
g. The ranges and viewing aspect angles are difficult to quantify.

Each of the above conditions, alone or in combination, introduce uncertainty. The unknown quantities far outnumber the known quantities. Unfortunately, in field and airborne radiometry, measurement scenarios like this are the rule rather than the exception. This document does not attempt to estimate the amount of uncertainty in every measurement situation from every cause. Even if that were possible, the result would not greatly improve the quality of the measurements. Instead, the focus is on general principles, methods of approaching common problems in calibration and upon a few representative instrument types. A number of strategies (rules of thumb, really) are given under measurement strategies that experience has shown will reduce the uncertainty in most measurements. It is best to avoid sources of error by good planning than to quantify them after the fact. There are many excellent text books for further reading that offer detailed procedures to estimate the uncertainty in a measurement. In Chapter 10, Measurement Uncertainty Estimation, of Reference 6b, is a detailed discussion on uncertainty estimation for low altitude measurements of tactical missiles but could be applied to other test scenarios.

None of the strategies that will be given are intended to be all-inclusive step-by-step recipes for success. Rather, the intent is to provide measurement personnel with sufficient insight into the mechanisms of measurement and causes of uncertainty to enable them to create and apply their own methods to their own unique situation. Standardization of method is neither possible nor desirable. In any radiometric measurement, complete documentation of the particular method used is almost always more important than the method itself.

7.10 Documentation and Presentation

The final reporting and documentation stage of a measurement is usually the least interesting and the lowest priority for the measurement personnel. By this time, the end of the project is in sight, the funding is nearly gone, and there is pressure to move on to new projects.

Unfortunately, the final documentation stage can be the most critical. All of the effort and care to reduce uncertainty through all of the previous stages, from the instrument characterization and calibration, to planning the measurement, and reducing the data, can be wasted if the final product is not documented adequately to enable the user to correctly interpret and apply the data.

Product quality will be improved as the measurement personnel gain more knowledge of how their data will be applied. Paragraph 7.9.1 described the requirements for documentation of the reduction process and of the formula and factor trail needed to establish credibility. The final report and data package mainly documents the target and measurement conditions. The exact

type and extent of the documentation required depends upon the application. Some typical applications of measurement data are:

a. Validation of a computer signature model (aircraft, missile, etc.).
b. Determination of countermeasures requirements (flares, jammers, etc.).
c. Calculation of threat missile lock-on ranges (relative to seeker bands).
d. Comparison of signature suppression devices and technologies (such as the engine Hover Infrared Suppression System (HIRSS), etc.).

The documentation requirements for validation of a computer model are the most extensive. As a general approach, sufficient information must be provided to recreate the target and its environment, exactly as measured. The examples here are for an aircraft, but most apply to other types of targets and vehicles. For an aircraft, the target documentation includes:

e. Engine parameters.
f. Aircraft size and shape.

An example of the environment for an airborne target includes:

g. Solar illumination.
h. Terrestrial illumination.

A rigorous validation will usually involve several iterations between model runs and perhaps additional reduction. The basic philosophy, and sometimes the challenge, is to get output from a computer model that exactly represents the target *as seen by the measurement instrument*. This often runs contrary to the instincts of modeling personnel who may have little measurement experience and feel that the measurement values should be operated on to produce the isolated components calculated by the model.

One difficult, but common example is that of a helicopter engine exhaust plume viewed in front of a section of fuselage that is itself warmed by the exhaust gases. Because exhaust plumes are translucent, any measurement of the plume includes the background behind the plume. Signature models; however, calculate values for exhaust plumes as they would exist in complete isolation from their surrounds or as viewed in front of a zero degree Kelvin background. Getting the model to produce output values that include the background as seen by the measuring instrument requires a knowledgeable user.

A test summary report as a minimum will include the information shown in Table 7-2. A test summary report typically accompanies a large digital data base such that all data are not presented; instead, examples of the data files are presented.

TABLE 7-2. TEST SUMMARY REPORT COMPONENTS

Components	Minimum Information Needed
Executive summary	• Test objectives • Participants • Dates • Location and altitude relative to sea level • Test matrix with IRIG date and times of milestone events such as ignition time or other trial initiation with clearly stated use of local time or Coordinated Universal Time (UTC).
Ancillary information	• Weather conditions with date and time tag • Sun azimuth and elevation (if appropriate) • Visibility • Time space position information (TSPI) such that range and viewing aspect angles to target can be derived. This can be a site survey of instruments and the target or time tagged digital data file with description if the target and/or instrument positions are dynamic. • Target power setting, velocity, and heading • Photographs
Instrument list and description	• Spectral and spatial responses and resolutions • Sample rates • Calibration factors and method of calibration • History of reference scans
Data format description	• Self explanatory
Stop-light Table	• A matrix of trials and instruments to show data availability. This is often referred to as "stop light table" with green indicating good data, red indicating data failure, and yellow indicating questionable data that requires additional analysis to determine data quality.
Measurement results	• Measurement results, or examples of measurement results, from each instrument including ancillary instruments with final units clearly defined.

7.11 References for Chapter 7

a. Moller, K. (1998). Optics (Chapter 16 "Scattering of Light", pg 553). University Science Books, Mill Valley, CA.

b. Brown, Col. R. (April 1996). Tactical Missile Signatures Measurement Handbook Gerber, G. (Editor), Joint Tactical Missile Signature (JTAMS) Joint Task Force (JTF), Infrared Information Analysis Center at Veridian Environmental Research Institute of Michigan (ERIM) International, Ann Arbor, MI.

This page intentionally left blank.

CHAPTER 8

TESTING SCENARIOS

In order to provide good test results, an important first step is to plan the test with a background of knowledge about the radiant source as well as the capability of instruments available to collect measurements. The test plan will define the source and measurement requirements, which are sometimes under less than ideal laboratory conditions. An approach using lessons learned from similar testing can provide a valuable start. The following paragraphs bring together various physical definitions relevant to testing with varied size targets, ranges, and surface properties of targets.

8.1 Geometric Size Considerations

Relative to the measuring optics, the target can be classified into the three categories of point source, finite source, and extended source. The radiant power from the different sources to the detector (Reference 8a) is illustrated in Figure 8-1. In Figure 8-1, E is the irradiance at the detector from the radiance of the extended source or the finite source, L, or the radiant intensity of the point source, I. Also in Figure 8-1, A_d is the area of the detector, r is the range from the optic to the source, and q is the focus distance. The focus distance q is equivalent to the focal length of the optic when r is much greater than q.

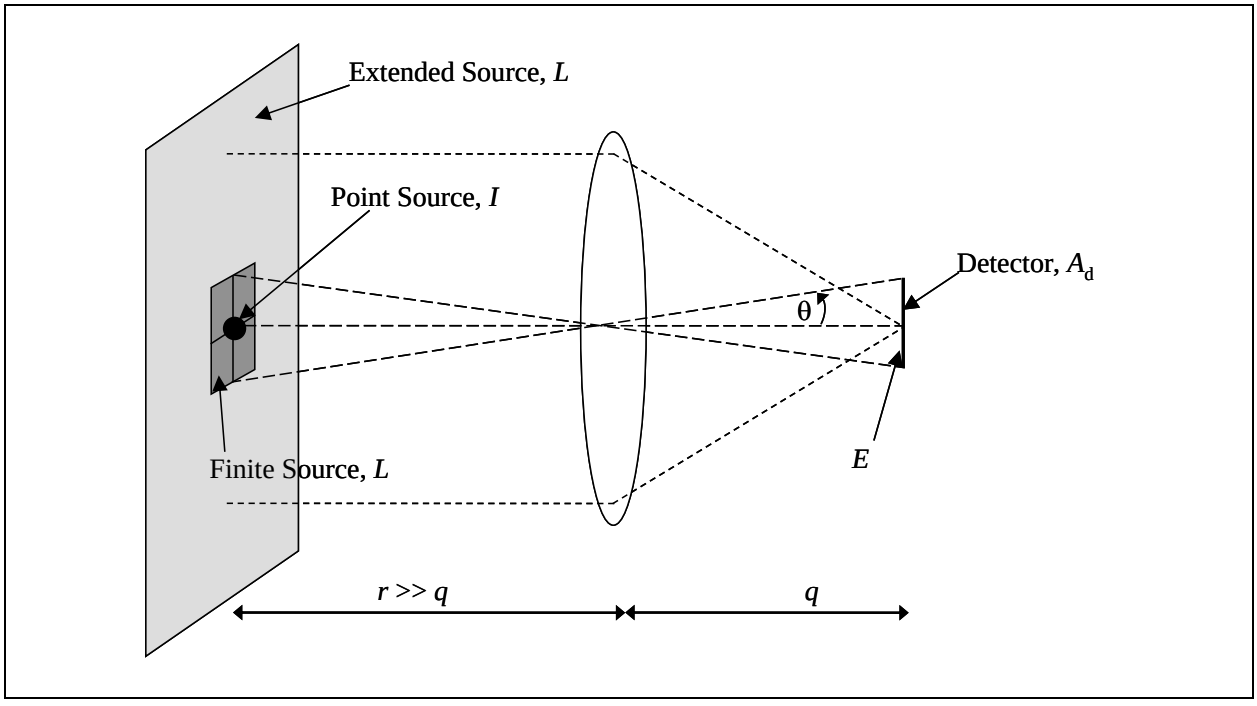

Figure 8-1. Radiant power transfer for various source types.

The irradiance, *E*, at the detector is summarized for ideal conditions by the following equations:

Point source: $E = 0.84\, I\, D_{lens}^2 / (r\, \lambda\, f/\#\, 2.44)^2$ (Eq. 8-1)

Where

I = intensity [W/sr]
D_{lens} = lens diameter [cm]
r = range[cm]
λ = wavelength [cm]
f/# = f-number (ratio of q to D_{lens}) where q is equivalent to the optic focal length when $r >> q$.

Finite source: $E = L\, A_{lens} / q^2 = \pi\, L / 4(f/\#)^2$ (Eq. 8-2)

Where

L = radiance [W/sr cm^2]
A_{lens} = lens area = $(\pi\, D_{lens}^2)/4$ [cm^2]

Extended source: $E = \pi\, L \sin^2 \theta = \pi\, L /(4(f/\#)^2 + 1)$ (Eq. 8-3)

Where

θ = half angle from detector to lens (degree)

Computed values for example cases are shown in the Figure 8-2, Figure 8-3, and Figure 8-4. All cases assume a lossless lens and an absolute zero temperature around the detector. Also, the irradiance is plotted as a function of f/#. The (+) symbol are included in the plots to indicate the standard full stop f-numbers seen on most camera lenses. Increasing standard full stop f/#'s are, for a fixed focal length, the lens diameter that causes a decrease in irradiance by a factor of two. The first five full standard f/# shown in the plots are f/1.4, f/2, f/2.8, f/4, and f/5.6. Note that the f/# for the standard f-stops are $2^{1/2}$, 2, $2^{3/2}$, 2^2, and $2^{5/2}$.

The first case (Figure 8-2) is for a point source. The image of a point source (unresolved object) will be spread out due to diffraction by the lens. For circular optics (the most common type) the diffraction pattern is an Airy pattern (Reference 8a). The Airy pattern is a central circular bright spot surrounded by a series of concentric rings with decreasing intensity. The distribution of flux in the central bright spot is not uniform but peaks in the center and decays rapidly out from the center. The central bright spot contains 84 percent of the flux and has diameter $2.44\, \lambda\, q/D_{lens}$. The 84 percent of the flux in the central bright spot is the 0.84 factor in Equation 8-1.

The second and third cases (Figure 8-3 and Figure 8-4) are for a finite source and an extended source, respectively. The radiances, L, in the examples are chosen to be 10 W/sr cm^2 and 11 W/sr cm^2, respectively, to illustrate the factor of two reduction in irradiance for increasing standard f-stop (+ symbols).

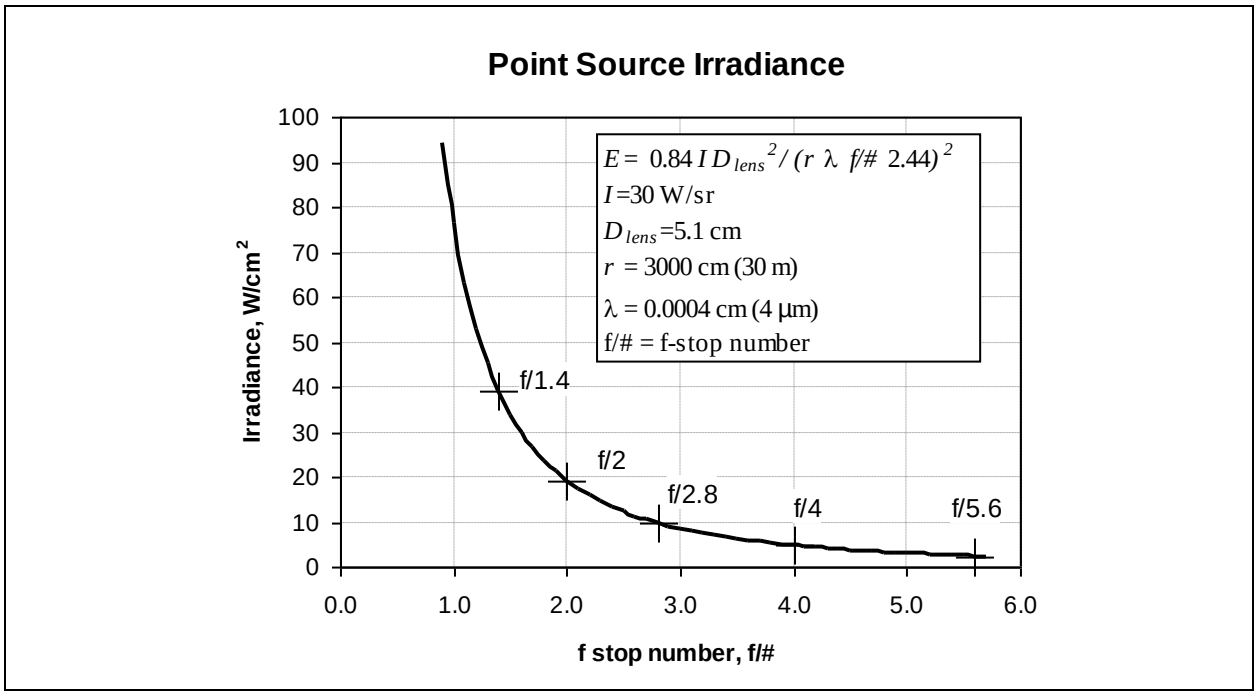

Figure 8-2. Point source irradiance example.

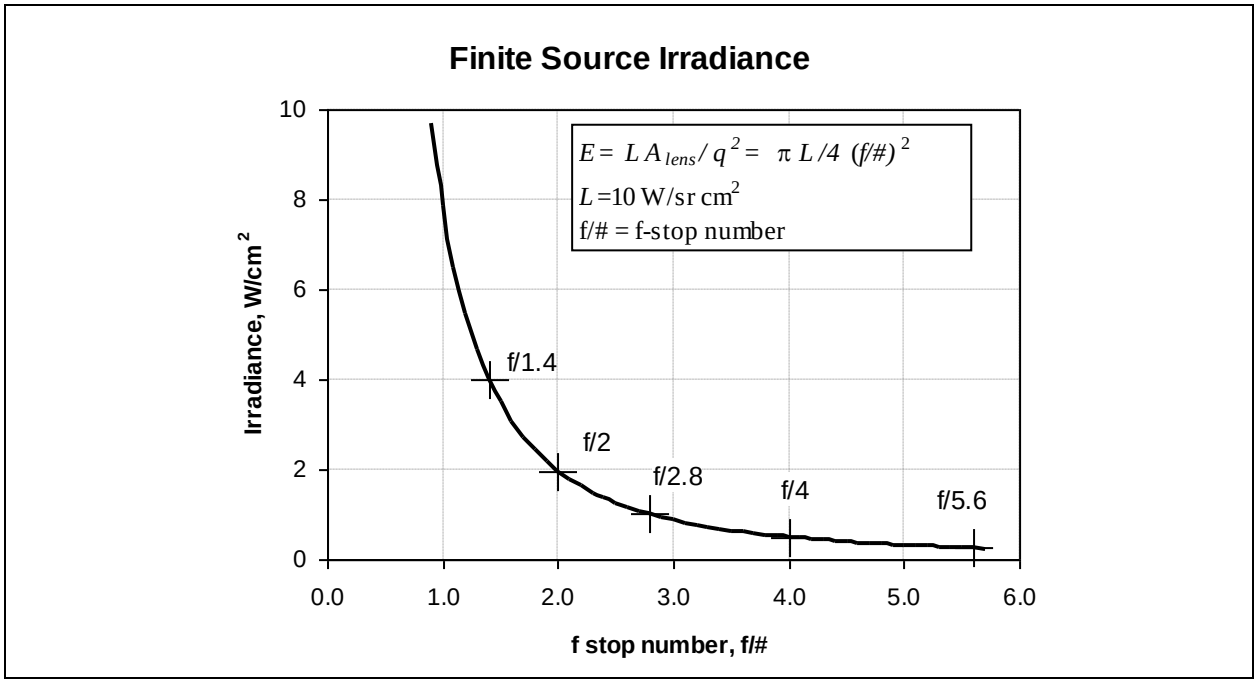

Figure 8-3. Finite source irradiance example.

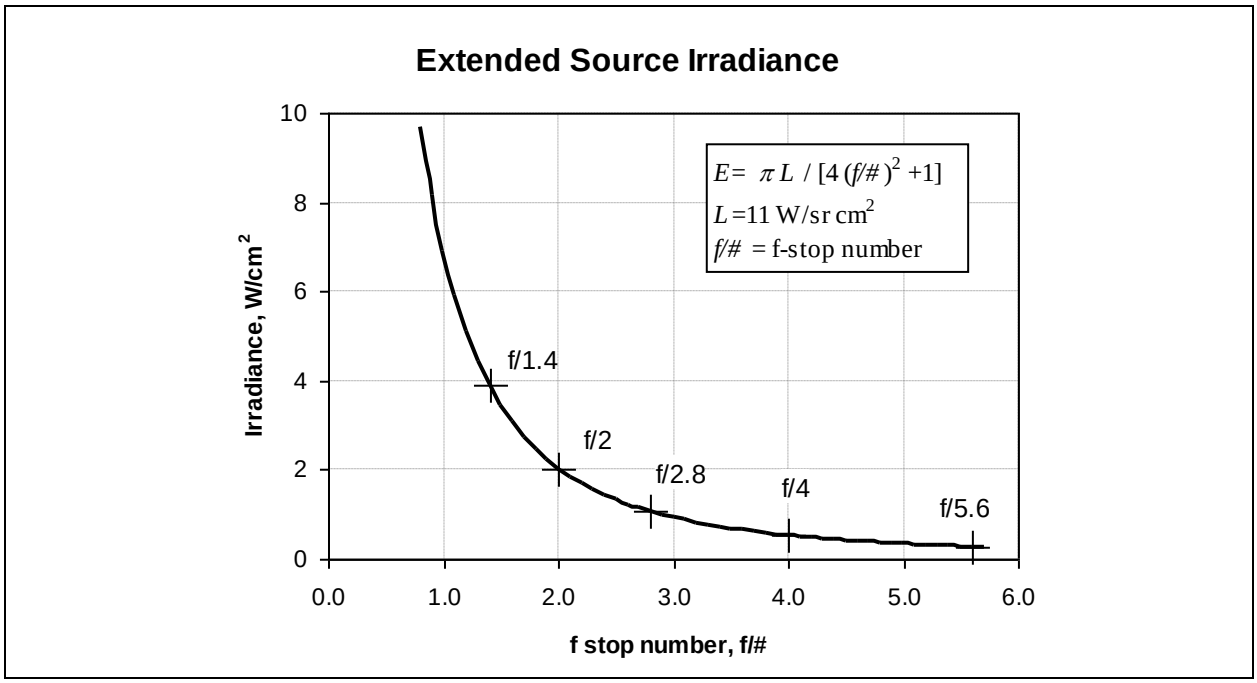

Figure 8-4. Extended source irradiance example.

The size of the target and the range to the target determine the optics needed to define the target in the FOV. For example, a component of the target such as the exhaust plume may be of interest to the exclusion of the remaining scene. Using simple geometry, the FOV in degrees that include a target length y at range r is given by FOV = 2 $\tan^{-1}$(y/2r). An example of FOV computations for a family of target lengths is shown in Figure 8-5. An example of using Figure 8-5 is to consider rotary wing aircraft IR signature measurements made at a range of 300 m with a 30 m target length. Tracing the y = 30 m plot to r = 300 m shows a 6 degree FOV optic is needed to include the 30 m length in the FOV. If the sensor is a radiometer or spectrometer with a single detector (i.e. no spatial resolution), then the target length would be an unresolved target.

It is important to consider the optics FOV and pixel size with measurements involving imagery. The target should include as many pixels as possible to maximize the spatial definition. Again using simple geometry, the footprint of a pixel at range *r* in either the horizontal or vertical dimensions is given by 2*r* $\tan^{-1}$(FOV/2 pixel count), where FOV is the total FOV of the imaging system. Figure 8-6 shows the pixel size obtained at various ranges and total FOV for a 256 x 256 CCD array. For a given range, the spatial resolution decreases (pixel footprint increases) as the total FOV increases. To increase spatial resolution, the total FOV must be decreased by using a longer focal length lens or by using a detector with greater pixel density.

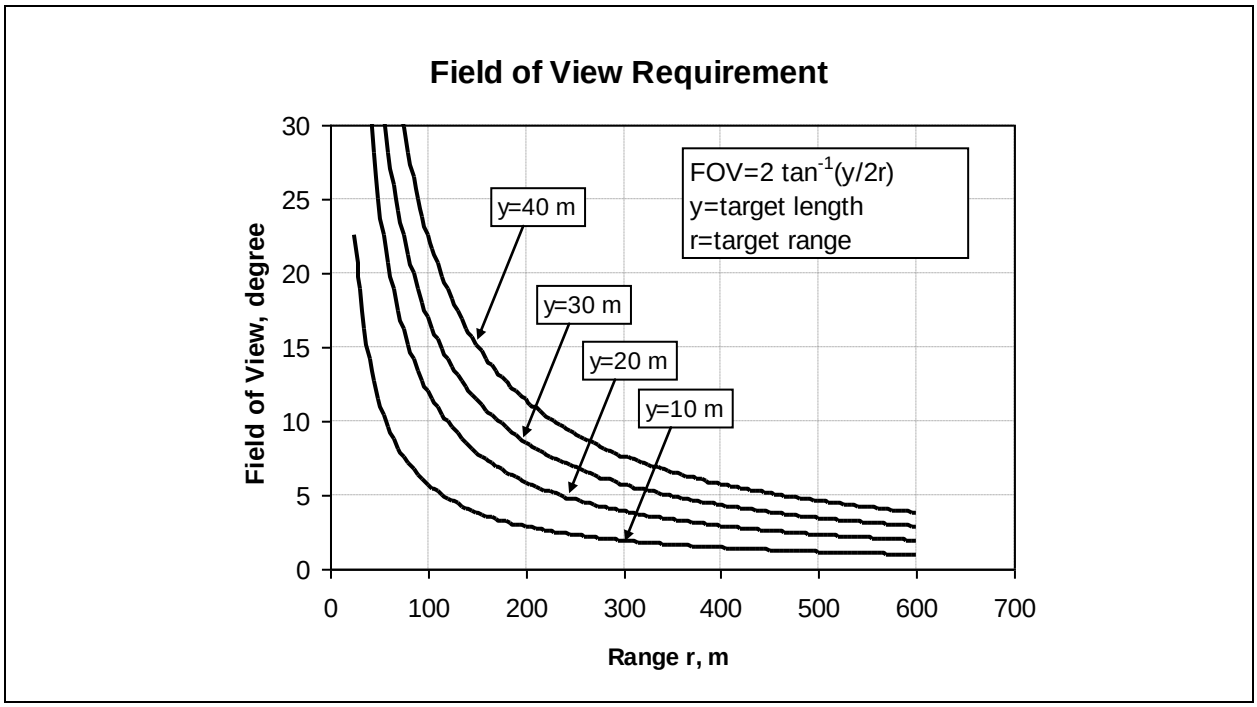

Figure 8-5. FOV requirement example.

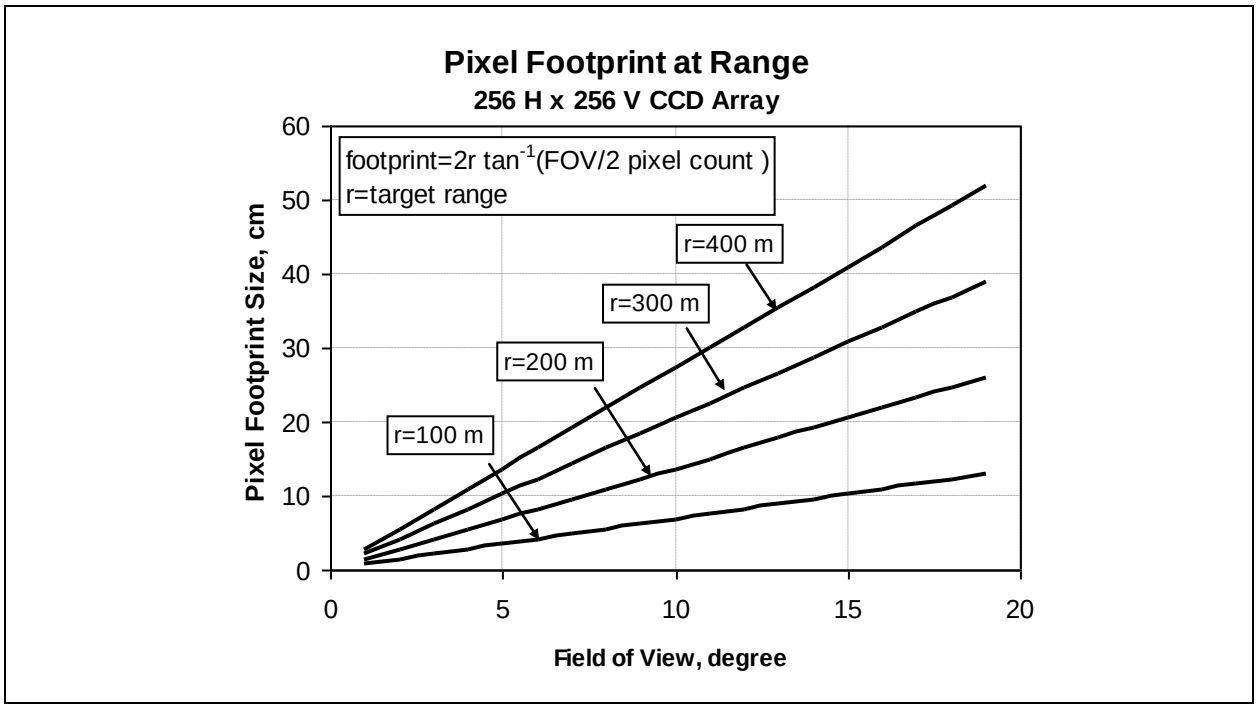

Figure 8-6. Pixel footprint length for a family of ranges as a function of total FOV.

8.2 Low Radiance Targets

Low surface emissivity and temperature, as well as long range targets, can result in radiance at the limit of detector responsivity. The capability to detect may be estimated with a signal-to-noise ratio (SNR) calculation. Definitions of the pertinent parameters are from Reference 8b and are listed as follows:

$$SNR = E_e / NEI_{BB} \quad \text{(Eq. 8-4)}$$

Where

E_e = Irradiance at the detector [W/cm2]

NEI_{BB} = Noise Equivalent Intensity [W/cm2] or the blackbody noise equivalent power or the amount of rms blackbody signal power incident upon the detector which produces a signal-to-noise ratio of unity in the detector.

$$NEI_{BB} = (\Delta f / A_D)^{1/2} / D_{BB}^*(\lambda, f) \quad \text{(Eq. 8-5)}$$

Where

Δf = The electrical noise equivalent bandwidth or the bandwidth of white noise whose integral power within that band is equal to the integrated power of the actual noise [Hz].

AD = The detector area (usually the area between the electrodes). For detectors, using integrating chambers, the entrance aperture area is usually the effective area [cm^2].

$D_{BB}^*(\lambda, f)$ = (cm $Hz^{1/2}$/W). A normalization of spectral detectivity with respect to Δf and A_D. Background conditions must be specified for background noise limited detectors.

The $D_{BB}^*(\lambda, f)$ values are defined for different materials in Reference 8b and are typically for a certain wavelength range and temperature. For the indium antimonide (InSb) (3 μm to 5 μm range and 77 K) example in Reference 8b, an approximate value of 10^{11} is given for D_{BB}^*. Based on this D_{BB}^* value, the NEI was calculated as shown in Figure 8-7. The measurement system may include some losses or gains that are not accounted for here. In this example, the signal must be greater than the NEI to be detectable.

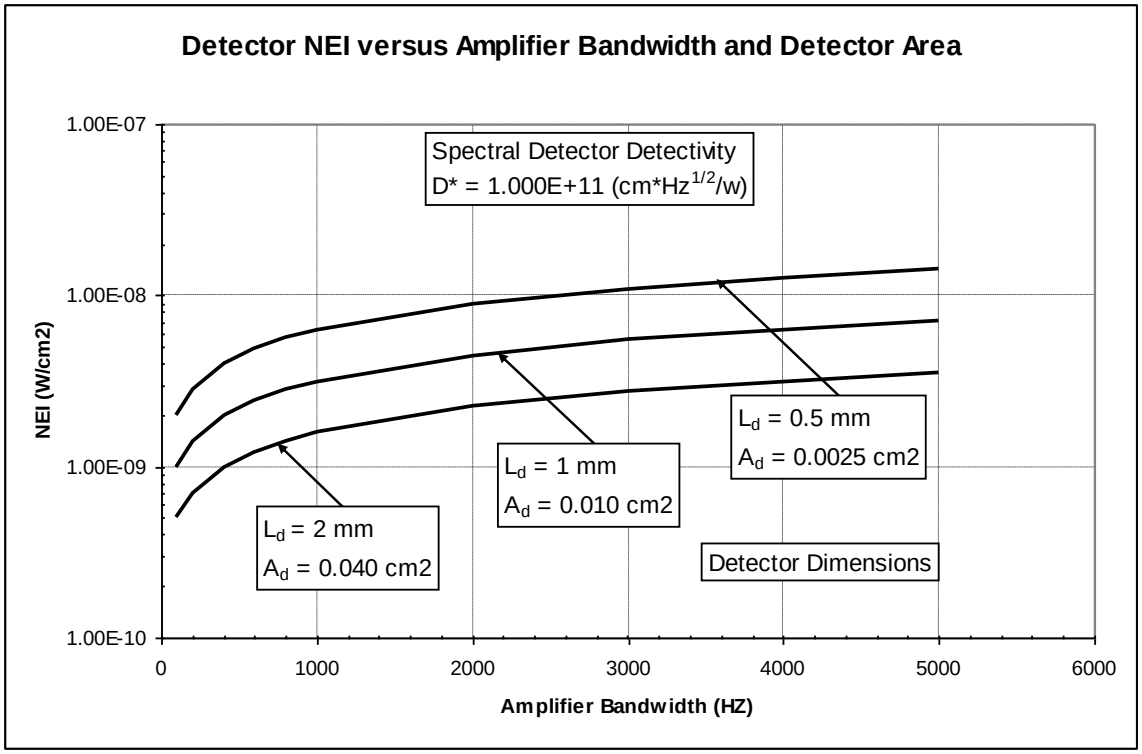

Figure 8-7. NEI calculation.

8.3 Long Range Testing

In long range testing, there is a signal drop due to the spreading of energy over a larger area and also due to atmospheric conditions causing absorption and scattering. The range reduction is the range-squared effect and is equal to 1/range^2 (paragraph 2.3.2). The atmospheric reduction is typically calculated by using an atmospheric model such as MODTRAN (Reference 8c). The MODTRAN model accounts for atmospheric conditions of interest, including time of year, time of day, temperature, pressure, and humidity.

8.3.1 Irradiance Reduction. The significance of irradiance reduction in the 3 μm to 5 μm MWIR band is shown in Figure 8-8 for a theoretical blackbody source.

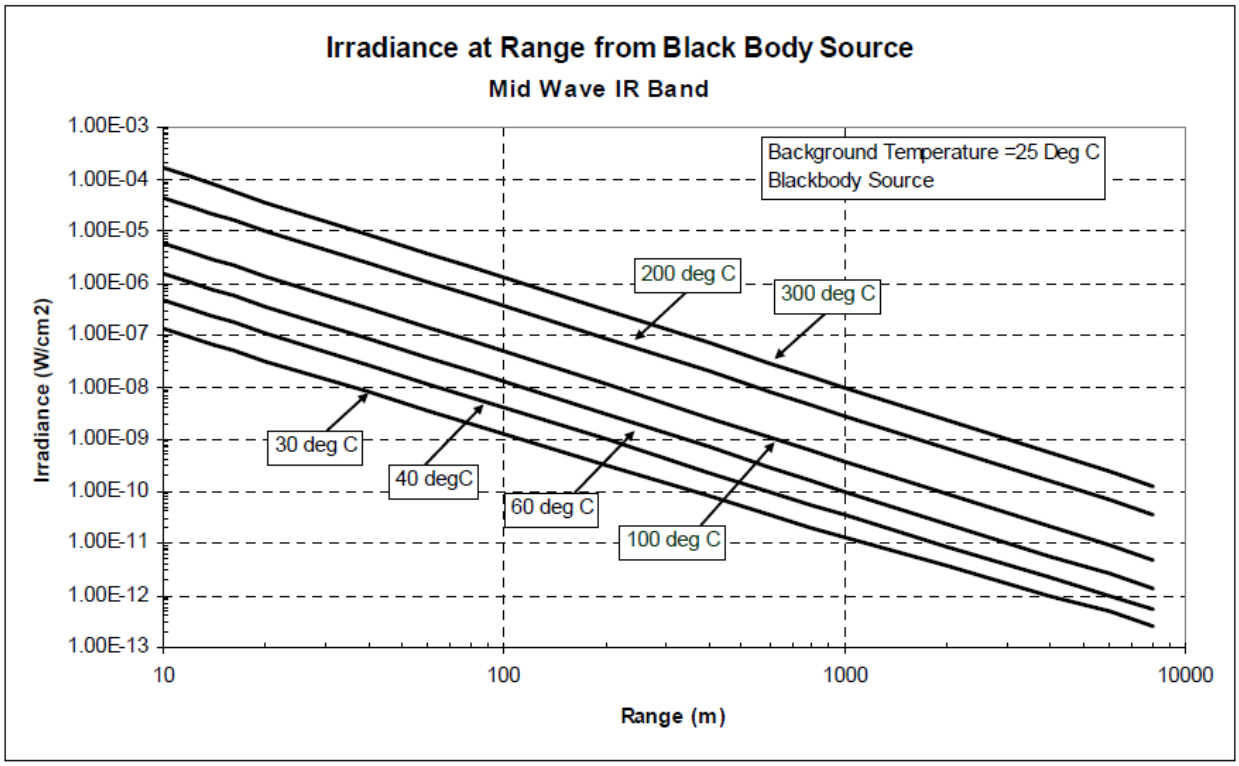

Figure 8-8. Irradiance reduction.

The primary reduction is due to the range-squared effect (1/range^2). For this case, atmospheric attenuation and path radiance for the assumed mid-latitude summer clear day is shown in Figure 8-9. The path irradiance originates from the warm air in the optical path and scattered solar radiance into the optical path. The path irradiance is an output of the MODTRAN model and is a strong function of path geometry and time of day. In general, when transmittance is high either because of a short range or because the measurement is within an atmospheric window, path radiance is low and the contrast between the target and the background is good. When the atmospheric transmittance is low, the path radiance increases and the contrast is decreased, making it harder to discriminate the target from the background.

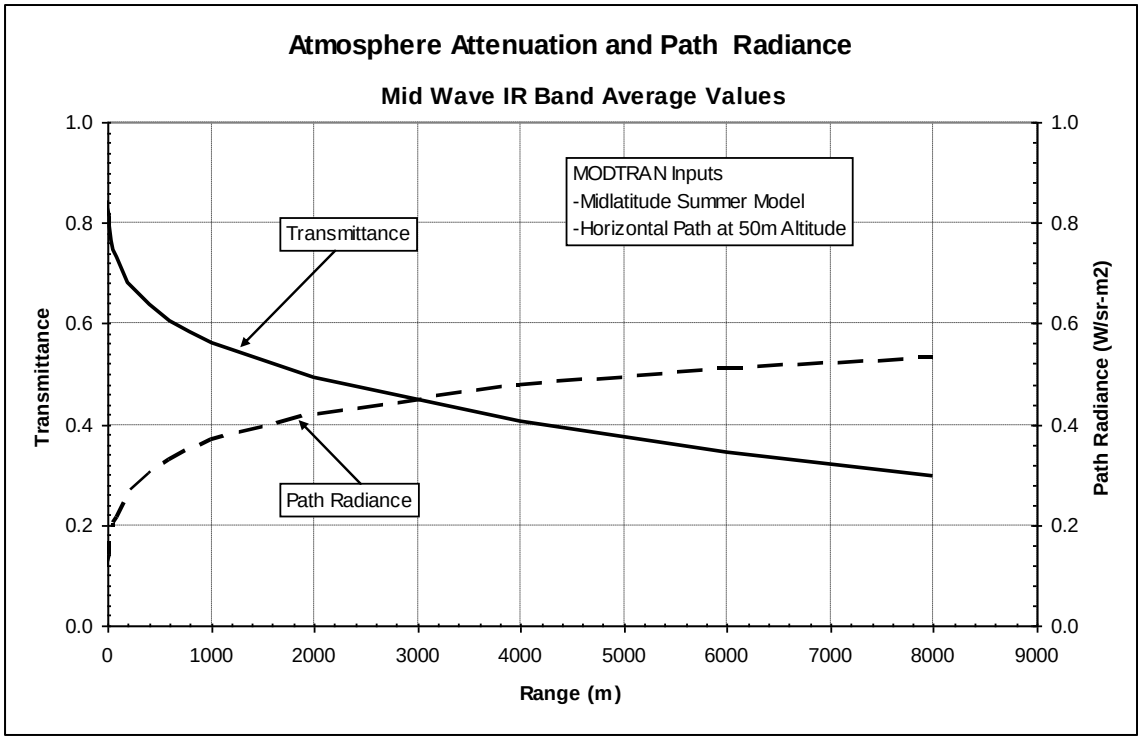

Figure 8-9. Radiance reductions due to the atmosphere, 3 μm to 5 μm MWIR band.

8.3.2 Atmospheric Band Average Transmission Values. In the calculations of Figure 8-9 the average values over the band are given; however, the attenuation is more accurately calculated at each wavelength because the radiance is being unequally distributed across the band (refer to Planck's Equation). The band average calculations have the highest accuracy around 425 ^{o}C in the 3 μm to 5 μm band. The use of an average transmittance will yield higher than actual radiances for low temperatures, and lower than actual radiances for high temperatures.

8.3.3 Calibrated Source at Range of Test. For long range testing, the source is likely to be of finite size and unresolved in the FOV. This case is the finite source case in Figure 8-3 with the radiant power density incident on the measuring instrument as irradiance L (W/cm^2). The example calculations in Figure 8-8 show the linear relationship on a log-log grid of irradiance versus range. A blackbody source placed at various ranges to the target location should produce a linear relationship similar to the theoretical case. More than one blackbody source should be used to cover the range of temperatures expected at the target. Irradiances obtained at the measuring instrument may be converted to radiant intensity I (W/sr) during data reduction. It is important to hold the blackbody source temperature to the value required for calibration. The temperature uncertainty computations in Figure 8-10 show the increase in radiance for a 10 ^{o}C rise in temperature. The error increases very rapidly for temperature levels below 100 ^{o}C.

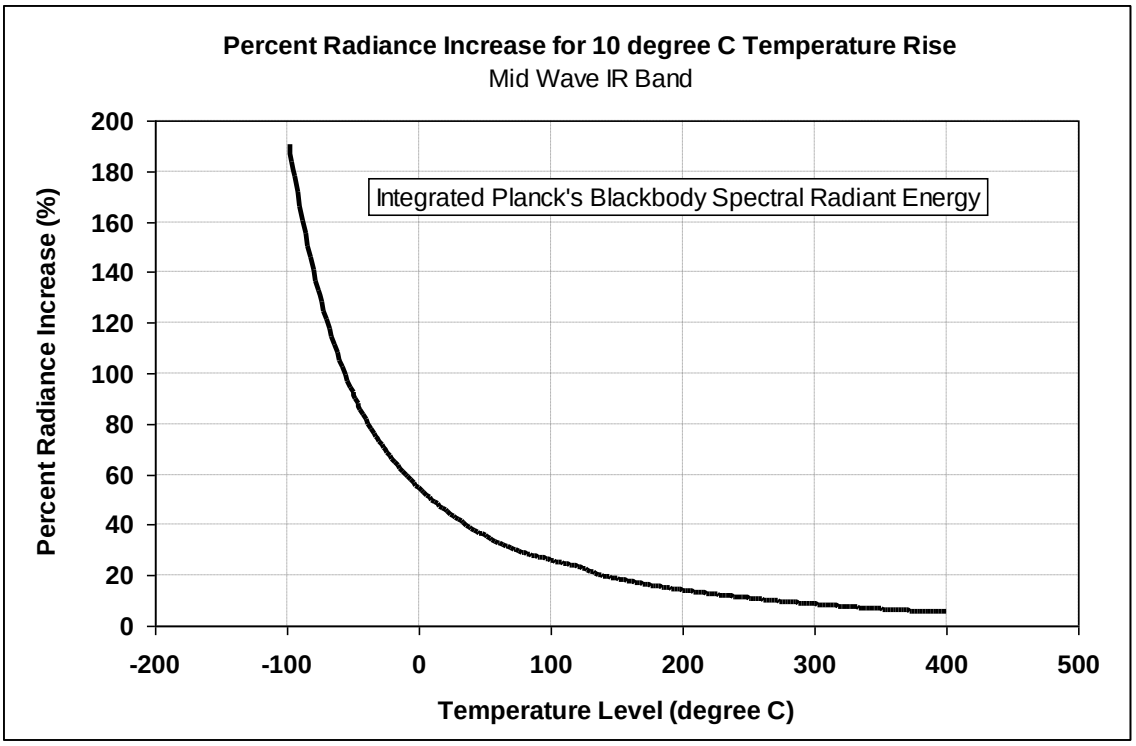

Figure 8-10. Radiance error resulting from temperature delta.

8.4 Short Range Testing

Testing at the closest range possible should be the goal in order to reduce the attenuating effects of atmosphere and the radiation spreading over increasing distances (inverse range squared effect). Also at close range, a high spatial resolution can be achieved providing detailed information about the heat generating components of the target. Even at close range, CO_2 and H_2O absorption bands can significantly reduce the radiant energy.

8.4.1 Atmospheric Attenuation. Figure 8-11 shows the wavelength regions in the MWIR range with high absorption. The CO_2 absorption near 2.7 μm and 4.3 μm wavelength is very strong and therefore the combustion products in engine exhausts are nearly attenuated at even the 300 m range. The H_2O absorption is present near 3.2 μm and is very strong near 6.0 μm which significantly, if not completely, attenuates the source radiation for a 300 m range.

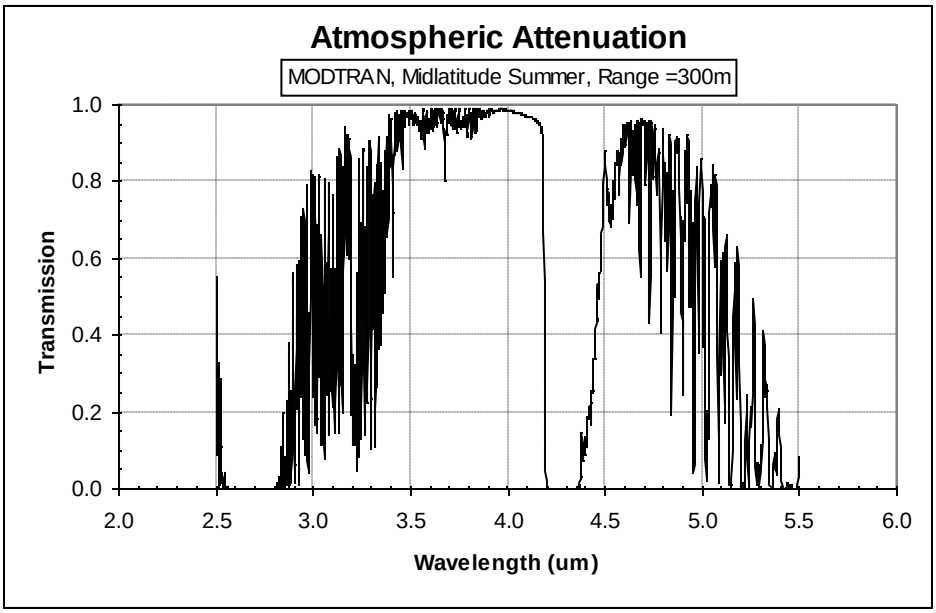

Figure 8-11. High atmospheric absorption bands.

8.4.2 Calibrated Source at Range of Test. For the short range test situation, the source is likely to be resolved in the FOV. This case is the extended source case in Figure 8-1 with the radiant power density incident on the measuring instrument can be measured as radiance I (W/sr cm^2).

8.5 Material Properties that Affect Optical Signature

Radiation incident on a surface can be absorbed, reflected, or transmitted. The fraction of energy is represented in the following conservation of energy equation:

$$E_{absorbed} + E_{reflected} + E_{transmitted} = 1 \qquad \text{(Eq. 8-6)}$$

For most solid surfaces, there is no transmitted energy at the surface and therefore the previous equation reduces to:

$$E_{absorbed} + E_{reflected} = 1 \qquad \text{(Eq. 8-7)}$$

A blackbody is defined to be one which emits the maximum amount of energy as possible ($E_{blackbody}$). Actual surfaces emit less than the maximum and are defined by surface emissivity ε as follows:

$$\varepsilon = E_{actual}/E_{blackbody} \qquad \text{(Eq. 8-8)}$$

A graybody is defined as a body with constant emissivity over all wavelengths and temperatures; where the constant is less than unity. Such an ideal body does not exist in practice but the assumption is a good approximation for many computations in engineering. When a surface is in equilibrium with its surroundings, the amount of absorption (or absorptivity, α) is equal to the amount of emission (or emissivity, ε) and then by Kirchhoff's Law

$$\alpha = \varepsilon \qquad \text{(Eq. 8-9)}$$

Emissivity values vary from near zero to 1.0 for actual materials as shown in Table 8-1 (Reference 8d). These are hemispherical emissivity values. It is important to consider the source temperature when determining the heat balance and surface temperature of an object in space with direct sun, for example. In this case, the absorption is at the solar temperature and emission is at the surface temperature. The characteristic α/ε ratio is used in spacecraft design to identify material uses. For example, a radiator design may involve the use of white paint ($\alpha / \varepsilon = 0.18/0.95 = 0.19$). Additionally, a heat absorber may choose polished chromium ($\alpha / \varepsilon = 0.49/0.08 = 6.13$). In general, emissivity for metals follows a trend of decreasing values with wavelength while emissivity for nonconductors follows the opposite trend.

TABLE 8-1. TYPICAL EMISSIVITY VALUES

Material	Surface Condition	0.6 um* Solar	1.8 um* 1371 °C	3.6 um* 538 °C	5.4 um* 260 °C	9.3 um* 38 °C
Aluminum	Polished	~0.30	0.19	0.08	0.05	0.04
	Oxidized	-	-	0.18	0.12	0.11
	Anodized at 1000 F	-	0.34	0.60	0.42	0.94
Brass	Polished	-	-	-	0.10	0.10
	Oxidized	-	-	-	-	0.61
Chromium	Polished	0.49	0.40	0.26	0.17	0.08
Copper	Polished	-	0.17	0.18	0.05	0.04
	Oxidized	-	-	0.77	0.83	0.87
Stainless Steel (18-8)	Polished	-	-	0.22	0.18	0.15
	Weathered	-	-	0.85	0.85	0.85
Brick	Red	0.70	-	-	-	0.93
	Fire Clay	-	~0.75	~0.7	-	0.9
Marble	White	0.47	-	0.93	-	0.95
Paper	White	0.47	-	0.93	-	0.95
Paints	White (ZnO)	0.18		0.91		0.95
	Cream	0.35	0.42	0.70	0.88	0.95
	Red	0.74	-	-	-	0.96
	Lampblack	0.97	0.97	-	0.97	0.96
Glass		Low	-	-	-	0.90

* Wavelength for which maximum radiance occurs at this temperature.

8.5.1 Material Directional Emissivity. A diffuse surface is one in which the emissivity is constant in all directions and is then known as Lambertian (i.e. follows Lambert's cosine law). Real surfaces differ from this ideal case. Directional surface emissivity for metals and nonconductors typically follow opposite trends as shown in Figure 8-12 and 8-13 (Reference 8c). For nonconductors, the emissivity decreases at large emission angles and for metals the emissivity increases at large emission angles.

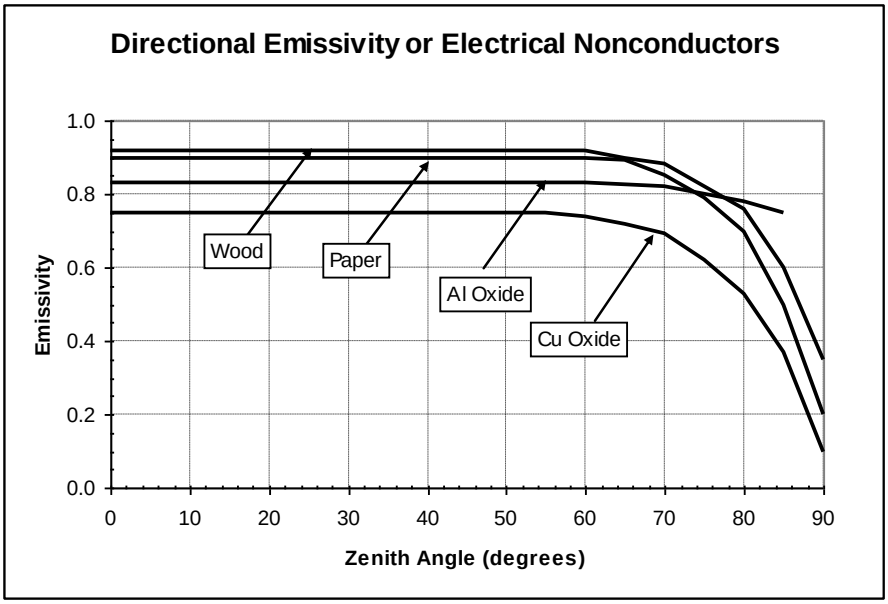

Figure 8-12. Directional emissivity variation for electrical nonconductors.

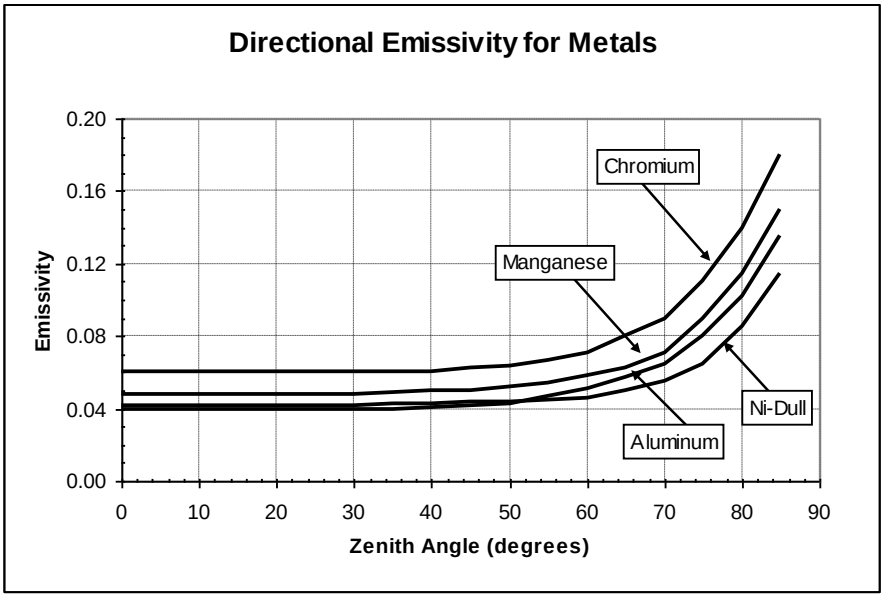

Figure 8-13. Directional emissivity variation for metals.

8.5.2 Material Directional Reflectance (MDR). The MDR is characterized through the Bidirectional Reflectance Distribution Function (BRDF). The BRDF is the ratio of reflected surface radiance and the incident surface irradiance. This generally refers to a mathematical model used to describe this characteristic material property. The model attempts to generalize the measured data. The data is dependent on wavelength and therefore the constants and parameters internal to the model will change in different wavelength regions. There are four basic parameters in the Sandford-Robertson reflectance model as shown in Table 8-2.

TABLE 8-2. BASIC SANDFORD-ROBERTSON REFLECTANCE MODEL PARAMETERS	
Parameter	**Description**
$\rho_D(\lambda)$	Diffuse spectral reflectance
$\varepsilon(\lambda)$	Spectral emissivity
b	Grazing angle reflectivity
e	Width of the specular lobe

The model equations (refer to Appendix D) are rather complex but can be easily implemented in a computer program to obtain numerical solutions. Example calculations were made based on the following parameters:

$$\rho_D(\lambda) = 0.02\ , \quad \varepsilon(\lambda) = 0.86, \quad b = 0.20, \quad e = 0.20 \qquad \text{(Eq. 8-10)}$$

The surface properties in total are shown in Figure 8-14. The diffuse reflectance is relatively small. Total reflectance is very high at the grazing angle where the emissivity is low. This is characteristic of an electrical nonconductor material.

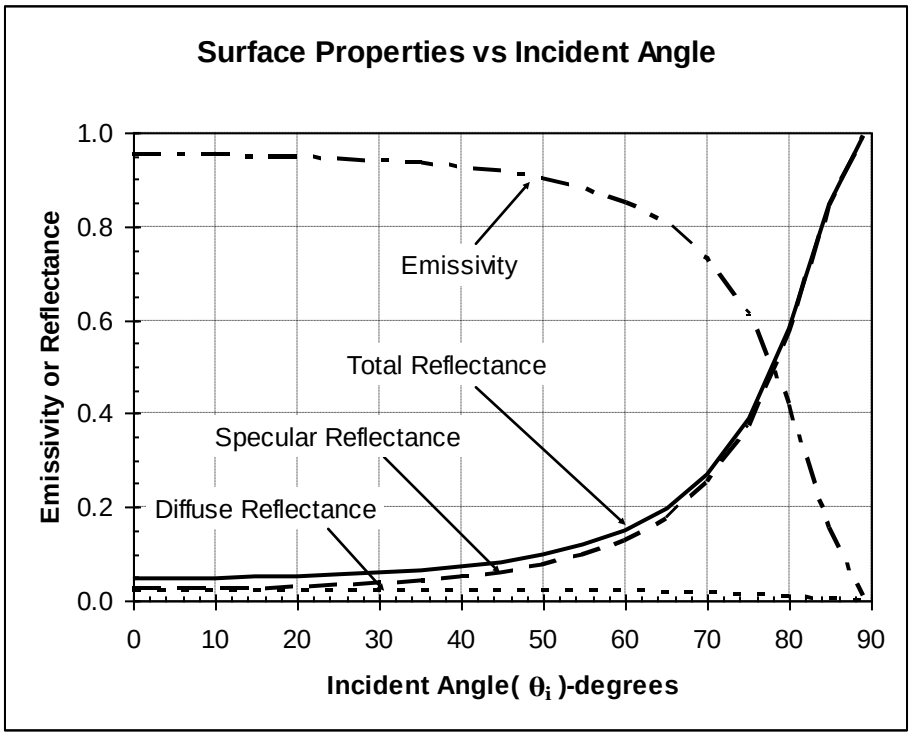

Figure 8-14. BRDF example surface properties.

The specular reflectance at various incident angles is shown in Figure 8-15. For angles less than the grazing angle 90 degrees, the reflectance peaks near the corresponding incident angle (for example, the reflectance for θ_i=60 ^{o} peaks near θ_r=65 ^{o}) and the peak value increases as the incident angle increases.

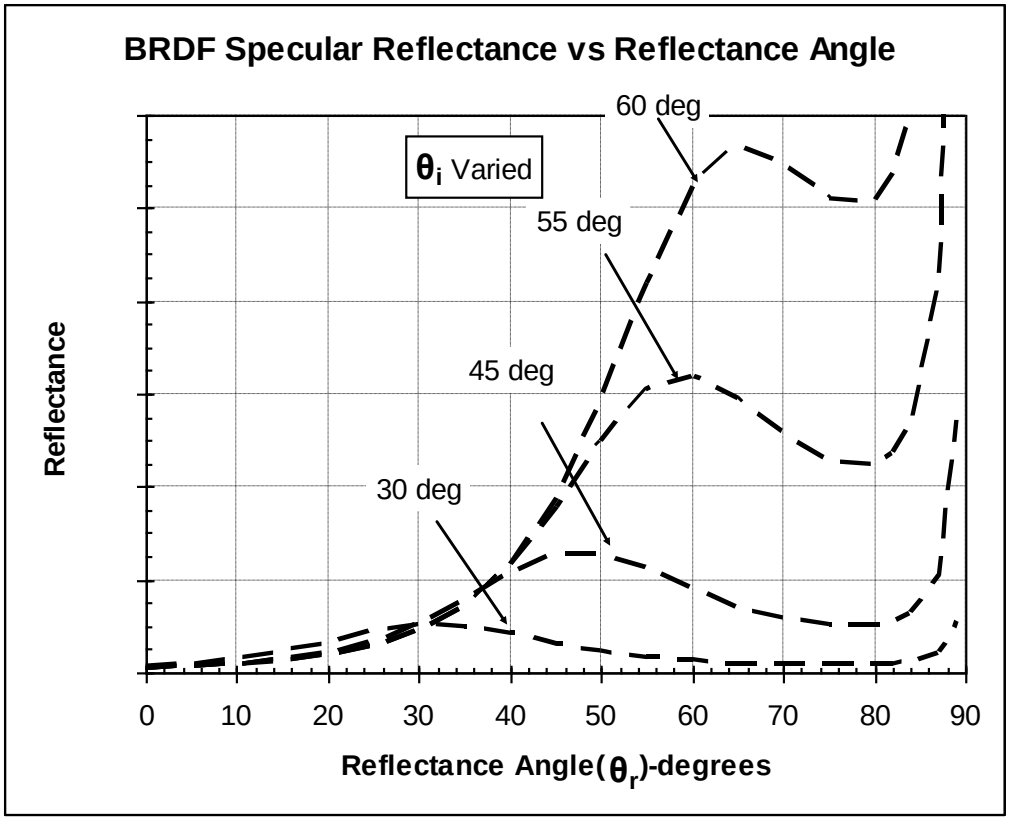

Figure 8-15. BRDF example specular reflectance.

8.5.3 Significance of Reflections. Testing in sunlight may add a complexity to a measurement especially when the material properties are not well known. The glint that appears from windshields and other reflective materials is evidence that the directional properties can dominate the energy received in a certain bandwidth. To illustrate this effect, computations were made of solar reflection at the surface of the earth surface versus the blackbody emission at a given surface temperature. The computations are presented in Figure 8-16, Figure 8-17, and Figure 8-18 for the NIR, MWIR, and LWIR ranges respectively, and for six fractional solar reflections (for example, 0.4 indicates 40 percent of the solar radiation in the wavelength band is reflected). Maximum solar energy occurs to the left side of the NIR range and therefore the impact of the solar reflections is expected to be highest in the NIR and diminish toward the LWIR range. The computations indicate agreement with the expected trend. The following assumptions were made in the computations:

a. Horizontal flat plate with sun positioned directly overhead
b. Extraterrestrial Solar Constant = 1353 W/m^2
c. Transmission coefficient for atmosphere = 0.7
d. Diffuse reflection of incident solar energy
e. Six fractional solar reflections from the flat plate (0.1, 0.2, 0.3, 0.4, 0.6, and 0.8).

In an actual case, the surface temperature will be determined by the heat balance associated with the different heat transfer mechanisms (conduction, convection, and radiation) with the environment.

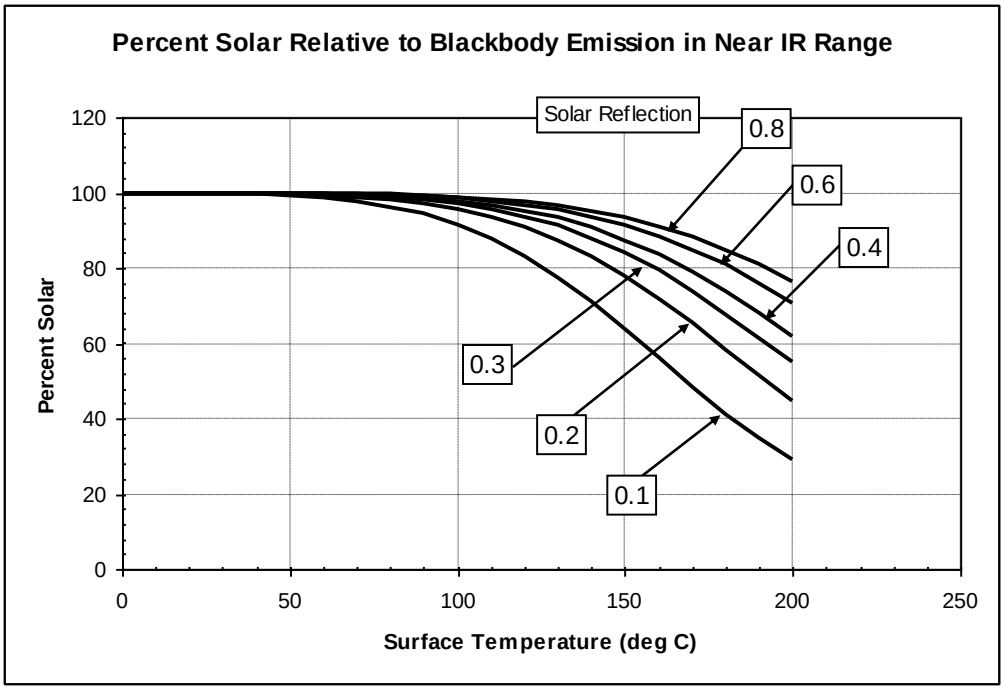

Figure 8-16. NIR solar reflectance effect.

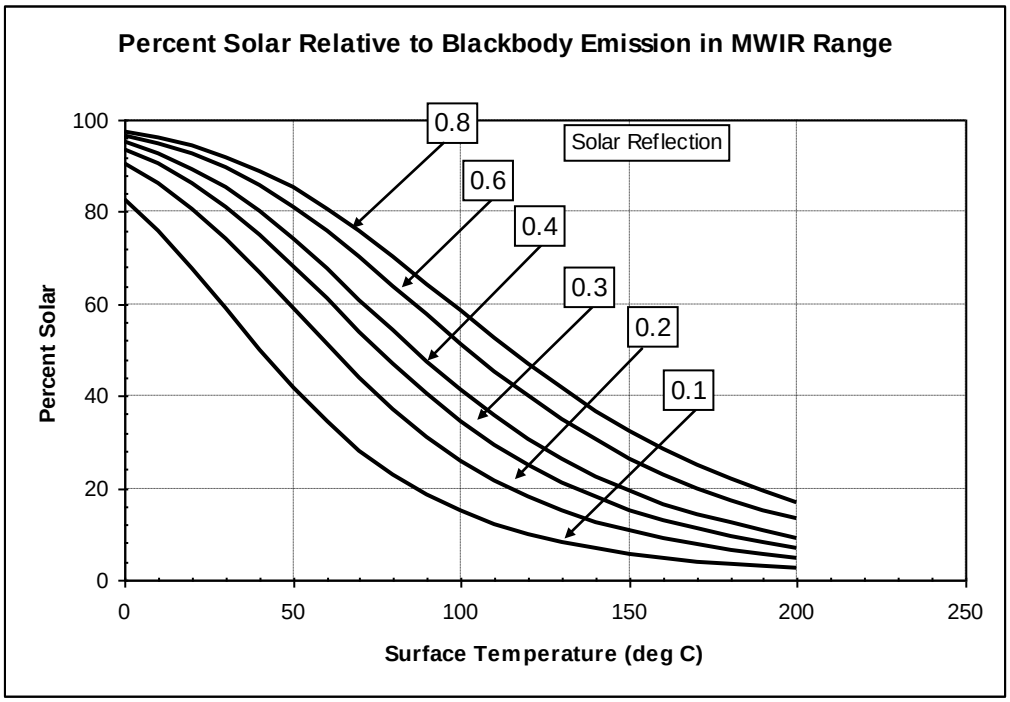

Figure 8-17. MWIR solar reflectance effect.

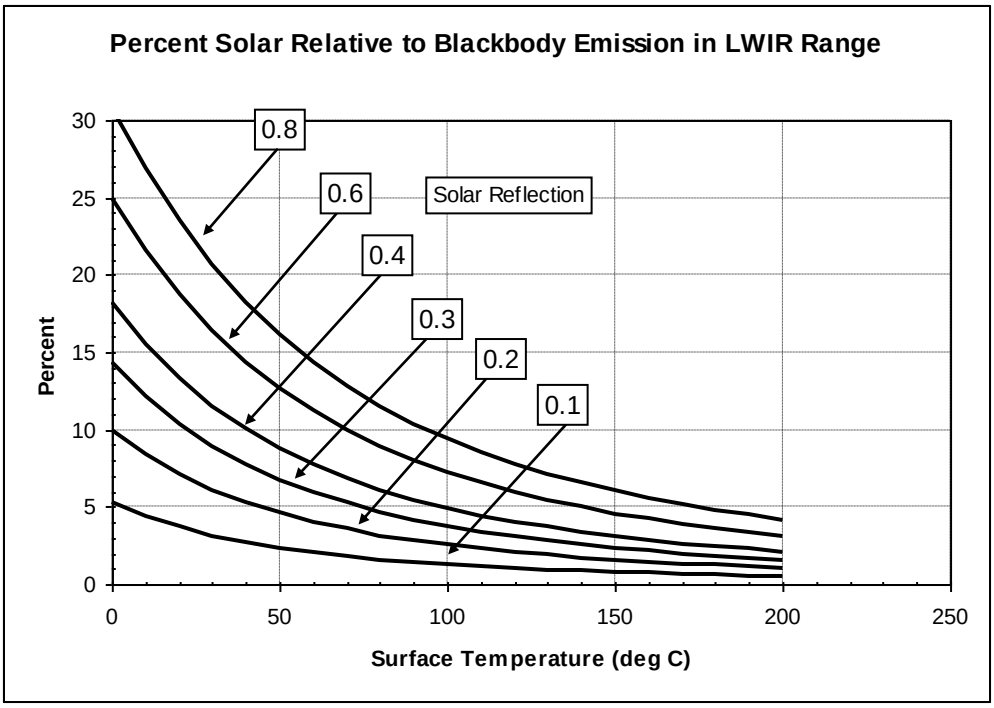

Figure 8-18. LWIR solar reflectance effect.

8.6 References for Chapter 8

a. Dereniak, E., Boreman, G. (1996). *Infrared Detectors and Systems* (pp 51-55). John Wiley & Sons Inc.

b. Wolfe, W., and Zissis, G. (1993). The Infrared Handbook (4th printing of 1985 edition, Chapter 11, pp 67-99). Infrared Information Analysis (IRIA) Center, Environmental Research Institute of Michigan (ERIM), a Defense Technical Information Center (DTIC) sponsored DoD Information Analysis Center.

c. Berk, A., Anderson, G., Acharya, P., Hoke, M., Chetwynd, J., Bernstein, L., Shettle, E., Matthew, M., and Adler-Golden, S. (Feb 11, 2003). MODTRAN4 User's Manual (Version 3 Revision 1), Air Force Research Laboratory (AFRL).

d. Kreith, F. (1965). Principles of Heat Transfer (2nd edition). International Textbook Company.

This page intentionally left blank.

CHAPTER 9

TARGET MEASUREMENTS IN PREDICTIVE SIGNATURE MODELS

Shoulder launched IR missiles present a growing threat to both military and civil aviation. These missiles are small, affordable, accurate, plentiful, and lethal. However, the threat from these missiles are vulnerable to advanced electronic countermeasure techniques including aircraft signature reduction, missile warning and active countermeasures sources like flares, directable lamps, and lasers. Mathematical simulation provides a cost-effective and very inclusive mechanism for evaluating the effectiveness of these techniques, but the simulation must also be accredited and validated to provide confidence in its utilization. Target model validation through field measurements adds to this accreditation.

The need to validate target models for simulations is important for many reasons. As with any theoretical model, inaccuracies may exist in representation of the actual target. In the overall simulation, the target model is combined with a missile model to define a missile fly-out for assessing target vulnerability and evaluating countermeasure effectiveness. The IR target presentation to a missile seeker requires valid representation of intensity, irradiance, and spatial distribution of the target and background signature for creditable analytical results. Also, the simulation requires accreditation to support design and operational testing of advanced countermeasure systems.

9.1 Signature Model Type and Complexity

There are typically three levels of complexity involved with mathematical representation of targets. In order of decreasing complexity, the three levels are:

a. The finite element model.
b. The one-dimensional equilibrium computation of temperatures and/or purely applied temperatures (possibly from a finite element model).
c. The multiple spheres radiance model.

The above representations also relate to the time and expense to develop the model as well as the field measurement data available for their validation. The advantages and disadvantages of each approach will be discussed in the following sub-paragraphs.

9.1.1 Finite Element Model. The finite element model is the most complete simulation of the heat transfer mechanisms that establish the object surface temperatures and, as a result, the spatial radiances. The model consists of a faceted wireframe that provides a three-dimensional (3D) description of the physical characteristics, material and surface properties, thermal nodes (groups of facets defining a thermal network), heat capacity definition of these thermal nodes, heat transfer connectors for conductive, convective, and radiative heat transfer between nodes, and thermal nodes utilized for heat sources and sinks to account for internal influences like an engine. The external contributions from solar loading, sky and ground radiances, and convection to ambient air are also included. The surface radiances are resolved at the pixel level to incorporate possible solar glint and combined with plume contributions to render the overall

spatially distributed signature. Table 9-1 lists attributes of the finite element model type organized as advantages and disadvantages.

TABLE 9-1. ADVANTAGES AND DISADVANTAGES OF FINITE ELEMENT MODEL

Advantages
Rendition of complete physical shape
Interactive with environment
Variable effects of internal heat sources (e.g. operating conditions)
Variable surface properties (e.g. BRDF inputs for reflectance)
Day and night conditions
Heat sink - transient effects
Plume definition
All surface temperatures - radiances potentially available at all view angles
Disadvantages
Time and expense to generate heat transfer connectors
Cost to obtain plume definition based on engine cycle deck and computational fluid dynamics (CFD) analysis
Time and expense for verification with field measurements
Cannot support high frame-rate real-time operations

9.1.2 One-dimensional Equilibrium Calculation or Applied Surface Temperature Model. This model offers the advantage of a geometrical three-dimensional faceted wireframe description of the physical configuration with the ability to determine temperatures by performing a one-dimensional equilibrium calculation or by applying surface temperature either computed by a more detailed model code or based on calibrated imagery measurements. Although a considerable amount of time and cost of model development are avoided, the versatility to use environments other than that in which measured data were gathered will be lost. Also, material property files with BRDF definitions must also be provided to support the proper viewer dependent signatures and the inclusion of environmental effects into the signatures. Table 9-2 lists advantages and disadvantages of the applied surface temperature model types.

TABLE 9-2. ADVANTAGES AND DISADVANTAGES OF ONE DIMENSIONAL EQUILIBRIUM AND APPLIED SURFACE TEMPERATURE MODELS
Advantages
Rendition of complete physical shape
Applied surface temperatures derived from physics based codes or measurements (imagery)
Surface radiances available at all view angles
Plume database support all aspect views
Disadvantages
May have limited plume definition
Limited to environment and operating conditions of measured data
Often cannot support high-frame rate real-time operations

9.1.3 Spheres Model. The spheres model is simplistic but can provide first-order simulation results when better models cannot be made available in an acceptable time frame. The model consists of a series of spheres whose radiance may be determined from imagery measurements or as the output of higher fidelity models. An approximation of the vehicle shape is made with the number and size of the spheres. Also, spatial hot spots are approximated in size at their locations about the aircraft. Caution should be used when interpreting the performance results utilizing this technique. Testing with full 3D facet models has shown that inaccurate assumptions about the missile performance are implied if the analysis is based solely on the spheres modeling approach. Table 9-3 lists attributes of the sphere model type organized as advantages and disadvantages

TABLE 9-3. ADVANTAGES AND DISADVANTAGES OF SPHERE MODEL
Advantages
Least time to implement
Sphere radiances derived from imagery measurements
Disadvantages
May skew missile performance results, resulting in inaccurate hit points
Sphere radiance, size, and location must be defined for each view (dependent on engineering judgment of the user)
Limited to environment and operating conditions of measured data
Limited plume definition

9.2 Expected Radiance Components

In IR signature measurements of aircraft, the settings of the instruments (e.g. radiometers) are critical to ensure the dynamic radiance span of the target is covered within the dynamic range and that the instruments are operating in the linear calibrated region. A good practice for minimizing testing costs, is to predict an estimated signature of the target in order to choose an appropriate dynamic range for the sensors. The prediction can be accomplished either by modeling or by searching historical databases.

9.2.1 Theoretical Radiance at Source. The following is an example of using a model to predict a theoretical source and the environment conditions. An aircraft consists of a hardbody and plume IR component at the source which are combined to a final result at measurement range. A combined exhaust plume and hardbody radiant intensity at the source is shown in Figure 9-1. The hardbody is represented by Planck's Equation for a blackbody temperature of 300 ^{o}C. The plume is represented in the 3 μm to 5 μm band as a spike whose width and central location are typical of aircraft exhaust plumes. Intensity values were chosen for illustrative purposes only. Due to the high exhaust plume contribution, instrument dynamic range could be over estimated.

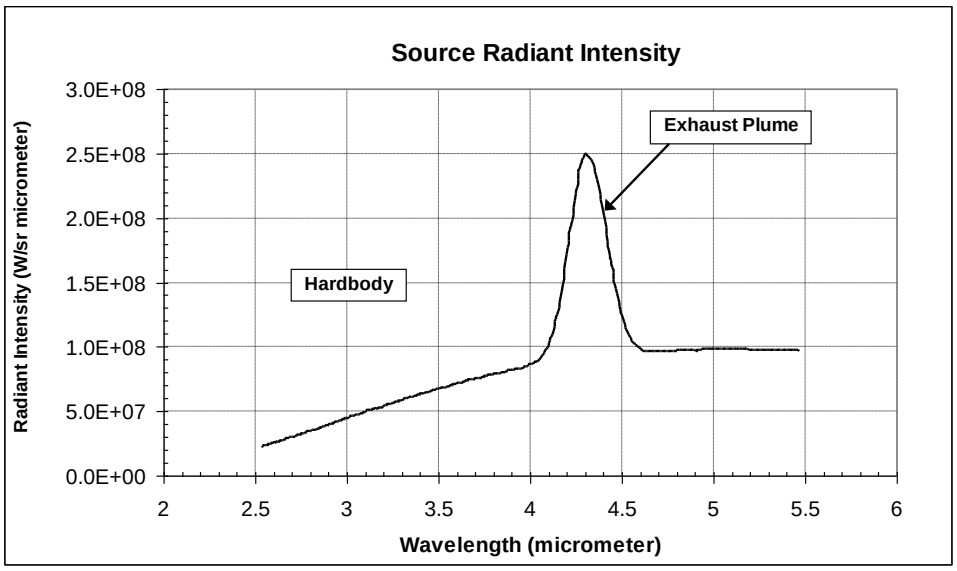

Figure 9-1. Source radiant intensity.

9.2.2 Theoretical Radiance at Measurement Range. In order to obtain a spatially unresolved measured target to support model development, where the FOV contains the entire aircraft body, the target range for a measurement event is typically chosen to be 300 m. Image data is helpful in discriminating the target from the background. It is often the case that spatially resolved image data are collected but that image data are spatially integrated in post-processing for comparison to the model output. At the 300 m range shown in Figure 9-2, the atmosphere has attenuated the radiant intensity, especially in the band from approximately 4.2 um to 4.3 5um. The exhaust plume attenuation is due to the atmospheric CO_2 absorption band centered near 4.3 μm. The exhaust emission is broader than the absorption band resulting in what is nicknamed the CO_2 red and blue spikes. An attempt has been made to estimate the exhaust contribution based on integrating below the two spikes and above a straight line from near

4.0 μm to 4.2 μm on the left side of Figure 9-2 to 4.35 μm to 5.1 μm on the right . Due to the near zero values (near 4.3 μm), it is not possible to use atmosphere model data (transmission) to inversely derive source values. In this example, the MODTRAN atmospheric model was used to compute the wavelength transmission values needed to prepare Figure 9-2. A detailed treatment of the atmospheric effects is described in Reference 9a.

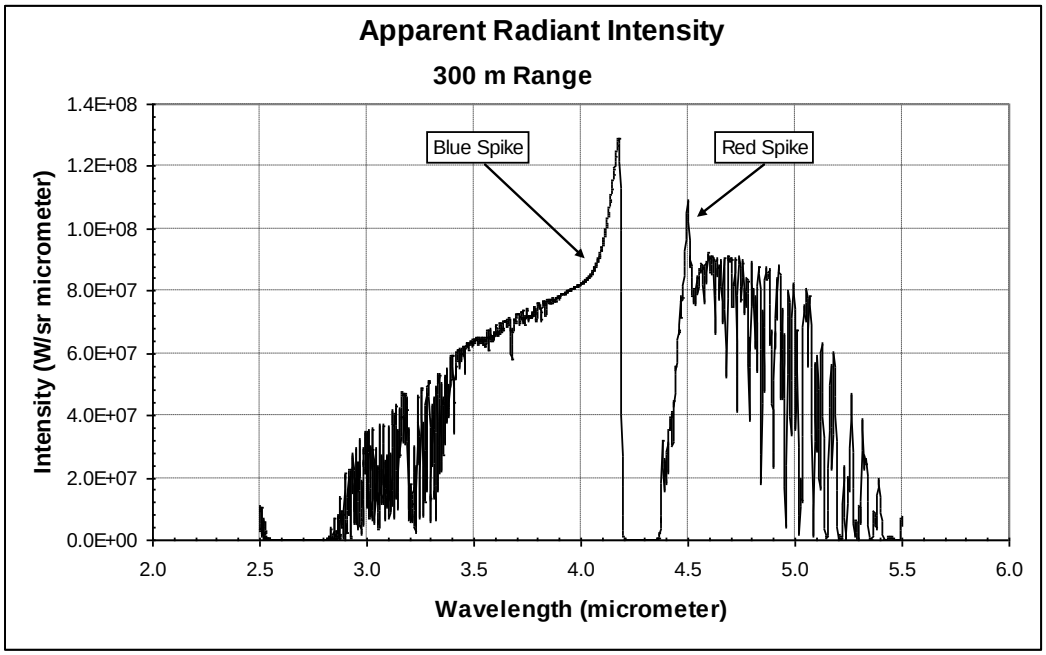

Figure 9-2. Example of exhaust spectral radiant intensity measured at a 300 m range.

9.3 Measurements Required

Data used for model development are categorized in Table 9-4 delineating the type of data and how the comparisons apply to validate the model, in terms of its entirety or components. Typical results used in these comparisons consist of surface temperatures, spectral intensities or radiances, and radiometric imagery. In addition, ancillary data pertaining to weather conditions, aircraft engine and maneuvering parameters, and observation range and aspects are used to adjust the model for the influences of these variables.

TABLE 9-4. DATA COMPARISONS

Measurement Type	Type of Data	Model Validation Application	Comments
Thermocouples with direct contact on surface points	Thermocouple • Data Temperatures	Comparison to values from finite element model Inputs to applied temperature model	
Passive radiometric with a spectrometer. The FOV contains the target and background	Spectral Data, 1.5 μm to 5.5 μm • Target and Background	Spectrally integrated in-band value comparison to all model types Corroboration with overall in-band value from other measurement methods	Valuable to estimate independent contributions from surfaces and plume(s)
Passive radiometric with an imager. The FOV contains the target and background but spatially resolved.	Radiometric effective imagery in the MWIR and LWIR • Target and background	Spatially integrated effective value comparison to all model types and measurement methods Fidelity of spatial distribution in finite element model	MWIR should capture entire range of radiances without saturating (may require two cameras with different gains) MWIR with relevant filters is preferred • LWIR also corroborates temperatures
Passive radiometric with a radiometer. The FOV contains the target and background.	Radiometer effective radiant intensity or irradiance in the NIR and MWIR • Target and background	In-band values comparison to all model types and measurement methods	NIR sensitive to solar wavelength and may pose measurement difficulty due to changing weather conditions

9.3.1 Spectral. Spectral data provides the structure of the signature over spectral regions of interest and permits direct comparison with the final output of the signature models. This comparison includes the methodology employed to account for atmospherics (attenuation, path radiance, and background), reflections of solar, ground, and atmospheric radiances, and panel-to-panel reflections. Reflections are also influenced by the surface properties defined in the model in terms of the BRDF input. Data used should consist of target measurements in terms of contrast intensities and the background radiance to facilitate the comparison with model output. The data should also permit separating the contributions from external surfaces in the continuum and those from the plume for comparison with values from the model. The structured data is integrated over multiple bandwidths, with or without inclusion of response functions, to provide

the various integral or effective signature levels pertinent to the individual seekers. Included in these integrals are values relevant to the accompanying imagery, discussed herein below. In this manner, the spectral results corroborate total signature values from imagery, lending to the credibility of both. Spectral data should be available from approximately 1 μm to 6 μm (NIR through MWIR) to permit integration over the various bandwidths of interest. Data in the LWIR spectrum are used mainly to support the associated imagery.

9.3.2 Radiometric Imagery. Imagery is used in place of, but more preferably in conjunction with, the temperature and spectral data to validate the appropriate components of the model. Imagery permits resolution of contributions over the configuration of the target, and the spatial distribution of effective radiances are used for comparison with model results. However, the use of imagery is bandwidth limited by the characteristic response of the instrument, which is why it is preferred to use imagery in conjunction with spectral data. As mentioned above, overall signatures from imagery are substantiated by corroborating with effective bandwidth values from associated spectral data. Because of restrictions on dynamic range for most cameras, it is common practice to use two similar optically banded cameras, boresighted and with different gain settings, to permit interlacing the data to provide imagery with adequate resolution to distinguish the required signature characteristics. Determination of source values from MWIR imagery is restricted by inaccuracies inherent to the use of bandwidth atmospheric transmittance especially for low levels of radiance. These inaccuracies diminish for longer wavelengths which allow LWIR radiance imagery to be utilized with some knowledge and judgment regarding surface properties and reflective contributors, to provide equivalent surface temperatures for corroboration with and extrapolation of results from thermocouple measurements.

9.3.3 Radiometer. Due to limited resources, either because of schedule or financial limitations, it is often the case that IR measurements are only taken with radiometers in the NIR and/or MWIR bands and with possibly uncalibrated imagery. Since radiometers do not have spatial resolution and spectral knowledge is limited to the optical bandwidth, this is far short of the data needed for the model developer to establish a validated model. However, there is some utility in that the data allows comparison of the overall signature of the model with measurements but requires the model developer to use engineering judgment about the contributions of exhaust plumes and spatial hot spots. For example, some insight to exhaust plume versus hot exhaust can be investigated with the measurements at aspect angles favoring one and not the other, although a series of aspect angle measurements should be considered in test planning.

9.3.4 Environments and Operating Conditions. Table 9-5 depicts a matrix of environments, or scenarios, representative of the variations of conditions for validating IR signature models for typical applications. The matrix includes variations of flight velocity from hover to maximum speeds for viewing angles from look-up to look-down with relevant sky and/or terrain backgrounds, during different times-of-day with hot-to-cold ambient temperatures. These variations are presented to provide minimum-to-maximum expected deviations of the radiances of the overall target and spatial distributions of individual contributors (i.e., engine hot parts, plume, and external surfaces), uniform and cluttered backgrounds, and contrast signatures. Table 9-6 lists typical data requirements.

TABLE 9-5. MATRIX OF ENVIRONMENTS

Operating Condition	**Elevation**	**Aspect Angle**
Hover, Cruise, and/or afterburner • Typical weight and configuration • Nominal temperature • Daytime	Look-up, co-altitude, and look-down	0 degree to 360 degree in 30 degree increments
Modify condition for maximum weight	Look-up and co-altitude	Select points for comparison to the nominal cases
Modify condition for maximum temperature	Look-up	Select points for comparison to the nominal cases
Modify condition for nighttime	Look-up	Select points for comparison to the nominal cases

TABLE 9-6. DATA REQUIREMENTS	
Operational Conditions	
Location	Latitude and Longitude
Range	~ 300 m
Altitude	~ Sea Level
Line of sight to aircraft	View to Cold Sky (Away from Sun)
IR Instrumentation	
Imaging radiometer	NIR, MWIR, and LWIR
Radiometer: Spectrometer	NIR, MWIR, and LWIR, Typically 1 μm to 12 μm range
Distance Measurement	IR laser range finder for full in-flight TSPI
Ancillary Data Requirements	
Time of day	IRIG time for each data event
Latitude and longitude	Test site location
Aircraft parameters	Turbine Gas Temperature (TGT), Aircraft heading
Background radiance	Sky/background radiance (line of sight to aircraft)
Calibration data:	All instrumentation: Spectral response filtered systems Intensity or radiance response
Weather data	Temperature, pressure, relative humidity (metrological data)
Field of View (FOV)	Must include entire aircraft including plume at range
Instrument gain settings	Set dynamic range to avoid saturation
General	
All aircraft operational data listed in Table 9-5 relevant to the time of signature measurements.	
Format	
Compatible with user PC software is preferred.	

9.4 Military IR Signature Model Programs

Several DoD sponsored and commercial codes are available to support the generation of IR signatures for both aircraft and ground vehicles. Some of the more well known codes include the Spectral and In-band Radiometric Imaging of Targets and Scenes (SPIRITS), the Composite Hardbody and Plume Program (CHAMP) and its real-time implementation RealTime CHAMP (RTC), the Multi-Service Electro-optic Signature (MuSES), and the Georgia Tech Signature (GTSIG) code.

Of the codes listed above, SPIRITS has long been the industry standard accepted as producing verified and validated IR aircraft signatures. The SPIRITS models are developed from, and rigorously verified and validated to, IR radiant intensity, spectral, multi-imaged, and multi-band measurement data which has been collected in flight. This measurement data is collected to bound the operational flight envelope of a given aircraft. The following sub-paragraphs provide a brief overview of each model.

9.4.1 Spectral and In-band Radiometric Imaging of Targets and Scenes (SPIRITS) Aircraft Model. In 1974, the Defense Advanced Research Projects Agency (DARPA) funded AFRL to accurately measure aircraft signatures in the IR with the Flying Infrared Signatures Aircraft (FISTA) and to develop a computer aircraft IR signature simulation capability using physics-based models. This aircraft signature modeling capability became the SPIRITS. To satisfy the need for accurate predictions for a variety of scenarios that had not been directly measured, the FISTA program undertook an ambitious program of model development, with support from many sponsors and contractors.

It was very apparent that, even when accurate measurements were available, a requestor of such data would find that the measurement bands would be different from those requested, the range to the target too different or the sun position or environment was different from the requestor's needs. The SPIRITS model was developed to predict the signature of an aircraft anywhere in its flight envelope, for any reasonable scenario, in a specified environment, and against a specified background. Since the code is based on the principles of physics, this allows modeling of new aircraft that that have not been measured. Such a model should be validated by flight measurements as soon as possible, but early modeling allows for early assessment of threat and vulnerability issues.

All current SPIRITS aircraft modules were developed from measurements by the FISTA program; however, any adequate series in-flight and ground measurements can be used. An example of a FISTA measurement compared to a SPIRITS signature is shown in Figure 9-3.

An advantage of the SPIRITS code is the availability of complete databases for a number of operational military aircraft. Access to the databases provides capability for generating accurate IR signatures for a wide range of altitudes and engine power settings. There are currently sixteen aircraft modules available. The QF-4 is included in the basic unclassified software and is in the tutorial section of the SPIRITS User Manual. The SPIRITS Technical Manual describes the component program modules. The 15 classified aircraft modules are:

C-130H (transport)	B-1B	C-5B	F-16C	737-700 (C-40)
AC-130 (gunship)	B-52H	C-5M	KC-135R	747-400F
AGM-86B (ALCM)	C-17A	F-15E	KC-10A	757-200

Note. When an aircraft module is installed it may incorporate classified information into SPIRITS.

The SPIRITS code has five major modules and a number of lesser supporting elements. The five major modules are:

a. Turbine Exit (TRBEXT) model engine exit plane calculation and hot parts.
b. Plume Flow Field (PFF): Standard Plume Flowfield (SPF), external turbo fan (EXTF)-3D Stream model, and the latest combustion research and flow technology aircraft (CRAFTAC) 3-Stream model. Non-symmetric nozzle models are in-development
c. Standard Infrared Radiation Model, version II (SIRRMII): Plume Radiation from flow field data
d. MODTRAN: (Moderate Resolution Atmospheric Transmission) model
e. HARDBODY: (Code Integration and Final Output)

The SPIRITS program is managed by the Joint Army-Navy-NASA-Air Force (JANNAF) Signature Panel of the Exhaust Plume and Signatures Subcommittee (EPSS) of the JANNAF Interagency Propulsion Committee (IPC).

The latest version for Linux and Windows, SPIRITS-AC2r2, is scheduled for release in summer 2010 through the Chemical Propulsion Information Analysis Center (CPIAC), Johns Hopkins University, Columbia Maryland (tel. 410-992-7300), http://www.cpiac.jhu.edu/.

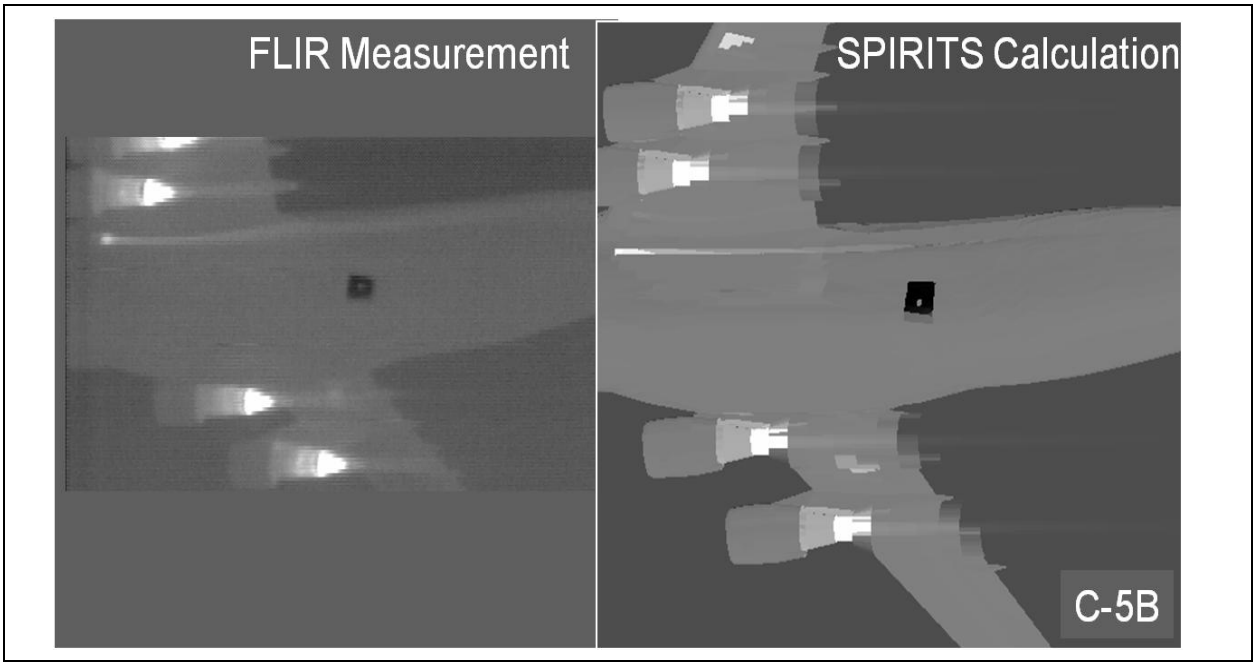

Figure 9-3. Sample FISTA data collections and SPIRITS signature generation.

9.4.2 Composite Hardbody and Missile Plume (CHAMP). The CHAMP program is a computer simulation used to provide time dependent high-fidelity IR simulations of airborne vehicles. The program was originally developed in 1993. Since that time, the AFRL Munitions Directorate, using their Kinetic Kill Vehicle Hardware-In-the-Loop Simulator (KHILS) facility located at Eglin AFB, has assumed the lead role in managing, maintaining, and upgrading

CHAMP. As a research and development (R&D) facility, KHILS is used to test advanced seeker concepts. Many of the advanced concepts require elements in the IR scenes that are currently not being modeled in other IR scene generators. For minimal resource investments, the computational structure of CHAMP allows it to readily serve as a test vehicle to explore new concepts. Figure 9-4 presents a comparison of measured IR imagery to CHAMP modeled IR imagery.

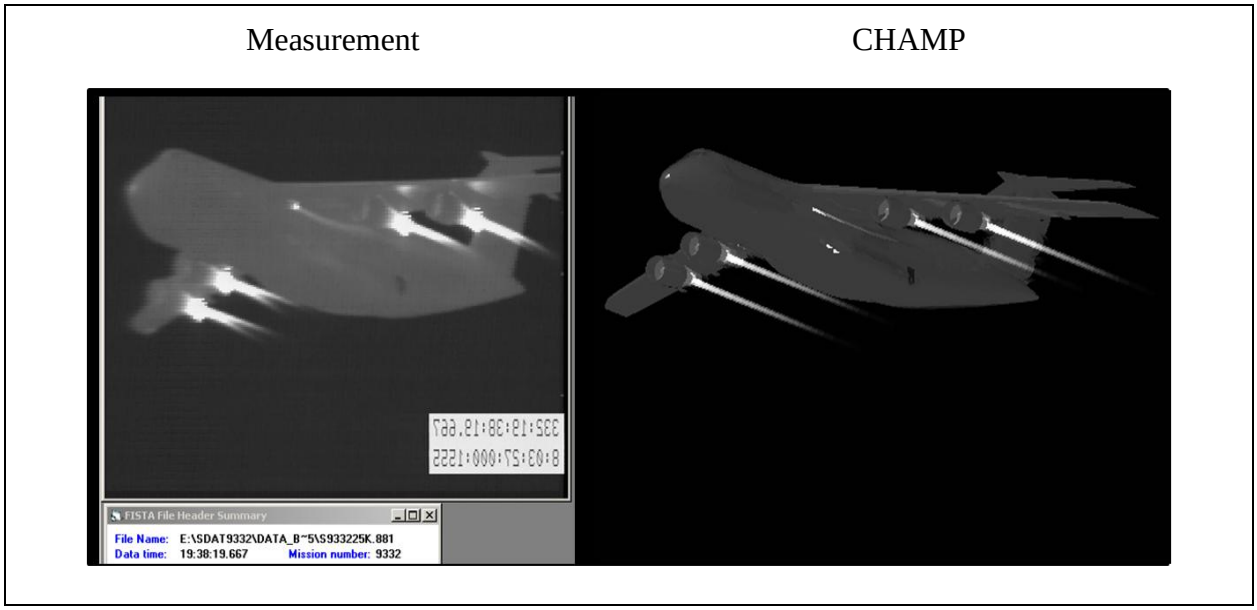

Figure 9-4. Example measurement to CHAMP signature comparison.

Computational efficiency has been one of the driving principals behind the development of the CHAMP program. Thermal modeling in CHAMP is a one-dimensional aerothermal heating implementation. More thermal detail can be represented in a CHAMP model than in a typical applied surface temperature model since temperatures are defined at the vertex level. In addition to a full three-dimensional polygon representation of an object, objects can be constructed from predefined objects like spheres, disks, and cylinders. Different material layers can also be applied in depth which provides added versatility.

The CHAMP user interface is programmable and allows users to readily create any type of scenario. The user input file is divided into several input classes or categories that guide the user through the necessary steps to build a scenario. These classes are Program Options, Library pathnames, Sensor, Surface and Temporal specifications.

In addition to CHAMP-only models, many of the validated SPIRITS models have been converted to CHAMP models including the C-130H, AC-130, B-1B, B-52H, C-17A, C-5B, C-5M, F-15E, F-16C, KC-135R, KC-10A, Boeing 737-700 (C-40), and the Boeing 747-400F. Several limited helicopter models have been constructed and validated to specific flight conditions. Many of these models have been transitioned to run in real-time in Real-Time CHAMP (RTC) to support hardware-in-the-loop (HIL) activities.

Originally developed to model aircraft targets, several ground vehicle models developed using the MuSES code (paragraph 9.4.4) have been adapted for use in CHAMP. Figure 9-5 shows a CHAMP rendering for a MuSES track armored vehicle.

The CHAMP is cross platform compatible for both Linux and Windows. The CHAMP aircraft models are distributed through the Chemical Propulsion Information Analysis Center (CPIAC), Johns Hopkins University, Columbia Maryland (tel. 410-992-7300).

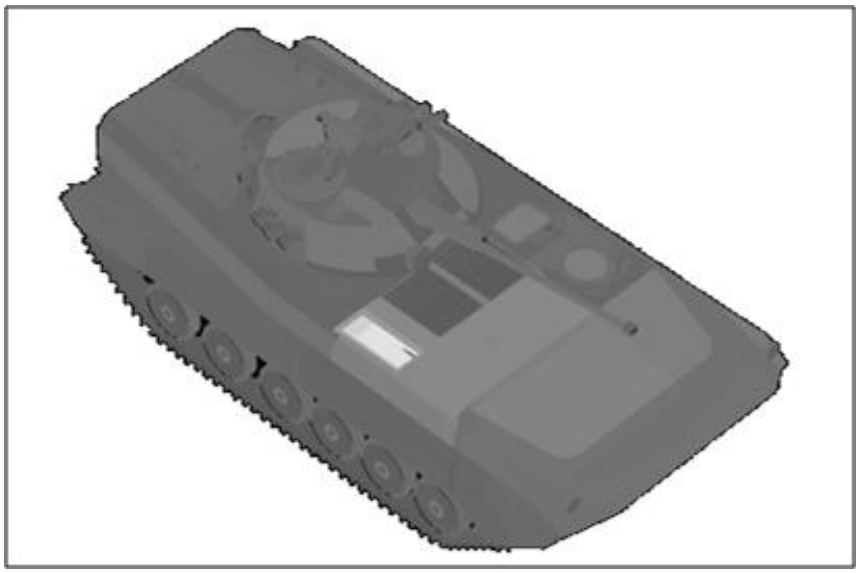

Figure 9-5. Example CHAMP rendering of a MuSES target.

9.4.3 Real-Time CHAMP (RTC). Real-Time CHAMP (RTC) is the real-time version of CHAMP capable of generating IR imagery for projection at the high frame rates needed for HIL simulation. Using NVidia video card technology to aid IR calculations, RTC is capable of generating 512 x 512 pixel scenes at frame rates greater than 90 Hz. Real-Time CHAMP relies on CHAMP to construct an input database of imagery data files to support real-time rendering. The latest development version of RTC, version 3 (RTC3), is a new architecture and is intended to fully utilize the capabilities of the massively parallel 128-bit video processors to provide CHAMP-like aircraft hardbody and full three-dimensional (3D) plume radiance transport calculations at real-time rates. In addition to aircraft targets, RTC3 supports maritime signature generation for small boats with full dynamic sea states, physical boat dynamics, bow spray, and speed dependent wakes. Both Linux and Windows versions are in development with aircraft plume analysis studies in process.

9.4.4 Multi-Service Electro-optic Signature (MuSES). The MuSES code is the next-generation IR signature prediction program developed to generate ground vehicle IR signatures. MuSES was designed to reconcile the previous disparity between the geometry required to predict vehicle signatures and the geometry used to design vehicles (Reference 9b). The solution was to use meshed computer-aided design (CAD) geometry. The MuSES code was built on the functionality of the Physically Reasonable Infrared Signature Model (PRISM), the Army's standard tool for IR signature and thermal modeling, and the functions of PRISM are integrated into MuSES. The implementation of several features within the code has allowed MuSES to find

increasing usage outside its primary function as a tool for designing ground vehicles. These features being: MuSES batch mode and the MuSES database file library interface, "tdfio" library. The “tdfio” MuSES output file format is a self contained file which includes all input and output information for a given signature, including the target physical description, operating state, and environmental state. Transient restart facility and user routines are described along with their application to synthetic natural environments, real-time scene generators, mission planning systems, and a continuously running temperature prediction system.

The MuSES, like SPIRITS and CHAMP, relies on a mesh facet geometry description of the target as well as material definitions. The radiation view factor module uses high-speed algorithms such as the hardware graphical hemi-cube technique and a software ray casting solution. The thermal radiation exchange is based on diffuse multiple bounce reflection for both the thermal radiosity solution and the IR signature output. Additional directionality using the BRDF module is available for signature output only. The surface temperatures are optionally initialized with a steady state solution, and then the simulation proceeds through time with a transient solution over the designated prediction time. The energy balance is based on linkages of radiation, convection, and conduction. MuSES will employ automatic link generation to create many of these linkages. The effects of aerodynamic heating will be included. Imposed heating is added as a function of time as well as time dependent temperatures for boundary conditions. Environmental effects are also included as boundary conditions. The user inputs include temperature, heat rate, convection coefficient, thickness, and surface/material assigned to each hardware part.

A customized thermal node menu provides the user with the options for specifying part (or node) types (e.g. assigned temperature, computed, and others). All of these model attributes can be entered interactively through the graphical user interface (GUI). To include the thermal effects of internal components, the user can insert simple isothermal solids; rectangular or cylindrical, engine solids with temperature/heat distributions, ducts with fluid flow, and simple heat exchangers.

MuSES displays the physical temperature of the modeled surface as a thermal image during the solution process. The image can be rotated and viewed at any direction throughout the thermal prediction simulation. Temperature and radiance output files are automatically created during the simulation thus providing the time-history.

9.4.5 Georgia Tech Signature (GTSIG) Code. The GTSIG (Reference 9c) is a library of computer programs funded by the Army to predict temperatures, blackbody emittance, and effective radiances of three-dimensional objects, accounting for the object’s interaction with an environment over a period of time. To produce high resolution IR signatures, GTSIG utilizes a three-dimensional finite difference thermal analyzer and a multi-surface radiosity model. The GTSIG is the component of the end-to-end simulation which predicts the temperatures and radiances of parts of objects (such as aircraft) and terrain materials. Outputs from GTSIG are used by the Georgia Tech Visible and Infrared Synthetic Imagery Testbed (GTVISIT) to compute the views of the world as seen by threat IR missiles.

GTSIG uses thermodynamic and heat transfer laws, material properties, and construction details of modeled objects to provide a rigorous yet more flexible approach to signature modeling than available using semi-empirical modeling. The outer surfaces of GTSIG objects are modeled as a set of connected triangles (facets). Neighboring facets deemed thermally identical by the modeler are combined into thermal nodes. The modeler also creates a thermal network identifying each node heat capacities and properties and the paths among the nodes by which heat can be conducted. Many current Army aircraft models are complex, containing thousands of facets and hundreds of thermal nodes.

Another feature of the model, or rather model input, concerns exhaust plumes. That is, plumes are part of the model, but are usually generated outside the model, and then input or called in. Generation of a plume begins with development of the gaseous flowfield, usually using Parabolized Navier Stokes (PNS) or computational fluid dynamics (CFD) technologies. The plume signature is then computed as a separate entity, utilizing ray-tracing techniques along multiple optical paths through the gaseous medium for either what is termed a correlated or uncorrelated application. Other than the attenuation of emissions from sources shadowed by the plume, other interactions between the plume and local aircraft surfaces are not modeled. A gaseous volume(s) is not included, per se, in the definition of the thermal model to account for plume heating of local airframe surfaces by radiation and/or possible convection. In some models, this plume heating is approximated by use of network connectors between select surface nodes and a plume or exhaust gas temperature input, but is specific to the flight condition (and relative plume shape and position); the user will need to modify as deemed appropriate. Furthermore, without plume physical definition to the model, view factors are not determined for including reflections of plume emissions from surface facets.

The GTSIG code generates the predictions required by GTVISIT for imagery to simulate the engagement of advanced threat IR missiles attacking aircraft protected by advanced countermeasures as depicted in Figure 9-6 (GTSIG model) and Figure 9-7 (GTVISIT image).

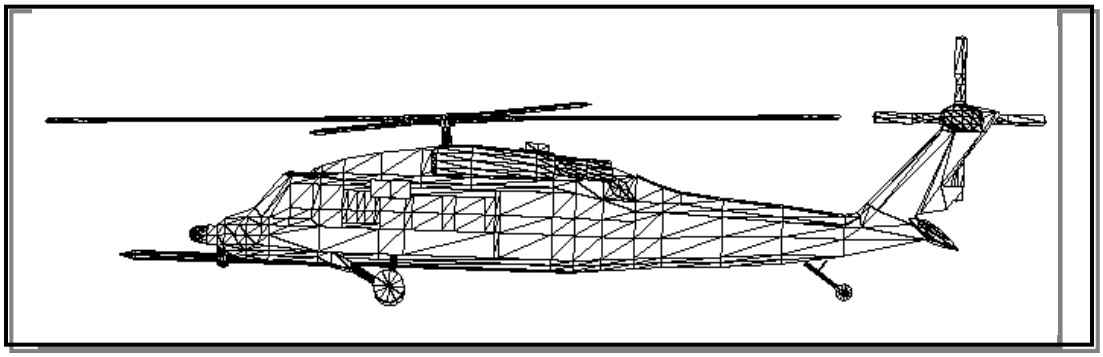

Figure 9-6. GTSIG faceted model (no external fuel tanks).

Figure 9-7. Example GTVISIT IR signatures generated from GTSIG output.

9.5 Enhanced Missile Signature (E-MSIG) Model

The Advanced Missile Signature Center (AMSC) at Arnold Engineering Development Center (AEDC) Arnold AFB, TN developed the E-MSIG model to support EO, UV, and IR simulations/simulators of surface-to-air missile (SAM) plume signatures. This simulation activity is required for Man Portable Air Defense System (MANPADS) missile systems, with the cognizance of The Defense Intelligence Agency Missile and Space Intelligence Center (DIA/MSIC).

The E-MSIG provides databases tailored to each of the seven currently modeled MANPADS missile systems using JANNAF predicted data called hypercubes that are scaled with measured UV, VIS, and IR signature data and that are refined to account for brief spikes in the measured data. Also provided are models of engineering unit measurements of UV, VIS, and IR signatures of tactical missile exhaust plumes from 0.2 μm to 25 μm in free-flight environments. Tailorable software extraction tools and sample test code also permit users to obtain signature outputs specific to their needs.

The model is essentially the output of the JANNAF predictive code suite (Viscous Interaction Performance Evaluation Routine (VIPER), standard plume flowfield (SPF), and Standard Plume Ultraviolet Radiation Code (SPURC), altered to capture the full spectral radiance values (which are usually treated as interim files and deleted), scaled to match measured signature data through the Model Extrapolation (MODEX) procedure (Reference 9d, and Reference 9e). To provide the altitudes, missile system velocity (Mach number), and aircraft missile-to-sensor aspect angles needed to support aircraft UV and IR sensor and missile system testing, E-MSIG first uses predictive UV, visible, or IR data from the validated government models (JANNAF) for missile motor nozzle exit conditions, plume flowfields, and radiometric signatures and plume-transmittance representations. These hyperspectral (UV, VIS, and IR) datasets are called hypercubes. Further, enhanced hypercube accuracy is provided by scaling the predictive data with extrapolated temporal bandpass corrections and by Gauss-Markov statistical refinements that more accurately represent signature spikes seen during missile flyout.

The signature measurements collected for the development and validation of the E-MSIG model are UV, VIS, and IR effective values with band radiometers to characterize high temporal

phenomena, spectra to identify emission features, and images to characterize the spatial extent and position of features such as Mach disks. Measurements are collected at as many aspect angles as possible and as fully across the altitude and velocity domains as safety and resources allow. Data are collected in the lowest background environment as possible. This is especially true for the VIS spectral region where all VIS data are collected during night trials. However, because the exhaust plume signatures are significantly greater than any signature component from solar heating, there is no effect from the position of the sun in the sky as there would be in, say, in aircraft or ground vehicle measurements. This lack of effect from the sun is fortunate because the signatures corrected for atmospheric attenuation are invariant to the time of day or position of the sun.

The AMSC has developed two versions of E-MSIG. The first version of E-MSIG (v 1.0) contains fully hyperspectral datasets (hypercubes) with measured and predicted plume radiant intensities for five of the missile motors currently modeled. The second version of E-MSIG (v 2.0), contains new features which have been added to two of the seven MANPADS models available via E-MSIG. A funded effort for all of the E-MSIG models to have the version 2.0 features, as well as atmospheric corrections and variations for timing and intensity data, is planned to be completed in late 2010. The new features in version 2.0 are:

a. Plume transmittance (in addition to radiant intensity).
b. Refinements for brief signature spikes, called sputter.
c. More efficient datasets employing sparse matrices that eliminate very rarely used points within the E-MSIG v 1.0 hypercubes.
c. Compression techniques for more efficient E-MSIG database storage and access.

The E-MSIG databases can be used with a wide variety of computing environments such as SGI, Unix, Linux, and Macintosh. Additionally, the modularity of the software libraries containing these datasets and the additional software extraction tools provided with E-MSIG permit users to employ multiple levels of access to measured and/or predictive data. Thus, for almost all test conditions, E-MSIG is currently used to support the full range of UV and IR simulations requiring MANPADS missile plume signature representations, including fully digital simulations (both real-time and non-real-time) as well as stimulations with software-in-the-loop or hardware-in-the-loop capabilities.

9.6 References for Chapter 9

a. Signature measurement Standards Group (SMSG) (publication date is to be determined (TBD). Weather and Atmospheric Effects on the Measurement and Use of Electro-Optical Signature Data, Range Commanders Council (RCC).

b. Sanders, J., Johnson, K., Curran, A., and Rynes, P. (2000). Ground Target Infrared Signature Modeling with the Multi-Service Electro-optic Signature (MuSES) Code, in Targets and Backgrounds VI: Characterization, Visualization, and the Detection Process, (Watkins, W., Clement, D., and Reynolds, R. editors), Proceedings of the Society of Photographic Instrumentation Engineers (SPIE) Vol. 4029.

c. Electro-optical (EO) Modeling and Analysis Group, Electro-Optical Systems Laboratory, Georgia Tech Research Institute Atlanta, GA. Georgia Tech Visible and Infrared Synthetic Imagery Testbed (GTVISIT) VIS/IR Image Rendering Code. http://eosl.gtri.gatech.edu/Default.aspx?tabid=132#GTVISIT (retrieved 2009).

d. Taylor, M., Pergament, H., Dietz, K., and Simmons, A. (May 15-17, 2000). Tactical Missile IR/UV Signature Databases Development and Validation. Briefing presented at the 25th Joint Army-Navy-NASA-Air Force (JANNAF) Exhaust Plume Technology Subcommittee Meeting, Nellis AFB, Las Vegas, NV.

e. Taylor, M., and Thorwart, M. (2006). Computational Toolkit for Generating Missile Signature Databases, Briefing presented at the 29th JANNAF Exhaust Plume Technology Meeting, Lockheed Martin Corp, Littleton, CO.

CHAPTER 10

FUTURE TOPICS

10.1 Objective

The collection, reduction, and analysis of quality radiometric data is a complex process involving the application of numerous scientific and engineering disciplines. To address every aspect of the process in a single manuscript would be impossible, and so this work is intended to serve as a living document and be updated as needed. During preparation and review of this standard, it became obvious that more expansive work in several areas would be beneficial. This chapter discusses the areas that the measurements community should address at a future time.

10.2 Atmospheric Correction

This document primarily addresses the process of making accurate measurements of the apparent signature of targets through careful characterization of the measuring instrument. Apparent signatures are those measured across an atmospheric path and include the attenuating effects of atmospheric absorption and scattering. The degree of attenuation depends on many complex variables which are often difficult to quantify at the time of measurement. These areas include measurement path length, altitude, measurement angle, meteorological conditions, molecular concentrations, and unique aerosol content. Apparent signature data satisfies the radiometric requirements for some project applications, but many programs require "source" signature data. That is, some customers require measurement data that have been corrected for any attenuating effects introduced in the measurements process and which ultimately convey radiometric properties intrinsic to the source.

Complex software models have been developed over the years to calculate atmospheric transmission and losses across optical bands of the electromagnetic spectrum. However, many of these models are difficult to use and the details of their application are not well-understood outside the atmospheric sciences community. The MODTRAN model, for example, is a common software model used to perform atmospheric correction for IR measurements. The model, developed and validated by the Air Force, can provide highly accurate and useful results when applied properly. However, few practitioners consider themselves proficient in its use. The sophisticated program relies on judicious selection of various computation modes, default atmospheric models, and a host of environmental variables to obtain useable results for even the simplest atmospheric path calculations.

The discussions of atmospheric effects on optical signatures (see paragraph 2.1, paragraph 2.6, and paragraph 4.4) have been cursory, and so more extensive work is needed in this area. The measurements community would greatly benefit from a reference document devoted to this subject matter. Specific topics that need to be addressed are atmospheric transmission losses, path radiance effects, refraction effects, and turbulence effects. Practical guidance for the selection of appropriate atmospheric models and their correct application to the measurements environment could significantly improve measurements accuracy on the test ranges. Furthermore, such a document could help introduce standards to the data reductions process, something that is woefully lacking at this juncture. To this end, the SMSG is currently

working on an RCC document entitled Weather and Atmospheric Effects on the Measurement and use of Electro-optical (EO) Signature Data.

10.3 Radiometric Data Reduction and Analysis Software

Radiometric data reduction and analysis is a computationally intensive process that lends itself to software implementation. For many years, measurement groups have been developing customized programs to govern data collection, reduction, and analysis for their respective test ranges and laboratories. There have been few attempts to standardize programming routines for common data reduction tasks. Furthermore, several recently developed commercial software packages are providing radiometric data reduction and analysis capabilities. These software packages have been employed with varying degrees of success and have drawn criticism from a number of test ranges. Although software is a common thread in the signatures community, there are few standards guiding its selection, implementation, and validation. Therefore, adding a section on software issues in future editions of this document would be very beneficial to the signatures community.

10.4 Aperiodic Transfer Function (ATF)

Most measurement scenarios addressed in this document involve fairly well resolved targets observed over relatively short ranges. However, some programs require signature measurements of very distant targets that subtend only a few pixels on a sensor focal plane array. In these cases, pixelization effects can dramatically impact the accuracy of radiometric data collection and analyses. The geometric projection of a complex target on a small number of square pixel elements often results in signal averaging which adds to measurement uncertainty. The ATF has been recommended as one potential technique for correcting pixelated radiometric data. The theory behind ATF has been well-formulated and documented but additional experimental work is needed to fully characterize and quantify ATF effects and develop practical guidelines for implementation. This work would greatly benefit DoD customers who require radiometric measurements of high-altitude targets from ground based sensors.

10.5 Real-time Compression

Advances in sensor size, resolution, and speed have led to dramatic increases in the volume of data produced by modern EO systems. Many real-time systems rely on sophisticated compression algorithms to stream data over bandwidth-limited networks and data links. A growing number of airborne sensors fall into this category and many of them are deployed on unmanned air vehicles (UAVs). Consequently, there is significant interest within the UAV community in characterizing the effects of data compression on the accuracy of signature measurements. Furthermore, additional research is needed to identify limiting factors and propose recommended compression techniques for preserving data integrity. A section addressing realtime compression and its potential impact on radiometric data products should be incorporated into this manuscript in a future revision.

10.6 Calibration Procedures

While this document provides an overview of the calibration process (paragraph 2.5 and paragraph 4.3) and presents generalized calibration strategies (section 7.6), a more thorough treatment of calibration procedures is needed. A reference work for accepted calibration procedures and techniques and practical examples of their application would greatly benefit the measurements community. The document should address the selection of calibration sources and temperature ranges appropriate to a given measurements task. Other topics should include selection of bandpass filters, reflected and scattered radiance, temperature of external optics, and traceability of sources and methods.

10.7 Polarization Measurements

Polarization can be an important discriminator of a target/threat to its background. Polarization can be exploited to penetrate scattering atmospheres as well as to characterize cloudy and hazy atmospheres to aid in interpretation of more general radiometric measurements. Polarization sensors are being considered for air- and ground-based platforms. A chapter on polarization, with particular emphasis on its impact to LWIR measurements, would be beneficial. The chapter should include discussions on specialized hardware required to measure polarized light, the calibration of such optical systems, and on the analysis of the measurements. The chapter should also include describe the state of the art of computer models related to polarization measurements.

This page intentionally left blank.

APPENDIX A

DETECTOR TYPES

1.1 Types of Electro-optical (EO) Detectors

The two basic types of EO detectors are thermal detectors and photon detectors. Thermal detectors absorb optical energy, carried by photons, which change some measurable detector characteristic. A quantum detector (also called photon or photoelectric detector) has an output proportional to the number of photons absorbed. The spectral response of a thermal detector is flat with wavelength while, since the energy of a photon is inversely proportional to its wavelength as Equation A-1, the spectral response of quantum detectors increases with longer wavelength as Equation A-2. Note that Equation A-2 uses a proportionality symbol to indicate the integration time is not accounted for. An illustration of the nominal spectral characteristics of ideal thermal and quantum detectors are shown in Figure A-1.

$$Q = \frac{hc}{\lambda} = \frac{1.24\ \text{eV}}{\lambda(\mu\text{m})} \qquad \text{(Eq. A-1)}$$

$$R(\lambda) \propto \frac{output(\text{amp, volt, or count})}{Q(\lambda)}$$

$$\propto output(\text{amp, volt, or count}) \times \frac{\lambda(\mu\text{m})}{1.24eV} \qquad \text{(Eq. A-2)}$$

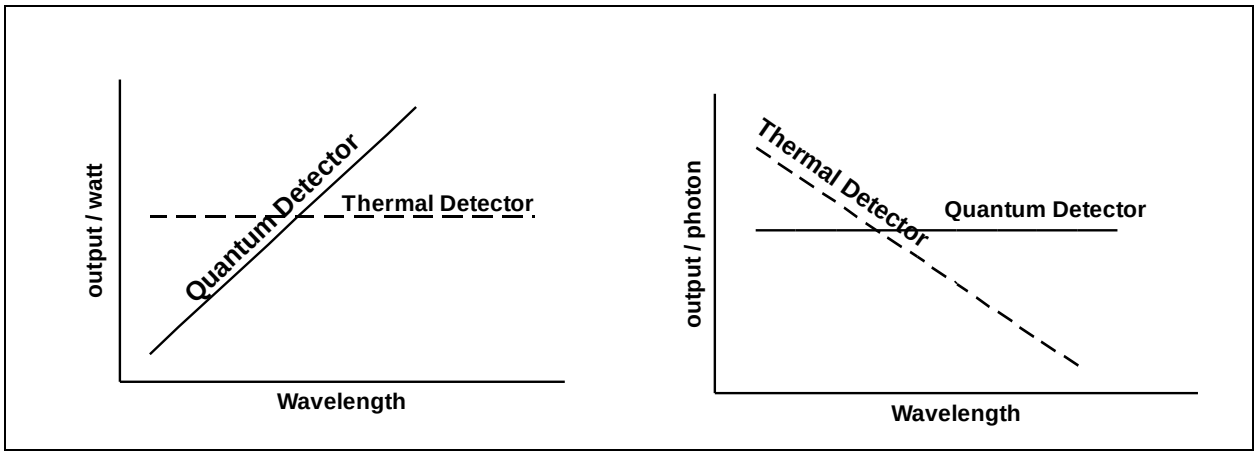

Figure A-1. Nominal spectral response of quantum and thermal detectors.

Although real detectors do not have the smooth response shown by the ideal response shown in Figure A-1, their spectral responses always show these nominal characteristics. Most target signature measurement systems today use quantum detectors because of their greater frequency response. Although the mechanism for producing an output is the conversion of photon energy to conduction electrons, the fact that each short wavelength photon carries more

energy than longer wavelength photons, results in an output versus energy curve with a slope of approximately 1 until a cutoff wavelength occurs. The cutoff wavelength occurs when each photon has insufficient energy to produce a conduction electron. In terms of spectral response, thermal detectors provide the advantage that their output is not dependent on the spectral distribution of radiant energy falling on the detector. This characteristic allows such systems to be calibrated in terms of irradiance rather than effective irradiance and makes correction of measured data much easier. But other characteristics such as time constant and responsivity make quantum detectors the usual choice for signature measurement systems. In certain applications, where the irradiance is high and frequency response is not an issue, the use of thermal detectors may be preferable to the use of quantum detectors.

There are many types of quantum detectors. Some quantum detectors require that a photon have sufficient energy to release an electron (photoelectric or photoemissive detectors). In order to produce a free electron, a photon must have more energy than the detector material's work function. Materials have been made with work functions low enough that photons of wavelength less than about 1.1 μm can produce free electrons. Other quantum detectors only require that the photon have sufficient energy to move an electron from a materials valence band to the conduction band (photoconductive and photovoltaic detectors). Since the energy gaps in various materials have a wide variation (including small energy gaps), response to optical energy of wavelengths much greater than 1.1 micrometers (even to millimeter wave wavelengths) are possible. Some typical detectors in these two categories are shown in Table A-1.

TABLE A-1. CATEGORIES OF ELECTRO-OPTICAL (EO) DETECTORS

Thermal	**Photoelectric/Photoemissive (<1.1μm)**	**Photovoltaic/Photovoltaic**
Thermocouples	Photomultiplier tubes	Silicon and germanium
Thermopiles	Photographic film	Indium gallium arsenide (InGAs)
Thermistor bolometers	Image converters	Lead sulphide and lead selenide (PbS/PbSe)
Golay cell	Vidicons	Indium antimonide (InSb)
		Mercury cadmium telluride (HgCdTe)

1.2 Detector Materials Applicable to Various Spectral Bands

Another factor that is required to obtain a high signal-to-noise ratio is to choose a detector system (detector, cryogenics, amplifier, etc) that has low noise and good responsivity in the spectral band of interest. The best way to quantify the noise in a detector is to determine its Noise Equivalent Power (NEP). The NEP is defined to be the radiant power required to produce a signal equal to detector noise. It is convenient to characterize detector materials using a quantity called "detectivity", which is the inverse of NEP. Detectors are generally characterized by a quantity called D* (dee-star) which is the detectivity for a unit square centimeter detector

area with an electrical bandwidth of 1 Hz. The D* of some detectors as a function of wavelength are shown in Figure A-2 (see Reference 1.2a). Note that the shape of the quantum detectors and thermal detectors are as described earlier. Detectors of other sizes and with other electrical bandwidths can easily be derived from D* as shown in Equation A-3.

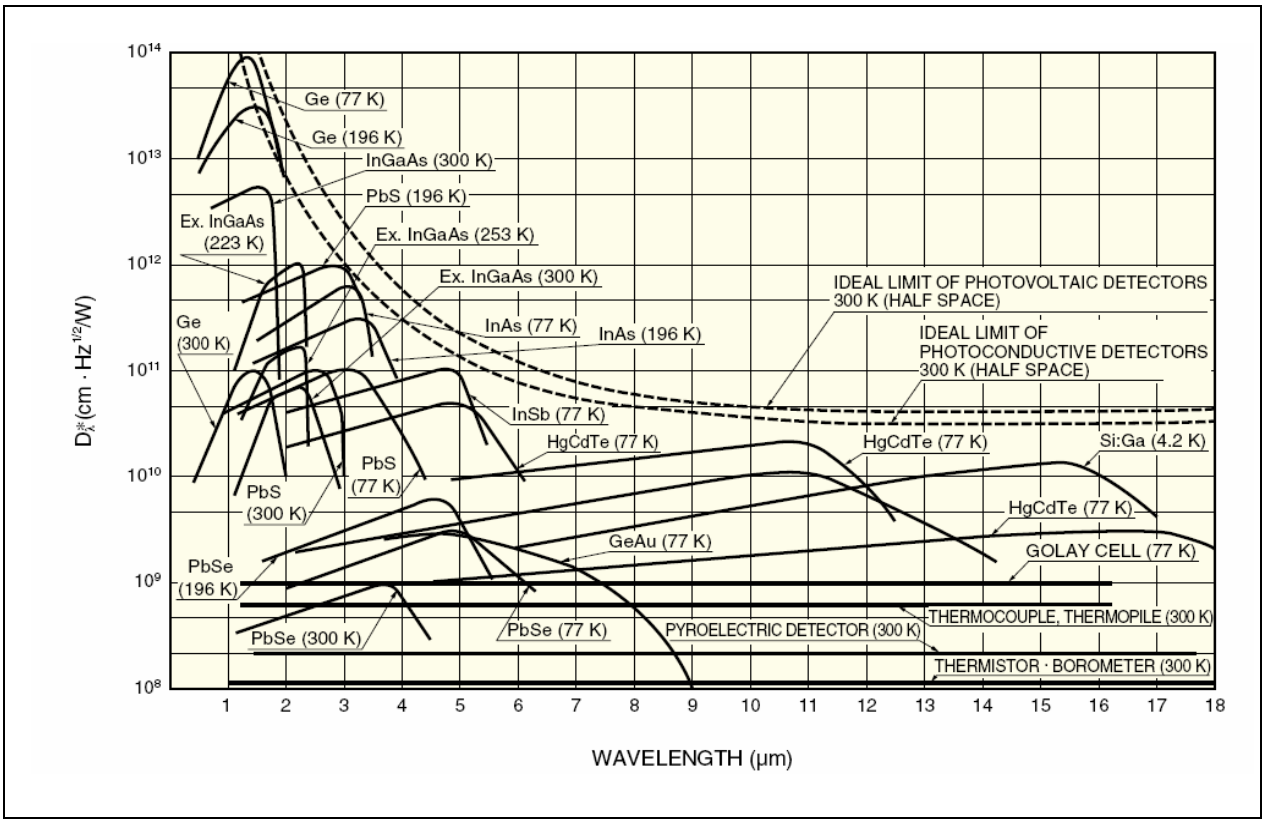

Figure A-2. D* for various electro-optical (EO) detectors.

$$NEP^* = \frac{1}{D^*} \qquad \text{(Eq. A-3)}$$

$$NEP = (NEP^*)(A_d \Delta f) = \frac{A_d \Delta f}{D^*} \qquad \text{(Eq. A-4)}$$

Where

A_d = the area of the detector
Δf = the amplifier bandwidth

The NEP represents the IR flux that must fall on the detector to produce a signal-to-noise of unity out of the detector. It does not represent the total measurement system noise. Amplifier noise and internal system radiation noise must also be considered.

1.2 Reference for Appendix A

a. Hamamatsu Photonics, Solid State Division. Characteristics and Use of Infrared Detectors, (Technical Information SD-12), Web site retrieval May 2008.

http://sales.hamamatsu.com/assets/applications/SSD/Characteristics_and_use_of_infrared_detectors.pdf.

This page intentionally left blank.

APPENDIX B

BLACKBODY FUNCTIONS

1.1 Planck's Blackbody Function

Planck's Law describes the spectral exitance of electromagnetic radiation at all wavelengths from a blackbody at its absolute temperature *T*. The spectral exitance of an ideal blackbody as a function of wavelength is given by Equation B-1.

$$M(\lambda,T) = \frac{2\pi hc^2}{\lambda^5}\frac{1}{e^{\frac{hc}{\lambda kT}}-1} \qquad \text{(Eq. B-1)}$$

Where

λ = wavelength
T = absolute temperature, K
h = Planck's constant, 6.626 069 x10^{-34} J s
c = the speed of light, 2.997 924 58 x 10^{8} m s^{-1}
k = Boltzman's constant, 1.380 650 4 x10^{-23} J K^{-1}
e = the base of the natural logarithm, 2.718 281

Equation B-1 can be rewritten in a more convenient form (Equation B-2) by combining the physical constants.

$$M(\lambda,T) = \frac{C_1}{\lambda^5}\frac{1}{e^{\frac{C_2}{\lambda T}}-1} \qquad \text{(Eq. B-2)}$$

Where

C_1 = 3.7418 x10^{4} W μm^4 cm^{-2}
C_2 = 1.4388 x10^{4} μm^{-1} K^{-1}

The surface of a blackbody is a Lambertian emitter. Using the relation between exitance and radiance for a Lambertian surface, M=πL, the spectral radiance of a blackbody is given by Equation B-3 and a more convenient form in Equation B-4. Figure B-1 presents spectral radiance for various blackbody temperatures.

$$L(\lambda,T) = \frac{2hc^2}{\lambda^5}\frac{1}{e^{\frac{hc}{\lambda kT}}-1} \qquad \text{(Eq. B-3)}$$

$$L(\lambda,T) = \frac{C_3}{\lambda^5}\frac{1}{e^{\frac{C_2}{\lambda T}}-1} \qquad \text{(Eq. B-4)}$$

Where

C_3=1.19105 x10^4 W μm^4 cm^{-2} sr^{-1}

C_2=1.4388 x10^4 μm^{-1} K^{-1}

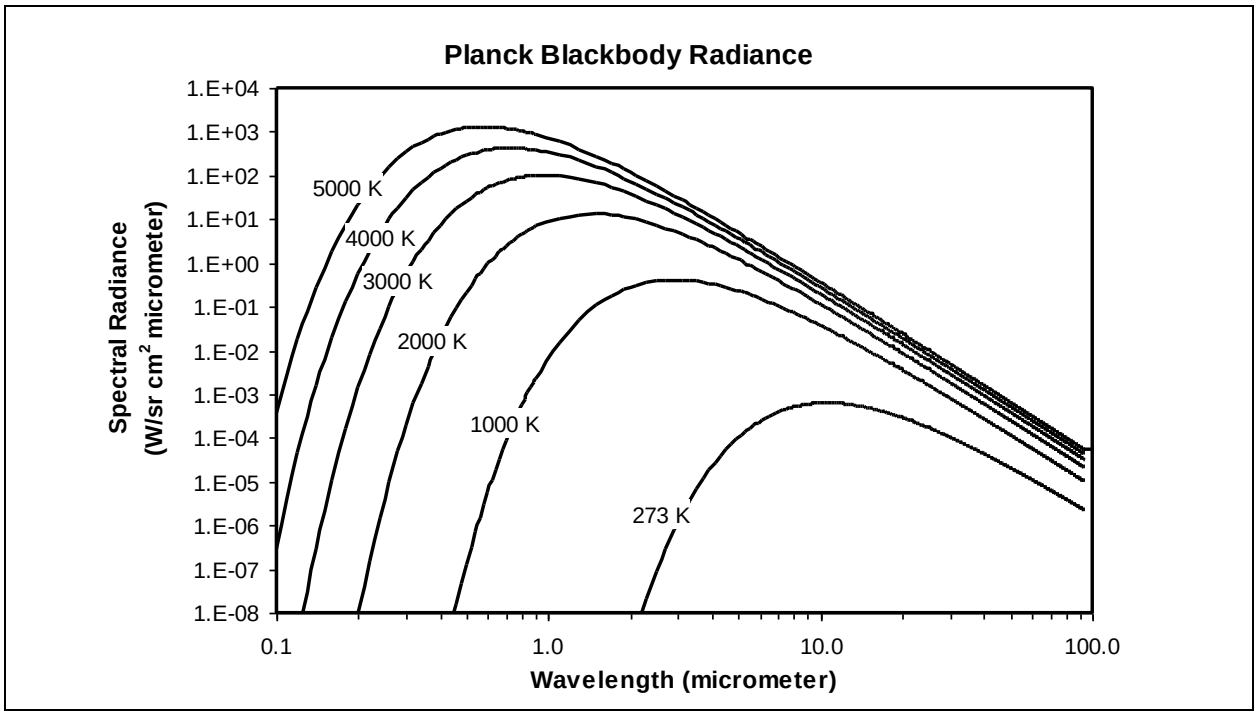

Figure B-1. Blackbody spectral radiance.

1.2 Wien's Displacement Law

Wien's Displacement Law states that there is an inverse relationship between the wavelength of the peak of electromagnetic radiation of a blackbody and its absolute temperature. Equation B-5 shows Wien's Law as a function of temperature. Figure B-2 shows the wavelength for which radiation is a maximum at a given black body temperature.

$$\lambda_{max} = \frac{b}{T} \qquad \text{(Eq. B-5)}$$

Where

λ_{max} = the peak wavelength, μm
T = the absolute temperature of the blackbody, K
b = the constant of proportionality, 2.897 768 5 x10^3 μm K

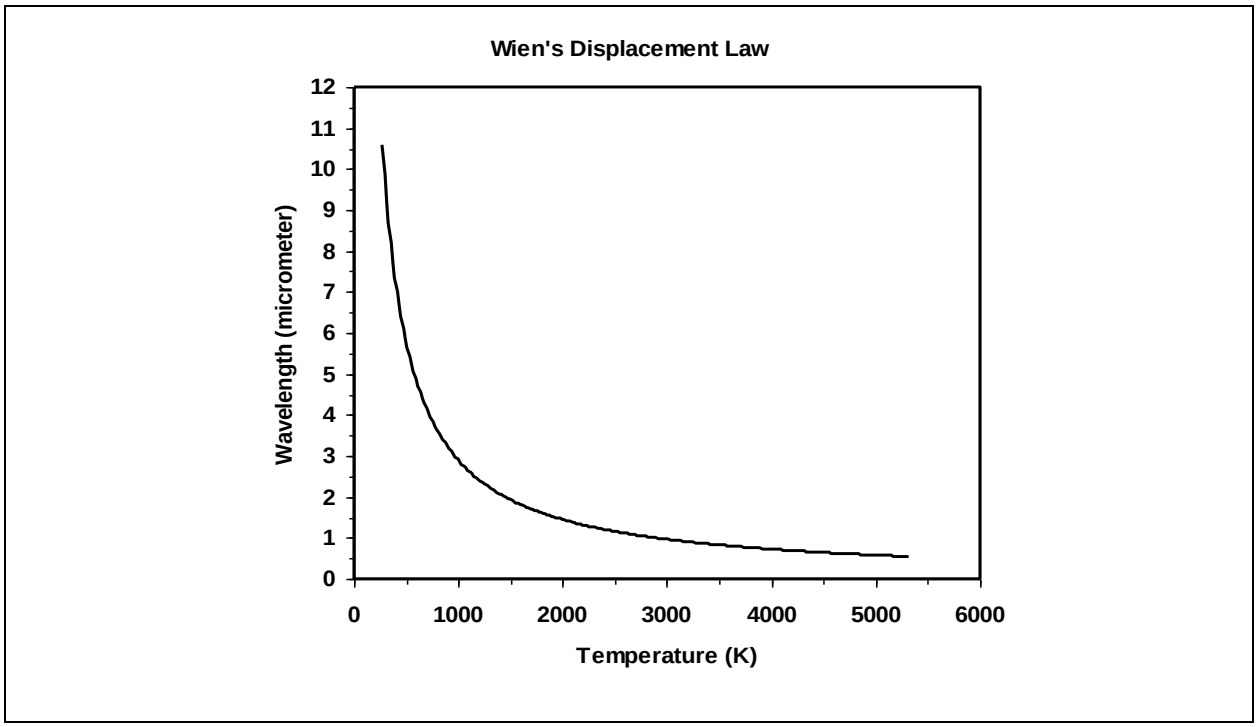

Figure B-2. Wavelength for maximum radiance.

1.3 Stefan-Boltzmann Law

The Stefan-Boltzmann Law states that the total electromagnetic radiation per unit surface area of a blackbody in unit time (emissive power) is directly proportional to the fourth power of the body's absolute temperature *T*. Equation B-6 shows the Stefan-Boltzmann Law as a function of temperature and includes an emissivity factor for the case in which a portion of the energy is radiated uniformly with wavelength (grey body). Figure B-3 presents the total emitted energy of a blackbody versus temperature.

$$M(T) = \varepsilon \sigma T^4 \qquad \text{(Eq. B-6)}$$

Where

$M(T)$ = the exitance of a blackbody, W/m^2
ε = the graybody emissivity (ε = 1.0 for blackbody)
σ = the Stefan-Boltzman constant, 5.670 400 $x10^{-8}$ J s^{-1} m^{-2} K^{-4}
T = the body absolute temperature, K

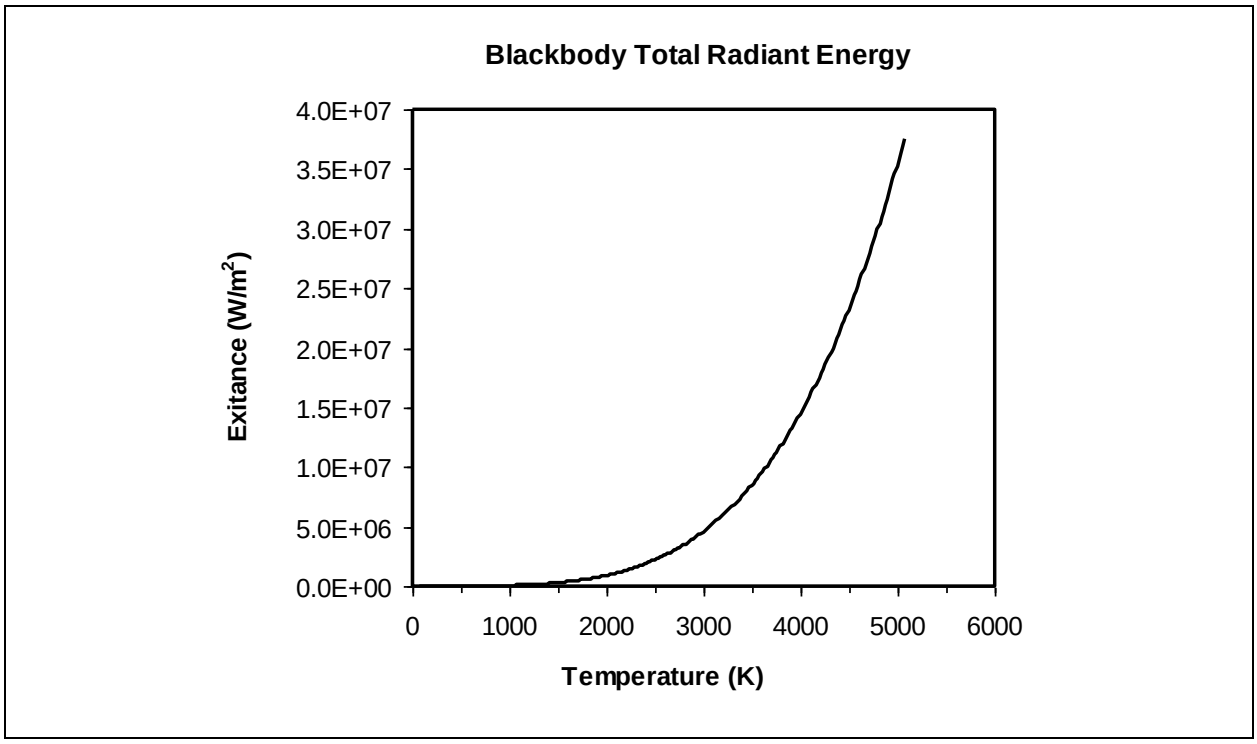

Figure B-3. Blackbody total radiant energy.

1.4 Spectral Emitters

The most general case (and realistic) is that for which emissivity depends on wavelength ($\varepsilon = \varepsilon(\lambda)$). Emissivity values vary from near zero to 1.0 for actual materials as shown in Table B-1 (see Reference 1.5a). These are hemispherical emissivity values. It is important to consider the source temperature when determining the heat balance and surface temperature of an object in space with direct sun, for example. In this case the absorption is at the solar temperature and emission is at the surface temperature. The characteristic α /ε ratio is used in spacecraft design to identify material uses.

Note.

A radiator design may involve the use of white paint (α /ε = 0.18/0.95 = 0.19).

A heat absorber may choose polished chromium (α /ε = 0.49/0.08 = 6.13).

In general, emissivity for metals follows a trend of decreasing values with wavelength while emissivity for nonconductors generally increases with wavelength. A low emissivity means little radiation is emitted at the wavelength while a high emissivity means the emitted radiation approaches the maximum possible given by Planck's Equation.

TABLE B-1. HEMISPHERICAL EMISSIVITY VALUES OF VARIOUS SURFACES

Material	Surface Condition	0.6 um* Solar	1.8 um* 1371 °C	3.6 um* 538 °C	5.4 um* 260 °C	9.3 um* 38 °C
Aluminum	Polished	~0.30	0.19	0.08	0.05	0.04
	Oxidized	-	-	0.18	0.12	0.11
	Anodized at 1000 °F	-	0.34	0.60	0.42	0.94
Brass	Polished	-	-	-	0.10	0.10
	Oxidized	-	-	-	-	0.61
Chromium	Polished	0.49	0.40	0.26	0.17	0.08
Copper	Polished	-	0.17	0.18	0.05	0.04
	Oxidized	-	-	0.77	0.83	0.87
Stainless Steel (18-8)	Polished	-	-	0.22	0.18	0.15
	Weathered	-	-	0.85	0.85	0.85
Brick	Red	0.70	-	-	-	0.93
	Fire Clay	-	~0.75	~0.7	-	0.9
Marble	White	0.47	-	0.93	-	0.95
Paper	White	0.47	-	0.93	-	0.95
Paints	White (ZnO)	0.18		0.91		0.95
	Cream	0.35	0.42	0.70	0.88	0.95
	Red	0.74	-	-	-	0.96
	Lampblack	0.97	0.97	-	0.97	0.96
Glass		Low	-	-	-	0.90

* Wavelength for which maximum radiance occurs at this temperature.

1.5 Reference for Appendix B

a. Kreith, F, (1965). Principles of Heat Transfer 2nd edition, International Textbook Company.

APPENDIX C

SOLID ANGLE

A solid angle is defined as the ratio of the area of a spherical cap to the square of the radius of the sphere. A spherical cap is the region of a sphere which lies above a plane that intersects the sphere. As illustrated in Figure C-1, the sphere has radius *R*, the plane intersecting the sphere is a circle with radius *a*, the length of a line along the sphere radius between the plane and the surface of the sphere is *h*, and the length of the radial line between the plane and the sphere origin is *(R-h).* In the spherical coordinate system, φ and θ are defined where

$$0 \le \theta \le 2\pi \text{ and } 0 \le \phi \le \pi$$

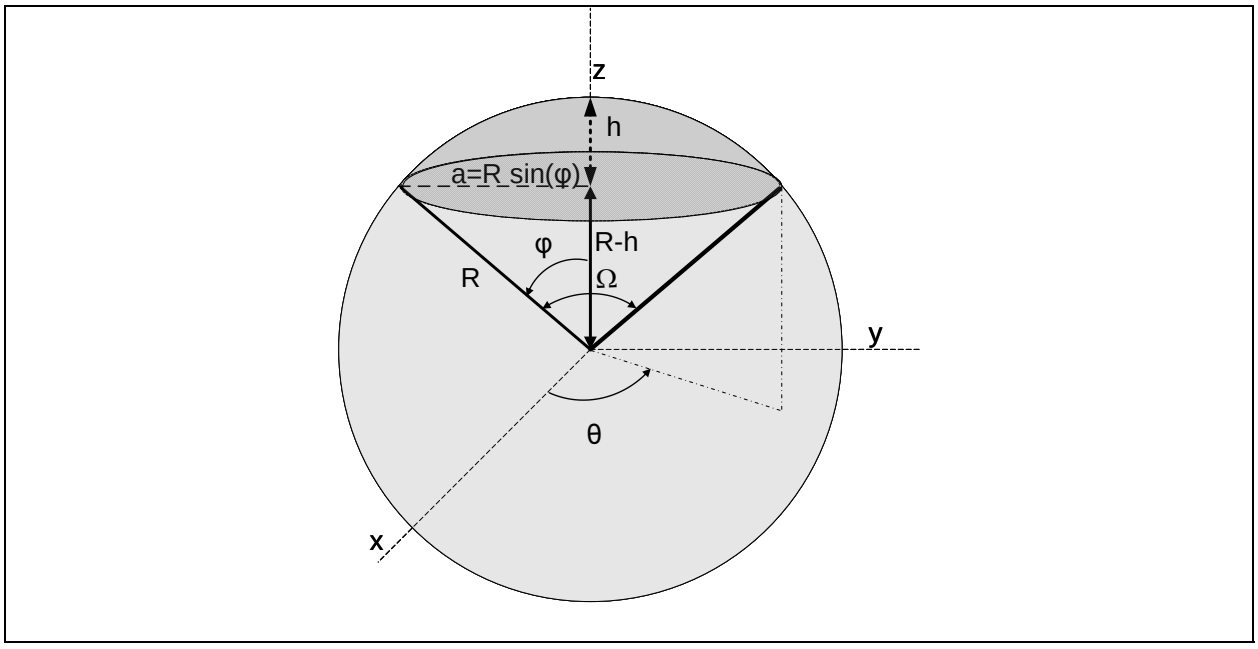

Figure C-1. Defining a solid angle, Ω.

From Figure C-1, we see the following relationships:

$$\cos(\phi) = \frac{R-h}{R} \qquad \text{(Eq. C-1)}$$

$$a^2 + (R-h)^2 = R^2 \qquad \text{(Eq. C-2)}$$

The surface area of a spherical cap A_{cap} is found using the well known integral for the surface area of a sphere except the limits of integration on φ are limited to 0 and $\cos^{-1}[(R-h)/R]$.

$$A_{cap} = R^2 \int_0^{2\pi} d\theta \int_0^{\cos^{-1}(\frac{R-h}{R})} \sin(\varphi) d\phi \qquad \text{(Eq. C-3)}$$

$$A_{cap} = 2\pi R^2 \left[-\cos(\phi)\right]_0^{\cos^{-1}(\frac{R-h}{R})}$$

$$A_{cap} = 2\pi R\, h \qquad \text{(Eq. C-4)}$$

By definition of the solid angle, we have

$$\Omega = \frac{2\pi R h}{R^2} \qquad \text{(Eq. C-5)}$$

An approximation frequently used in radiometry is that the solid angle Ω can be approximated by the ratio of the area of the circle and $(R\text{-}h)^2$ for large R. The approximation is convenient in that the area of the circle can be thought of as the clear aperture area of collection optics A_{optic} or the area of the field of view (FOV) at the target plane A_{FOV} as illustrated in Figure C-2.

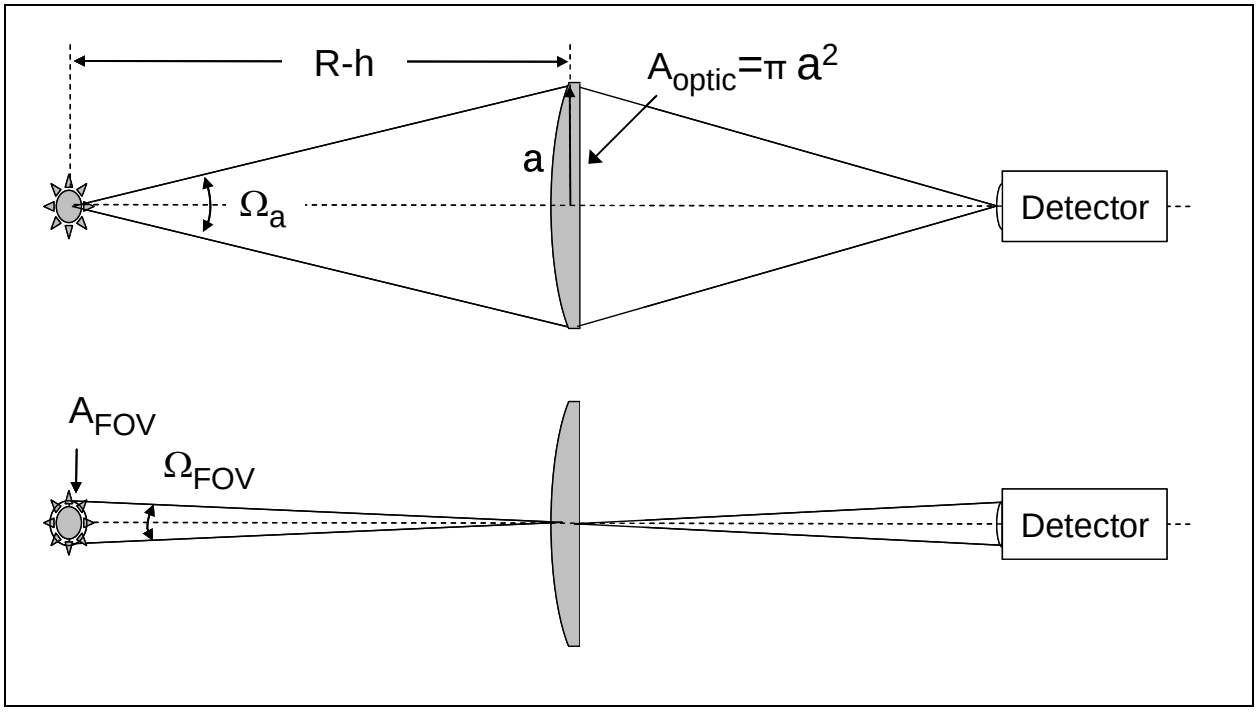

Figure C-2. Illustration of the use of an approximation to the solid angle related to the sensor optical parameters.

The following discussion proves that the range criterion for this approximation is easily met in most situations. The area of the base of the spherical cap in Figure C-1 is πa^2. The approximation to the solid angle is then

$$\Omega_a = \frac{\pi a^2}{(R-h)^2} \qquad \text{(Eq. C-6)}$$

Where

The subscript *a* is used to identify the solid angle Ω_a as the approximation using the area of circle and the range from the circle to the sphere origin.

We will compare Ω_a to Ω for *R* as positive multiples of the circle radius *a*. Replace *R* in Equation C-2 with multiples of *a*, *R*=*ma* where *m* is any positive number, and solve for *h*.

$$a^2 + (am-h)^2 = (am)^2$$

$$(am-h)^2 = a^2m^2 - a^2$$

$$h = a(m - \sqrt{m^2-1}) \qquad \text{(Eq. C-7)}$$

Using Equation C-7 in Equation C-5 and Equation C-6 we write Ω and Ω_a in terms of the multiple *m*.

$$\Omega = \frac{2\pi\left(m-\sqrt{m^2-1}\right)}{m} \qquad \text{(Eq. C-8)}$$

$$\Omega_a = \frac{\pi}{m^2-1} \qquad \text{(Eq. C-9)}$$

Figure C-3 is a graph of the solid angle Ω and the approximation Ω_a as the range *R* increases relative to the circle radius *a*. Figure C-4 is the percent difference of the approximation to the solid angle calculated as $Y = 100 \times (\Omega_a - \Omega)/\Omega$.

Both Figure C-3 and Figure C-4 clearly show that the approximation is good for ranges that are on the order of 30 times the radius of the circle. A one percent difference is seen if the range is about 10 times the radius of the base circle and a difference of less than 0.1 percent is seen if the range is 30 times the radius of the base circle. An example in terms of optical apertures is to consider a mirror with radius 0.5 m (1 m diameter) for the collection optic. Then, a 0.1 percent error is realized for a 15 m range.

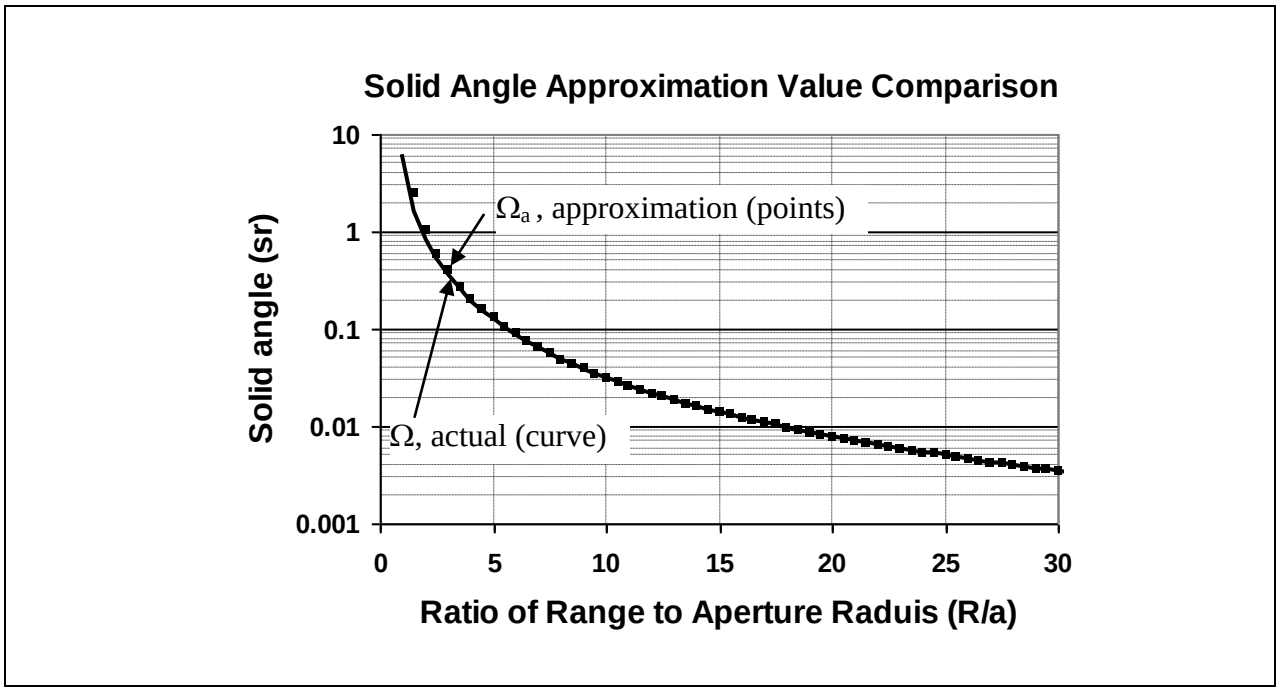

Figure C-3. Approximation to solid angle Ω_a and actual solid angle Ω for increasing range.

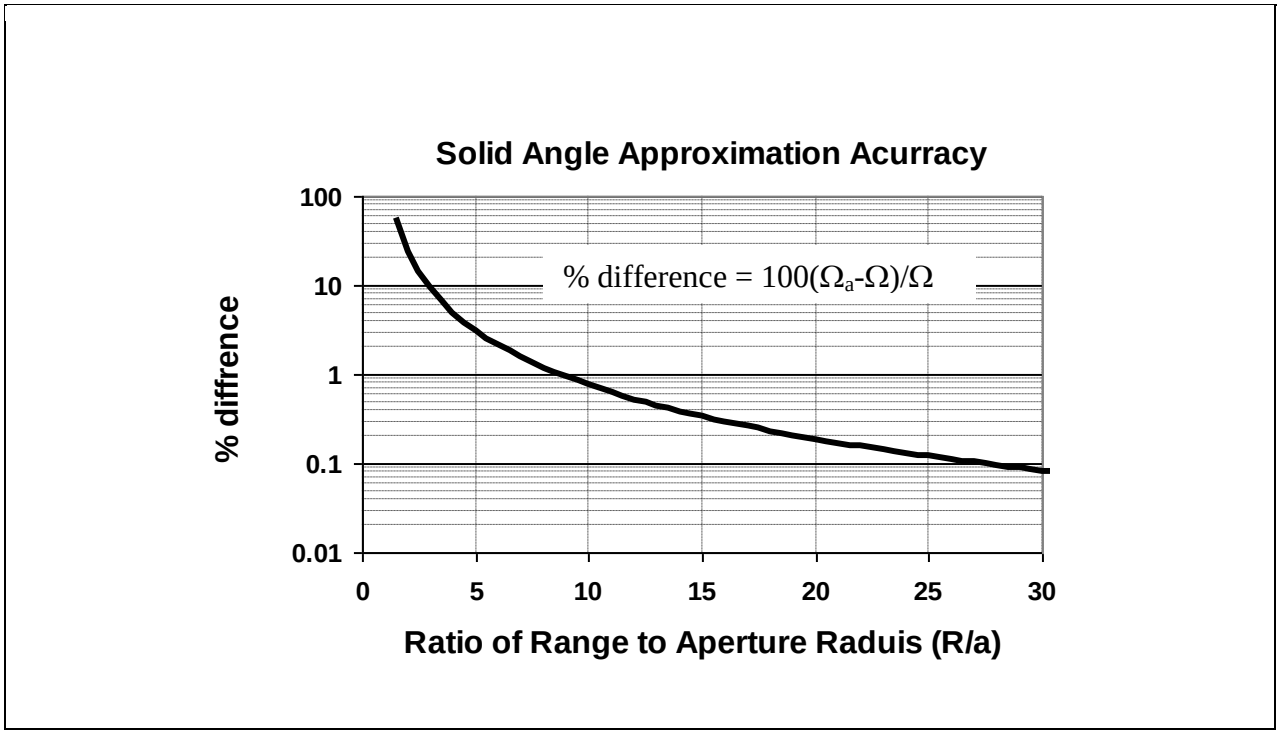

Figure C-4. Percent difference between the approximation Ωa and Ω for increasing range.

APPENDIX D

SANDFORD-ROBERTSON BIDIRECTIONAL REFLECTANCE DISTRIBUTION FUNCTION (BRDF) EQUATIONS

1.1 Sandford-Robertson BRDF Equations

The Sandford-Robertson Bidirectional Reflectance Distribution Function (BRDF) equation is presented in Equation D-1 below as a reference. The equation relates the spherical angles of the incident beam, θ_i and φ_i, to the spherical angles of the reflected beam, θ_r and φ_r, from a surface. The equation has two primary terms, one for the diffuse component and one for the specular component. The terms are determined by fitting to data collected with a BRDF device.

$$BRDF(\theta_i,\phi_i;\theta_r,\phi_r) = f_d(\theta_i,\phi_i;\theta_r,\phi_r) + f_s(\theta_i,\phi_i;\theta_r,\phi_r) \qquad \text{(Eq. D-1)}$$

a. <u>The diffuse component</u>.

$$f_d(\theta_i,\phi_i;\theta_r,\phi_r) = \frac{1}{\pi}\frac{g(\theta_r)\rho_D g(\theta_i)}{G(b)^2} = \frac{1}{\pi}\frac{g(\theta_r)}{G(b)}\frac{g(\theta_i)}{G(b)}\rho_D$$

Where

$$g(\theta) = \frac{1}{1 + b^2\tan^2\theta}$$

$$G(b) = \frac{1}{1 - b^2}\left\{1 - \frac{b^2}{1 - b^2}\ln\left(\frac{1}{b^2}\right)\right\}$$

b. <u>The specular component</u>.

$$f_s(\theta_i,\phi_i;\theta_r,\phi_r) = \frac{1}{4\pi}\rho_s(\theta_i)\frac{h(\alpha)}{H(\theta_i)\cos(\theta_r)} = \frac{1}{4\pi}\left[1 - (\rho_D + \varepsilon_H)\frac{g(\theta)}{G(b)}\right]\frac{h(\alpha)}{H(\theta_i)}\frac{1}{\cos(\theta_r)}$$

$$\rho_s(\theta_i) = 1 - (\rho_D + \varepsilon_H)\frac{g(\theta_i)}{G(b)}$$

$$h(\alpha) = \frac{1}{\left\{e^2\cos^2\alpha + \sin^2\alpha\right\}^2} = \frac{1}{\left\{(e^2 - 1)\cos^2\alpha + 1\right\}^2}$$

$$\cos\alpha = \frac{\cos\theta_i + \cos\theta_r}{\sqrt{2(1 + q)}}$$

$$q = \cos\theta_i\cos\theta_r + \sin\theta_i\sin\theta_r(\cos\phi_i\cos\phi_r + \sin\phi_i\sin\phi_r)$$

$$H(\theta_i) = \frac{1}{2e^2}\left[(1 - e^2)\cos\theta_i + \frac{2e^2 + (1 - e^2)\cos^2\theta_i}{\sqrt{(1 - e^2)\cos^2\theta_i + 4e^2}}\right]$$

1.2 Relationships and Definitions

a. Relationships.

$$\rho_{tot}(\theta_i) = 1 - \frac{g(\theta_i)}{G(b)}\varepsilon_H = 1 - \varepsilon(\theta) = \rho_d(\theta_i) + \rho_s(\theta_i)$$

$$\varepsilon(\theta) = \frac{g(\theta_i)}{G(b)}\varepsilon_H$$

$$\rho_s(\theta_i) = 1 - (\rho_D + \varepsilon_H)\frac{g(\theta_i)}{G(b)} \quad \text{inferring..} \ \rho_d(\theta_i) = \frac{g(\theta_i)}{G(b)}\rho_D$$

b. Definitions.

$\rho_D(\lambda)$	=	Diffuse spectral reflectance
$\varepsilon(\lambda)$	=	Spectral emissivity
b	=	Grazing angle reflectivity
e	=	Width of the specular lobe

APPENDIX E

NON-SI PHOTOMETRIC QUANTITIES

1.1 Historical Photometric Quantities

Use of SI units is recommended for photometric measurements and use of non-SI units is discouraged (Reference 1.3a). However, since non-SI units are still encountered, a list of some of the most often encountered quantities is presented in Table E-1 for conversion only. Note that the candela replaced the quantity "candle power" in 1948, but the term candle power will at times be found in older documents. For reference, a candle power is approximately equal to 0.981 cd.

TABLE E-1. NON-SI PHOTOMETRIC QUANTITIES

Name	Quantity	Symbol	Units	Conversions
Phot	Illuminance	pt	lm/cm^2	1 pt = 10^4 lx
Lux	Illuminance	lx	lm/m^2	1 lx = 1 lm/m^2
Nox	Illuminance	nx	lm/m^2	1 nx = 10^{-3} lx
Foot-candle	Illuminance	fc	lm/ft^2	1 fc =10.764 lx
Candela	Luminous intensity	cd	lm/sr	1 cd = 1 lm/sr
Stilb	Luminance	sb	cd/cm^2	1 sb = 10^4 cd/m^2
Nit	Luminance	nt	cd/m^2	1 nt = 1 cd/m^2
Skot	Luminance	st	cd/ft^2	1 st = $3.183x10^{-4}$ cd/m^2
Lambert	Luminance	L	cd/cm^2	1 L = 3183 cd/m^2
Apostilb	Luminance	asb	cd/m^2	1 asb = 0.3183 cd/m^2
Meter-Lambert	Luminance	m L	cd/m^2	1 m L = 0.3183 cd/m^2
Foot-Lambert	Luminance	ft L	cd/ft^2	1 ft L = 3.4263 cd/m^2

Note. For non-si photometric quantities information, see Reference1.3b).

1.2 Compare Unit Lux To Unit Foot-Candle

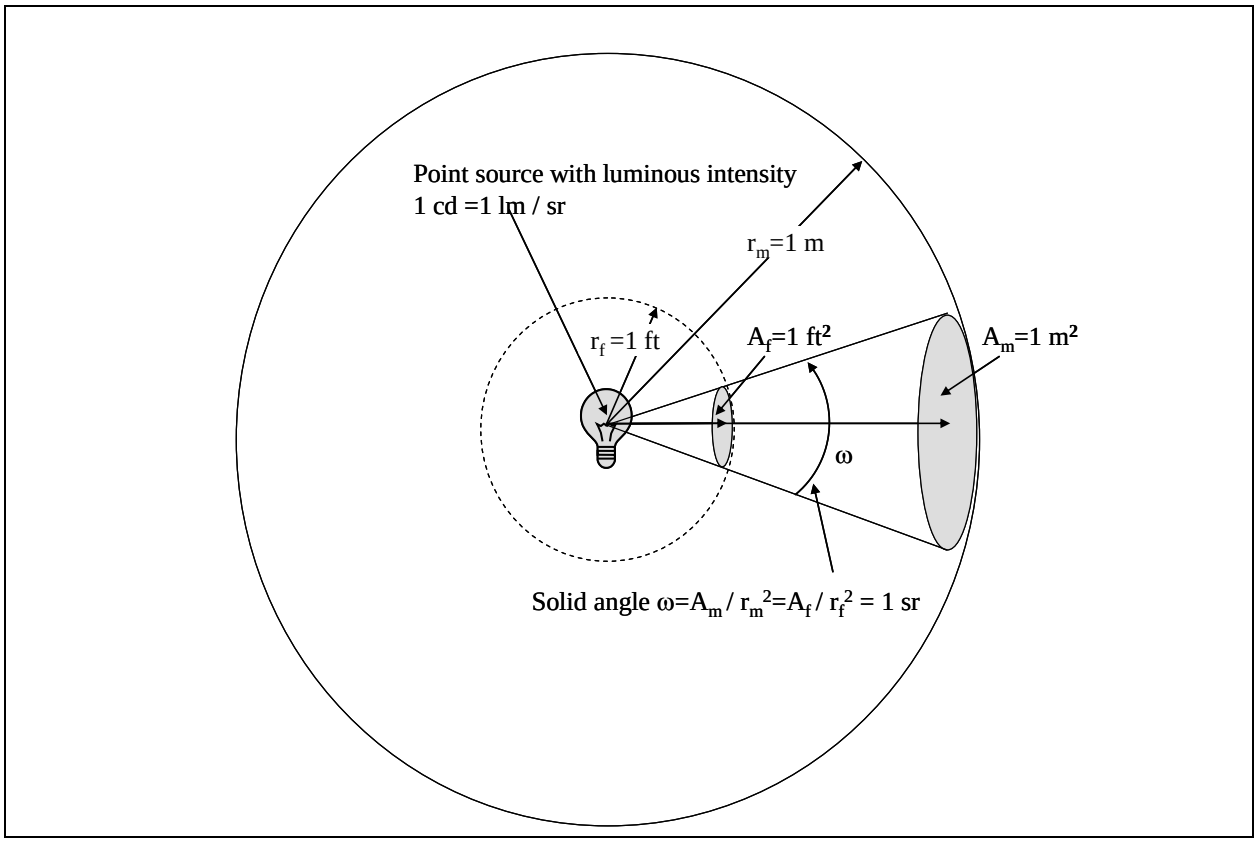

Figure E-1. Illustration to compare the unit lux to the unit foot-candle.

The area of a sphere subtended by a 1-sr solid angle is equal to the square of the radius (see Figure E-1 above). The illuminance from a 1 cd (candela) source on the surface of a sphere with radius r=1 m is 1 lx (1 lm/m^2). The illuminance from the same source on a sphere with radius r=1 ft is 1 fc (foot-candle). Because the surface of the 1-ft radius sphere is closer to the source than the surface of a 1-m radius sphere, the unit fc is greater than the unit lx. The conversion is 1 fc = 10.76 lx.

Proof.

Given.

The source has luminous intensity is I_v = 1 cd = 1 lm/sr

Illuminance at 1-m radius sphere is $E_{v,m} = \frac{I_v}{r_m^2} = 1 \text{ lm/m}^2$

Illuminance at 1-ft radius sphere is $E_{v,f} = \frac{I_v}{r_f^2} = 1 \text{ fc}$

Then

$$\frac{E_{v,f}}{E_{v,m}} = \frac{r_m^2}{r_f^2} = \frac{(3.048\ \text{ft})^2}{(1\ \text{ft})^2} = 10.76$$

Therefore,

1 fc = 10.76 lx

It is also obvious from the above example why SI eliminated the unit foot-candle, fc, from the list of derived SI units. Not only does it use an English unit of length, but more seriously, the form of the unit foot-candle implies length times luminous intensity, which it is not. The unit foot-candle only has meaning through a definition. It is impossible to conduct algebra on the unit foot-candle in any meaningful way to derive additional units of measure or to convert to other units.

1.3 References for Appendix E.

a. Ohno, Y. (1997). Photometric Calibrations, NIST Special Publication 250-37. U.S. Department of Commerce Technology Administration, National Institute of Standards and Technology (NIST).

b. Wolfe, W. and Zissis, G. (1998). The Infrared Handbook. The Infrared Information Analysis (IRIA) Center, Environmental Research Institute of Michigan, June 1993.

This page intentionally left blank.

GLOSSARY

apparent: A term to indicate the radiometric quantity includes atmospheric attenuation effects.

blackbody: An ideal body that completely absorbs all radiation and therefore appears black at all wavelengths. A perfect blackbody has an emissivity of unity at all wavelengths. The emissions from a blackbody are modeled by Planck's Blackbody Law.

Bidirectional Reflectance Distribution Function (BRDF): Unified notation for the specification of reflection for a surface in terms of the incident and reflected beam geometry.

charge-coupled device (CCD): A self-scanning semiconductor device, usually of a linear or two dimensional array of individual detector elements placed at the focal plane of an imager or of a spectrometer.

computational fluid dynamics (CFD): The science of using models to predict flowfields.

Composite Hardbody and Missile Plume (CHAMP): A computer simulation used to provide time dependent high-fidelity IR simulations of airborne vehicles.

(D*, D-star): A figure of merit to designate the relative sensitivity of a detector. Higher D* values indicate greater sensitivity.

Effective: A term to indicate the radiometric quantity is related to the spectral response of the measuring system. The subscript "e" is used to indicate an effective quantity, such as L_e.

Electro-optical (EO): The technology associated with electrical devices which are designed to interact with optical electromagnetic radiation.

Emissivity: The ratio of a source radiance to that of a perfect blackbody at the same temperature and wavelength.

Enhanced Missile Signature (E-MSIG): Spectral, spatial and temporal models of the UV through IR signatures of tactical missile exhaust plumes, developed by the Defense Intelligence Agency/ Missile and Space Intelligence Center (DIA/MSIC), Redstone Arsenal, AL, and the Arnold Engineering Development Center, Arnold AFB, TN.

FEL: FEL is the lamp-type designation (not an acronym) of the American National Standards Institute (ANSI).

field of regard: Total spatial extent covered by an optical system, usually only used for a spatial extent when a smaller FOV or IFOV is mechanically scanned over a large area.

FIR: Far IR, 30 μm to 1 000 μm wavelength span of the electromagnetic spectrum.

FOV: Field of view, the maximum spatial extent in source (target) space that can be seen by an optical system.

FPA: Focal plane array; a linear or two-dimensional matrix of detector elements (pixels) usually used at the focal plane of an imaging system.

Fourier Transform Spectrometer (FTIR): Synonymous with Michelson spectrometer and FTS.

Fourier Transform Spectrometer (FTS): Synonymous with FTIR spectrometer and Michelson spectrometer.

graybody: Similar to a blackbody absorber/emitter except the spectral emissivity is a constant less than unity (also spelled as greybody).

Georgia Tech Signature Code (GTSIG): A library of computer programs whose development is sponsored by the Army to predict temperature, blackbody emittance, and effective radiances of three-dimensional objects, accounting for the object's interaction with an environment over a period of time.

Georgia Tech Visible and Infrared Synthetic Imagery Testbed (GTVISIT): A computer program that uses the GTSIG output as inputs to compute the views of the world as seen by threat IR missiles.

hyper-spectral: A type of spectral imager that has high spectral resolution but possibly compromised spatial resolution, where the terms high and low are subjective.

Integrated Data Requirements List (IDRL): (1) A list that relates the specific test data requirements to data sources, accuracy specifications, frequency of collection, method of collection, and point of responsibility, (2) A list of parameters identifying what will be collected during a particular test event.

instantaneous field of view (IFOV): The spatial extent in source (target) space that can be seen by a single detector and a single pixel in a detector pixel array.

infrared (IR): 0.76 μm to 1 000 μm wavelength span of the electromagnetic spectrum.

Inter-range Instrumentation Group (IRIG): Here referring to the digital time code standard.

Joint Tactical Missile Signature (JTAMS): An OSD JTF program (1993-1996) to determine standard practices and procedures to collect, interpret, and archive tactical missile exhaust plume UV and IR signatures.

Lambertian: A diffuse surface that has the special property that the radiance is constant with viewing angle.

long wave IR (LWIR): 6 μm to 30 μm wavelength span of the electromagnetic spectrum.

Model Extrapolation Procedure (MODEX): A procedure to create modeled data for missile flight conditions that are impossible or too costly to measure and to overcome inaccuracies in the predictive code suite.

Moderate Resolution Atmospheric Transmission (MODTRAN): The atmospheric model developed by the AFRL Space Vehicles Directorate.

multi-spectral: A type of spectral imager with high spatial resolution but possibly compromised spectral resolution, where the terms high and low are subjective.

mid-wave IR (MWIR): 2.7 μm to 6 μm wavelength span of the electromagnetic spectrum.

near IR (NIR): 0.75 μm to 1.83 μm wavelength span of the electromagnetic spectrum.

nomograph (or nomogram): A graphical calculating device, a two-dimensional diagram designed to allow the approximate graphical computation of a function; it uses a coordinate system other than Cartesian coordinates.

optical radiation: 0.01 um to 10 000 um wavelength span of the electromagnetic spectrum.

photometry: Science of measuring light which is the integrated radiant power within the visible region of the electromagnetic spectrum, weighted by the response of a human observer.

photopic vision: Vision by the cones of the eye, requires high luminance conditions.

Parabolized Navier Stokes (PNS): Equations used to predict the flowfields.

radiometry: Science of measuring radiant power for wavelength in the optical region of the electromagnetic spectrum.

scotopic vision: Vision by the rods of the eye, vision in low luminance conditions.

short wave IR (SWIR): 1.83 μm to 2.7 μm wavelength span of the electromagnetic spectrum.

Staring Focal Plane Array (SFPA): A type of imager that does not use optical or mechanical scanning of the FOV or modulation such as from a chopper.

Spectral and Inband Radiometric Imaging of Targets and Scenes (SPIRITS): Code developed by the Air Force Research Laboratory.

source (1): An origination of radiant power; a point source if the physical extent is small compared to the FOV of the observing system; an extended source if the physical extent is large relative to the FOV of the observing system.

source (2): A term use to indicate that atmospheric attenuation effects are not included in the radiometric value; either the atmospheric attenuation is unity or the effect has been numerically removed from the apparent value.

spectroscope: A device used for separating light into component colors for analysis.

spectroscopist: One who investigates by means of a spectroscope; one skilled in the use of the spectroscope.

time after trigger (TATR): Used as a time tag on data that are not yet correlated to an ignition time or other test initiation event.

time constant: A characteristic of an electro-optical (EO) detector. It is the time required to change the output value to 63% of the final steady state value in response to a change in input stimulus. $[1-\exp(-t/\tau_c)]$ is 0.63 for $t = \tau_c$ where τ_c is the time constant. It is an experimentally determined value of a detector. For t very much greater than τ_c, $[1-\exp(-t/\tau_c)]$ approaches 1.0 and steady state is reached.

time-space-position information (TSPI): The 3-dimensional coordinates of an object at a specific time.

ultraviolet radiation (UV): 0.01 μm to 0.38 μm wavelength span of the electromagnetic spectrum.

visible radiation (VIS): 0.36 μm to 0.83 μm wavelength span of the electromagnetic spectrum.

This page intentionally left blank.